Localiser et comprendre le risque de mortalité d'arbres sous l'effet du changement climatique : approche multi-échelles combinant modélisation statistique et mécaniste

Cathleen Petit

THÈSE POUR OBTENIR LE GRADE DE DOCTEUR

DE MONTPELLIER SUPAGRO

En Ecologie et Biodiversité

École doctorale GAIA – Biodiversité, Agriculture, Alimentation, Environnement, Terre, Eau

Unité de recherche 629 - Ecologie des Forêts Méditerranéennes

INRA

Localiser et comprendre le risque de mortalité d'arbres forestiers sous l'effet du changement climatique

Approche multi-échelles combinant modélisation statistique et mécaniste

Locate and understand the mortality risk of forest tree under climate change

Multi-scale approach combining statistical and mechanistic modelling

---

Présentée par

Cathleen PETIT-CAILLEUX

Soutenue le 21-02-2020 devant le jury composé de :

Guillaume Charrier, Chargé de recherche, INRAe	**Examinateur**
Wolfgang Cramer, Directeur de recherche, IMBE-CNRS	**Président du jury**
Hendrik Davi, Directeur de recherche, INRAe	**Co-directeur de thèse**
Anne Duputié, Maître de conférence, CNRS-University Lille 1	**Examinatrice**
François Lefèvre, Directeur de recherche, INRAe	**Co-directeur de thèse**
Sylvie Oddou-Muratorio, Directrice de recherche, INRAe	**Directrice de thèse**
Annabel Porté, Directrice de recherche, INRAe-Université de Bordeaux	**Rapporteure**

Avant-propos

Dans cette thèse, je me suis intéressée à l'impact du changement climatique sur les risques de mortalité d'arbres forestiers européens. Le hêtre a été mon modèle d'étude et à l'aide d'outils de modélisations statistiques et basés sur les processus, j'ai intégré des connaissances provenant des domaines de l'écophysiologie, gestion forestières et génétiques. Le but était de modéliser des risques de mortalité actuels et futurs liés aux stresses de sécheresse et de gelée tardive aussi bien à l'échelle de l'arbre que de l'espèce. Ainsi cette thèse nous a permis de comprendre les mécanismes physiologiques entraînant un risque de mortalité élevé et de localiser les zones à fort risque d'extinction pour guider les gestionnaires forestiers.

La thèse se compose en parties générales qui sont rédigées en français et en trois articles scientifiques rédigés en anglais. Cette thèse a été financé par le projet GenTREE à partir du 17 octobre 2016. Les données utilisées dans le premier chapitre ont été fournie par la Réserve Naturelle Nationale de la Forêt de la Massane.

Remerciements

"Écrire des remerciements de thèse, cela n'est pas si anodin" (1).

Les relations des êtres vivants entre eux et avec leur environnement m'ont toujours captivé. Comme l'a fait remarquer Eric Hobsbawm, la théorie de l'évolution de Darwin a permis de ré-inclure l'humain dans ces êtres vivants et de supprimer la démarcation entre les sciences naturelles et les sciences humaines et sociales (2). Il n'est donc pas étonnant qu'en plus de l'écologie, un de mes autres centres d'intérêt majeur est la sociologie. C'est sûrement pourquoi je me suis demandée : comment est ce que j'ai pu faire une thèse ? Où cela va-t-il me mener ? En effet, parmis les doctorant de ma génération, je fais partie des 2.2 % venant d'une classe social d'artisan/commerçant (3). Cependant le chemin est encore long avant de pouvoir me prétendre chercheure. En effet, il y a 52% de femmes en doctorat de science agronomique et écologique mais ce pourcentage se réduit à 44 % des effectifs pour des postes de maître de conférence, puis à 25 % de professeures (4). C'est pour tout le chemin que j'ai déjà parcouru, et qu'il me reste à faire que je souhaite remercier les personnes qui m'ont encouragé et qui ont cru en moi.

Tout d'abord, je tiens à remercier les personnes qui m'ont permis de réaliser cette thèse, mes encadrant.e.s, Sylvie Oddou-Muratorio, Hendrik Davi et François Lefèvre. Je remercie tout particulièrement, Sylvie pour ton encadrement, qui a tenu bon pendant tout ce temps, en me redirigeant quand cela commençait à dévier et en relisant inlassablement mon travail. A Hendrik Davi pour ton enthousiasme et ta confiance dans mes idées et capacitées. A François Lefèvre pour nos discussions enrichissantes et ton optimisme permanent. Vous avoir tous les trois en encadrement c'était du boulot, riche en échanges et compromis, mais particulièrement génial (surtout grâce à cette petite semaine de formation EDEN).

(1). Quentin Verreycken, "Anatomie des remerciements de thèse", in ParenThèses, publié le 07/12/2015, `https://parenthese.hypotheses.org/1127` (consulté le 30/05/2020).

(2). « L'écologie scientifique, une science impliquée ? », Écologie & politique, vol. 51, no. 2, 2015, pp. 55-64. `https://doi.org/10.3917/ecopo.051.0055`

(3). Parcours dans l'enseignement supérieur : devenir des bacheliers 2008 Note d'information n°6 - Septembre 2018. MENESR-DGESIP/DGRI-SIES

(4). ces chiffres sont équivalent, voir moindre dans les instituts de recherche public

Je remercie sincèrement Annabel Porté et Wolfgang Cramer d'avoir accepté d'être les rapporteur.e.s de ma thèse ainsi que Anne Duputié et Guillaume Charrier qui ont accepté d'en être les examinateur.ices. Merci aussi aux membres de mon comité de suivi de thèse, Marta Benito-Garzon, Nicolas Delpierre, Isabelle Chuine, Bruno Fady, Xavier Morin et Silvio Schueler pour les échanges très enrichissants, leur bienveillance et leurs conseils.

Je remercie chaleureusement tous mes collaborateurs et collègues. Tout particulièrement l'équipe de la Massane pour tous ces échanges et les sessions terrains dans cette magnifique hêtraie. Jean-André Magdalou, Joseph Garrigue et Elodie Magnanou. Didier Betored et William Brunetto pour m'avoir accompagnée sur le terrain. Frédéric Guibal et Nicolas Mariotte pour la formation carotte (d'arbre). François de Coligny et Nicolas Beudez pour avoir répondu à mes appels à l'aide liés au codage sous java et l'utilisation de la plateforme CAPSIS. Merci à Emily Walker pour tous tes conseils en statistiques. A Marie-Claude et Laurent des gestionnaires d'unités exceptionnel.le.s !

Merci au bâtiment forêt pour ces pauses café améliorées, discussions variées, repas annuels synonymes de bonne humeur et d'après-midi de digestions. Au groupe du journal club qui m'a permis d'ouvrir ma culture scientifique. Aux "vieilles" du bâtiment avec qui j'ai adoré trainer et qui m'ont entraîné (ou essayé) à la piscine, à la course à pied ou aux manif (Annabel, Florence). Merci à Maurane pour nos échanges musicaux, toujours de très bon goût.

Cette partie des remerciements qui reflète la vie (finalement) hyperactive que j'ai eu à Avignon (c'était pas gagné dans cette ville), était la plus dure à écrire car vous avez été à mes côté en permanence et dans toutes sortes d'aventures.

Merci à la cohorte de thésards qui est maintenant docteur.e.s, avec qui ces trois années à l'URFM sont passées très vite. Par ordre d'apparition, merci à ma co-bureau du tonnerre, sans toi je serai encore en train de maudire des virgules sous R et jamais, mais au grand jamais, je n'aurais couru de semi-marathon avec 300m de dénivelé ! A Maxime, le roi des forêts, quelqu'un sur qui on peut compter ! A Valentin, le petit sorcier de la pluie, pour nos discussions et les innombrables soirées. A Violette, l'artiste, pour tes expressions imagées et toute l'aide que tu m'as apporté (merci pour la relecture de mails, la prise de recul sur le stress et j'en passe).

Un (grand) MERCI aux non-perms du patio pour tous ces moments partagés, pour l'aide apportée durant ces trois années et qui m'ont notamment soutenu et ont suivi dans la mise en place de notre espace vert (Laeticia, Lucile, Claire, Myriam, Victor).

Merci à tou.te.s mes ami.es qui ont eu la gentillesse de corriger mon français (Camille, Coline, Val). Merci au groupe de "La pâte !" pour toutes nos discussions enflammées, votre soutien, nos expéditions rando, nos repas gastronomiques et soirée films ; ces moments resteront inoubliables.

Merci à mes coloc, qui m'ont supporté et accepté. La grande Steph, pour ton ouverture d'esprit et ton entrain. A Elisa, the rousse on fire, pour nos 11h de rando avec 10kg sur le dos (oui oui on y est presque…). A Alice et Léo, mes bobo révolutionnaires préférés. Aux colocs de la Cabrière, merci pour m'avoir laisser squatter chez vous !

Merci aux membres d'ACACIA et surtout aux bureaux (Max, Anne-So, Camille, Coline, Stéph, Carla, Violette, Alice, Marie, Enrico, Hussein et The Maria) pour toutes ces activités scientifiques, culturelles et sociales. Merci aux ami.e.s d'Avignon pour ces moments d'évasions (particulièrement à Emma, Robin, le Gang des italiens et des Libanais, La coloc de Montplaisir). Merci au staff de l'Explo, Gille, Flo, Mathieu (autrement connu sous le pseudonyme de Loïc), Ben, Olivia, Sevda, Yohan et Margotte pour leur bonne humeur permanente et pour nous accueillir tous les jeudi et plus ! Merci à mes acolytes de plongée, Mélanie et Kévin, qui m'ont abandonnée lâchement à Avignon avec tinder et frutz.

Un grand MERCI à tous ceux qui m'ont permis de tenir durant ces 15 années de scolarité puis 10 ans d'études supérieures. Sans oublier les politiques sociales françaises et européennes, que je souhaite encourager, car être boursière m'a permis de poursuivre mes études dans des conditions décentes, voir presque normale.

A mes ami.e.s de toujours, Ophélie S., Thomate et Axel avec qui j'ai grandi, merci d'être encore là ! Merci à tous mes amies de Jussieu, avec qui j'ai passé des années formidables à faire les 400 coups et qui sont toujours partant pour de nouvelles aventures : Clémence, tout le groupe de licence (notamment Luis, Louis, Fanny et Captain), les zouzs du master Tam et Faustine.

A Loreleï et Aurélien, après toutes ces années et malgré mon franc parlé surdéveloppé, vous êtes toujours présent, prêt à râler, argumenter, cancaner et me remonter le moral. Merci à vous deux !

Je remercie tout particulièrement ma famille, mon père et ma mère qui m'ont donné le goût de l'écologie, l'envie d'apprendre et m'ont laissé développer ma curiosité. Vous m'avez toujours encouragé à votre manière et pour cela je ne vous remercierai jamais assez. A mon petit frère, pour nos échanges variés et peu productifs, qui sont essentiels pour moi et qui me rappellent d'où je viens.

Pour finir, je remercie le Val pour m'avoir supportée, sans toi, je n'aurais peut être pas fini ma thèse.

Liste non exhaustive, mais sachez que si nos chemins se sont déjà croisés, je te remercie pour l'échange positif (ou négatif) que nous avons eu.

La science consiste à faire ce qu'on fait en sachant et en disant que c'est tout ce qu'on peut faire, en énonçant les limites de la validité de ce qu'on fait.

Pierre Bourdieu, Questions de sociologie, 1984

Table des matières

Introduction générale

1 Les forêts européennes et leur devenir

Les forêts fournissent de nombreux biens et services écosystémiques, essentiels à la société, l'économie, et au bien-être humain. Elles sont une source d'approvisionnement de nombreux biens (nourriture, médicament, énergie, matériaux), permettent la filtration de l'air et de l'eau le déroulement des cycles biogéochimiques, préviennent l'érosion des sols, abritent plus des trois quarts de la biodiversité terrestre mondiale et sont un moyen de limiter l'augmentation du CO_2 (stockage de carbone) dans l'atmosphère (Daily et al., 1997). La FAO définit une forêt comme étant : une terre ayant un couvert arboré (ou une densité de peuplement équivalente) supérieur à 10% et une superficie supérieure à 0,5 hectare et dont les arbres doivent avoir une hauteur minimale de cinq mètres à maturité [5].

(5). http://www.fao.org/3/I9535FR/i9535fr.pdf

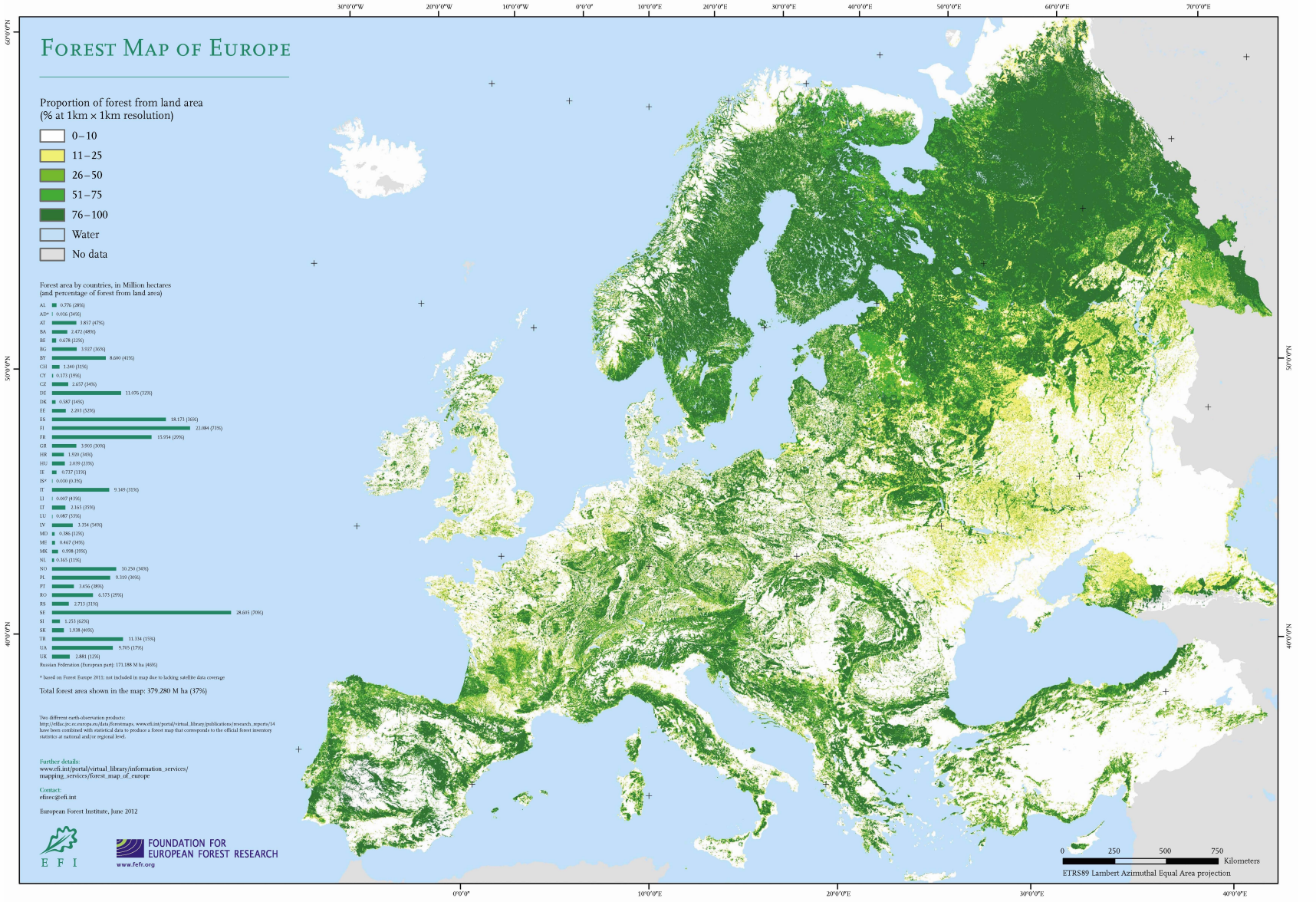

Figure I.1: Distribution des forêts en Europe

1.1 La forêt européenne en quelques chiffres

En Europe, la forêt s'étend sur 366 millions d'hectares d'espace non continu et représente 10% des surfaces forestières mondiales (Union Européenne et Fédération de la Russie en Europe) [6] (Figure I.1). La couverture forestière varie fortement entre les pays allant de plus de 60 % pour la Suède à moins de 10% pour les Pays-Bas. Contrairement à la tendance générale des surfaces forestières dans le monde, la surface des forêts européennes tend à augmenter suite à l'abandon progressif des terres agricoles (i.e. déprises agricoles). Entre 1990 et 2010, les surfaces de forêts ont ainsi augmenté de 11 millions d'hectares [7]. En 2015 en Europe, on compte 4% de forêts dites primaires (c'est-à-dire non modifiées par l'humain), 9% de plantations et 87% de forêts «semi-naturelles», c'est-à-dire façonnées par l'Humain. Les forêts européennes sont majoritairement détenues par des propriétaires privés (environ 51% des surfaces, contre 49% de forêts publiques) [8].

L'atlas européen des forêts distingue 14 grandes catégories de forêts : boréales (conifères); hémiboréales et némorales (conifères, conifères et feuillus mélangés); conifères alpin; chênaies , chênes et bouleaux acidophiles; mésophytes à feuilles caduques; hêtraies; hêtraie de montagne; feuillus thermophiles; feuillus à feuilles persistantes; conifères des régions méditerranéennes, anatoliennes et macaronésiennes; marécageuses; plaines inondables; non riveraine d'aulnes, de bouleaux ou de trembles; et d'espèces d'arbres introduites (voir table : "European Forest Types : tree species matrix" (Pividori et al., 2016). La distribution des espèces dans ces écosystèmes dépend principalement du climat, du sol, de l'altitude, de la topographie, de l'histoire des glaciations et des interactions biotiques.
Malgré l'augmentation de leurs surfaces, des menaces pèsent sur les forêts européennes. Environ 6% de ces forêts sont endommagées par des facteurs biotiques et abiotiques. La majorité de ces dégâts sont causés par des facteurs abiotiques, dont les sécheresses, les incendies (particulièrement dans la zone méditerranéenne), les inondations, les tempêtes (en moyenne, au cours des soixante dernières années, il y a deux tempêtes majeures par an) et la pollution atmosphérique (émissions provenant du trafic routier ou des installations industrielles). A cela, il faut ajouter la fragmentation des forêts découlant de la construction d'infrastructures de transport représentant un risque pour la biodiversité [9]. Les facteurs biotiques comme les insectes (notamment les scolytes), les cervidés et les maladies, représentent, pour le moment, une part infime des dégâts subis dans les forêts européennes. Le régime de ces différentes perturbations (intensité, fréquence) est et sera affecté par les changements climatiques et globaux en cours

(6). https://foresteurope.org/

(7). https://www.touteleurope.eu/actualite/forets-et-surfaces-boisees-en-europe.html

(8). https://foresteurope.org/wp-content/uploads/2016/08/summary-policy-makers.pdf

(9). http://www.europarl.europa.eu/factsheets/fr/sheet/105/l-union-europeenne-et-les-forets

et prévus.

1.2 Effets attendus des changements climatiques sur les forêts

L'augmentation du CO_2 est un des moteurs du **changement climatique** et l'un des éléments essentiels de la physiologie des plantes. Le changement climatique se traduit par un changement dans les régimes de précipitations, et une augmentation des températures moyennes (Figure I.2). En outre, on observe et on attend une augmentation en intensité et en fréquence des événements extrêmes (i.e. tempêtes, inondations, sécheresses, gelées tardives, feux). Ces changements peuvent avoir des impacts majeurs sur les forêts et leurs **services écosystémiques**, notamment parce qu'ils sont susceptibles d'entraîner un risque accru de mortalité des arbres (Hauck et al., 2015). Comme les arbres sont les espèces majeures de ces ecosystèmes forestiers, leurs mortalités massives auraient des conséquences importantes sur la diversité des espèces associées et la composition des communautés forestières. Il est aussi attendu une perte économique entre 21 et 50% de la valeur des forêts européennes d'ici 2071-2100 (Hanewinkel et al., 2012). Il est donc urgent de prévoir l'avenir des forêts européennes et d'évaluer la résilience de leurs services écosystémiques, afin de mettre en œuvre des politiques publiques d'atténuation des effets et d'adaptation au changement climatique.

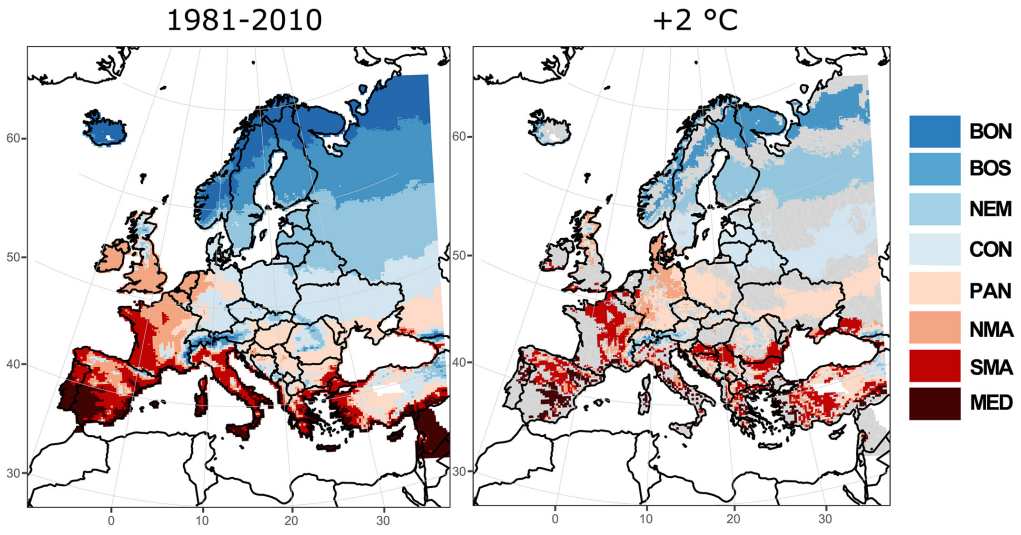

Figure I.2: Déplacement des zones agro-climatiques en Europe vers le nord en réponse au changement climatique. a) Zonage agroclimatique de l'Europe basé sur la longueur de la saison de croissance et la somme des températures actives médiane de cinq simulations différentes de modèles climatique CORDEX pendant la période de référence (1981-2010). (b) Médiane du déplacement des zones agroclimatiques sous un réchauffement global de surface de 2°C selon le scénario RCP8.5. Les zones grises représentent les régions où aucun changement par rapport à la période de référence n'est simulé. Les zones agroclimatiques identifiées sont nommées comme suit (en allant du nord au sud) : nord boréal (BON), sud boréal (BOS), némoral (NEM), continental (CON), pannonien (PAN), nord maritime (NMA), sud maritime (SMA) et Méditerranée (MED). (Figure adaptée à partir de Ceglar et al. 2019)

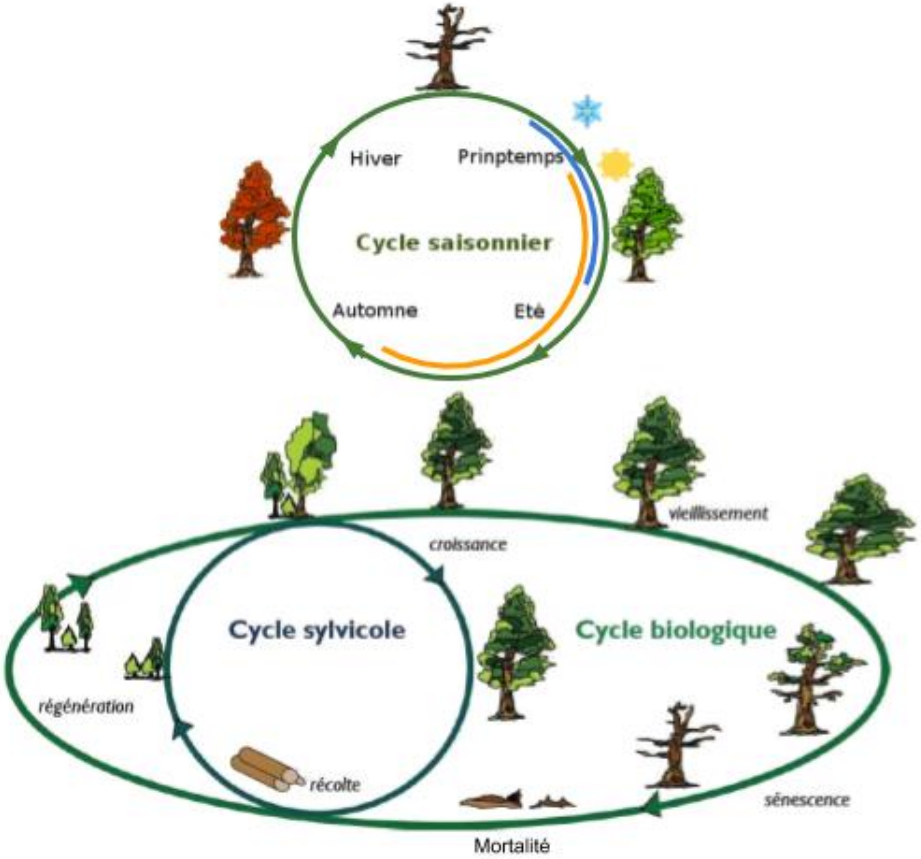

Figure I.3: Cycle de vie et cycle saisonnier d'un arbre. a) Cycle saisonnier : Les arbres développé différentes stratégies d'évitement des stress climatiques au fil des saisons, notamment les feuillus avec la perte des feuilles avec l'approche de l'hiver. Au printemps, avec l'augmentation des températures et de la longueur des jours, les bourgeons débourrent. Cependant, les jeunes feuilles sont sensibles aux gelées (phase bleue). De plus à partir de la production des feuilles, les arbres ont besoin de puiser de l'eau pour la photosynthèse. Durant toute la saison de végétation (du débourrement à la chute des feuilles), les arbres sont sensibles à la sécheresse (phase orange). b) Cycle de vie : Les arbres ont une durée de vie longue, ils peuvent suivre un cycle biologique sans sylviculture (grand cercle) ou avec sylviculture (petit cercle). La sylviculture raccourcit le temps entre deux générations. Adapté de ©ONF

Plusieurs études et rapports ont signalé une augmentation du dépérissement des forêts et de la mortalité des arbres, à la fois la mortalité dite de fond, non catastrophique (Van Mantgem et al., 2009; Lorenz & Becher, 2012) et la mortalité massive et catastrophique due à des événements extrêmes d'intensités et de fréquences variées (Mueller et al., 2005; Allen et al., 2010; Lorenz & Becher, 2012). Pour prédire comment ce nouveau régime de mortalité des arbres affecterait la structure et la composition des forêts (Anderegg et al., 2015; Choat et al., 2018), nous devons mieux comprendre les rôles respectifs des divers facteurs et mécanismes sous-jacents à la mortalité des arbres au cours de leur cycle de vie (Figure I.3). La plupart des déclins de populations d'arbres forestiers européens sont attendus aux marges sud (en Europe) de la distribution des espèces (**read-edge**). Ils devraient être principalement causés par de graves sécheresses, résultant de l'augmentation des températures moyennes et de la diminution des précipitations prévues par la plupart des modèles climatiques. Avec l'augmentation des températures moyennes, il est aussi attendu une augmentation du risque de mortalité des espèces sensibles à l'accumulation de températures lors du débourrement des bourgeons. En effet, deux réponses sont attendues, à commencer par un débourrement plus précoce dans l'année, augmentant les risques de dégâts foliaires importants liés aux gelées tardives (Augspurger 2009 – Figure I.4). Néanmoins, si les exigences de températures froides n'ont pas été respectées, dans certains cas le débourrement peut être retardé (Hänninen & Tanino, 2011), comme il a été observé au Tibet (Yu et al., 2010).

L'augmentation du CO_2 peut aussi avoir des effet bénéfique et permettre d'atténuer l'impact climatique sur les forêts. En effet, si dans le sud de l'Europe, il est attendu une diminution de la productivité des forêts, l'inverse est possible dans le nord (Härkönen et al., 2019). De plus, plusieurs études estiment que les limites nord de distribution des espèces sont principalement dues aux températures trop basses qui empêcheraient la reproduction des arbres (Morin et al., 2008). Ainsi, l'augmentation des températures permettrait aux marges nord de devenir des zones d'extensions des espèces (**leading-edge**).
Ces influences antagonistes, avec des effets négatifs et positifs attendus du changement climatique sur les processus écophysiologiques, induisent une forte incertitude quant à son impact sur le risque de mortalité des arbres.

1.3 Adaptation et adaptabilité des populations d'arbres face au changement climatique

La capacité des arbres forestiers à répondre aux changements climatiques en cours et prédit pourrait en outre jouer un rôle important. Les populations d'arbres forestiers peuvent en effet migrer pour suivre leur optimum bioclimatique, ou s'adapter sur place aux changements de leur environnement soit sur le court terme par la **plasticité phénotypique** (Encadré 1), soit au fil des générations par l'**adaptation géné-**

Figure I.4: (a) Observation de dégâts de gelées tardives sur le Hêtre au Ventoux juin 2019 ©Petit-Cailleux. (b) Dépérissement foliaire chez le Hêtre à la Massane ©ReserveLaMassane.

tique. L'importante diversité d'environnements à laquelle sont exposés les arbres forestiers est associée à la fois à une grande plasticité et au développement d'adaptations locales au sein des aires de distribution de chaque espèce (Alberto et al., 2013). Les tests de provenances forestiers sont un outil de choix pour quantifier ces phénomènes. Ils permettent de mettre en évidence les phénomènes d'adaptation locale et de plasticité des caractères phénotypiques. Dans l'exemple de *Pinus sylvestris* sur la Figure I.6, les tests de provenances montrent que la survie de chaque provenance diminue quand la distance de transfert augmente, illustrant la plasticité de la réponse. En outre, la population centrale paraît être localement adaptée, car elle montre la survie relative maximale en local; en revanche l'optimum de survie de la population nordique est légèrement décalé vers le Sud. Cette maladaptation des populations aux marges est probablement le fruit des flux de gènes asymétriques depuis le centre de l'aire. Ces tests de provenance ont aussi permis de quantifier la différenciation génétique entre provenances des caractères physiologiques impliqués dans la réponse au climat (chez le Hêtre : Hajek et al. 2016) ou encore des besoins en températures pour le débourrement (Kramer et al., 2017).

Ces patrons d'adaptation locale et de différenciation génétique des caractères suggèrent que les populations d'arbres forestiers se sont adaptées avec succès aux variations climatiques passées au cours de la recolonisation post-glaciaire. Par conséquent, étant donné leur grande taille, leurs niveaux élevés de diversité intra-population et leurs capacités de flux de gènes, les populations d'arbres sont également considérées comme ayant un potentiel d'adaptation (ou **adaptabilité**) élevé face au changement climatique (Savolainen et al., 2007; Alberto et al., 2013). Cependant, les capacités d'évolution génétique des populations d'arbres sur une courte période restent en grande

Encadré 1 : La plasticité phénotypique

La plasticité phénotypique est la courbe de réponse d'un caractère d'un génotype dans une gamme de possibles environnementaux. La plasticité peut être adaptative si la variation du caractère en question accroît la valeur sélective de l'individu (Nicotra et al., 2010), mal-adaptative si elle la diminue (Ghalambor et al., 2007) ou neutre si elle ne la modifie pas. Face aux enjeux de conservation de la biodiversité et aux enjeux des nouvelles politiques pour limiter l'impact humain sur la biodiversité, il est souhaité d'avoir déjà en place des populations avec des génotypes peu plastiques, car peu "sensibles" au changement environnemental (dans la gamme environnementale 1, par contre, plastique dans la gamme environmental 2 (voir figure ci-dessous)). Si on prend en exemple un trait hypothétique, qui varie d'une réponse faible à forte, selon un gradient de l'environnement, d'un environnement défavorable à favorable, avec deux génotypes A et B. Si l'environnement évolue vers un changement favorable, des individus plastiques (génotype A) tireront des avantages plus rapide et auront une réponse forte du caractère dans un environnement favorable contrairement à des individus peu plastiques (génotype B). Cependant, la plasticité adaptative peut également aider au processus d'adaptation en produisant une réponse première rapide aux changements environnementaux et empêchant une extinction trop rapide suite à un changement d'environnement (Chevin et al., 2010).

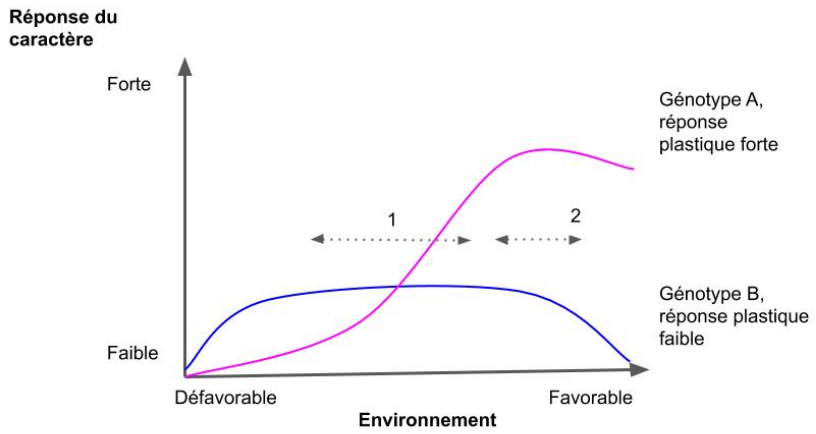

Figure I.5: Schéma représentant la gamme de réponse plastique d'un caractère dans une gamme environnemental allant de défavorable à favorable. En rose, le génotype A fortement plastique. En bleu, le génotype B peu plastique. En ligne pointillée deux gammes environnementales.

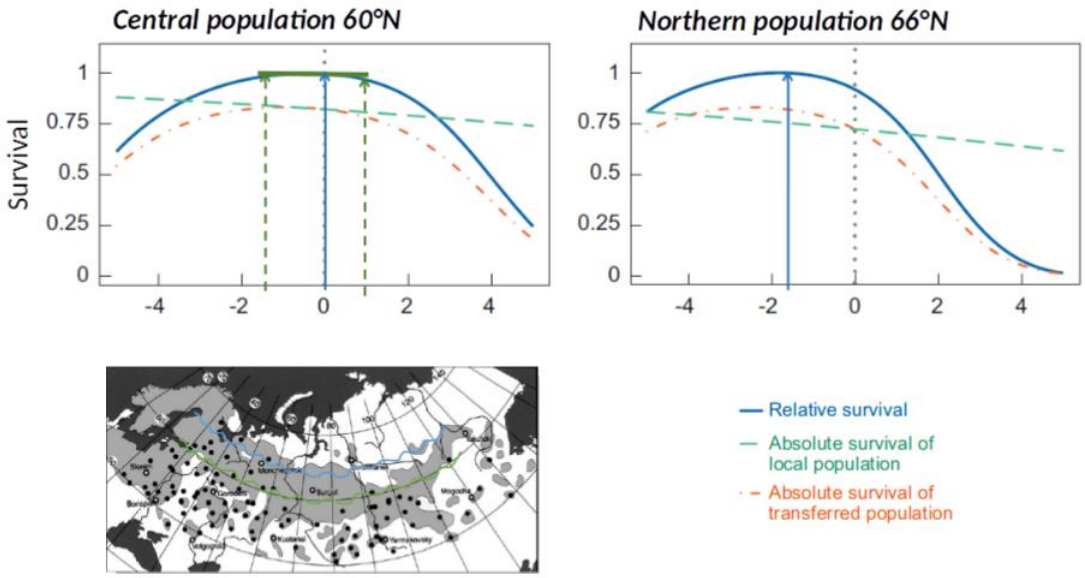

Figure I.6: Fonctions de réponse de la survie de Pinus sylvestris au transfert latitudinal, basée sur les tests de provenances. Ces graphiques considèrent une population centrale de latitude 60°N (en vert sur la carte de distribution) et une population nordique de latitude 66°N (en bleue sur la carte de distribution). L'axe des abscisses montrent les différences de latitudes entre les populations du centre et du nord et leur site de transfert, les chiffres positifs indiquant un transfert latitudinal vers le nord. Les lignes bleus en gras montrent la survie relative de chaque population (centrale à gauche ou nordique à droite), par comparaison à celle des autres populations sur chaque site de transfert. Les lignes tiret-point montrent la survie absolue des populations transférées (orange) ou locales (vert). Les flèches verticales bleues pointent l'optimum latitudinal maximisant la survie relative. Figure adaptée de (Savolainen et al., 2007), d'après (Rehfeldt et al., 2002).

partie méconnues, d'autant plus que la vitesse du changement climatique en cours est susceptible de dépasser le potentiel de réponse adaptative naturelle des populations locales pour de nombreuses espèces d'arbres (Kuparinen et al., 2010).

1.4 La sylviculture comme outil pour favoriser l'adaptation des essences forestières ?

C'est dans ce contexte que les pratiques sylvicoles entrent en jeu comme outils permettant potentiellement de réduire l'impact du changement climatique sur les espèces forestières (Encadré 2 pour un exemple des pratiques sylvicoles sur le Hêtre). La plus grande partie des forêts européennes sont déjà sous contrôle humain par le biais de la sylviculture et ces pratiques d'aménagement et de gestion forestière peuvent aussi contribuer à adapter les forêts au changement climatique (gestion pour l'adaptation). Futuyma 2010 a identifié quatre facteurs limitants de l'adaptation génétique sur lesquels la pratique forestière peut avoir un impact direct ou indirect : le manque de diversité génétique, la stochasticité démographique (sélection à contre-courant), la **dérive génétique** et le flux génétique asymétrique (par exemple aux limites des aires de distribution). De plus, Kuparinen et al. 2010 ont identifié un autre facteur limitant potentiellement affecté par la pratique forestière : la faible mortalité.

Les pratiques de gestion peuvent être classées en fonction de leur impact sur les peuplements forestiers, depuis des pratiques à fort impact comme par exemple, le remplacement des espèces existantes par de nouvelles espèces plus adaptées, jusqu'à des pratiques à faible impact (Lefèvre et al., 2014). Ces dernières consistent typiquement à accélérer le rythme naturel de l'adaptation via la plasticité ou la réponse à la sélection naturelle, en jouant sur les paramètres de ces processus (ex. augmenter les flux de gènes, raccourcir la durée de vie des peuplements etc.). Ces stratégies utilisent la ressource génétique locale, intégrée écologiquement dans son environnement actuel pour accélérer les processus évolutifs naturels et s'appuient sur la régénération naturelle. Elle ne se produisent que des changements progressifs, limités par le potentiel adaptatif de la ressource locale, mais elle est souple et permet de lever l'incertitude écologique liée à l'introduction de matériel génétique.

Une stratégie intermédiaire consiste à transférer par plantation du matériel génétique pré-adapté, pour injecter ces adaptations dans d'autres populations de la même espèce. L'enrichissement de la ressource locale avec une certaine quantité de matériel étranger peut augmenter le potentiel d'adaptation et d'accélérer l'évolution tout en limitant l'incertitude écologique due à l'introduction. Par exemple, en France, l'Office National des Forêts (ONF), porte un programme pilote (projet Giono - ONF) consistant à sélectionner des graines issues de populations de Hêtre et de Chêne du Sud de la France, déjà soumises aux effets du changement climatique et adaptées à des conditions de sécheresse, pour enrichir les peuplements des régions plus au nord de la France (Verdun). Ce programme participe aussi à la conservation des populations

Encadré 2 : Principaux types de sylviculture en Europe

Une sylviculture est définie d'abord par son régime, c'est-à-dire l'origine des arbres (graines versus rejet, régénération naturelle versus artificielle). On distingue traditionnellement la **futaie**, dont les arbres, nés d'une graine, développent généralement un tronc unique ou fût, du **taillis**, où plusieurs tiges, issues de bourgeons réactivés par une coupe, partent d'une même base et forment une cépée. Le deuxième élément définissant une sylviculture est le mode de traitement des peuplements, qui détermine la répartition des classes d'âge. Si les arbres sont tous sensiblement du même âge, le traitement est dit « régulier ». Si au contraire, tous les âges sont représentés dans une certaine proximité, le traitement est dit « irrégulier ». Dans ces travaux, nous avons distingué 3 grands systèmes sylvicoles, relevant tous de la sylviculture régulière (even-aged forestry) :

— **La futaie régulière avec coupe de régénération à blanc** (Even-aged forest management with clear-cut) : lorsque le peuplement est arrivé à maturité, il est récolté en bloc et la nouvelle génération est installée en une fois, par graines.

— **La futaie régulière avec coupes de régénérations progressives** (Even-aged forest management with shelter-wood) : le passage d'une génération à la suivante se fait par régénération naturelle, et s'étale sur plusieurs années, voire plusieurs décennies.

— **Les systèmes à courtes rotation** (short rotation), principalement les taillis à courte rotation, dans lesquels tous les arbres sont coupés puis repoussent en même temps.

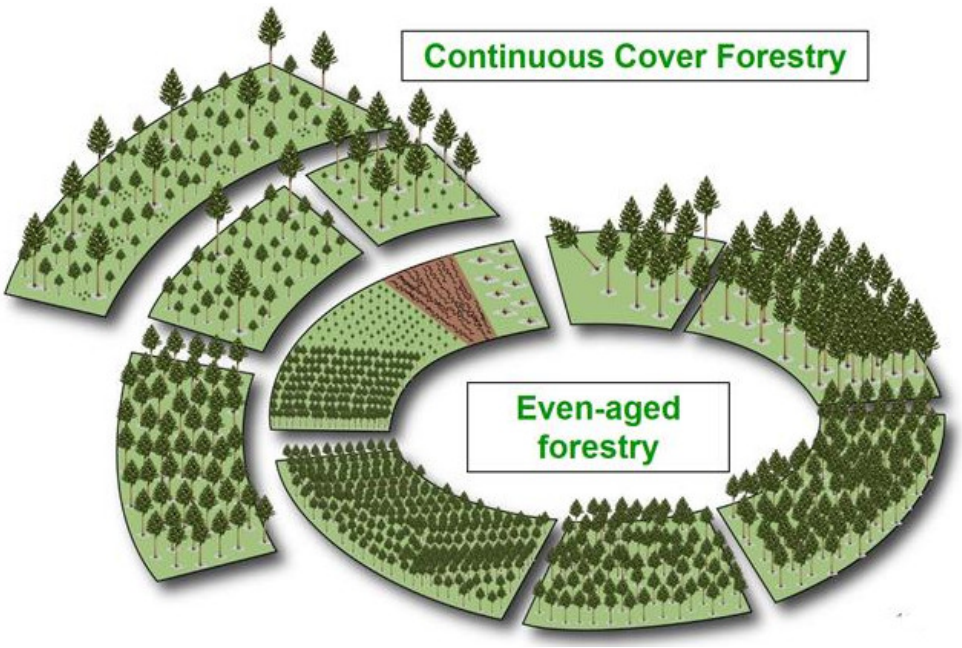

Figure I.7: comparaison de traitement régulier (even-aged forestry) et irrégulier

(continuous cover forestry)

transférées. Le transfert de matériel génétique permet potentiellement des évolutions drastiques des populations locales et le sauvetage génétique des populations transférés, mais elle induit un risque à court terme de mauvaise adaptation (maladaptation) aux conditions locales actuelles. Pour atténuer les risques de perte de biodiversité et de maladaptation, il faut réduire au minimum les incertitudes quant à l'intégration écologique des ressources génétiques des populations transférées dans le nouveau site sous les climats futurs. Une troisième stratégie intermédiaire, serait de combiner les deux précédentes.

En raison de l'importance et de la diversité du patrimoine génétique des populations naturelles d'arbres forestiers, leurs **ressources génétiques** représentent donc un élément central dans le potentiel d'adaptation des forêts dans le cadre du **changement climatique**. Il est urgent d'évaluer dans quelle mesure la **plasticité phénotypique**, l'adaptabilité et/ou les pratiques de gestion peuvent affecter le risque de mortalité des arbres sous changement climatique.

2 Processus écophysiologiques impliqués dans la mortalité des arbres en réponse aux événements climatiques

2.1 Impact de la sécheresse sur la physiologie d'un arbre

Dans le cadre conceptuel général de la notion de risque (Encadré 3), le risque de mortalité résulte de la combinaison de l'aléa, de la vulnérabilité et de l'exposition des individus et des populations aux stress climatiques. L'écophysiologie s'intéresse en particulier aux rôles conjoints de l'aléa et de la vulnérabilité. La mortalité est déclenchée par plusieurs facteurs (aléa) et implique de nombreux processus physiologiques sous-jacents, souvent en interaction entre eux, qui jouent sur la vulnérabilité des arbres. Les facteurs déclenchant la mortalité comprennent les événements climatiques extrêmes avec l'augmentation de leurs fréquences et intensités (i.e., sécheresse, tempête, inondation, neige abondante, gel tardif, feu de forêt), les changements soudains dans les interactions biotiques (i.e. nouveaux ravageurs, espèces envahissantes), mais aussi les perturbations climatiques ou biotiques à long terme (i.e., les déficits récurrents en eau, changements dans la compétition au niveau communautaire) (Maraun et al., 2003; McDowell et al., 2011). Ces facteurs peuvent agir en interaction : par exemple, la sécheresse peut accroître la sensibilité des arbres aux ravageurs (Durand-Gillmann et al., 2014; Anderegg et al., 2015) ou la sensibilité des peuplements au feu

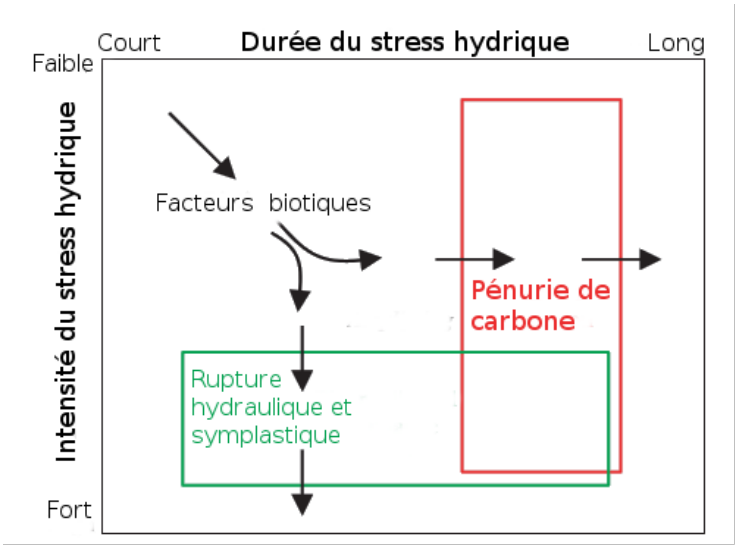

Figure I.8: Relation théorique entre la durée de la sécheresse, la diminution relative de la disponibilité en eau (intensité) et les mécanismes à l'origine de la mortalité. La défaillance du système hydraulique se produit si l'intensité de la sécheresse est suffisamment forte pour pousser une plante au-delà de son seuil de dessiccation irréversible; ce phénomène de cavitation a généralement lieu avant que les réserves de carbones ne soient épuisées, mais ne conduit pas nécessairement seul à la mortalité. On suppose que les réserves de carbone parviennent à épuisement lorsque la durée de la sécheresse est suffisamment longue pour réduire la photosynthèse en deçà du stock de carbone nécessaire pour le maintien du métabolisme. L'action des agents biotiques, tels que les insectes et les pathogènes, peut amplifier ou être amplifiée à la fois par l'épuisement des réserves de carbone et la défaillance hydraulique. (Adapté de McDowell et al. (2011)).

(Brando et al., 2014). Enfin, un seul facteur climatique peut jouer sur plusieurs processus physiologiques sous-jacents, avec potentiellement des rétroactions entre ces processus, comme dans le cas de la sécheresse (McDowell et al. 2011, Figure I.8). Dans cette thèse, deux facteurs relevant des événements extrêmes ont été étudié, dont l'impact est déjà observé et dont l'amplification est attendue : la sécheresse et les gelées tardives.

La mortalité en réponse à la sécheresse est généralement considérée comme étant due à la défaillance hydraulique, à l'épuisement des réserves carbonées ou à la combinaison de ces deux processus (McDowell & Sevanto, 2010; Anderegg et al., 2012; Adams et al., 2017) (Figure I.8). La défaillance hydraulique est la perte de conductance résultant d'une embolie importante du xylème, c'est-à-dire la formation de vapeur d'eau ou de bulles d'air dans le xylème en raison de la forte tension dans la colonne d'eau allant du sol à la canopée (Tyree & Sperry, 1989). Pour éviter une défaillance hydraulique, les arbres peuvent fermer leurs stomates avant d'atteindre le point d'embolie du xylème (propre à l'espèce) (Cowan & Farquhar, 1977). Cependant, la fermeture des stomates réduit mécaniquement l'activité photosynthétique, forçant l'arbre à assurer son métabolisme de base en utilisant ses réserves de carbone, qui peuvent éventuellement s'épuiser, en particulier pendant une longue sécheresse. L'épuisement des réserves de carbone entraîne à terme la mort de l'arbre. De nombreuses études expérimentales sur les conséquences de la sécheresse suggèrent que la défaillance hydraulique est la cause la plus fréquente de mortalité des arbres, ou du moins, la première étape vers des processus en cascade menant à la mortalité (Choat et al., 2018; McDowell et al., 2011). Néanmoins, il est difficile de mesurer le stock de carbone de l'arbre et de reproduire des conditions naturelles en expérimentation. Un phénomène largement observé suite à des événement de sécheresses est la défoliation (i.e. dessiccation de branche de la canopé) (Figure I.4 b). Ce phénomène peut aussi être une stratégie de résistance/d'évitement à l'embolie (Bréda et al., 2006). En effet, en réduisant leur canopée les arbres transpirent moins et donc utilisent moins d'eau. Cependant, quand ce phénomène est récurrent, il devient un indicateur de mauvaise santé de l'arbre et précède la mortalité (Penuelas & Boada, 2003; Bréda et al., 2006; Carnicer et al., 2011).

Mais les relations entre les flux de carbone et d'eau, les moyens de compensation et le rôle des facteurs biotiques pendant et après la sécheresse sont encore loin d'être compris dans leur globalité (McDowell et al., 2011; O'Brien et al., 2014; Meir et al., 2015; Adams et al., 2017; Feng et al., 2018).

2.2 Impact des gelées tardives sur la physiologie d'un arbre

Les dommages dus au gel ont lieu lorsque l'exposition aux températures froides dépasse le seuil de sensibilité de la plante (Williams et al., 2008; Charrier et al., 2015) (Figure I.4). Le risque de dommages dus aux gelées printanières dépend étroitement de la coïncidence entre la phénologie du débourrement et la séquence climatique des

Encadré 3 : Définition du risque de mortalité et des concepts associés

Selon les domaines de recherche ou pour les gestionnaires, les concepts de vulnérabilité, de risque et d'adaptation peuvent être définis et interprétés de manière différentes. Dans cette thèse nous nous sommes basés sur le rapport IPCC 2014 pour définir la notion de risque mortalité lié aux événements extrêmes de sécheresses et gelées tardives, et les concepts associés de sensibilité, adaptabilité, vulnérabilité, aléa et exposition (Figure I.9).

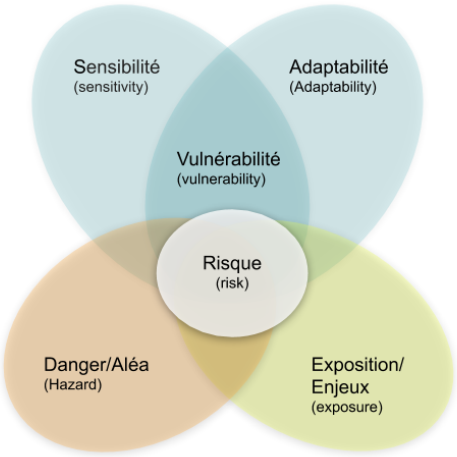

Figure I.9: Concepts clés de la thèse sur les risques, l'adaptation et la vulnérabilité liés aux changements climatiques.

Le Risque (Risk) est défini par l'IPCC comme la « probabilité d'occurrence de tendances ou d'événements dangereux que viennent amplifier les conséquences de tels phénomènes lorsqu'ils se produisent. » Dans cette thèse, je considère le risque de mortalité lié aux changements climatiques (i.e. sécheresses et gelées tardives), et ce risque est évalué par la combinaison de trois indices : le pourcentage de perte de conductance (PLC) comme indice du risque de mortalité par défaillance hydraulique; le niveau de réserve carbonées, comme indice du risque de mortalité par épuisement des réserve carbonées; et le nombre de jours de gelées tardives, comme indice du risque de mortalité dues aux gelées tardives.

La Sensibilité (Sensitivity) est définie par l'IPCC comme le "Degré selon lequel un écosystème ou une espèce est influencé, positivement ou négativement, par la variabilité du climat ou les changements climatiques". Dans cette thèse, je considère en particulier les variations de sensibilité aux sécheresses et gelées tardives entre individus, qui peuvent être dues à des différences d'environnement (compétition, variation microlocales) et/ou à des différences de la réponse physiologique aux stress, qui dépend des effets ontogéniques, plastiques et génétiques

contrôlant l'expression des caractères.

L'adaptabilité ou capacité d'adaptation (Adaptability or Adaptive capacity) est définie par l'IPCC comme « la faculté d'ajustement des écosystèmes, leur permettant de limiter d'éventuels dommages, ou de profiter des changements ». Dans le cadre de cette thèse, les capacités d'adaptation des arbres sont la plasticité phénotypique, qui est modélisée dans CASTANEA, et la capacité de réponse à la sélection des populations, qui est considérée partiellement. CASTANEA simule la capacité plastique des arbres à éviter le stress hydrique en fermant leurs stomates : cette réponse plastique réduit le risque de cavitation, mais augmente le risque d'épuisement des réserves carbonées. La notion de capacité de réponse à la sélection est abordée dans le chapitre 3, où la variabilité génétique disponible dans une « population » détermine son risque de mortalité.

La vulnérabilité (Vulnerability) est définie par l'IPCC comme la « propension ou prédisposition à subir des dommages. La vulnérabilité englobe divers concepts ou éléments, notamment les notions de sensibilité ou de fragilité et l'incapacité de faire face et de s'adapter.» Dans cette thèse, la vulnérabilité aux sécheresses et gelées tardives résulte de l'intégration d'une part de la sensibilité à ces événements climatiques, et d'autre part de la capacité d'adaptation liée à la plasticité des individus et à la variabilité génétique présente dans la population.

Le danger ou Aléa (Hazard) est défini par l'IPCC comme «l'éventualité d'un phénomène ou d'une tendance physique, naturel susceptible d'entraîner des pertes concernant la fourniture de services rendus par les écosystèmes. Ce terme se rapporte en général aux phénomènes dangereux associés au climat ou à leurs impacts physiques ». Dans cette thèse, l'aléa est défini par le climat, et en particulier par les phénomènes de sécheresses et de gelées tardives.

L'exposition (Exposure) est définie par l'IPCC comme la « Présence d'espèces ou d'écosystèmes, de ressources ou de services environnementaux dans un lieu ou dans un contexte susceptibles de subir des dommages ». Dans cette thèse, cette notion d'exposition n'a pas été explicitement prise en compte. Elle pourrait résulter des enjeux spécifiques liés à la présence de l'espèce en un lieu donné.

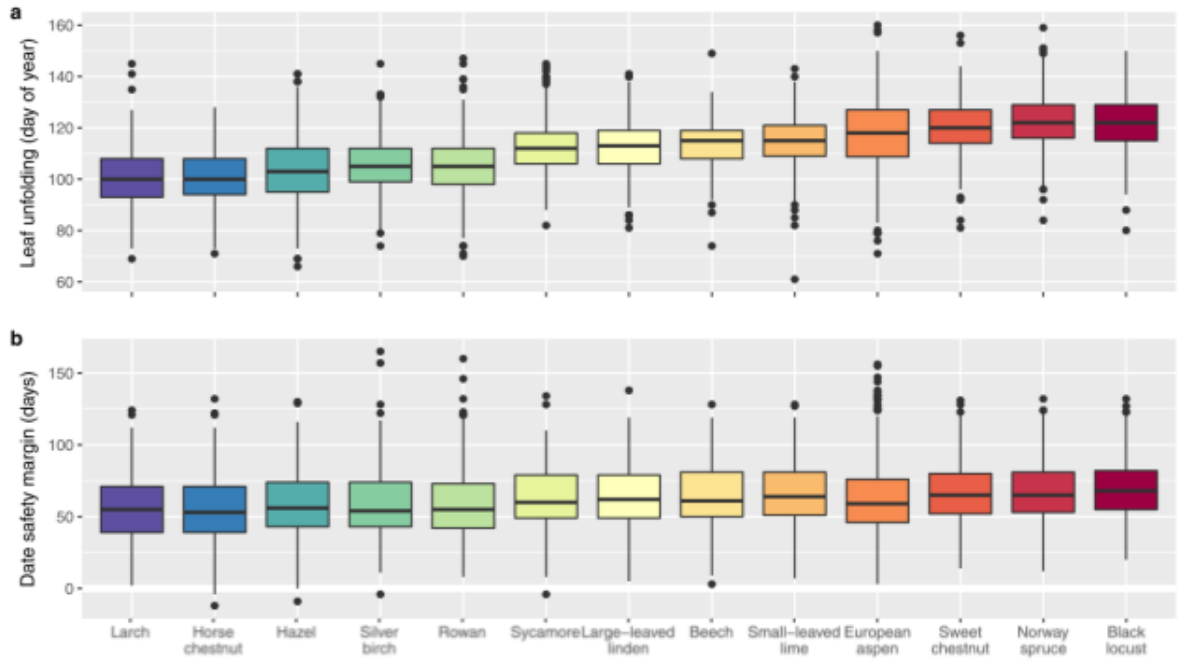

Figure I.10: Répartition des dates de débourrement et risque de gel (marge de sécurité en nombre de jour). Boîtes à moustache représentant : (a) les dates de débourrement, (b) les marges de sécurité en nombre de jour entre la date de débourrement et le dernier gel observé. Les boîtes comprennent les 25e, 50e et 75e percentiles. Les espèces sont classées des espèces à feuilles au débourrement précoces (bleu) aux espèces à feuilles au débourrement tardives (rouge) selon les dates médianes de déploiement des feuilles. Adapté de Bigler & Bugmann 2018.

basses températures (Figure I.10). Bien que des marges de sécurité (i.e. nombre de jours entre la dernière gelée observée et le début du débourrement) relativement importantes soient actuellement observées chez de nombreuses espèces d'arbres et d'arbustes tempérés (Dantec et al., 2015; Bigler & Bugmann, 2018), ces marges de sécurité peuvent diminuer avec le changement climatique, en raison de l'avancée des dates de débourrement des arbres (Augspurger, 2009).

Il existe plusieurs stratégies de réponse face au dégâts subis après une gelée, qui dépendent des espèces d'arbres et du degré de dommages : (1) Si les dégâts ne sont pas trop importants, l'arbre peut garder des feuilles partiellement endommagées durant toute la saison de végétation ; (2) Si les dégâts sont trop importants, certaines espèces produisent une nouvelle cohorte de feuilles (nouveau débourrement foliaire) (Augspurger, 2009; Menzel et al., 2015), cependant le temps nécessaire pour produire ces nouvelles feuilles entraîne une saison de croissance plus courte (Lenz et al., 2013) et

implique une baisse d'accumulation de réserves carbonées, (3) La dernière possibilité est la mort de l'arbre, si ce dernier n'a pas assez de réserves pour produire de nouvelles feuilles.

2.3 La variabilité des réponses aux stress explique la difficulté de comprendre et d'anticiper la mortalité des arbres

Un des défis dans l'étude de la mortalité est de prendre en compte la variabilité spatio-temporelle de la vulnérabilité des arbres. Par exemple, la sensibilité aux stress climatiques peut varier d'un arbre à l'autre au sein d'une population en fonction (i) de l'hétérogénéité spatiale locale des ressources disponibles, en particulier l'eau du sol (Nourtier et al., 2014); (ii) de l'hétérogénéité des cycles de développement individuel, et des contraintes héritées qui jouent sur la morphologie et l'anatomie des arbres (Vanoni et al., 2016); (iii) de la variation interindividuelle de la réponse physiologique aux stress, qui dépend des effets ontogéniques, plastiques et génétiques contrôlant l'expression des caractères (Vitasse et al., 2009; Anderegg et al., 2015). La sensibilité peut également varier dans le temps au cours de l'année pour un individu ou une population donnée, notamment à travers les processus phénologiques sensibles aux variations climatiques, comme le débourrement.

Prendre en compte simultanément le rôle de l'aléa, des processus physiologiques et de leurs variations entres individus ou populations nécessite des approches expérimentales ou de modélisation appropriées.

3 Modélisation de la mortalité des arbres

Le long cycle de vie et les caractéristiques écologique et biologique des arbres (i.e. taille, accessibilité des organes, etc..), font qu'il est difficile d'utiliser des approches purement expérimentales pour comprendre l'impact du changement climatique sur le risque de mortalité. Le recours à la modélisation permet d'intégrer les différents mécanismes liés à la mortalité des arbres, et d'étudier leurs effets combinés sur tout le cycle de vie de l'arbre. Plus généralement, en science, un modèle est une «représentation graphique, mathématique, symbolique, physique ou verbale ou une version simplifiée d'un concept, phénomène, relation, structure, système ou un aspect du monde réel». Les objectifs généraux des modèles sont (1) de faciliter la compréhension de systèmes complexes (2) d'aider à la prise de décision en simulant des scénarios hypothétiques, (3) d'expliquer, de contrôler et de prédire les événements sur la base des observations passées. En intégrant différents processus d'écologie et d'évolution (interactions biotique et abiotique, adaptation génétique, plasticité, flux/migration des gènes) à différentes échelles dans un cadre de modélisation, l'écologie prédictive peut améliorer notre compréhension de la façon dont ces processus peuvent contribuer à

la réponse adaptative des populations aux changements climatiques (Dawson et al., 2011). L'appréhension des effets du changement climatique à large échelle par l'écologie prédictive est une discipline qui se développe de plus en plus et qui combine la modélisation et les connaissances différentes disciplines (écologie fonctionnelle et évolutive, génomique, climatologie, Mouquet et al. 2015). Par le développement de modèles prédictifs quantitatifs appropriés, l'écologie prédictive vise à déduire, à partir des modèles, les états futurs de la réalité (prévisions), à extrapoler ces modèles à des domaines où il existe une certaine incertitude sur les valeurs des principaux paramètres (projections) et à décrire les trajectoires ou comportements possibles du système réel, selon le choix des valeurs des paramètres susceptibles de subir l'effet des actions humaines (scénarios) (Harfoot et al., 2014). Les modèles en écologie sont notamment utilisés pour deux types de prédictions : la prédiction corroborative est liée à la validation des théories, et la prédiction anticipative est liée à la description des futurs possibles (Marris 2018). L'un des principaux défis de l'écologie prédictive est d'aborder la complexité des systèmes écologiques, en simplifiant notre compréhension de ces systèmes.

La modélisation est un outil de choix pour comprendre et prédire le risque de mortalité des arbres forestiers en réponse aux sècheresse et gelées tardives. Il est détaillé en particulier ci-dessous les approches de modélisation tenant compte explicitement de la variation de l'aléa climatique (par exemple, entre scénarios climatiques), des variations de sensibilité aux sècheresse et gelées tardives entre individus, et des capacités d'adaptation des individus et des populations face à ces stress climatiques.

3.1 Les modèles statistiques de mortalité : points forts et limites

Les approches statistiques utilisent des données de suivis forestiers ou d'inventaires forestiers pour tester comment les facteurs endogènes (par exemple liés à la taille et au taux de croissance des arbres et des peuplements) et les facteurs exogènes (l'environnement biotique et abiotique, ainsi que la gestion sylvicole) affectent la probabilité individuelle de mortalité ou le taux de mortalité à l'échelle du peuplement. Au cours des dernières décennies, de nombreuses études statistiques ont comparé les mortalités observées entre espèces ou populations sur de grands gradients climatiques et ont démontré l'effet globalement positif de l'intensité de la sécheresse sur la mortalité. Les approches statistiques de ce type n'expliquent généralement qu'une proportion limitée de la variance des taux de mortalité (Allen et al., 2010; Greenwood et al., 2017; Taccoen et al., 2019), mais, la précision des prédictions augmente généralement quand le modèle inclut des covariables individuelles comme la croissance, la taille et/ou la compétition des arbres. Ces différents résultats démontre la capacité des modèles statistiques à tenir compte de la variabilité entre individus de la sensibilité aux facteurs associés à la mortalité, et aussi l'importance écologique de cette variabi-

lité interindividuelle de la sensibilité (Monserud, 1976; Hülsmann et al., 2017).

Une limite majeure de ces approches statistiques est la difficulté d'interpréter leur résultats pour comprendre les mécanismes causaux de la mortalité. Des études statistiques récentes ont tenté d'inclure les caractères fonctionnels impliqués dans la réponse au stress en tant que covariables supplémentaires pour améliorer la précision de la prédiction de la mortalité. Par exemple, Carnicer et al. 2011 ont montré que les tendances de la défoliation correspondent aux tendances de la mortalité dans les forêts d'Europe du Sud. Benito Garzón et al. 2018 ont constaté que la mortalité augmentait dans les populations dont les marges de sécurité hydraulique étaient négatives pour 15 espèces sur les 25 étudiées. Taccoen et al. 2019, ont montré que la mortalité de 19 espèces sur 43 était sensible au signal de changement climatique et ce signal expliquait en moyenne 6% de la mortalité observée. Mais la difficulté à mesurer sur un grand nombre d'individus de populations les caractères fonctionnels impliqués dans la réponse au stress limites le développement de modèles d'inférence statistique à base écophysiologique.

Les principaux avantages des approches statistiques sont donc : (1) leur capacité à tenir compte d'un nombre potentiellement élevé de facteurs et de processus déclenchant la mortalité, (2) leur capacité à tenir compte de la variabilité entre individus de sensibilité aux facteurs associés à la mortalité. Cependant, il faut garder à l'esprit que les modèles statistiques tiennent peu compte de la colinéarité entre les facteurs, de la non-linéarité des effets et du caractère non-aléatoire inhérents aux populations naturelles (i.e. le fait que chaque génotype n'ait pas été placé aléatoirement dans l'espace). De plus, la précision des prévisions statistiques diminue considérablement en dehors de la zone étudiée (Hülsmann et al., 2017).

3.2 Modèles de simulation basés sur les processus : points forts et limites

En foresterie, les modèles basées sur les processus (PBM, pour process-based models, comprennent : 1) des modèles biophysiques et écophysiologiques, initialement développés pour simuler les flux de carbone et d'eau dans les écosystèmes forestiers , 2) des modèles de dynamique forestière, qui intègrent les principaux processus de la dynamique forestière (i.e. régénération, croissance, mortalité) et 3) des modèles de dynamique évolutive, qui simulent l'évolution des traits adaptatifs dans les population sous l'effet des forces évolutives (i.e. sélection, flux de gènes, dérive, mutation). Parmi ces trois grandes catégories, seuls les modèles biophysiques et écophysiologiques permettent de tenir compte explicitement de l'effet des aléas climatiques sur la mortalité dans un contexte de changement climatique. En effet, les modèles de dynamique forestière ont été initialement développés pour simuler la dynamique des peuplements en environnement constant, même s'ils tendent à incorporer de plus en plus de mé-

canismes écophysiologiques.

Les modèles biophysiques et écophysiologiques commencent largement à être utilisés pour étudier les facteurs environnementaux et les processus physiologiques qui provoquent la mortalité des arbres. Par exemple, en utilisant le modèle CASTANEA, Davi & Cailleret 2017 (CASTANEA [10] - Annexe 1) ont montré que la mortalité d'*Abies alba* dans le sud de la France résultait de la combinaison de l'épuisement des réserves carbonées lié à la sécheresse et des attaques de parasites. Dans une autre étude, Mcdowell et al. 2013 ont constaté à l'aide de six modèles différents, que la mortalité dépendait davantage de la durée du stress hydrique que d'un seuil physiologique précis. L'un des principaux avantages des modèles basés sur les processus est leur capacité à prédire la mortalité sous de nouvelles combinaisons de variables dans un environnement en évolution (notamment, sous climat futur avec des concentration de CO_2 encore jamais observées). Les simulations faites avec ces modèles permettent d'avoir des projections spatiales des zones à fort risque de mortalité. Les PBM trouvent en général une augmentation des risques de stress hydrique dans les zones xériques de la distribution des espèces, et une augmentation de la croissance dans les zones froides due à l'augmentation de la saison de végétation (Sánchez-Salguero et al., 2017; Morin et al., 2008). Cependant il n'y a pas de consensus sur les risques de mortalité future, ni sur la localisation précise de ces risques (Cheaib et al., 2012). Par exemple, pour Sperry et al. 2019, le risque de mortalité dépend fortement du ratio entre augmentation de température et concentration de CO_2 dans l'atmosphère.

Un inconvénient majeur des PBM est qu'il est nécessaire de calibrer localement un nombre important de paramètres avant de les utiliser (plus de 120 dans le modèle CASTANEA). Généralement, certains paramètres sont supposés constant au sein d'une espèce donnée, mais cette approximation peut réduire la précision de la prédiction dans des peuplements pour lesquels le modèle n'a pas été calibré. De plus, les modèles basés sur les processus biophysiques et écophysiologiques négligent généralement la variabilité des paramètres entre individus au sein des populations, sauf quelques exceptions (Berzaghi et al., 2019). Prendre en compte la variabilité génétique intra- et inter-population des paramètres permettrait de mieux prédire la gamme possible de réponse des espèces face aux changements climatiques.

En conclusion, les approches de modélisation statistiques et celles fondées sur les processus semblent complémentaires, et de nombreux auteurs suggèrent de les comparer, ou même de les combiner (Hawkes, 2000; O'Brien et al., 2017; Seidl et al., 2011).La comparaison de ces approches se fait déjà pour la prédictions de l'impact du changement climatique sur l'aire de distribution des espèces et permettent de définir des zones d'extensions et d'extinctions (Cheaib et al., 2012). Les modèles corrélatifs de distributions d'espèces (cSDM) sont des outils majoritairement utilisés, bien que

(10). `https://www.overleaf.com/read/nmyvszjkfxxh`

remis en question pour étudier ces effets (Journé et al., 2019), contrairement aux modèles PBM, qui sont-eux plus complexes et nécessitant plus de données.

4 Objectifs et structure de la thèse

Le changement climatique en particulier les événements climatiques extrêmes comme les sécheresses et gelées tardives menacent les forêts et les services écosystémiques qu'elles rendent. Malgré leur grande capacité plastique et leur diversité génétique, les forêts ne pourraient pas être en mesure de répondre à la vitesse du changement climatique. La longue longévité des arbres rend difficile la mise en place d'expérimentation pour comprendre les impacts du changement climatique sur l'ensemble du cycle de vie des arbres et le rôle de la sylviculture dans cette dynamique. C'est pourquoi la modélisation des processus écophysiologiques intégrant la diversité génétique est un outil indispensable pour prendre en compte l'impact du changement climatique sur les risques de mortalité des arbres. Dans ce contexte, les principaux objectifs de cette thèse sont :

1. de comprendre les processus écophysiologiques à l'origine de la mortalité chez les arbres soumis au changement climatique,
2. de prédire les risques de mortalité des principales espèces d'arbres européens dans le futur,
3. d'évaluer comment la diversité génétique et la sylviculture peuvent les atténuer.

Ce projet s'appuie sur des approches de modélisation croisée pour évaluer des stratégies de gestion innovantes pour la conservation de la diversité des populations sous changement climatique.

Pour cela, les questions suivantes ont été abordés (déclinées dans les différents chapitres de la thèse par article, dont un soumis et les deux autres en préparations) :

— Quels sont les mécanismes entraînant la mortalité d'un feuillu (*Fagus sylvatica*), dans la marge xérique de sa distribution ? Pour répondre à cette question, j'ai utilisé des modèles statistiques et un modèle basé sur les processus (CASTANEA) dans une population des Pyrénées orientales, La Massane, dans laquelle un suivi longitudinal de la mortalité, de la croissance et du dépérissement était disponible (Chapitre I).

— Quels sont les risques de mortalité à l'échelle de la distribution Européenne de 5 essences majeures européenne, et quel est l'impact de la sylviculture sur ces risques de mortalité passés et futurs ? Pour répondre à cette question, j'ai utilisé CASTANEA à large échelle, et j'ai testé différents scénarios climatiques et sylvicoles (Chapitre II).

— Quel est le rôle de la variabilité génétique intra- et inter-population sur le risque de mortalité des populations d'arbres face aux changement climatiques ? Pour

répondre à cette question, j'ai utilisé CASTANEA à large échelle avec le Hêtre comme cas d'étude (Chapitre III) .

Chapitre II

Combiner des modèles statistiques et un modèle basé sur les processus pour comprendre les causes de la mortalité du Hêtre dans une population en marge xérique

1 Contexte et méthodes

Plusieurs études font état d'une augmentation du déclin des forêts, à la fois en termes de mortalité de fond (i.e. non catastrophique) (Van Mantgem et al., 2009; Lorenz & Becher, 2012) et de mortalité massive et catastrophique due à des événements extrêmes (Allen et al., 2010; Lorenz & Becher, 2012; Mueller et al., 2005). Un des enjeux majeurs en écologie est la compréhension et la prédiction de la mortalité des arbres pour permettre la conservation des populations et l'adaptation des politiques sylvicoles. Les interactions entre les différents facteurs et les processus physiologiques à l'origine de la mortalité des arbres, ainsi que la variabilité inter-individuelle de la vulnérabilité aux stress climatiques, doivent encore être identifiées et évaluées.
Dans cette étude, nous avons étudié une hêtraie au sein d'une réserve naturelle en gestion naturelle (i.e. sans intervention sylvicole), pour identifier et quantifier les facteurs de risque de mortalité du Hêtre. Nous avons utilisé des données de dépérissement, croissance et mortalité sur 4323 hêtres européens (*Fagus sylvatica* L.) suivis depuis 2002 dans une population de marge sèche. Nous avons combiné deux types d'approches permettant de distinguer l'influence des facteurs climatiques et biotiques sur la probabilité de mortalité et les mécanismes sous-jacent à l'échelle individuel et de la parcelle. Des modèles statistiques ont été utilisés pour quantifier les effets de la compétition, de la croissance, de la taille et du dépérissement des arbres sur la mortalité. Un modèle basé sur les processus écophysiologiques (PBM) a été utilisé pour séparer les différents mécanismes à l'origine des variations temporelles et inter-individuelles de la mortalité en simulant les réserves de carbone, la conductance hydraulique et les gelées tardives en réponse au climat.

Cette étude à été réalisé en partenariat avec les gestionnaires de la Réserve Naturelle de la Forêt de La Massane. La Massane est une hêtraie de 336 ha située dans les Pyrénées orientales françaises entre 600 et 1127m d'altitude. Cette population située au sud de la distribution du Hêtre est à la jonction des climats méditerranéen et montagneux. Aucune exploitation forestière n'a été autorisée depuis 1886 et la forêt a été classée comme réserve en 1974. Le Hêtre est l'arbre dominant de la canopée, représentant environ 68% de la surface terrière de la forêt. Une parcelle clôturée de 10 ha exclut le pâturage des vaches depuis 1956. Tous les arbres de cette parcelle protégée ont été géoréférencés et suivis individuellement depuis 2002. Ma tâche dans ce projet était d'expliquer la mortalité des hêtres observée dans la réserve intégrale. Pour cela la première tâche accomplie a été de préparer et d'analyser les carottes d'arbres pour en extraire la croissance annuel de 91 arbres cibles. J'ai ensuite participé à une campagne de géoréférencement précis de hêtres à la Massane pour cartographier plus précisément la distribution spatiale des arbres. Puis j'ai mis au point la procédure d'étude (i.e. l'utilisation de différents outils de modélisation à différentes échelles pour explorer les différentes causes de mortalité).

En parallèle de cette étude sur le risque de mortalité, une deuxième étude sur l'im-

pact de la défoliation des arbres sur la croissance et la reproduction a été menée 1. Nos résultats suggèrent que tout en diminuant leur croissance, certains grands arbres défoliés contribuent encore à la reproduction par la production de graines et la pollinisation. Ce déclin non-coordonné de la croissance et de la fécondité au niveau individuel en réponse au stress peut compromettre l'évolution des traits de résistance aux stress au niveau des populations et accroître la vulnérabilité des arbres forestiers.

Cette étude a été soumise dans la revue PCIecology en Mai 2019, et est en cours de re-soumission dans cette même revue.

2 Combining statistical and mechanistic models to identify the drivers of mortality within a rear-edge beech population

Mots-cléfs : *Fagus sylvatica L.*, regression logistiques , modèle basé sur les processus, modèle de dynamique de végétation, CASTANEA, analyse longitudinale , défoliation.

Title:

Combining statistical and mechanistic models to identify the drivers of mortality within a rear-edge beech population

Authors:

Cathleen Petit-Cailleux[1], Hendrik Davi[1], François Lefèvre[1], Joseph Garrigue[2], Jean-André Magdalou[2], Christophe Hurson[2,3], Elodie Magnanou[2,4], and Sylvie Oddou-Muratorio[1].

Adresses

[1]INRA, UR 629 Ecologie des Forêts Méditerranéennes, URFM, Avignon, France

[2]Réserve Naturelle Nationale de la Forêt de la Massane, France

[3]Fédération des Réserves Naturelles Catalanes, Prades, France

[4]Sorbonne Université, CNRS, Biologie Intégrative des Organismes Marins, BIOM, F-66650 Banyuls-sur-Mer, France

Keywords: *Fagus sylvatica* L., logistic regression, process-based model, dynamic vegetation model, CASTANEA, longitudinal analysis, defoliation.

Abstract

Since several studies have been reporting an increase in the decline of forests, a major issue in ecology is to better understand and predict tree mortality. The interactions between the different factors and the physiological processes giving rise to tree mortality, as well as the individual between-tree variability to mortality risk, still need to be identified and assessed.

This study is based on a survey of 4323 European beeches (*Fagus sylvatica* L.) since 2002 in a rear-edge population within a natural reserve. We combined two types of approaches: (1) statistical models were used to quantify the effects of competition, tree growth, size and decline on mortality and (2) an ecophysiological process-based model (PBM) was used to separate out the different mechanisms giving rise to temporal and inter-individual variations in mortality by simulating carbon reserves, hydraulic conductance and late frosts in response to climate.

The mortality rate at population level was associated to the combination of conductance loss, carbon reserve depletion and occurence of late frosts simulated with the PBM. In the statistical models, the individual probability of mortality decreased with increasing mean growth, and increased with increasing crown defoliation, earliness of budburst, fungi presence and increasing competition. The interaction between tree size and defoliation was significant, indicating a stronger increase in mortality associated to defoliation in smaller than larger trees. Finally, the PBM predicted a higher conductance loss together with a higher level of carbon reserves for trees with earlier budburst, while the ability to defoliate the crown was found to limit the impact of hydraulic stress at the expense of the accumulation of carbon reserves.

We discuss the convergences and divergences obtained between statistical and process-based approaches and we highlight the importance of combining them to identify the different processes underlying mortality, and the factors modulating the individual risk of mortality.

Introduction

Global changes have been repeatedly reported to be the cause of forest decline and tree mortality, both in terms of background, non-catastrophic mortality (Van Mantgem et al. 2009, Lorenz and Becher 2012) and of massive, catastrophic mortality due to extreme, 'pulse' events (Allen et al. 2010; Lorenz and Becher 2012; Mueller et al. 2005). To predict how such a new regime of trees mortality will impact upon forest structure, composition and ecosystem services (Anderegg et al. 2015a; Choat et al. 2018), we need to better understand the respective roles of the various drivers and mechanisms underlying tree mortality.

Studying mortality poses several well-recognized challenges, in particular because it is triggered by several factors and involves several underlying and interacting physiological processes. The factors triggering mortality include extreme, pulse climatic events (i.e. repeated drought, storms, floods, heavy snow, late frosts, wildfires) or sudden changes in biotic interactions (i.e. emerging pests, invasive species), but also long-term climatic or biotic perturbations (i.e. recurrent water deficits, changes in competition at the community level) (Maraun et al. 2003; McDowell et al. 2011). Moreover, these factors can have interactive effects. For instance, drought may increase trees' sensitivity to pests (Durand-Gillmann et al. 2014; Anderegg et al. 2015b) or predispose them to wildfires (Brando et al. 2014). Finally, a single factor triggering mortality may involve several underlying physiological processes, with several thresholds leading to mortality and potential feedback between them (McDowell et al. 2011). This is exemplified by drought, which is usually considered to trigger mortality through the combination of hydraulic failure and carbon starvation (Adams et al. 2017; Anderegg et al. 2012; McDowell et al. 2011). Hydraulic failure is the loss of conductance resulting from major xylem embolism, i.e. the formation of water vapour or air bubbles within xylem due to high water tension from soil to canopy (Tyree and Sperry 1989). To avoid hydraulic failure, trees can close their stomata before reaching the xylem species-specific embolism point (Cowan and Farquhar 1977). However, stomata closure mechanically reduces photosynthetic activity, forcing the tree to ensure basal metabolism by using carbon reserves, which can eventually become depleted, particularly during a long period of drought, leading to mortality through carbon starvation. Many experimental studies on drought suggest that hydraulic failure is the most frequent cause of tree mortality, and at least, is often the initial step to trigger a number of interacting processes leading to mortality (Choat et al. 2018). Nevertheless, the relationship between carbon and water fluxes, and the role of biotic factors during and after drought, remains to

be clarified (Adams et al. 2017; Feng et al. 2018; McDowell et al. 2011; Meir, Mencuccini, and Dewar 2015; O'Brien et al. 2014).

Another challenge when studying mortality is that the physiological processes governing tree mortality may vary in space and time. For instance, the risk of mortality may vary among individual trees within a population according to (i) the local spatial heterogeneity of resources availability, especially soil water (Nourtier et al. 2014); (ii) the heterogeneity in an individual tree's life history, and in particular the effects of past stresses on tree morphology and anatomy (Vanoni et al. 2016); (iii) the inter-individual variation of physiological responses to stresses, which depends on ontogenic, plastic, and genetic effects controlling the expression of traits (Anderegg 2015a; Vitasse et al. 2009). Risk of may also vary through time for a given individual/population, not only because of temporal climatic variation but also through individual variations in phenological processes. This is well illustrated by the risk of late frost damage, which is closely related to the coincidence between temporal patterns of budburst phenology, and the climatic sequence of low temperatures. Although relatively large safety margins were found regarding the risk of late frost damage during budburst across many European temperate tree and shrub species (Bigler and Bugmann 2018), these safety margins may reduce with climate change, due to budburst in trees occurring earlier (Augspurger 2009). When young leaves have been damaged, some species can reflush, i.e. produce another cohort of leaves (Augspurger 2009; Menzel, Helm, and Zang 2015), but the time required to reflush reduces the length of the growing season (Lenz et al. 2013), and may lead to mortality if trees do not have enough reserves to do this.

Available approaches to investigate the multiple drivers and processes underlying tree mortality can be classified into two broad categories: statistical, phenomenological approaches vs process-based, mechanistic approaches. Statistical approaches use forest inventory data to test how endogenous factors (e.g. related to tree/stand size and growth rate) and exogenous factors (biotic and abiotic environment, including management) affect stand- or individual- mortality. By comparing species or populations over areas with large climatic variations, such studies have demonstrated the overall effect of drought severity on mortality, although usually explaining only a limited proportion of the variance found in causes of mortality (Allen et al. 2010; Greenwood et al. 2017). Moreover, probabilities of mortality have been predicted with a higher accuracy when individual covariates for tree growth, size and/or competition were included in the statistical models, highlighting the importance of inter-individual variability in the threshold for mortality (Hülsmann, Bugmann, and Brang 2017; Monserud 1976). Recent statistical studies have attempted to include functional traits involved in the response to stress as additional covariates to improve the

accuracy of mortality prediction. For instance, Carnicer et al. (2011) showed that defoliation trends are consistent with mortality trends in southern European forests. Benito-Garzón et al. (2018) found that mortality increased in populations with negative hydraulic safety margins for 15 species out of the 25 studied. Overall, the main advantage of statistical approaches is their ability to account for a potentially high number of factors and processes triggering mortality and for individual variability in the threshold for mortality. However, these statistical models barely deal with the usually low temporal resolution of mortality data, missing information on the cause of tree death, and non-randomization inherent in natural population designs. In addition, the accuracy of statistical predictions dramatically decreases outside the studied area (Hülsmann, Bugmann, and Brang 2017).

On the other hand, biophysical and ecophysiological process-based models (PBMs), initially developed to simulate carbon and water fluxes in forest ecosystems, are also useful to investigate the environmental drivers and physiological processes triggering tree mortality. For example, using the PBM CASTANEA, Davi & Cailleret (2017) showed that mortality of silver fir in southern France resulted from the combination of drought-related carbon depletion and pest attacks. Using six different PBMs, Mcdowell et al. (2013) found that mortality depended more on the duration of hydraulic stress than on a specific physiological threshold. A main advantage of PBMs is their ability to understand the physiological drivers of mortality and to predict mortality under new combinations of forcing variables in a changing environment. However, they need a large number of parameters to be calibrated, which makes it difficult to have a precise projection in other populations where the model has not been precisely calibrated and validated. Moreover, biophysical and ecophysiological PBMs generally do not take into account individual tree characteristics (i.e. related to ontogenic, plastic and/or genetic variation). Hence, statistical and process-based approaches appear as complementary, and many authors have called for studies comparing or combining them (Hawkes 2000; O'Brien et al. 2017; Seidl et al. 2011).

An important tree of pan-European forests, the European beech (*Fagus sylvatica* L.) combines a widespread distribution (from northern Spain to southern Sweden and from England to Greece) and a high sensitivity predicted to climate change (Cheaib et al. 2012; Kramer et al. 2010). In particular, bioclimatic niche models predict a future reduction of this species at the rear edge of its range over the next few decades (particularly in the southern part of its distribution), in response to reduced rainfall (Cheaib et al. 2012; Kramer et al. 2010). This prediction is consistent with this species' well-known sensitivity to summer droughts. For example, more frequent extreme droughts have been associated with beech with weaker growth (Dittmar, Zech, and Elling 2003; Jump, Hunt, and Penuelas 2006; Knutzen et al. 2017), altered physiological performances (Bréda et al. 2006) and

increased defoliation (Penuelas and Boada 2003). However, the low mortality rate observed so far in beech has led some authors to propose that this species presents a higher heat stress tolerance and metabolic plasticity when compared to other tree species (García-Plazaola et al. 2008). This apparent paradox between a low mortality and a high sensitivity to climate makes beech an interesting model species to study.

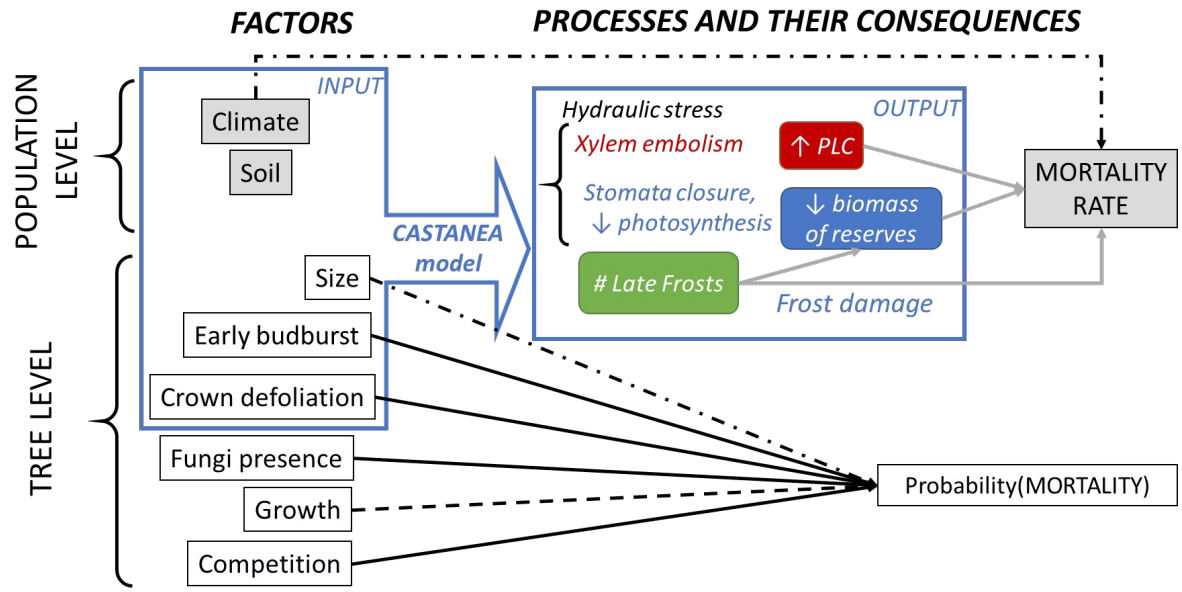

Figure 1: Combining statistical and process-based models to study variables and processes involved in tree mortality at population and tree-level. The right text in square boxes indicates the measured factors and response variables considered in statistical models (white background = individual level; grey background = population level), while the italic text indicates the focal processes (no boxes) and stress-related output variables (boxes with rounded corners) simulated with the PBM CASTANEA. The blue box on the left delineates the input variables of CASTANEA. At the top, grey arrows indicate the relationships considered to link stress-related output variables simulated by CASTANEA with observed mortality rate at population level, while the thin black arrows indicate the relationships considered in the statistical model for mortality at population level. At the bottom, the thick black arrows indicate the relationships considered in the statistical model for the probability of mortality at individual level (solid lines: expected positive effect; dashed lines: expected negative effect; nonlinear effects were expected for size, as well as interaction effects between size on the one hand and all other factors). PLC – percentage of loss of conductance.

In this study, we used a combination of statistical regression models, and the PBM CASTANEA (Figure 1), to investigate patterns of mortality within a population located at the warm and dry ecological margin for European beech (42° 28' 41" N, 3° 1' 26" E; Supplementary Fig. S1). Mortality, decline (crown defoliation and fungi presence), size, growth, competition and budburst were characterised in a set of 4323 adult trees over a 15 year-period from 2002 to 2016. CASTANEA was used to simulate the number of late frost days (integrating tree phenology), the percentage of loss

of conductance (PLC) and the biomass of carbon reserves in response to stress. Specifically, we addressed the following issues: (1) When and how do climate variations trigger mortality at population level; and (2) how do factors varying at tree-level modulate the individual tree's probability of mortality? To answer the first issue, we used CASTANEA simulations at population-level to study the relationship between the simulated response variables and the observed mortality rate. We also tested the impact of climatic variables related to drought duration and intensity on the population-level mortality rate with a beta-regression model. To answer the second issue, we used on the one hand logistic regression to characterise the respective effects of exogenous and endogenous factors on the individual probability of mortality (see detailed expectations on Figure 1), and on the other hand CASTANEA to investigate how differences in tree size, phenology, and defoliation affected the physiological responses to stress.

Materials and Methods

Study site

La Massane is a forest of 336 ha located in the French eastern Pyrenees ranging from 600 to 1127 m.a.s.l. Located in the south of the beech range, the forest is at the junction of Mediterranean and mountainous climates with a mean annual rainfall of 1260 mm (ranging from 440 to 2000 mm) and mean annual temperature of 11°C (with daily temperature ranging from -10°C to 35°C) (Supplementary Fig. S2). No logging operations have been allowed since 1886 and the forest was classified as a reserve in 1974. European beech is the dominant tree in the canopy representing about 68% of basal area of the forest. Beech is in mixture with downy oak (*Quercus pubescens* Willd), maple (*Acer opalus* Mill., *Acer campestris* L., *Acer monspessulanum* L.), and holly (*Ilex aquifolium* L.). A 10 ha fenced plot has excluded grazing from cows since 1956. All trees from this protected plot have been geo-referenced and individually monitored since 2002 (Supplementary Fig. S3).

We estimated the soil water capacity (SWCa) through soil texture, soil depth and percentage of coarse elements measured in two soil pits. Secondly, we estimated the mean Leaf Area Index (LAI) by using hemispherical photographs (Canon 5D with Sigma 8mm EXDG fisheye). We computed the LAI and clumping index following the methodology described by Davi et al. (2009). SWCa and LAI were measured at population level.

Individual tree measurements

This study is based on the characterisation of twelve variables in 4323 beech trees in the protected plot over the period from 2002 to 2016 (Table 1). Note that beech sometimes produces stump shoots resulting in multiple stems from a single position (coppice), but that here, every stem of all the coppices was individually monitored and subsequently referred to "tree".

Table 1: Quantitative and categorical variables measured at individual level. All the variables were measured in 4323 trees, except for H_{2002} (1199 trees). The "Cat" column indicates both the category (i.e. size, growth, competition, decline, phenology) and whether it is endogenous (Endo) or exogenous (Exo). The "YMeas." column indicates the year of measurement; note that all the variables were measured only once, so when 2 dates are given they indicate the period over which the variable is computed.

Quantitative variables measured at individual level							
Code	**Variable**	**Cat**	**YMeas.**	**mean**	**min**	**max**	**unit**
DBH_{2002}	Diameter at breast height measured in 2002	Size Endo	2002	21.65	10	116	cm
DBH_{2012}	Diameter at breast height measured in 2012	Size Endo	2012	22.84	10	116	cm
MBAI	Mean basal area increment between 2002 and 2012.	Growth Endo	2002-2012	4.66	0	95	$cm^2.year^{-1}$
H_{2002}	Height measured in 2002	Size Endo	2002	8.8	2	26	m
DEFw	Cumulated and weighted defoliation score	Decline Endo	2003-2016	0.14	0	1	
Nstem	Number of stems observed in the coppice	Compet Exo	2002	1.54	1	11	
$Compet_{intra}$	Intra-specific competition index	Compet Exo	2002	2.74	0	11.43	
$Compet_{intra+}$	Intra-specific competition index accounting for within-coppice competition	Compet Exo	2002	1.03	0	12.69	
$Compet_{tot}$	Total competition index, accounting for within-coppice competition	Compet Exo	2002	4.63	0.12	19.98	

Categorical variables measured at individual level					
Code	**Variable**	**Cat**	**YMeas.**	**Level**	**Number of trees**
Fungi	Presence (1) or absence (0) of the saproxylic fungus	Decline Endo	2003-2016	1: 0:	414 3913
Budburst	Early (1) or late (0) budburst	Phenology Endo	2002	1 0	237 4090

Tree mortality was recorded every year from 2003 to 2016, based on two observations (in autumn, based on defoliation and in spring, based on budburst). A tree was considered to have died at year *n* when (1) budburst occurred in the spring of year *n* but (2) no leaves remained in the autumn of year *n*, and (3) no budburst occurred in year *n*+1. All the 4323 trees were alive in year 2003 (Supplementary Fig. S4). We computed the annual mortality rate (τ_n) for each year *n* as:

$$\tau_n = \frac{N_{dead,n}}{N_{alive,n-1}} \quad \text{(Equation 1)},$$

where $N_{dead,n}$ (respectively $N_{alive,n}$) is the number of dead (respectively alive) trees in year *n*.

Diameter at breast height (DBH) was measured 1.30 m above ground level in 2002 and 2012. As we focused on the drivers of mature tree mortality, only trees with DBH_{2002} greater than 10 cm were retained for analysis. Individual growth was measured by the mean increment in basal area (MBAI) between 2002 and 2012, estimated as:

$$MBAI_i = (\pi(DBH_{2012} - DBH_{2002})^2/4)/NyearsAlive_i \quad \text{(Equation 2)},$$

where $NyearsAlive_i$ is the number of years where individual *i* was observed being alive. Height in 2002 was estimated for a subset of 1199 trees.

A bimodal pattern in budburst phenology had been previously reported in La Massane (Gaussen 1958; Perci du Sert 1982). Some trees were observed to systematically initiate budburst about two weeks before all the others. Here, the monitoring allowed budburst phenology to be surveyed as a binary categorical variable, distinguishing trees with early budburst from the others.

The presence of defoliated major branches was recorded each year between 2003 and 2016 (except 2010) as a categorical measure (DEF = 1 for presence; DEF = 0 for absence). These annual measures were cumulated and weighted over the observation period for each individual as:

$$DEFw_i = \frac{\sum_{j=1}^{NyearsAlive_i} ¿_j}{NyearsAlive_i} \quad \text{(Equation 3)},$$

Year 2010 was not included in $NyearsAlive_i$. DEFw is an ordered variable integrating (without disentangling) the recurrence of defoliation and the ability to recover from defoliation. The presence of fructification of the saproxylic fungus *Oudemansiella mucida* (Schrad.) was recorded as a categorical measure (Fungi = 1 for presence; Fungi = 0 for absence). Given that once observed, the fructification persists throughout the subsequent years, we analysed it as a binary variable.

Competition around each focal beech stem was estimated by the number of stems in the coppice (*Nstem*) as an indicator of within-coppice competition. We also computed competition indices accounting simultaneously for the diameter (DBH_{2002}) and the distance (d_{ij}) of each competitor *j* to the competed individual *i*, following Martin and Ek (1984):

$$Compet_{i,dmax} = \frac{1}{DBH_{2002i}} \sum_{j=1}^{N_{compet}} DBH_{2002j} \exp\left[\frac{-16\, d_{ij}}{DBH_{2002i} + DBH_{2002j}}\right] \quad \text{(Equation 4)},$$

where N_{compet} is the total number of competitors in a given radius dmax (in m) around each focal individual *i*. Only trees with $DBH_{2002} > DBH_{2002\ i}$ are considered as competitors. Such indices were shown to describe more accurately the competition than indices relying on diameter only (Stadt et al. 2007). We computed this competition index in three ways. The intra-specific competition index $Compet_{intra}$ only accounts for the competition of beech stems not belonging to the coppice of the focal tree. The intra-specific competition index $Compet_{intra+}$ accounts for all beech stems belonging, or not, to the coppice of the focal tree. The total competition index $Compet_{tot}$ accounts for all stems and species. We considered that stems located less than 3 m away from the focal stem belonged to the same coppice. The three indices were first computed at all distances from 1 m (or 3 m for $Compet_{intra}$) to 50 m from the target tree, with 1 m steps. We then retained d_{max} = 15 m in subsequent analyses, because all indices reached a ceiling after this distance value, suggesting that in a radius greater than 15 m, the increasing number of competitors is compensated for by distance.

Climate data

Local climate has been daily monitored *in situ* since 1976 and 1960 for temperature and precipitation/mean relative humidity, respectively. In order to obtain a complete climatic series (from 1959 to 2016), we used the quantile mapping and anomaly method in the R package "meteoland" (De Caceres et al. 2018), considering the 8-km-resolution-SAFRAN reanalysis (Vidal et al. 2010) as reference.

From the corrected climate series, we derived the daily climatic input variables for CASTANEA, which are the minimum, mean and maximum temperatures (in °C), the precipitation (mm), the wind speed ($m.s^{-1}$), the mean relative humidity (%) and the global radiation ($MJ.m^{-2}$). We also computed two standardised precipitation-evapotranspiration indices (SPEI), varying between -2 (indicating aridity) and 2 (indicating wetness), using the R package "SPEI" (Beguería and Vicente-Serrano 2017). The cumulated SPEI from June to August with a three-month buffer (SPEI3_JJA) was used as an indicator of average drought level during the vegetative season. The lowest monthly SPEI-value over the vegetative season (SPEI1_dryVg) was used as an indicator of drought intensity (see Appendix 1 for details).

Simulations with CASTANEA

Model overview: CASTANEA is a PBM initially developed to simulate carbon and water fluxes in forest ecosystems with no spatial-explicit representation of trees (Dufrêne et al. 2005). A tree is abstracted as six functional elements: leaves, branches, stem, coarse roots, fine roots and reserves (corresponding to non-structural carbohydrates). The canopy is divided into five layers of leaves. Photosynthesis is half-hourly calculated for each canopy layer using the model of Farquhar et al. (1980), analytically coupled to the stomatal conductance model proposed by Ball et al. (1987). Maintenance respiration is calculated as proportional to the nitrogen content of the considered organs (Ryan 1991). Growth respiration is calculated from growth increment combined with a construction cost specific to the type of tissue (De Vries, Brunsting, and Van Laar 1974). Transpiration is hourly calculated using the Monteith (1965) equations. The dynamics of soil water content (SWCo; in mm) is calculated daily using a three-layer bucket model. Soil drought drives stomata closure via a linear decrease in the slope of the Ball et al. (1987) relationship, when relative SWCo is under 40% of field capacity (Granier, Biron, and Lemoine 2000; Sala and Tenhunen 1996). In the carbon allocation sub-model (Davi et al., 2009; Davi & Cailleret 2017), the allocation coefficients between compartments (fine roots, coarse roots, wood, leaf and reserves) are calculated daily depending on the sink force and the phenological constraints. CASTANEA model was originally developed and validated at stand-scale for beech (Davi et al. 2005).

Focal processes and output variables: In this study, we focussed on three response variables simulated by CASTANEA: (1) the biomass of reserves (BoR) as an indicator of risk of carbon starvation, (2) the percentage of loss of conductance (PLC) as an indicator of risk of hydraulic failure, and (3) the number of late frost days (NLF) as an indicator of risk of frost damage. Note that we did not simulate mortality with CASTANEA because the thresholds in PLC, NLF and BoR triggering mortality are unknown. These variables were simulated using the CASTANEA version described in Davi and Cailleret (2017) with two major modifications. First, for budburst, we used the one-phase UniForc model, which describes the cumulative effect of forcing temperatures on bud development during the ecodormancy phase (Chuine, Cour, and Rousseau 1999; Gauzere et al. 2017). We simulated damage due to late frosts (see details in Appendix 2) and considered that trees were able to reflush after late frosts. We calculated NLF as the sum of late frost days experienced after budburst initiation.

Second, we implemented a new option in CASTANEA to compute PLC following the Pammenter and Willigen (1998) formula:

$$PLC = \frac{1}{1 + e^{slope\left(\Psi_{leaf} - \Psi_{P50}\right)}} \qquad \text{(Equation 5)},$$

with Ψ_{leaf} (MPa) the simulated midday leaf water potential, Ψ_{50} (MPa) the species-specific potential below which 50% of the vessels are embolized, and *slope* a constant fixed to 50.

The leaf water potential Ψ_{leaf} was calculated as:

$$\Psi_{leaf}(t+1) = \Psi_{soil}(t+1) - \frac{TR}{3600} \times R_{SoilToLeaves} + \frac{\Psi_{leaf}(t)}{\Psi_{soil}(t+1) + TR \times R_{SoilToLeaves}} \times e^{\frac{deltaT}{R_{SoilToLeaves} \times Cap_{SoilToLeaves}}} \text{(Equation 6)}$$

where the soil water potential (Ψ_{soil} MPa) was calculated from daily SWCo (Campbell 1974). Ψ_{leaf} was calculated hourly (deltaT = 3600s) based on the sap flow (TR in $mmol.m^{-2}.leaf^{-1}$) simulated following the soil-to-leaves hydraulic pathway model of Loustau et al. (1990). We used a single resistance ($R_{SoilToleaves}$ in $MPa.m^{-2}.s^{-1}.kg^{-1}$, following Campbell 1974) and a single capacitance ($Cap_{SoilToleaves}$ in $kg.m^{-2}.MPa^{-1}$) along the pathway. $R_{SoilToleaves}$ was assessed using midday and predawn water potentials found in the literature.

We added a binary option in CASTANEA to simulate branch mortality and defoliation as a function of PLC. If the PLC at year *n* was >0, the LAI at year *n* was reduced by the PLC value for trees able to defoliate (option “Defoli-able”). Otherwise, PLC has no consequences on LAI.

Simulation design: The aim of the first simulations was to investigate whether response variables simulated by CASTANEA correlated with patterns of observed mortality at population scale. We simulated a population of 100 trees representing the variability in individual characteristics observed in La Massane in terms of height-diameter allometry, DBH, leaf area index and budburst phenology (Appendix 2). We also simulated a range of environmental conditions representing the observed variability in SWCa and tree density. CASTANEA was validated based on ring width patterns (Appendix 2). Values of focal output variables (PLC, NLF and BorR) were then averaged across the 100 trees. We also computed a composite risk index (CRI) for each year *n* combining the simulated PLC, NLF and BoR as follows:

$$CRI_n = \left(\frac{PLC_n}{max(PLC)} + \frac{NLF_n}{max(NLF)} \right) - \frac{BoR_n}{max(BoR)} \qquad \text{(Equation 7)},$$

Note that each term is weighted by its maximal value across all years, so that the contribution of the three drivers to risk is balanced. The possible range of CRI is [-1; 2].

The second simulation aimed at investigating the differences in physiological responses between individuals with different characteristics. We simulated eight individuals corresponding to a complete cross design with two size categories (5 and 40 cm in DBH), two budburst types (early and normal), and two defoliation levels (option “Defoli-able” activated or not).

Statistical models of mortality

Population-level: We used a beta-regression model to investigate the effects of climate on annual mortality rate at population-level. Beta-regression models predict a response variable varying between [0; 1] and account for features like heteroscedasticity or asymmetry, which are commonly obtained in time-series of annual mortality rates. We investigated the following model for mortality at year *n* (with *n* varying from 2004 to 2016):

$$\tau_n = \text{SPEI1\_dryVg}_n \times \text{SPEI3\_JJA}_n \text{ (Equation 8)},$$

where SPEI1_dryVg is lowest monthly value of SPEI during the vegetative season; and SPEI3_JJA is cumulated SPEI from June to August computed over three months. As the number of observations (years) was low, we focussed on these two predictors expected to cause mortality based on beech ecology (Bréda et al. 2006).

Beta-regression was fitted with the R package ‘betareg’ (Cribari-Neto and Zeileis 2010). The variables were scaled before fitting the model. Model validity was checked based on the leverage points (i.e. points having a greater weight than expected by chance) with the Cook's distance (Cook distance < 0.5 indicate no leverage). We evaluated the goodness-of-fit with the Brier test score (Brier 1950). We evaluated the sensitivity and specificity of the model using the receiver operating characteristic (ROC) curve.

Individual-level: We used logistic regression models to investigate how tree characteristics affect the individual probability of mortality ($P_{mortality}$). This approach is appropriate for a binary response variable and a mixture of categorical and quantitative explanatory variables, which are not necessarily normally distributed (Hosmer and Lemeshow 2000). We considered the following complete logistic regression model:

$$P_{mortality} = [\text{DEFw} + \text{Fungi} + \text{Budburst} + \text{MBAI} + (\text{Nstem OR Compet}_{intra} \text{ OR Compet}_{intra+} \text{ OR Compet}_{tot})] \times (\text{DBH}_{2002} + \text{DBH}_{2002}^2) \text{ (Equation 9)}$$

where the predictors defoliation (DEFw), growth (MBAI), size (DBH_{2002}) and competition (Nstem or the Compet indices) were quantitative variables, and the presence of fungi (Fungi) and budburst phenology (Budburst) were categorical variables. We included both a linear and quadratic effect of

DBH_{2002} by specifying this effect as a polynomial of degree 2. Interaction effects of the previous predictors with this polynomial were included.

All variables were scaled before fitting the model. To select the best competition-related variables, we first fitted the model described by equation 9 with each competition term successively (Appendix 3). Then, we used a stepwise procedure to select the most parsimonious model based on AIC. When two models had similar AIC (delta < 2) (Arnold 2010), the one with fewer variables (most parsimonious) was selected. Model validity and fit quality were checked using similar tools as for the beta-regression model.

Collinearity resulting from correlations between predictor variables is expected to affect the statistical significance of correlated variables by increasing type II errors (Schielzeth 2010). To evaluate this risk, we first checked for correlation among predictors included in equation 9 (Fig. S5). We also computed the variation inflation factor (VIF) with the R package "car". A threshold of VIF < 4 is commonly accepted to show that variables are not excessively correlated and do not render the model unstable.

We expressed the results in terms of odds ratios, also called relative risk, indicating the degree of dependency between variables. For instance, the odds ratio for mortality as a function of budburst characteristics (early or normal) is:

$$Oddsratio_{EarlysvsNormal} = \frac{Odds_{Early}}{Odds_{Normal}} \qquad \text{(eq 10)},$$

With $Odds_{Early} = \frac{P_{mortality}(Early)}{1 - P_{mortality}(Early)}$ and $Odds_{Normal} = \frac{P_{mortality}(Normal)}{1 - P_{mortality}(Normal)}$.

We computed odds ratios with "questionr" the R package (Barnier, Briatte, and Larmarange 2018). The interactions were visualized with the package "jtools" (Long 2018).

Results

Population-level patterns of mortality

The total mortality rate between 2004 and 2016 was 23% (Figure 2; Table S1). After 2004 (2.6%), two peaks of high mortality were observed, in 2006-2007 (3.3% in 2006) and in 2010 (2.9%). The lowest mortality rate was observed in 2008 (0.8%).

CASTANEA simulated inter-annual variations in the PLC: the mean PLC value varied among years, from 1% in 2004 and 2005 to 31% in 2006 (Fig. 2a). The mean simulated biomass of carbon reserves (BoR) varied among years, from 51 $gC.m^{-2}$ in 2006 to 354 $gC.m^{-2}$ in 2011. Finally, the number of late frost days (NLF) varied among years, from 0.2 in 2016 to 7.56 days in 2010 (Fig. 2c). The variation in the composite risk index (CRI) integrated these different responses (Fig. 2d), showed a peak in 2006 (drought), in 2010 (late frost) and in 2012 (combination of frost and drought).

None of the response variables simulated by CASTANEA (NLF, PLC, BoR) was significantly correlated to annual variation in mortality rate. The only significant correlation was observed between CRI and the annual mortality rate ($r = 0.58$, p-value = 0.04). Hence, inter-annual variations in CRI were a good predictor of the mortality rate, except in year 2007.

Figure 2: Stress-related output variable simulated with CASTANEA from 2004 to 2016: (a) percentage of loss of conductance (PLC); (b) biomass of reserves in gC.kg^{-1} (BoR); (c) number of late frost days (NLF);. (d) Composite risk index (CRI) integrating a+b+c. The black line is the mean of simulation, and the grey area represents the inter-individual variation from the 1st to the 3rd quartile. The yellow line is the mortality rate observed in La Massane.

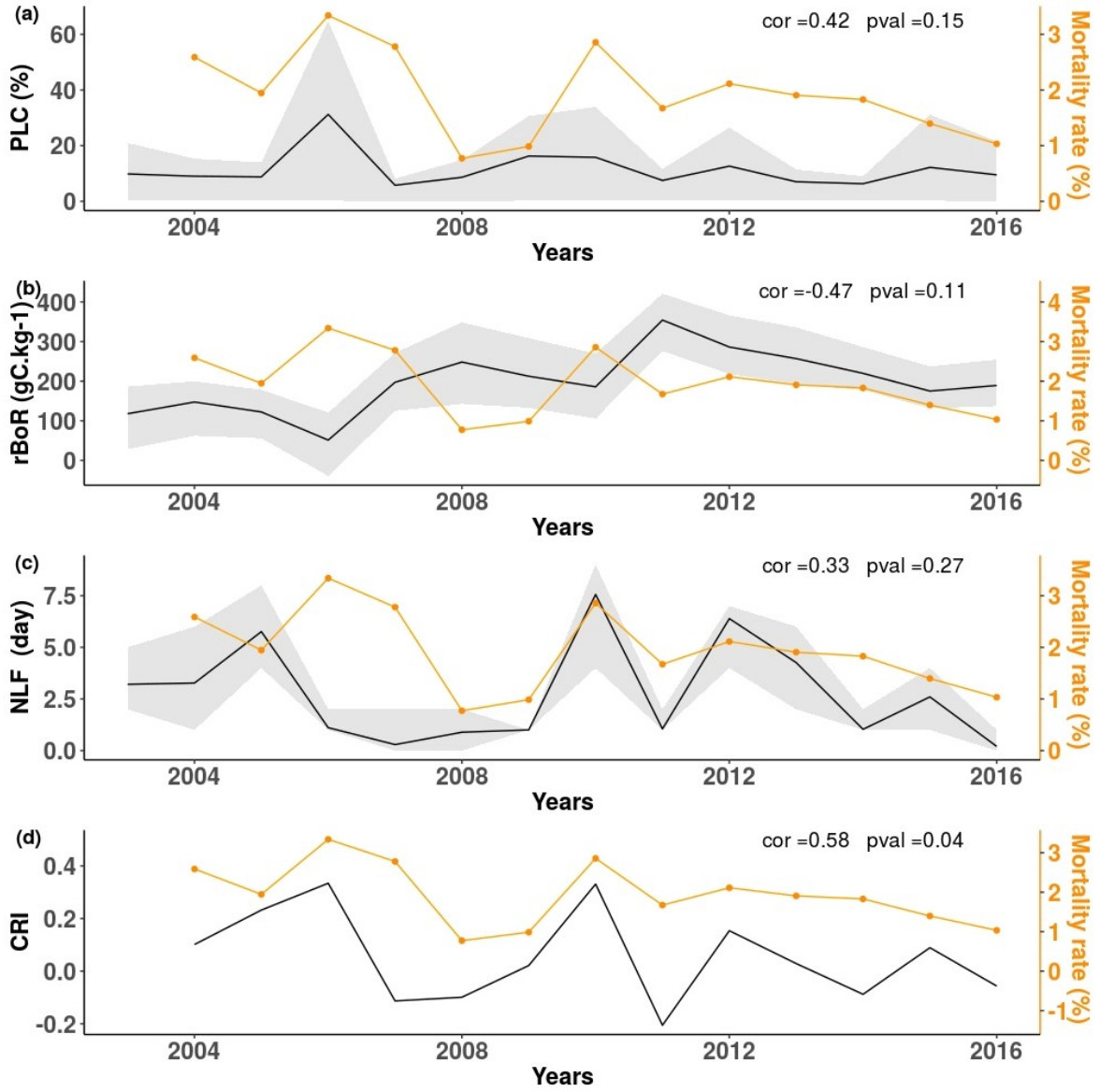

The beta-regression model revealed a significant impact of climate variables on the observed mortality rate at population-level (Appendix 1). SPEI1_dryVg, SPEI3_JJA and their interactions explained 32% of the variation in mortality rate between years. This model had both fair validity and goodness-of-fit. For low values of SPEI3_JJA (i.e. during dry summers), mortality increased with decreasing SPEI1_dryVg (i.e., increasing drought intensity). However, non-expected interaction

effects were observed for high values of SPEI3_JJA (i.e. during wet summers), where mortality increased with increasing SPEI1_dryVg (i.e., decreasing drought intensity).

Statistical model of mortality at individual level

Table 2: Effects of variables varying at tree-level on the individual tree's probability of mortality. Variables are defined in Table 1. Effects were estimated with a logistic regression model (equation 9). β is the maximum likelihood estimate, with its estimated error (SE), z-value, and associated p-value. OR is the odds ratio.

Variables	β	SE	z value	p-value	OR
DEFw	6.91	0.26	26.29	< 2.2 e-16	1.0 e03
DBH_{2002}	-11.59	5.15	-2.25	2.42 e-02	9.22 e-06
DBH_{2002}^2	22.25	4.95	4.50	6.86 e-06	4.60 e09
MBAI	-5.91e-02	1.06 e-02	-5.55	2.80 e-08	0.94
Budburst	0.81	0.17	4.69	2.69 e-06	2.25
Nstem	0.12	3.60 e-02	3.42	6.24 e-04	1.13
Fungi	0.56	0.14	3.94	8.10 e-05	1.75
DEFw:poly(DBH_{2002})1	-55.17	14.81	-3.73	1.95 e-04	1.10 e-24
DEFw:poly(DBH_{2002})2	32.09	16.81	1.91	5.63 e-02	8.64 e13
poly(DBH_{2002})1:MBAI	0.37	0.45	0.83	0.41	1.45
poly(DBH_{2002})2:MBAI	-0.83	0.44	-1.89	5.90 e-02	0.43

All the variables listed in equation 9 were retained in the best model and had a significant main effect on the probability of mortality (Table 2). This model explained 49% of the observed mortality and had both a high validity and goodness-of-fit (Appendix 3). Defoliation had the strongest linear effect on mortality: the relative probability of mortality increased by 1000 times for a one-unit increase in DEFw. Then, the probability of mortality was 2.25 higher for trees with earlier budburst as compared to others, and 1.75 higher for trees bearing fungi fructifications as compared to others. Among the competition-related variables, N_{stem} was selected as it was associated with the lowest AIC. The probability of mortality increased with increasing Nstem, and decreased with increasing MBAI. Regarding the effect of tree size, the polynomial of degree 2 corresponded to a U-shape and traduced a higher relative probability of mortality for both the smaller and the larger trees (Table 3, Appendix 3).

Interaction effects between size and defoliation on mortality were significant: the probability of mortality increased more rapidly with DEFw for small rather than larger trees, and at an equal level of defoliation, the probability of mortality was always higher for smaller trees (Fig. 3a, Table 2). Interaction effects between size and growth on mortality were also significant: the decrease in the probability of mortality with increasing mean growth was evident mostly for small trees (Fig. 3b).

These results were robust for the choice of the competition variable (Nstem versus competition indices), for the choice of the size variable (height instead of diameter) and for the consideration of size (DBH_{2002}) as a quantitative versus categorical variable (Appendix 3). Finally, we obtained convergent results with an alternative approach (survival analysis) which account simultaneously for both levels of variability (individual and temporal) in our data set (Appendix 4).

Process based model at individual scale

Simulations with CASTANEA showed that inter-individual differences in tree size, phenology, and defoliation, together with the intensity of climatic stress, affected the physiological responses to stress. The magnitude of the individual effects on tree risk of mortality differed during a drought year (2006), a frost year (2010) and a good year (2008, 2014 or 2016) (Fig. 4). The loss of conductance was higher for trees with early budburst and for larger trees, but this effect was only evident in drought years (Fig. 4a). Moreover, during drought, the ability to defoliate decreased the risk of cavitation (Fig. 4a) but increased the risk of carbon starvation (Fig. 4b). By contrast, phenology only poorly affected the biomass of reserve (BoR): even during a frost year, trees with earlier budburst did not reduce their BoR, due to their ability to reflush (Fig. 4b). BoR was always lower for large tree, even without stress. This was to be expected, because there is no explicit competition for light in CASTANEA. Hence large trees and small trees have a relatively similar photosynthesis when it is scaled by soil surface (large trees photosynthesize slightly more because they have a stronger LAI). Large trees, on the other hand, have a larger living biomass and thus a higher level of respiration, which leads to lower reserves.

Figure 3: Interaction effects in the logistic regression model at individual-level (a) between diameter (DBH_{2002}) and weighted defoliation (DEFw). (b) between DBH_{2002} and the mean growth in basal area (MBAI). Regression lines are plotted for three values of DBH_{2002}, corresponding to ± 1 standard deviation (10.7 cm) from the mean (22 cm). Confidence intervals at 95% are shown around each regression line.

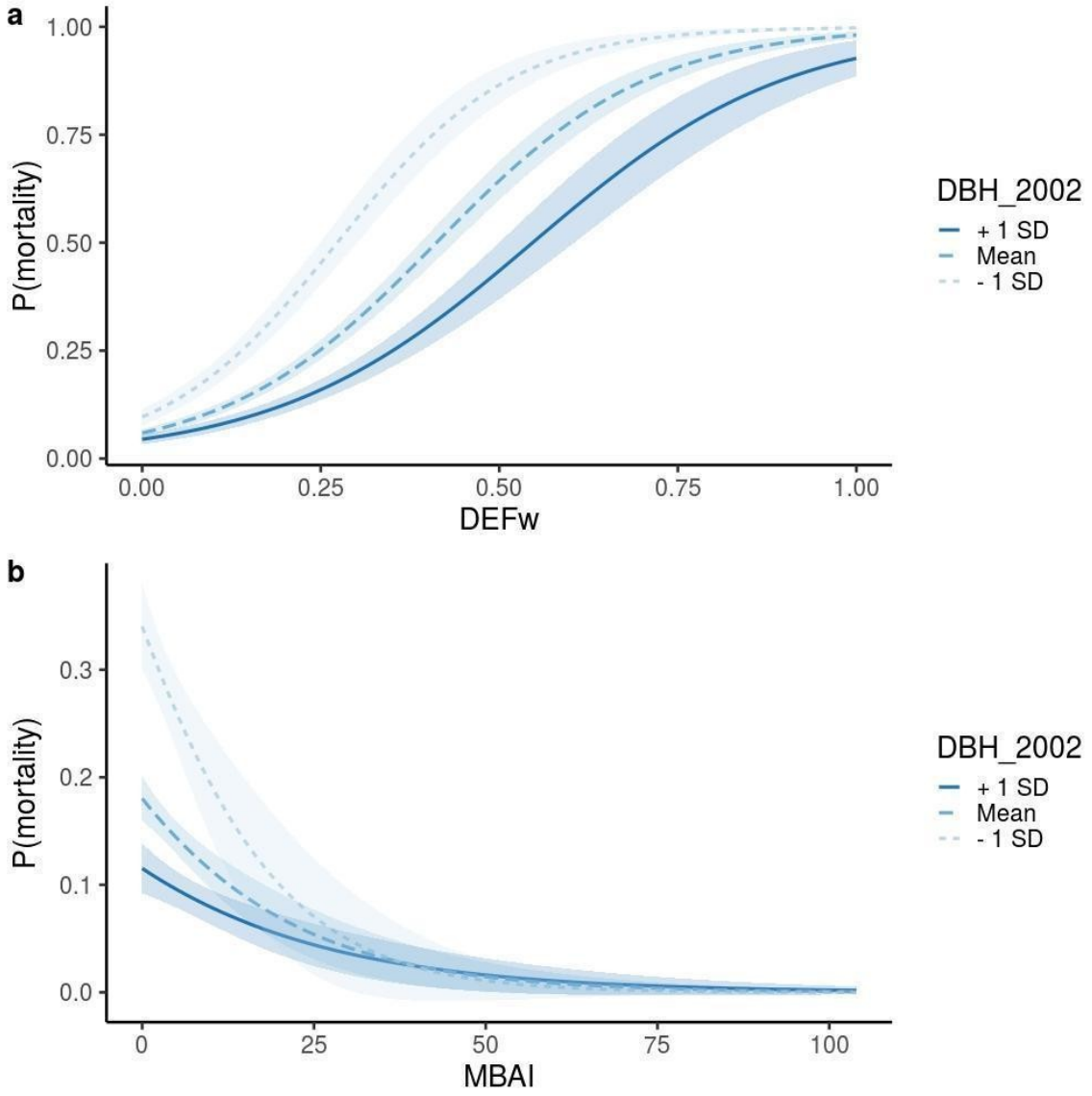

Figure 4: Physiological proxies of the risk of mortality simulated for eight trees differing in size, defoliation and budburst phenology. We focus on three key years**:** 2006 (drought); 2008 (no stress); 2010 (late frosts). Colours indicate the DBH at the beginning of the simulation: 5 cm (light blue) versus 40 cm (dark green). Triangles (respectively round) indicate individuals with early (respectively "normal") budburst. Empty (respectively full) indicate individuals able (respectively not able) to defoliate.

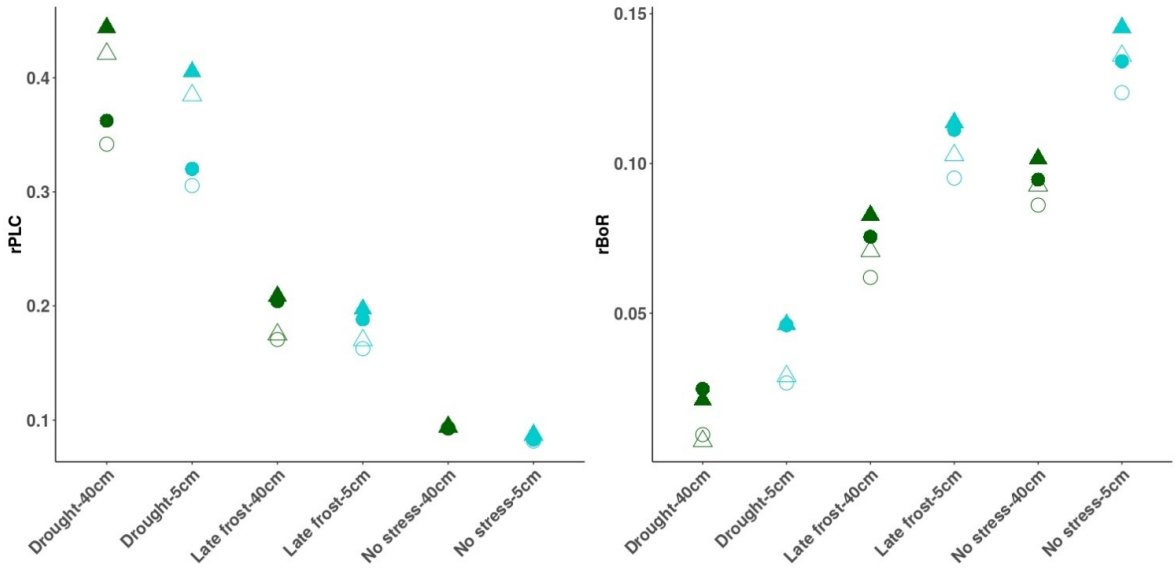

Discussion

By combining statistical and process-based models at population and tree-level (Figure 1), this study shed new lights on when and how climate variations trigger mortality and how factors varying at tree-level modulate the individual risk of drought and frost stresses (Table S2).

Increasing population-level rate of mortality in response to drought and frost

The annual mortality rates observed in this study ranged between 0.7 and 3.3% (mean value = 2%). This is at the upper range of the few mortality estimates available for beech. Hülsmann et al. (2016) reported annual mean rates of mortality of 1.4%, 0.7% and 1.5% in unmanaged forests of Switzerland, Germany and Ukraine, with a maximum mortality rate of 2.2%. Archambeau et al. (2019) estimated even lower mortality rates (mean annual value = 3.8×10^{-3}%, range = 3.7×10^{-3}% to 3.8×10^{-3}%) from European forest inventory data (including managed and unmanaged forests). Overall, these mortality rates are low when compared to other tree species; for instance, according to the French national forest inventory, the average mortality is 0.1% for beech against 0.3% on average for other species and 0.4% for spruce or 0.2% for silver fir (IFN 2016). The relatively high value observed here may result from the absence of management, combined with the population location being at the dry, warm margin of species distribution (Fig. S1), where most population

extinctions are expected in Europe (Thuiller et al. 2005). However, we cannot rule out that these different mortality estimates are also affected by the size threshold in inventories, which differ between studies (including smaller trees automatically increases the mortality rate).

We showed that inter-annual variations in the observed mortality rate at population-level were significantly associated with variations in the composite risk index (CRI) integrating the number of late frost days (NLF), the percentage of loss of conductance (PLC) and the biomass of carbon reserves (BoR) simulated by CASTANEA. This association was not found when the three response variables simulated by CASTANEA were considered separately, highlighting that patterns of mortality in beech are driven by a combination of drought, and late-frost, stresses. In particular, simulations showed that in 2010 (a year without drought), the high mortality rate coincided with an extreme late frost event. This is consistent with the study of Vanoni et al (2016), which showed that both drought and frost could contribute to beech mortality. These results are also consistent with the emerging consensus that mortality at dry, warm margins is not due either to carbon starvation or hydraulic failure, but is rather the result of a balance of all these responses (e.g. McDowell et al. 2011; Sevanto et al. 2014).

This study also found a significant relationship between the observed mortality rate and SPEI variables computed from climatic series. A major role of SPEI on mortality has already been found by Archambeau et al. (2019) in beech, by Davi and Cailleret (2017) in silver fir, or by Carnicer et al., (2011) in 12 European tree species. Here, the statistical regression model including only SPEI variables suggested that mortality was triggered by summer droughts, including both the pulse effects of severe drought (through SPEI1_dryVg) but also long-term effects of repeated droughts (through SPEI3_JJA). Our results additionally suggest an interaction between long-term and pulse effects of drought on mortality i.e. the risk of mortality increased more than the sum of risks predicted by each factor separately. However, the biological interpretation of some of these interaction effects was not evident. This may be due to the low number of observations, with only 14 years in the mortality survey. This may also confirm that integrative measurements of the response to stresses, such as the CRI proposed here, allow a better understanding of when and how mortality occurs than purely stress-related climatic variables.

In future developments, the CRI could be refined in several ways. Its different components could be weighted based on ecophysiological knowledge. The CRI could also benefit from taking into account the temporal dynamics of mortality, such as the existence of positive or negative post-effects across years. The low number of observations in this study compelled us not to account for these lagged effects, which probably explains why the CRI failed to predict the high mortality

observed in 2007. Indeed, the high mortality of 2007 is probably due to the lagged effect of the 2006 drought. Such lags between the weakening of a tree and its final death were shown for beech in Vanoni (2016) and silver fir in Davi & Cailleret (2017).

Inter-individual variation in the risk of drought and frost

The large number of trees individually monitored in this study provided us with an exceptionally large sample size to test for the effects of factors modulating individual risk of drought and frost in beech. Firstly, we found that a higher mean growth was associated with a lower probability of mortality, as previously demonstrated (Cailleret and Davi 2011; Gao et al. 2018). This decrease in mortality with increasing mean growth was evident mostly for small trees as already reported in beech seedlings (Collet and Le Moguedec 2007) and other species (Kneeshaw et al. 2006; Lines, Coomes, and Purves 2010), but not in adult beech trees to our knowledge.

Secondly, we found that increased defoliation was associated with increasing mortality. This result was expected from previous studies (Dobbertin and Brang 2001, Carnicer et al. 2011), although the consequences of defoliation are still being debated for beech. Senf et al. (2018) showed that defoliation was associated with tree decline, while Bauch et al., (1996) and Pretzsch (1996) found that the growth of highly defoliated beech trees did not decrease and could even increase in some cases. Our simulations comparing trees able, or not able, to defoliate, shed light on the multiple effects of defoliation on mortality. This was achieved by showing that defoliation indeed decreased carbon reserves in good years but could also limit the loss of hydraulic conductance during dry years. We also observed a significant interaction between defoliation and tree size on mortality, showing that small trees were more vulnerable to mortality in response to defoliation than large trees. However, we cannot rule out that this effect is due in part to the categorical method used to survey defoliation, which does not take into account the percentage of crown loss. Hence, defoliation may be biased with respect to size, such that small and defoliated trees will on average have a higher proportion of canopy loss, and therefore be more impacted than large and defoliated trees.

Thirdly, both statistical and process-based approaches found that trees with early budburst were more prone to die. By contrast, Robson et al. (2013) showed that trees with early budburst were not more vulnerable to mortality, but rather grew better, consistent with our simulations where trees with early budburst accumulate more reserves during good years. This discrepancy may be due to the location of our studied population at the rear-edge of beech distribution, where earlier budburst dates are observed due to higher temperature and may expose trees to a higher risk of late frost. It may be that the presence of trees with very early budburst in the studied

population makes it somewhat unusual, although similar cases have been observed elsewhere (Gaussen 1958; Perci du Sert 1982). In CASTANEA simulations, the higher risk of mortality of early trees resulted rather from a higher risk of hydraulic failure than a higher impact of late frosts. This is because trees with early budburst have a longer vegetation season and they develop their canopies faster, which also mechanically increases their water needs. Altogether, the relationships between phenology and mortality deserve further investigation, especially since the spatio-temporal variation of budburst patterns under climate change may produce complex spatio-temporal patterns of stresses (Vanoni et al. 2016).

Regarding the effect of size, the results differed between the statistical approach, where large trees died less than small ones, and the simulations, which predicted a greater risk of drought of large trees. There may be several explanations for this discrepancy. The first reason is that CASTANEA simulates an average tree without explicit competition for light and water; hence not accounting for the higher observed background mortality in small trees as compared to large ones (Figure S7). In addition, CASTANEA also does not account for individual dominance status, which can affect the current carbon balance of a tree and hence its capacity to mitigate stress. In the studied population, large trees are more likely to be dominant, with better access to light resources promoting carbon accumulation, as compared to small trees, which are more likely to be suppressed. Another reason is that tree size may vary with environmental factors in the studied population, such that large trees have a tendency to occur on better soils. Therefore, the size effect observed through the statistical approach may reveal the confounding effect of spatial soil heterogeneity, not taken into account in the PBM. A measurement of water availability at individual tree level would be necessary to address this issue but was out of the scope of this study.

Combining statistical and process-based approaches to identify the causes of tree risk of mortality

These two approaches illustrate the classical compromise between a fine understanding of physiological mechanisms driving mortality, with complex and expensive PBMs, versus high precision local mortality predictions, with statistical models requiring less data, but having a weaker ability to generalize. Most often, studies adopt either of the two approaches, and generally statistical approaches prevail (Hülsmann et al. 2016; Seidl et al. 2011). However, the two approaches are highly complementary, and combining them allows the deciphering of the respective roles of the drivers and mechanisms underlying tree mortality and understanding their variability among individuals or years (Hawkes 2000; O'Brien et al. 2017; Seidl et al. 2011). The two approaches can be simply compared as done in this study at the individual level, or they can be

more finely integrated as done when we analysed the correlation between the observed mortality rate and the simulated variables related to the response to stress. An upper level of integration would be inverse modelling, where observed mortality rates could be used to infer the physiological thresholds (e.g. in BoR, PLC and NLF) likely to trigger mortality (Davi & Cailleret 2017).

This study also illustrated a classical difficulty in combining statistical and process-based approaches, related to the difference between observed variables and PBM parameters. For instance, the comparison of defoliated and non-defoliated trees does not have exactly the same meaning when using CASTANEA and the statistical approach. In CASTANEA, we compared trees, able versus unable, to defoliate, while these average trees share on average the same edaphic conditions. In the statistical approach, we compared trees with different levels of defoliation, but which also probably did not share the same edaphic and biotic conditions: Defoliation was thus also likely to be an indicator of the fertility of the environment, such that on shallow soils, defoliation was stronger and the probability of mortality increased. Hence, the correlation does not necessarily involve a causal relationship between defoliation and mortality.

The major benefits of our approach combining different approaches (statistical, process-based) at different scales (population, individual) is that it allows us to disaggregate ecological patterns observed at an upper scale (population, multi-year period), and get back to patterns observed at a lower scale where processes operate (individual, year). This ability to aggregate/disaggregate patterns is acknowledged as a powerful approach to understand apparent contradictions between patterns observed at different scales (Clark et al. 2011). There are however some limitations to the approaches we used here. First, none of them could fully account for the non-independence of climatic effects on mortality between years. Indeed, the effect of climatic variables at a given year may depend on other variables expressed in previous years. This was observed in beech, where several drought years finally led to a growth decline (Jump et al. 2006; Knutzen et al. 2017; Vanoni et al. 2016) or a modification in sap flow (Hesse et al. 2019). Moreover, the processes driving mortality may change through time as the most sensitive individuals are progressively eliminated, and/or the surviving trees become less and less sensitive (i.e. acclimation Niinemets 2010). Finally, the statictical model at the individual level could not fully make use of the repeated measurements of mortality over the years, partly because other individual variables were measured only once over the study period (except defoliation). Survival analyses could unfortunately not fully address this limitation (Appendix 4), and the development of a finely tuned Bayesian approach was out of the scope of this study. Besides methodological improvements, another extension to the present study would be to combine statistical and process-based

approaches at a larger spatial scale, among populations across climatic gradients. This would allow the investigation of whether the respective drought and late frost sensitivity differ between the rear, core and leading edge of species distribution, as suggested by Cavin and Jump (2017).

Data accessibility

The data set analysed in this preprint is available online under the zenodo repository (https://doi.org/10.5281/zenodo.3519315**)**. Raw data can be obtained from JG, JAM and CH.

Supplementary material

The process-based model CASTANEA is an open-source software available on capsis website: http://capsis.cirad.fr/

Supplementary materials (Figures and Tables) for this preprint are available on bioRxiv (XXX).

Author Contributions

JAM, JG, CH and EM measured and mapped all the trees. CP performed the wood core analyses. CP, FL and SOM designed and ran the statistical models. CP and HD ran the PBM. CP drafted the manuscript, and all authors contributed to its improvement.

Acknowledgments

We are grateful to M. Cailleret, B. Fady, and N. Martin Saint Paul for discussions and comments on a previous version of this manuscript. We thank N. Mariotte for wood core sampling, and F. Guibal for their analyses. SOM and HD were funded by the EU ERA-NET BiodivERsA projects TIPTREE (BiodivERsA2-2012-15) and the ANR project MeCC (ANR-13-ADAP-0006). CP received funding from the European Union's Horizon 2020 research and innovation programme under grant agreement No. 676876 (GenTree).

Conflict of interest disclosure

The authors of this preprint declare that they have no financial conflict of interest with the content of this article. SOM is one of the PCIEcology recommenders.

References

Adams, Henry D. et al. 2017. “A Multi-Species Synthesis of Physiological Mechanisms in Drought-Induced Tree Mortality.” Nature Ecology and Evolution 1(9):1285–91.

Akaike, Hirotugu. 1987. “Factor Analysis and AIC.” Pp. 371–86 in. Springer, New York, NY.

Allen, Craig D. et al. 2010. “A Global Overview of Drought and Heat-Induced Tree Mortality Reveals Emerging Climate Change Risks for Forests.” Forest Ecology and Management 259(4):660–84.

Anderegg, W. R. L. et al. 2012. “From the Cover: The Roles of Hydraulic and Carbon Stress in a Widespread Climate-Induced Forest Die-Off.” Proceedings of the National Academy of Sciences 109(1):233–37.

Anderegg, William R. L. 2015a. “Spatial and Temporal Variation in Plant Hydraulic Traits and Their Relevance for Climate Change Impacts on Vegetation.” New Phytologist 205(3):1008–14.

Anderegg, William R. L. et al. 2015b. “Tree Mortality from Drought, Insects, and Their Interactions in a Changing Climate.” New Phytologist 208(3):674–83.

Archambeau, Juliette et al. 2019. “Similar Patterns of Background Mortality across Europe Are Mostly Driven by Drought in European Beech and a Combination of Drought and Competition in Scots Pine.” Agricultural and Forest Meteorology, 2020, vol. 280, p. 107772.

Arnold, Todd W. 2010. “Uninformative Parameters and Model Selection Using Akaike’s Information Criterion.” Journal of Wildlife Management 74(6):1175–78.

Augspurger, Carol K. 2009. “Spring 2007 Warmth and Frost: Phenology, Damage and Refoliation in a Temperate Deciduous Forest.” Functional Ecology 23(6):1031–39.

Ball, J. Timothy, Ian E. Woodrow, and Joseph A. Berry. 1987. “A Model Predicting Stomatal Conductance and Its Contribution to the Control of Photosynthesis under Different Environmental Conditions.” Pp. 221–24 in Progress in photosynthesis research. Springer.

Barnier, Julien, François Briatte, and Joseph Larmarange. 2018. “Questionr: Functions to Make Surveys Processing Easier.”

Bauch, Josef. 1986. “Characteristics and Response of Wood in Declining Trees from Forests Affected by Pollution.” IAWA Journal 7(4):269–76.

Beguería, Santiago and Sergio M. Vicente-Serrano. 2017. “SPEI: Calculation of the Standardised Precipitation-Evapotranspiration Index.”

Benito Garzón, Marta et al. 2018. “The Legacy of Water Deficit on Populations Having Experienced Negative Hydraulic Safety Margin.” Global Ecology and Biogeography 27(3):346–56.

Bigler, Christof and Harald Bugmann. 2018. “Climate-induced shifts in leaf unfolding and frost risk of European trees and shrubs.” Scientific Reports 8(1):1–10.

Brando, Paulo Monteiro et al. 2014. “Abrupt Increases in Amazonian Tree Mortality Due to Drought-Fire Interactions.” Proceedings of the National Academy of Sciences of the United States of America 111(17):6347–52.

Bréda, Nathalie, Roland Huc, André Granier, and Erwin Dreyer. 2006. “Temperate Forest Trees and Stands under Severe Drought : A Review of Ecophysiological Responses , Adaptation Processes and Long-Term Consequences.” Annals of Forest Science 63(6):625–44.

Brier, Glenn W. 1950. “Verification of Forecasts Expressed in Terms of Probability.” Monthey Weather Review 78(1):1–3.

De Caceres, Miquel, Nicolas Martin-StPaul, Marco Turco, Antoine Cabon, and Victor Granda. 2018. “Estimating Daily Meteorological Data and Downscaling Climate Models over Landscapes.” Environmental Modelling and Software 186–96.

Cailleret, Maxime et al. 2017. “A Synthesis of Radial Growth Patterns Preceding Tree Mortality.” Global Change Biology 23(4):1675–90.

Cailleret, Maxime and Hendrik Davi. 2011. “Effects of Climate on Diameter Growth of Co-Occurring Fagus Sylvatica and Abies Alba along an Altitudinal Gradient.” Trees 25(2):265–76.

Campbell, Gaylon S. 1974. “A Simple Method for Determining Unsaturated Conductivity from Moisture Retention Data.” Soil Science 117(6):311–14.
Carnicer, Jofre et al. 2011. “Widespread Crown Condition Decline, Food Web Disruption, and Amplified Tree Mortality with Increased Climate Change-Type Drought.” Proceedings of the National Academy of Sciences 108(4):1474–78.
Cavin, Liam and Alistair S. Jump. 2017. “Highest Drought Sensitivity and Lowest Resistance to Growth Suppression Are Found in the Range Core of the Tree Fagus Sylvatica L. Not the Equatorial Range Edge.” Global Change Biology 23(1):362–79.
Cheaib, Alissar et al. 2012. “Climate Change Impacts on Tree Ranges: Model Intercomparison Facilitates Understanding and Quantification of Uncertainty.” Ecology Letters 15(6):533–44.
Choat, Brendan et al. 2018. “Triggers of Tree Mortality under Drought.” Nature 558(7711):531–39.
Chuine, Isabelle, P. Cour, and D. D. Rousseau. 1999. “Selecting Models to Predict the Timing of Flowering of Temperate Trees: Implications for Tree Phenology Modelling.” Plant, Cell and Environment 22(1):1–13.
Clark, James S. et al. 2011. “Individual-Scale Variation, Species-Scale Differences: Inference Needed to Understand Diversity.” Ecology Letters 14(12):1273–87.
Collet, Catherine and Gilles Le Moguedec. 2007. “Individual Seedling Mortality as a Function of Size, Growth and Competition in Naturally Regenerated Beech Seedlings.” Forestry 80(4):359–70.
Cowan, I. R. and G. D. Farquhar. 1977. “Stomatal Function in Relation to Leaf Metabolism and Environment.” Symposia of the Society for Experimental Biology 31:471–505.
Cribari-Neto, Francisco and Achim Zeileis. 2010. “Beta Regression in R.” Journal of Statistical Software 34(2).
Davi, H. et al. 2005. “Modelling Carbon and Water Cycles in a Beech Forest. Part II.: Validation of the Main Processes from Organ to Stand Scale.” Ecological Modelling 185(2–4):387–405.
Davi, H., C. Barbaroux, C. Francois, and E. Dufrêne. 2009. “The Fundamental Role of Reserves and Hydraulic Constraints in Predicting LAI and Carbon Allocation in Forests.” Agricultural and Forest Meteorology 149(2):349–61.
Davi, Hendrik and Maxime Cailleret. 2017. “Assessing Drought-Driven Mortality Trees with Physiological Process-Based Models.” Agricultural and Forest Meteorology 232:279–90.
Dittmar, Christoph, Wolfgang Zech, and Wolfram Elling. 2003. “Growth Variations of Common Beech (Fagus Sylvatica L.) under Different Climatic and Environmental Conditions in Europe—a Dendroecological Study.” Forest Ecology and Management 173(1–3):63–78.
Dobbertin, Matthias and Peter Brang. 2001. “Crown Defoliation Improves Tree Mortality Models.” Forest Ecology and Management 141(3):271–84.
Dufrêne et al. 2005. “Modelling Carbon and Water Cycles in a Beech Forest Part I : Model Description and Uncertainty Analysis on Modelled NEE.” Ecological Modelling 185:407–36.
Durand-Gillmann, Marion, Maxime Cailleret, Thomas Boivin, Louis Michel Nageleisen, and Hendrik Davi. 2014. “Individual Vulnerability Factors of Silver Fir (Abies Alba Mill.) to Parasitism by Two Contrasting Biotic Agents: Mistletoe (Viscum Album L. Ssp. Abietis) and Bark Beetles (Coleoptera: Curculionidae: Scolytinae) during a Decline Process.” Annals of Forest Science 71(6):659–73.
Farquhar, G. D., S. von Caemmerer, and J. A. Berry. 1980. “A Biochemical Model of Photosynthetic CO2 Assimilation in Leaves of C3 Species.” Planta 149(1):78–90.
Feng, Xue et al. 2018. “The Ecohydrological Context of Drought and Classification of Plant Responses.” Ecology Letters, November 1, 1723–36.
Gao, Shan et al. 2018. “Dynamic Responses of Tree-Ring Growth to Multiple Dimensions of Drought.” Global Change Biology 24(11):5380–90.

García-Plazaola, José Ignacio, Raquel Esteban, Koldobika Hormaetxe, Beatriz Fernández-Marín, and José María Becerril. 2008. “Photoprotective Responses of Mediterranean and Atlantic Trees to the Extreme Heat-Wave of Summer 2003 in Southwestern Europe.” Trees 22(3):385–92.
Gaussen, H. 1958. “Le Hêtre Aux Pyrénées Espagnoles.” Pp. 185–91 in Actas del tercer congreso internacional de estudios pirenaicos, Gerona.
Gauzere, J. et al. 2017. “Integrating Interactive Effects of Chilling and Photoperiod in Phenological Process-Based Models. A Case Study with Two European Tree Species: Fagus Sylvatica and Quercus Petraea.” Agricultural and Forest Meteorology 244–245:9–20.
Gillner, Sten, Nadja Rüger, Andreas Roloff, and Uta Berger. 2013. “Low Relative Growth Rates Predict Future Mortality of Common Beech (Fagus Sylvatica L.).” Forest Ecology and Management 302:372–78.
Granier, A., P. Biron, and D. Lemoine. 2000. “Water Balance, Transpiration and Canopy Conductance in Two Beech Stands.” Agricultural and Forest Meteorology 100(4):291–308.
Greenwood, Sarah et al. 2017. “Tree Mortality across Biomes Is Promoted by Drought Intensity, Lower Wood Density and Higher Specific Leaf Area” edited by J. Chave. ECOLOGY LETTERS 20(4):539–53.
Hawkes, Corinna. 2000. “Woody Plant Mortality Algorithms: Description, Problems and Progress.” Ecological Modelling 126(2–3):225–48.
Hesse, Benjamin D., Michael Goisser, Henrik Hartmann, and Thorsten E. E. Grams. 2019. “Repeated Summer Drought Delays Sugar Export from the Leaf and Impairs Phloem Transport in Mature Beech” edited by M. Dannoura. Tree Physiology 39(2):192–200.
Hijmans, Robert J., Steven Phillips, John Leathwick, Jane Elith, and Maintainer Robert J. Hijmans. 2017. “Package ‘Dismo.’” Circles 9(1):1–68.
Hosmer, David W. and Stanley Lemeshow. 2000. Applied Logistic Regression.
Hülsmann, Lisa et al. 2016. “Does One Model Fit All? Patterns of Beech Mortality in Natural Forests of Three European Regions.” Ecological Applications 26(8):2463–77.
Hülsmann, Lisa, Harald Bugmann, and Peter Brang. 2017. “How to Predict Tree Death from Inventory Data – Lessons from a Systematic Assessment of European Tree Mortality Models - SUPP.” Canadian Journal of Forest Research (April):cjfr-2016-0224.
Hülsmann, Lisa, Harald Bugmann, Maxime Cailleret, and Peter Brang. 2018. “How to Kill a Tree: Empirical Mortality Models for 18 Species and Their Performance in a Dynamic Forest Model.” Ecological Applications 28(2):522–40.
IGN. 2016. La Mortalité. France. https://inventaire-forestier.ign.fr/IMG/pdf/2018_mortalite.pdf
Jump, Alistair S., Jenny M. Hunt, and Josep Peñuelas. 2006. “Rapid Climate Change-Related Growth Decline at the Southern Range Edge of Fagus Sylvatica.” Global Change Biology 12(11):2163–74.
Kneeshaw, Daniel D., Richard K. Kobe, K. David Coates, and Christian Messier. 2006. “Sapling Size Influences Shade Tolerance Ranking among Southern Boreal Tree Species.” Journal of Ecology 94(2):471–80.
Knutzen, Florian, Choimaa Dulamsuren, Ina Christin Meier, and Christoph Leuschner. 2017. “Recent Climate Warming-Related Growth Decline Impairs European Beech in the Center of Its Distribution Range.” Ecosystems 20(8):1494–1511.
Kramer, Koen et al. 2010. “Modelling Exploration of the Future of European Beech (Fagus Sylvatica L.) under Climate Change-Range, Abundance, Genetic Diversity and Adaptive Response.” Forest Ecology and Management 259(11):2213–22.
Lebourgeois, F., N. Bréda, E. Ulrich, and A. Granier. 2005. “Climate-Tree-Growth Relationships of European Beech (Fagus Sylvatica L.) in the French Permanent Plot Network (RENECOFOR).” Trees 19:385–401.

Lenz, Armando, Günter Hoch, Yann Vitasse, and Christian Körner. 2013. “European Deciduous Trees Exhibit Similar Safety Margins against Damage by Spring Freeze Events along Elevational Gradients.” New Phytologist 200(4):1166–75.
Lines, Emily R., David A. Coomes, and Drew W. Purves. 2010. “Influences of Forest Structure, Climate and Species Composition on Tree Mortality across the Eastern US” edited by A. Hector. PLoS ONE 5(10):e13212.
Long, Jacob A. 2018. “Jtools: Analysis and Presentation of Social Scientific Data.”
Lorenz, Martin and Georg Becher. 2012. Forest Condition in Europe.
Loustau, D., A. Granier, F. El Hadj Moussa, M. Sartore, and M. Guedon. 1990. “Evolution Saisonnière Du Flux de Sève Dans Un Peuplement de Pins Maritimes.” Annales Des Sciences Forestières 47(6):599–618.
Van Mantgem, Phillip J. et al. 2009. “Widespread Increase of Tree Mortality Rates in the Western United States.” Science 323(5913):521–24.
Maraun, Mark, Jörg-Alfred Salamon, Katja Schneider, Matthias Schaefer, and Stefan Scheu. 2003. “Oribatid Mite and Collembolan Diversity, Density and Community Structure in a Moder Beech Forest (Fagus Sylvatica): Effects of Mechanical Perturbations.” Soil Biology and Biochemistry 35(10):1387–94.
Martin, George L. and Alan R. Ek. 1984. “A Comparison of Competition Measures and Growth Models for Predicting Plantation Red Pine Diameter and Height Growth.” Forest Science 30(3):731–43.
McDowell, Nate G. et al. 2013. “Evaluating Theories of Drought-Induced Vegetation Mortality Using a Multimodel-Experiment Framework.” New Phytologist 200(2):304–21.
McDowell, Nate G. et al. 2011. “The Interdependence of Mechanisms Underlying Climate-Driven Vegetation Mortality.” Trends in Ecology & Evolution 26(10):523–32.
Meir, Patrick, Maurizio Mencuccini, and Roderick C. Dewar. 2015. “Drought-Related Tree Mortality: Addressing the Gaps in Understanding and Prediction.” New Phytologist 207(1):1443–47.
Menzel, Annette, Raimund Helm, and Christian Zang. 2015. “Patterns of Late Spring Frost Leaf Damage and Recovery in a European Beech (Fagus Sylvatica L.) Stand in South-Eastern Germany Based on Repeated Digital Photographs.” Frontiers in Plant Science 6:110.
Monserud, Robert A. 1976. “Simulation of Forest Tree Mortality.” Forest Science 22(4):438–44.
Monteith, J. L. 1965. “Evaporation and Environment. The State and Movement of Water in Living Organisms. Symposium of the Society of Experimental Biology, Vol. 19 (Pp. 205-234).”
Mueller, Rebecca C. et al. 2005. “Differential Tree Mortality in Response to Severe Drought: Evidence for Long-Term Vegetation Shifts.” Journal of Ecology 93(6):1085–93.
Niinemets, Ülo. 2010. “Responses of Forest Trees to Single and Multiple Environmental Stresses from Seedlings to Mature Plants: Past Stress History, Stress Interactions, Tolerance and Acclimation.” Forest Ecology and Management 260(10):1623–39.
Nourtier, Marie et al. 2014. “Transpiration of Silver Fir (Abies Alba Mill.) during and after Drought in Relation to Soil Properties in a Mediterranean Mountain Area.” Annals of Forest Science 71(6):683–95.
O’Brien, Michael J. et al. 2017. “A Synthesis of Tree Functional Traits Related to Drought-Induced Mortality in Forests across Climatic Zones. Journal of Applied Ecology 54(6):1669–86.
O’Brien, Michael J., Sebastian Leuzinger, Christopher D. Philipson, John Tay, and Andy Hector. 2014. “Drought Survival of Tropical Tree Seedlings Enhanced by Non-Structural Carbohydrate Levels.” Nature Climate Change 4(8):710–14.
Pammenter NW and Vander Willigen C. 1998. “A Mathematical and Statistical Analysis of the Curves Illustrating Vulnerability of Xylem to Cavitation.” Tree Physiology 18(Equation 1):589–593.
Penuelas, Josep and Martí Boada. 2003. “A Global Change-Induced Biome Shift in the Montseny Mountains (NE Spain).” Global Change Biology 9(2):131–40.

Perci du Sert, Th. 1982. Relations Entre La Phenologie et La Morphologie Du Hêtre Dans Le Massif Des Albères.
Pretzsch, Hans. 1996. “Growth Trends of Forests in Southern Germany.” Pp. 107–31 in Growth Trends in European Forests. Berlin, Heidelberg: Springer Berlin Heidelberg.
Robson, T. Matthew, Erwin Rasztovits, Pedro J. Aphalo, Ricardo Alia, and Ismael Aranda. 2013. “Flushing Phenology and Fitness of European Beech (Fagus Sylvatica L.) Provenances from a Trial in La Rioja, Spain, Segregate According to Their Climate of Origin.” Agricultural and Forest Meteorology 180:76–85.
Ryan, Michael G. 1991. “Effects of Climate Change on Plant Respiration.” Ecological Applications 1(2):157–67.
Sala, A. and J. D. Tenhunen. 1996. “Simulations of Canopy Net Photosynthesis and Transpiration in Quercus Ilex L. under the Influence of Seasonal Drought.” Agricultural and Forest Meteorology 78(3–4):203–22.
Schielzeth, Holger. 2010. “Simple Means to Improve the Interpretability of Regression Coefficients.” Methods in Ecology and Evolution 1(2):103–13.
Seidl, Rupert et al. 2011. “Modelling Natural Disturbances in Forest Ecosystems: A Review.” Ecological Modelling 222(4):903–24.
Senf, Cornelius et al. 2018. “Canopy Mortality Has Doubled in Europe’s Temperate Forests over the Last Three Decades.” Nature Communications 9(1):4978.
Sevanto, Sanna, Nate G. Mcdowell, L. Turin Dickman, Robert Pangle, and William T. Pockman. 2014. “How Do Trees Die? A Test of the Hydraulic Failure and Carbon Starvation Hypotheses.” Plant, Cell and Environment 37(1):153–61.
Stadt, Kenneth J. et al. 2007. “Evaluation of Competition and Light Estimation Indices for Predicting Diameter Growth in Mature Boreal Mixed Forests.” Annals of Forest Science 64(64):477–90.
Thuiller, Wilfried, Sandra Lavorel, M. B. Araujo, Martin T. Sykes, and I. Colin Prentice. 2005. “Climate Change Threats to Plant Diversity in Europe.” Proceedings of the National Academy of Sciences 102(23):8245–50.
Tyree, M. T. and J. S. Sperry. 1989. “Vulnerability of Xylem to Cavitation and Embolism.” Annual Review of Plant Physiology and Plant Molecular Biology 40(1):19–36.
Vanoni, Marco, Harald Bugmann, Magdalena Nötzli, and Christof Bigler. 2016. “Drought and Frost Contribute to Abrupt Growth Decreases before Tree Mortality in Nine Temperate Tree Species.” Forest Ecology and Management Journal 382:51–63.
Vidal, Jean-Philippe, Eric Martin, Laurent Franchistéguy, Martine Baillon, and Jean-Michel Soubeyroux. 2010. “A 50-Year High-Resolution Atmospheric Reanalysis over France with the Safran System.” International Journal of Climatology 30(11):1627–44.
Vitasse, Yann et al. 2009. “Leaf Phenology Sensitivity to Temperature in European Trees: Do within-Species Populations Exhibit Similar Responses?” Agricultural and Forest Meteorology 149(5):735–44.
De Vries, F. W. T. Pennin., A. H. M. Brunsting, and H. H. Van Laar. 1974. “Products, Requirements and Efficiency of Biosynthesis a Quantitative Approach.” Journal of Theoretical Biology 45(2):339–77.

Appendices

Four supplementary appendices are available on bioRxiv (XXX):

Appendix 1: Beta-regression model for mortality rate at population-level

Appendix 2: CASTANEA calibration and simulations

Appendix 3: Logistic regression models for the probability of mortality at tree-level

Appendix 4: Survival analysis of the probability of mortality at tree- and year-levels

3 Supplementary online material

Supplementary Materials for the manuscript "Combining statistical and mechanistic models to identify the drivers of mortality within a rear-edge beech population", by Cathleen Petit-Cailleux, Hendrik Davi, François Lefevre, Christophe Hurson, Joseph Garrigue, Jean-André Magdalou, Elodie Magnanou and Sylvie Oddou-Muratorio

Figure S1: European climatic niche of *Fagus sylvatica* as depicted by the sum of precipitation and the mean annual temperature. For the 1358 locations (black empty dots) where beech is documented as present by Georg von Wühlisch (2008), we used climate series available from Weedon et al. (2014) to compute average values of each climatic variable from 1976 to 2008**.** The red full dot is the studied site of La Massane.

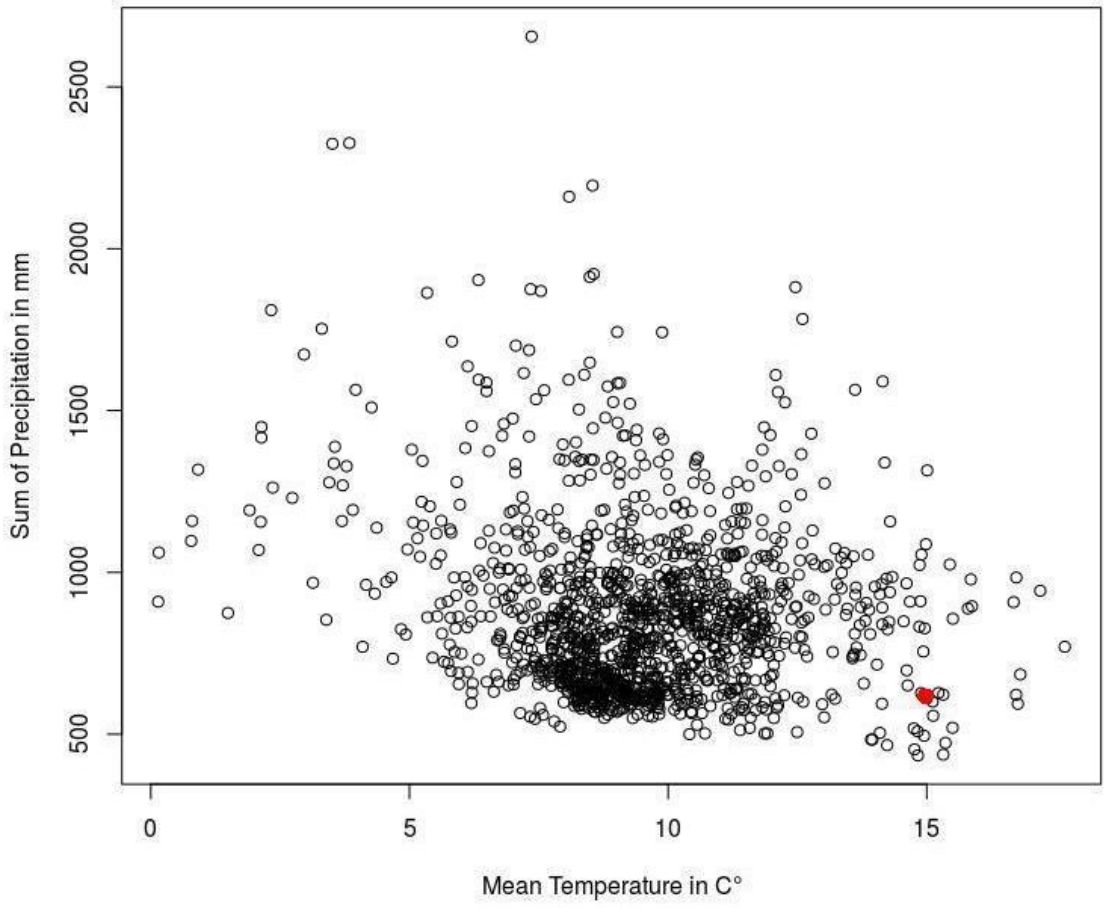

Georg von Wühlisch. **2008**. *EUFORGEN Technical Guidelines for genetic conservation and use for European beech (Fagus sylvatica).* Rome, Italy.

Weedon GP, Balsamo G, Bellouin N, Gomes S, Best MJ, Viterbo P. **2014**. The WFDEI meteorological forcing data set: WATCH Forcing Data methodology applied to ERA-Interim reanalysis data. *Water Resources Research* **50**: 7505–7514.

Figure S2: Ombro-thermic diagram of the studied site (La Massane) between 1976 and 2016. The blue histogram represents the average amount of precipitation per month, with vertical bars showing their standard deviation. The black curve represents the average temperature of each month, and the dotted lines represent its standard deviation.

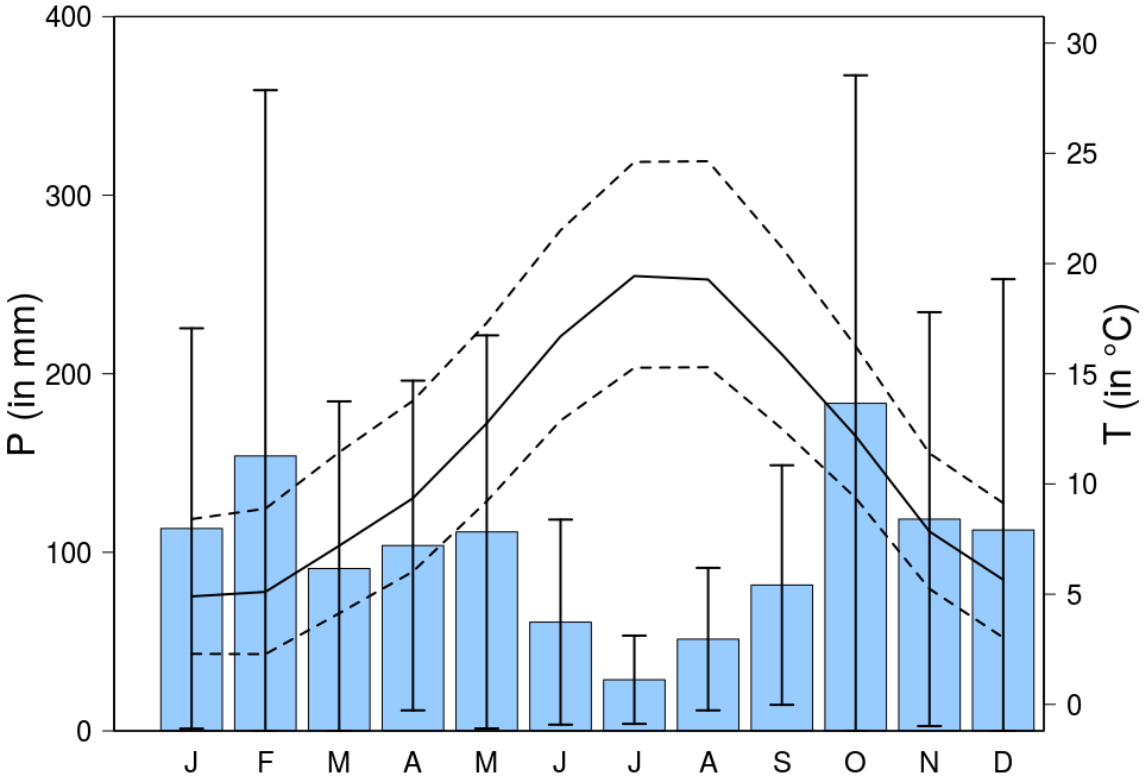

Figure S3: Spatial distribution of trees in the studied site La Massane. Dot's size is proportional to tree diameter at breast height (DBH_{2002}) and only tree with DBH2002> superior to 10 cm are shown (and studied).

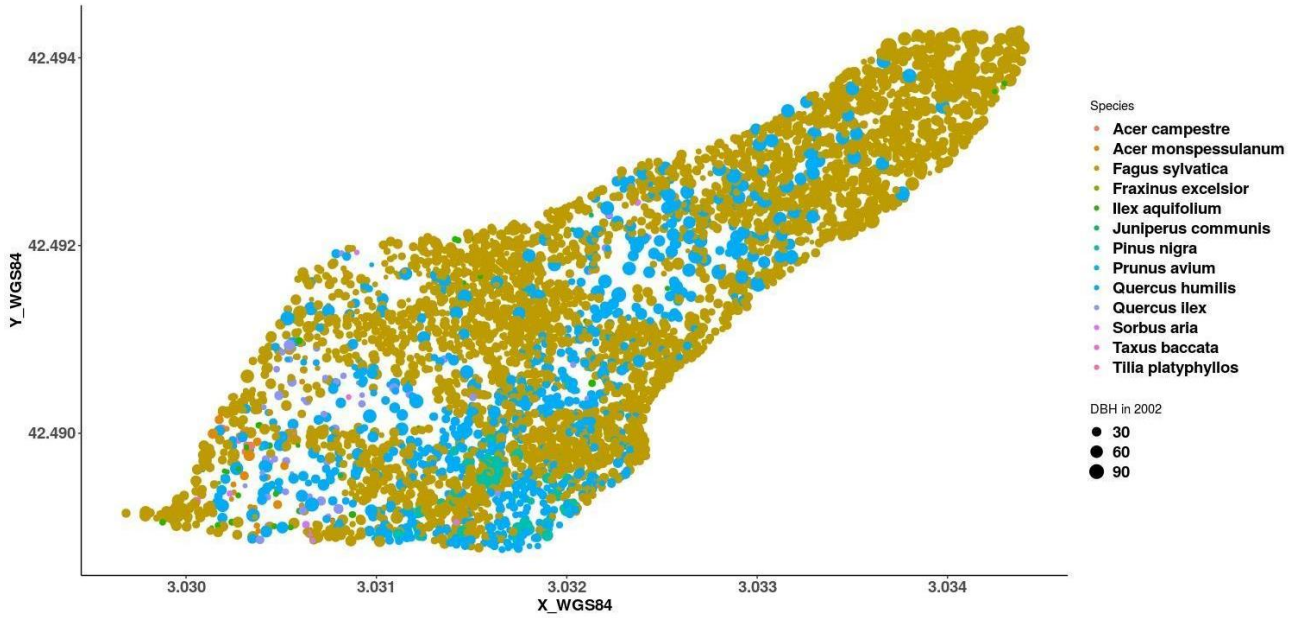

Figure S4: Spatial distribution of alive (blue dots) and dead (pink dots) beech trees at the end of the studied period (2004-2016). Dot's size is proportional to DBH_{2002}.

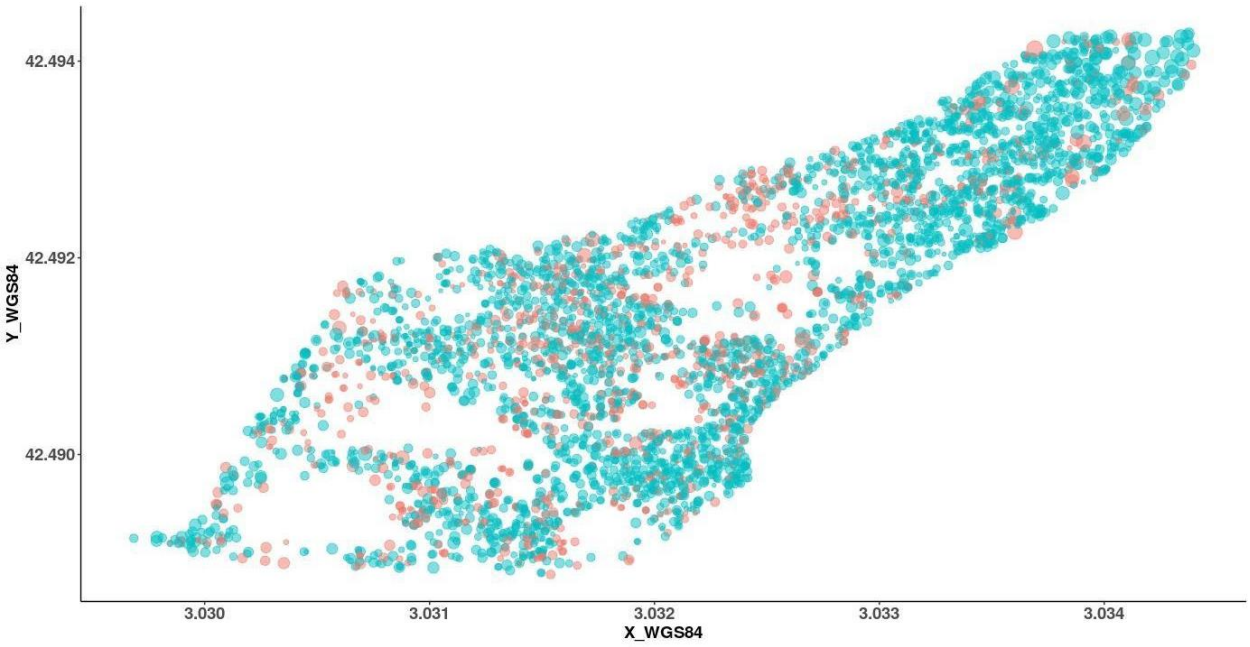

Figure S5: Pairwise distribution and correlations among quantitative variables (see table 1 for notations)

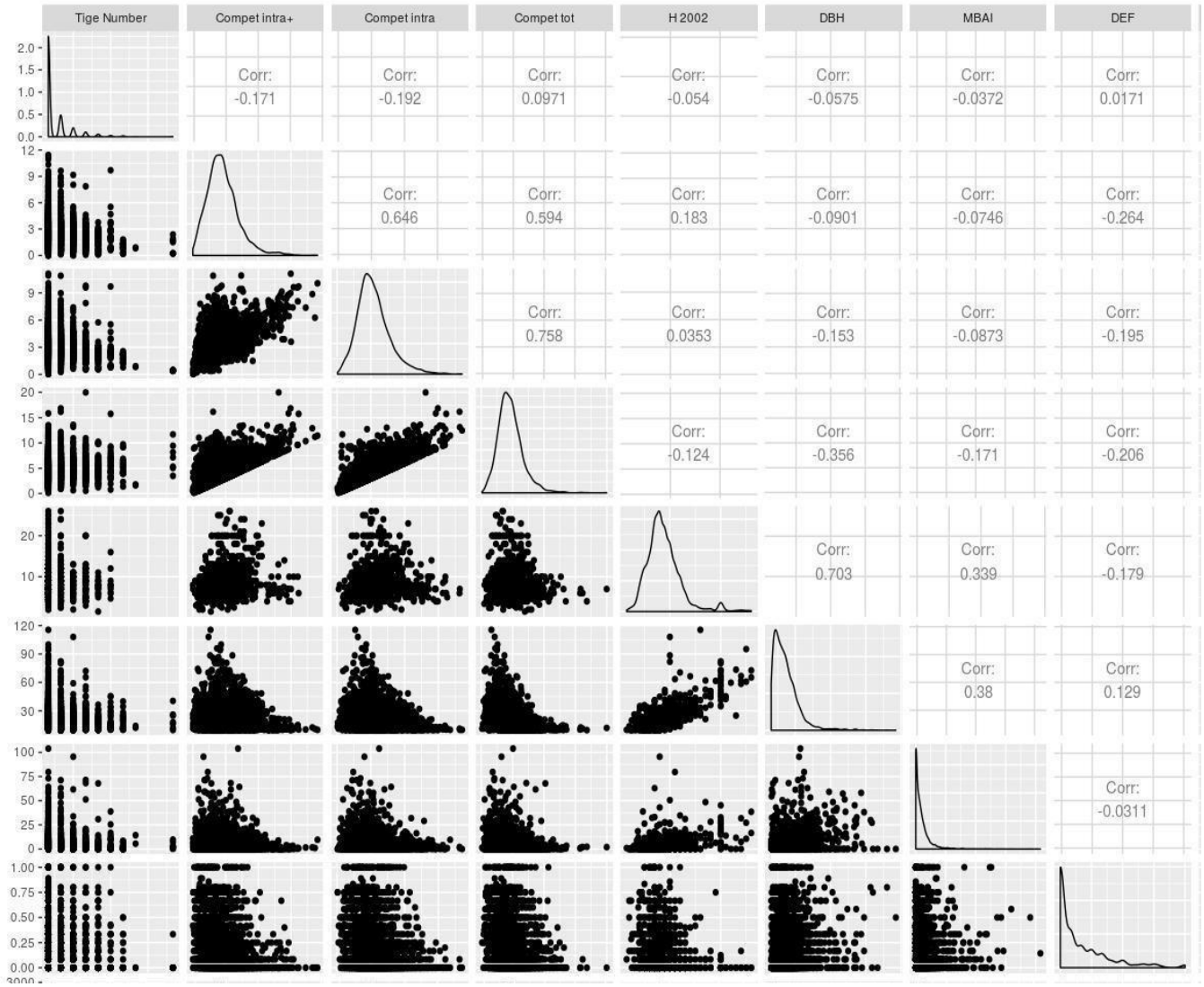

Figure S6: Impact of budburst phenology on Percentage of Loss of Conductance (PLC) and Biomass of reserve (BoR) simulated by CASTANEA. Triangles indicate trees with early budburst. Round symbol with dashed lines indicate trees with normal budburst . The initial DBH at the beginning of the simulation was 40 cm, and trees were not able to defoliate.

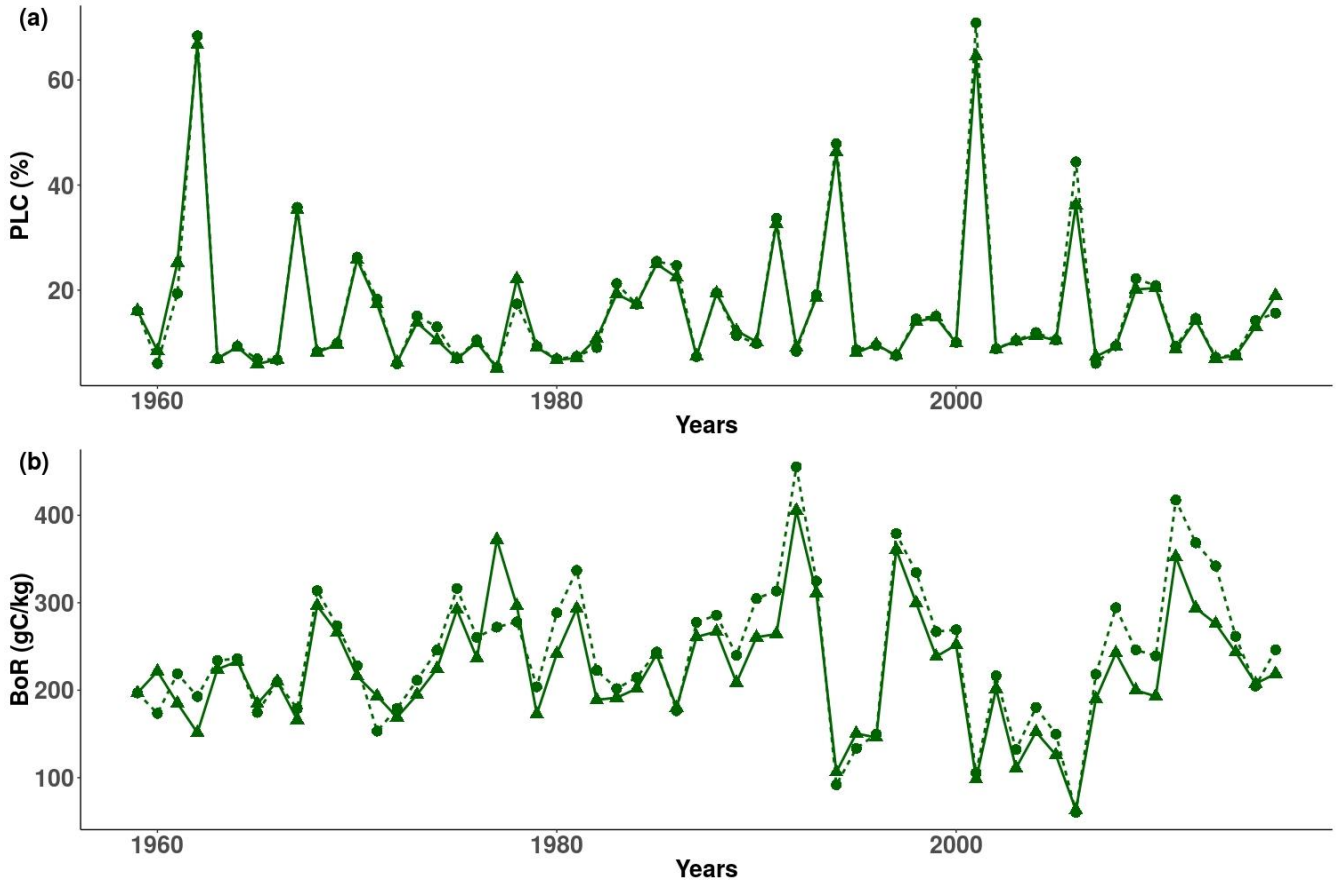

Table S1 - Observed mortality rates, measured climatic variables and simulated stress-related output variables of CASTANEA from year 2004 to year 2016.

Year	2004	2005	2006	2007	2008	2009	2010	2011	2012	2013	2014	2015	2016
Mortality rate in %	2.6	1.9	3.3	2.8	0.8	1.0	2.9	1.7	2.1	1.9	1.8	1.4	1.0
SPEI3_JJA	2.73	1.14	-2.39	0.12	-0.26	-1.67	0.91	0.88	-0.09	0.66	0.16	-1.43	-0.33
SPEI_dryVg	-0.26	-1.57	-1.45	-0.95	-0.78	-0.6	-0.74	-1.27	-0.02	0.47	-0.95	-1.63	0.31
PLC	0.09	0.09	0.31	0.06	0.09	0.16	0.16	0.08	0.13	0.07	0.06	0.12	0.1
BoR	147.32	122.12	51.1	197.17	248.22	212.43	185.71	354.24	286.18	256.9	219.7	175	18912
NLF	3.27	5.76	1.11	0.29	0.89	1.00	7.56	1.05	6.39	4.26	1.03	2.6	0.2

Table S2: Summary of the main effects of the studied variables on mortality, both at population-level (1) and tree-level (2).

(1) When and how do climate variations trigger mortality at population level ?			
Variables	**Related climate stress**	**Statistical model**	**PBM**
SPEI3_JJA	average drought level	Significant main and interaction effects	Not meaningful
SPEI_dryVg1mt	drought intensity		
NLF (number of late frost days)	late frost	Not available	Not directly correlated with observed mortality rate
PLC (percentage of loss conductance)	drought	Not available	Not directly correlated with observed mortality rate
BoR (Biomass of reserve)	late frost &drought	Not available	Not directly correlated with observed mortality rate
CVI	PLC + NLF - BoR	Not available	Positively correlated with observed mortality rate
(2) How do factors varying at tree-level modulate the individual tree's probability of mortality?			
Variables		**Statistical model**	**PBM**
Crown defoliation		Associated to a strong increase in mortality, especially for small trees	Associated to a lower BoR but also to a lower PLC
Size (DBH)		The smallest and the largest trees had a higher mortality	Large trees had always a lower BoR, and a higher PLC in drought year
Growth (MBAI)		Fast-growing trees had a lower mortality (evident only for small trees)	Not tested
Budburst phenology		Tree with earlier budburst had a higher mortality	Tree with earlier budburst had a lower PLC in drought year
Competition (Number of stems)		Increasing competition was associated to a higher mortality	Not tested
Presence of fungi		Tree with fungi had a higher mortality	Not tested

4 Appendices

Appendices for the manuscript "Combining statistical and mechanistic models to identify the drivers of mortality within a rear-edge beech population", by Cathleen Petit-Cailleux, Hendrik Davi, François Lefevre, Christophe Hurson, Joseph Garrigue, Jean-André Magdalou, Elodie Magnanou and Sylvie Oddou-Muratorio

Contents

Appendix 1: Beta-regression model for mortality at population-level.

1–SPEI variables considered in the beta-regression model

The Standardised Precipitation-Evapotranspiration Index (SPEI) is a multiscalar drought index based on climatic data varying between -2 and 2. It can be used for determining the onset, duration and magnitude of drought conditions with respect to normal conditions. We used the package SPEI (Beguería & Vicente-Serrano, 2017) to compute monthly SPEI-values from 1970 to 2015 considering two possible period of references for the "normal conditions" (respectively one and three month before the considered period). We gave the same weight to all previous months and used a uniform distribution to do it. Moreover, we modified the calibration of evapotranspiration (ETP), adapted to crop in SPEI package; we used instead the ETP estimation provided by the mechanistic model (CASTANEA). Then, for each of the two monthly SPEI series, we computed 2 SPEI variables for each year from 1970 to 2015. SPEI3_JJA is the mean SPEI computed over June, July and August, taking into account the precipitation of from April to August. SPEI1_dryVg is the minimum SPEI reach over April to August, taking into account the precipitation of from April to August,

Note that the SPEI3_JJA represent the drought over June, July and August with SPEI computed from the last three months. Hence, the months are weighted as 1,2,3,2,1 (April, May, June, July, August). Values of the variables are in the table S2.

2 – Model fit

Table A1.2: Parameter estimates and related statistics for beta-regression model described by equation 8. β is the maximum likelihood estimate, with its estimated error (SE), z-value, and associated p-value (Pr(>|z|). OR is the odds ratio. VIF is the generalized collinearity diagnostic value (variance inflation factor).

Variables	β	**Std.Error**	**z-value**	**p-value**	**OR**	**VIF**
SPEI1_dryVg	-0.15	0.16	-0.96	0.33	$8.60e^{-1}$	1.16
SPEI3_JJA	0.37	0.16	2.25	0.02	1.46	3.51
SPEI1_dryVg:SPEI3_JJA	0.31	0.16	1.89	0.06	1.36	3.28
(phi)	435.	172.6	2.53	0.01	$2.07e^{18}$	

	9				9	

3 –Model validation

The best model had a good validity (VIF < 4) and goodness-of-fit (0.42 of R^2) (Table A1.2) VIF were computed with the package “car” (Fox & Weisberg, 2011). With the diagnostic plot (Figure A1.3), we did not observe any trends in the residues, which means that there is no detectable temporal autocorrelation. We observed that 3 years have a higher impact than expected randomly on the model prediction 2004, 2006 and 2015 (ie. cook distance > 0.5). For the first two leverage points, this is not surprising since these two years have high mortality rates.

Figure A1.3: Diagnostic plot of the beta-regression. From the top left to the bottom right: Residuals vs. indices of observation; Cook’s distance plot; Generalized leverage vs predicted values; Residuals vs linear predictor.

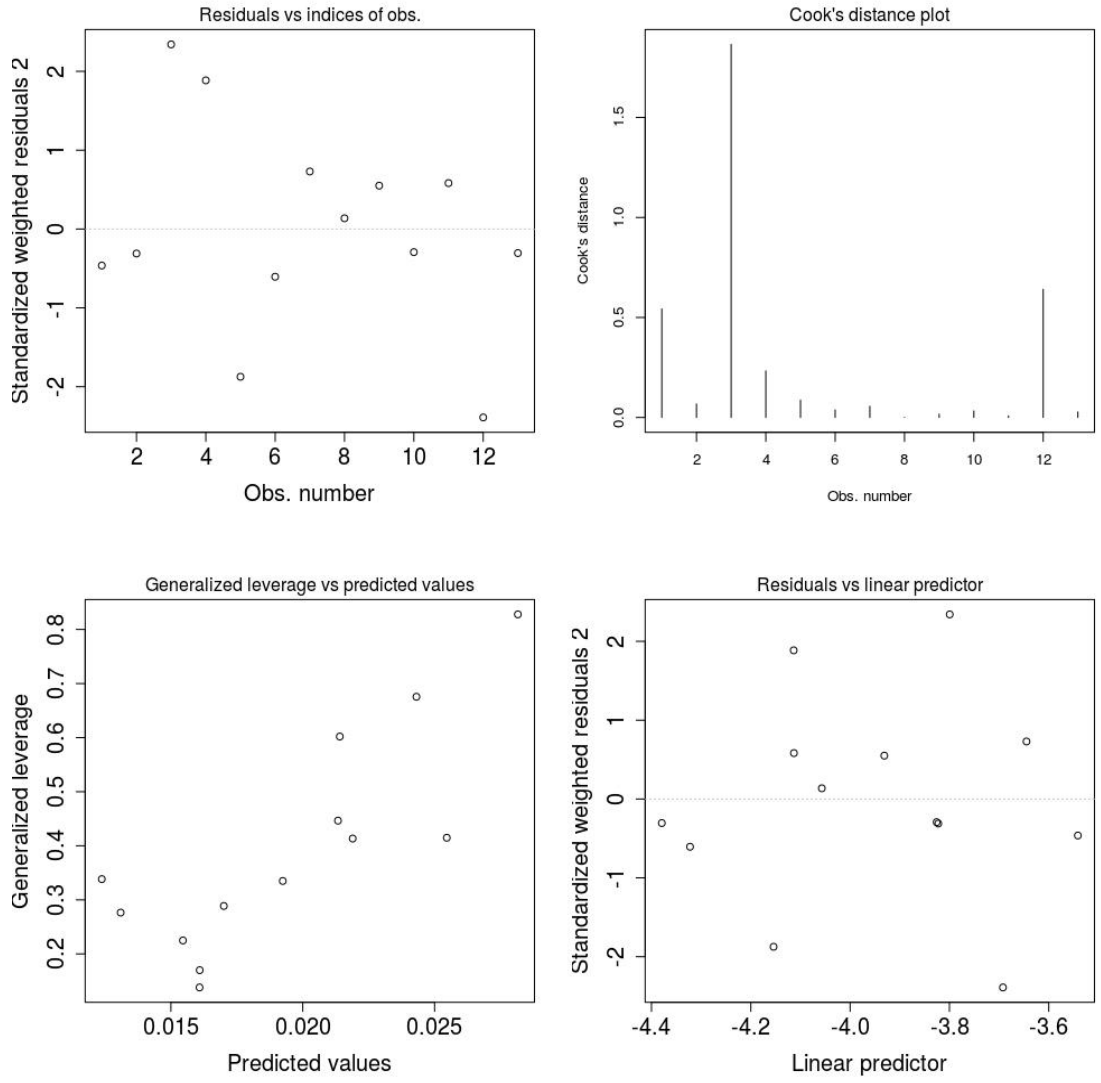

Appendix 2: CASTANEA details, calibration and simulations

1 - Modelling late frost damage

Here, we used the UniForc model a one-phase model, describing the cumulative effect of forcing temperatures on bud development during the ecodormancy phase (Chuine et al., 1999). Budburst occurs when the accumulated rate of forcing R_f (Eqn. 1) reaches F∗:

$$\sum_{d=t_0}^{t_f} R_f(T_d) \geq F^*$$

R_f is calculated as a sigmoid function

$$\frac{1}{1+e^{-d_t(T_d-T_{50})}}$$

with d_T the positive slope and T_{50} the mid-response temperature of the sigmoid function.

The level of frost damage was estimated using the following equations :

$$leafFrostDamage(t+1)=min\left(1;leafFrostDamage(t)+\frac{1}{1+\exp\left(BF*frostHardiness-T_{min}\right)}\right)$$

With T_{min} the minimal daily temperature, DL the day length and BF is a factor estimated as following:

$$BF=-0.3-1.5\times\exp\left(0.1\times frostHardiness\right)$$

The frost hardiness was calculated as following:

$$frostHardiness(t+1)=frostHardiness(t)\times\frac{4}{5}+\frac{1}{5}\times\left(FH_{minfe}+CR\times\left(dFHti+dFHpi\right)\right)$$

$$With\begin{cases}if\left(T_{min}>T_{e1}\right)dFHti=0\\if\left(T_{min}<T_{e1}\wedge T_{min}>T_{e2}\right)dFHti=¿\\if\left(T_{min}<T_{e2}\right)dFHti=FHtfemax\end{cases}FHtfemax-\frac{FHtfemax}{T_{e1}-T_{e2}}\times\left(T_{min}-T_{e2}\right)$$

$$With\begin{cases}if\left(DL>NL2\right)dFHpi=0\\if\left(DL<NL1\right)dFHpi=FHpfemax\\if\left(DL<NL2\wedge DL>NL1\right)dFHpi=FHpfemax-\frac{FHpfemax}{NL1-NL2}\times\left(DL-NL2\right)\end{cases}$$

Then the effect of these damages was modeled according to three modalities: no effect, an effect with a definite decrease of the LAI, a decrease of the LAI followed by a new leaf flush. When unfolding leaves are affected by frost, decreased of leaf area index (LAI) is simulated every day using the following equation:

$$LAI=LAI_{initial}\left(1-leafFrostDamage\right)$$

2 - Calibration

We simulated a population of 100 trees representing the mean (and possibly the variability) in individual characteristics observed in La Massane in terms of height-diameter allometry (fixed), diameter (variable), leaf area index (fixed) and budburst phenology (variable).

The values of DBH were randomly drawn for each mean individual in a gamma law with mean and standard deviation measured in the whole population.

Budburst was simulated following equation 1-3 detailed in Oddou-Muratorio and Davi (2014), with the inter-individual variability in budburst date generated by varying a single parameter, FcritBB, the critical value of the state of forcing, which is most commonly referred to as the temperature sum required for budburst. We considered that the population was composed of 10 trees with a low FcritBB-value (early budburst), and of 90 trees with a the FcritBB-value observed for beech (“normal” budburst).

We also simulated a range of SWCa conditions representing the variability in SWCa in the site (TableA2.1). Height-diameter allometry (agF) was computed by simple linear regression (agF =1.26746). The LAI-value measured in La Massane is 4.48.

Inventory files for CASTANEA simulation are available in the Zenodo repository : https://doi.org/10.5281/zenodo.3519315 .

Table A2.1 Values of parameters used for simulations at population-level. Distribution law used to draw parameters values (S.Law); respective mean and standard deviation (sd) for the Gaussian law; respective shape and rate of the Gamma law. Units of the variables.

Variables	S.Law	Mean	sd	shape	rate	units
SWCa	Gaussian	167.90	22.88	-	-	
Fcrit for trees with early budburst	Gaussian	41	5	-	-	
Fcrit for other trees	Gaussian	33	5	-	-	
DBH	Gamma	-	-	0.80	0.06	cm

2- Validation

Method: To evaluate CASTANEA simulations, we used ring width profiles measured on 100 beech trees from the study site with contrasted size and defoliation characteristics. Cores were extracted in February 2016 at 1.30m above ground. After sanding, cores were scanned at 1200 dpi. Boundary rings were read using. Nine trees were excluded due to fungal contamination presence or unreadable ring width (indistinguishable RW or friable wood). Ring width were measured, and each individual series was cross-dated to check for missing rings and dating errors using the softwares Cdendro 9.0 and CooRecorder v 9.0 (Cybis Elektronik & Data AB. Sweden).

Results and discussion: Annual ring widths simulated by CASTANEA over the period from 1959 to 2015 were significantly correlated to the observed ring widths with an R^2 of 0.58 (p.value = 2.7e-6). (Fig. A2.1). Beyond this global correlation, two discrepancies between simulated and observed growth were noticeable (Fig. A2.2). CASTANEA simulated a trend in decreasing ring width, which was not mirrored in observed ring widths. Moreover, during two periods (from 1981 to 1992 and from 2000 to 2015), CASTANEA simulated depressions in ring widths, which were not mirrored in observed ring widths. This can be due to a slackening of competition in the observed population due for instance to tree mortality. Indeed, CASTANEA does not account for changes in tree dominance status, which can affect their current carbon balance and hence their growth.

Figure A2.1 observed (x-axis) vs simulated ring width (y-axis) from 1960 to 2015. Full line is the first bissectrice. Simulated ones are overestimated but the correlation of variations is significant 0.58 (pval= $2.66.10^{-6}$) .

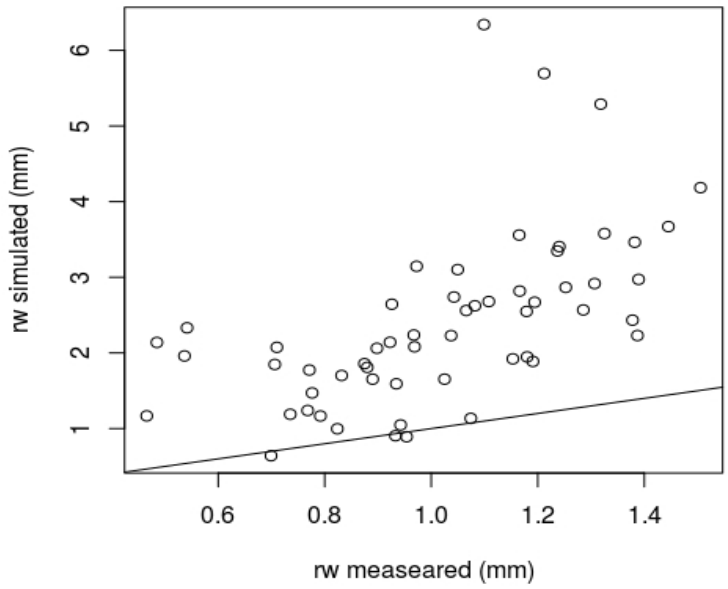

Figure A2.2 observed Ring width (grey) vs simulated ring width (blue) from 1960 to 2015. Grey dotted line is the mean observed ring width chronology. The grey envelope corresponds to the maximum and minimum ring width observed. Blue line is the mean simulated ring width. Blue envelope is the maximum and minimum simulated ring width.

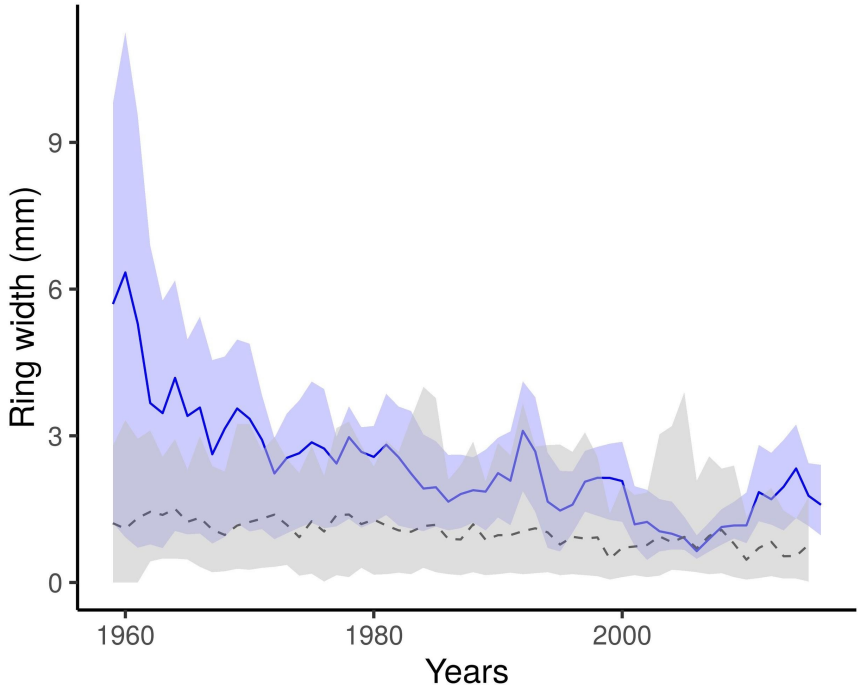

Appendix 3: Logistic regression models for the probability of mortality at tree-level

This appendix aims to present the procedure of variable selection for the logistic regression model presented in equation 9 in the main document:

$$P_{mortality} = [DEFw + Fungi + Budburst + MBAI + (Nstem \textbf{ OR } Compet_{intra} \textbf{ OR } Compet_{intra+} \textbf{ OR } Compet_{inter})] \times (DBH_{2002} + DBH_{2002}^2)$$

where $P_{mortality}$ is the individual probability of mortality; defoliation (DEFw), growth (MBAI), size (DBH_{2002}) and competition (Nstem and the Compet indices) factors were quantitative variables, while fungus presence (Fungi) and budburst phenology were categorical variables.

The section (1) presents the procedure for variable selection. Sections 2 to 4 present three alternative models where (2) DBH is considered as a categorical variable (instead of quantitative variable), (3) only non-clonal trees (ie with Nstem=1) are considered and (4) height in 2002 is considered instead of DBH.

1- Variables and model selection

Table A3.1 Comparison between models. This table was built using MuMin package, and gives the name of the model ("step_" are the model after stepwise selection); the variables present in the model, degree of freedom (df) ; the log-likelihood (logLik); the value of the information criterion used (AICc) ; the delta AIC (delta); and 'Akaike weight' (weight).

Model Name	Variables	df	logLik	AICc	delta	weight
step_Nstem	Fungi+Budburst+ Nstem+ (MBAI+ DEFw)×(DBH_{2002}+ DBH_{2002}^2)	12	-1 631.58	3 287.23	0	0.95
step_intra	Fungi+Budburst+ (MBAI +DEFw)×(DBH_{2002}+ DBH_{2002}^2)	11	-1 637.12	3 296.31	9.08	0.01
step_intra+	Fungi+Budburst+ (MBAI+DEFw)×(DBH_{2002}+ DBH_{2002}^2)	11	-1 637.12	3 296.31	9.08	0.01
step_tot	Fungi+Budburst+MBAI+DEFw ×(DBH_{2002}+ DBH_{2002}^2)	11	-1 637.12	3 296.31	9.08	0.01
model_Nstem	[DEFw+Fungi+Budburst+MBAI+ Nstem] ×(DBH_{2002}+ DBH_{2002}^2)	18	-1 630.55	3 297.25	10.02	0.01
model_intra	[DEFw+Fungi+Budburst+M	18	-1	3	12.39	0

+	BAI+ $Compet_{intra+}$]×(DBH_{2002}+ DBH_{2002}^2)		631.73	299.62		
model_intra	[DEFw+Fungi+Budburst+MBAI+ $Compet_{intra}$]×(DBH_{2002}+ DBH_{2002}^2)	18	-1 634.07	3 304.30	17.07	0
model_tot	[DEFw+Fungi+Budburst+MBAI+ $Compet_{tot}$]×(DBH_{2002}+ DBH_{2002}^2)	18	-1 634.65	3 305.46	18.23	0

Table A3.2 Variables influences in the best model (step_Nstem) and model validation. Df are the degrees of freedom. Dev is the deviance associated. AIC is the AIC of the model if the variable is removed. LRT is the likelihood ratio test between the complete model and the model with the variable removed, with its associated p-value. $GVIF^{1/2df}$ is the generalized collinearity diagnostic value taking into account the different dimensions of the variables with Df. The Brier score of the model is 0.11 and the goodness of fit (GoF) computed with the roc curve (area under the curve) is 0.82.

Variables	**Df**	**Dev.**	**AIC**	**LRT**	**p-value**	**GVIF**	**$GVIF^{1/2df}$**
DEFw	1	4348	4370	1084.89	< 0.001	1.224	1.106
DBH_{2002}+DBH_{2002}^2	2	3291.8	3311.8	28.69	< 0.001	5.584	1.537
MBAI	1	3305	3327	41.83	< 0.001	1.540	1.241
Budburst	1	3283.7	3305.7	20.5	< 0.001	1.013	1.007
Nstem	1	3274.2	3296.2	11.09	< 0.001	< 0.001	1.005
Fungi	1	3278.2	3300.2	15.09	< 0.001	1.198	1.095
DEFw: (DBH_{2002}+DBH_{2002}^2)	2	3279.2	3299.2	16.08	< 0.001	6.293	1.584
MBAI: (DBH_{2002}+DBH_{2002}^2)	2	3267.5	3287.5	4.35	0.1141	4.534	1.459

Fig A3.1: ROC curve. Percent of true positives (sensitivity 49%) against percent of false positives (1 – specificity 51%). The percentage of true negatives is 96% and the percentage of false negatives is 4%.

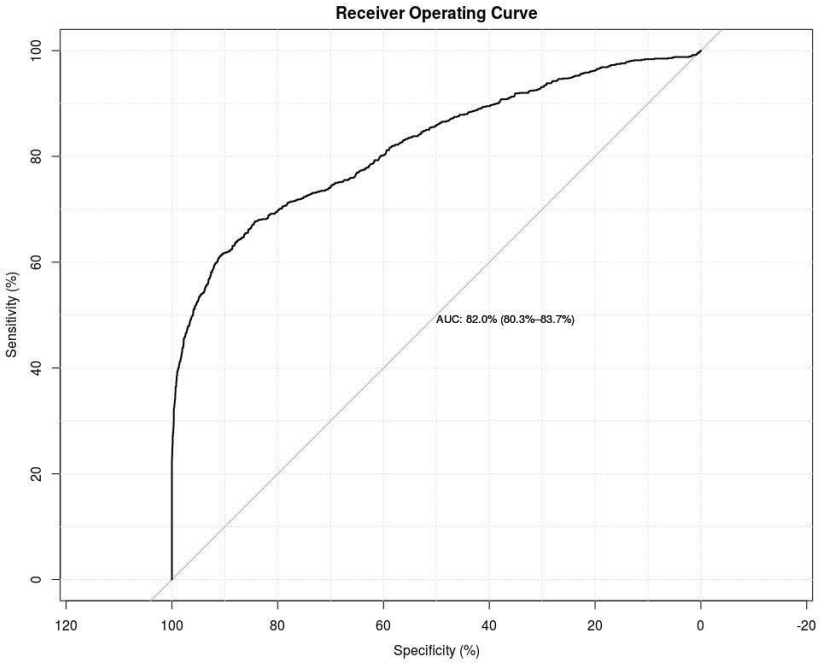

Figure A3.2: Cook's distance plot. Stand Pearson residuals and their leverage. If the point is out of 0.5, it has a big influence in the model.

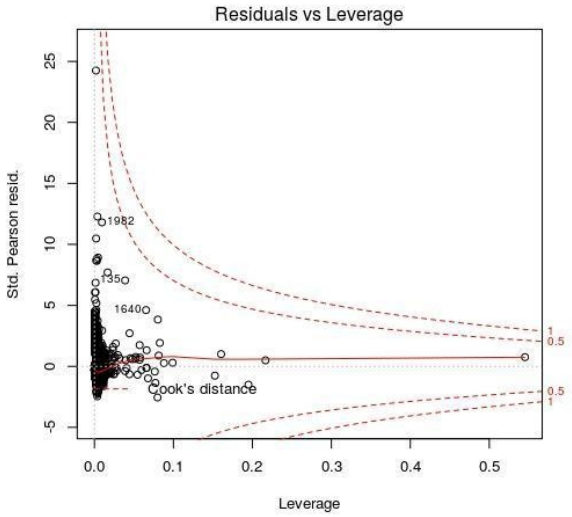

2- Alternative model where DBH is considered as a class qualitative variable

To take into account the U-shaped relationship between mortality and DBH, we also tested a model with DBH considered as a 4-level categorical variable. We distinguished four DBH-classes: Class 10-20cm with 1280 individuals, class 21-30cm

with 1312 individuals, class 31-40cm with 411 individuals and class >40cm with 200 individuals. This model wrote as follows :

$P_{mortality}$ **=** [DEFcum + Fungi **+** Budburst**+** MBAI **+**

(Nstem **OR** $Compet_{intra}$**OR** $Compet_{tot}$ **OR** $Compet_{intra\ +}$)] * Class_DBH (equation A3.2)

We applied the same procedure as in the main article to select first the best competition variable, and then use the step AIC procedure to select the best model.

Table A3.3: Parameter estimates and related statistics in the best model (eq. A3.2). β is the maximum likelihood estimates and SE its estimated error. We give the z value and the associated p-value of the test that β is significantly different from zero. OR is the estimated odds ratios.

Variables	β	SE	z value	p-value	OR
DEFw	7.512	0.364	20.653	< 0.001	1830.1
class_DBH21-30	-0.253	0.172	-1.471	0.141173	0.776
class_DBH31-40	-1.102	0.302	-3.646	< 0.001	0.332
class_DBH>40	-0.204	0.467	-0.436	0.663	0.816
MBAI	-0.077	0.017	-4.606	< 0.001	0.926
Budburst (Early)	0.783	0.172	4.544	< 0.001	2.189
Nstem	0.122	0.036	3.388	< 0.001	1.130
Fungi (Presence)	0.493	0.143	3.443	< 0.001	1.637
class_DBH21-30:MBAI	-0.037	0.027	-1.373	0.169	0.964
class_DBH31-40:MBAI	0.081	0.020	4.142	< 0.001	1.085
class_DBH>40:MBAI	-0.059	0.038	-1.534	0.125	0.943
DEFw:class_DBH21-30	-1.575	0.560	-2.813	< 0.001	0.207
DEFw:class_DBH31-40	-2.100	0.822	-2.556	< 0.001	0.122
DEFw:class_DBH>40	0.243	0.025	3.437 2	0.254	-1.416

Table A3.4 Variables influences in the best model (eq. A3.2) and model validation. Df are the degree of freedom. Dev. is the deviance associated. AIC is the AIC of the model if the variable is removed. LRT is the likelihood ratio test between the complete model and the model with the variable removed, with its associated p-value. GVIF1/2df is the generalized collinearity diagnostic value taking into account the different dimensions of the variables with Df. The Brier score of the model is 0.11 and the goodness of fit computed with the roc curve (area under the curve) is 0.83.

Variables	Df	Dev.	AIC	LRT	p-value	$GVIF^{1/2df}$
DEFw	1	3975.9	4003.9	725.57	< 0.001	1.523
class_DBH	3	3266.7	3290.7	16.39	< 0.001	1.798
MBAI	1	3279.7	3307.7	29.42	< 0.001	2.258
Budburst	1	3269.6	3297.6	19.31	< 0.001	< 0.001
Nstem	1	3261.2	3289.2	10.88	< 0.001	1.005
Fungi	1	3261.9	3289.9	11.57	< 0.001	1.084
class_DBH:MBAI	3	3291.1	3315.1	40.75	< 0.001	1.595

DEFw:class_DBH	3	3261.7	3285.7	11.34	0.0100	1.848

3 - An alternative model with competition index as a proxy for competition.

To test the robustness of the model to the choice of the competition predictor, we first reduced the data set by excluding all trees belonging to a coppice (keeping only tree with Nstem =1). Then, we fitted the following model

$$P_{mortality} = [DEFcum + Fungi + Budburst + MBAI + (Compet_{intra} \textbf{ OR } Compet_{tot})] * (DBH + DBH^2) \text{ (equation A3.3)}$$

We applied the same step AIC procedure as in the main article to select the best model The fit of this model revealed that all the variables had a significant effect on the probability of mortality except competition. Moreover, these effects were consistent with those estimated in the main part of this manuscript.

Table A3.5: Parameter estimates and related statistics for the best model (eq. A3.3). β is the maximum likelihood estimates and SE its estimated error. We give the z value and the associated p-value of the test that β is significantly different from zero. OR is the estimated odds ratios.

Variables	β	SE	z value	p-value	OR
DEFw	6.912	0.263	26.312	< 0.001	857.030
DBH_{2002}	-12.189	5.141	-2.371	< 0.001	0.927
DBH_{2002}^2	22.306	4.949	4.507	0.104	$1.6\ 10^{-4}$
MBAI	-0.060	0.011	-5.573	< 0.001	$5.76\ 10^{6}$
Budburst	0.842	0.172	4.899	< 0.001	2.413
Fungi	0.580	0.142	4.092	< 0.001	1.919
DEFw: DBH_{2002}	-56.404	14.792	-3.813	0.03	$3.9\ 10^{-16}$
DEFw: DBH_{2002}^2	32.591	16.851	1.934	0.02	537.8
DBH_{2002}:MBAI	0.381	0.454	0.839	0.551	0.687
DBH_{2002}^2:MBAI	-0.835	0.443	-1.884	0.105	0.379

Table A3.6 Variables influences in the best model (eq. A3.3) and model validation. Df is the number of degree of freedom. Dev. is the deviance associated. AIC is the AIC of the model when the variable is removed. LRT is the likelihood ratio test between the complete model and the model with the variable removed, with its associated p-value. GVIF1/2df is the generalized collinearity diagnostic value taking into account the different dimensions of the variables with Df. The Brier score of the model is 0.24 and the goodness of fit computed with the roc curve (area under the curve) is 0.82.

Variables	Df	Dev.	AIC	LRT	Pr(>Chi)	GVIF	$GVIF^{1/2df}$
DEFw	1	2915.6	2935.6	713.39	< 0.001	1.258	1.122
MBAI	1	2236.2	2256.2	34.01	< 0.001	1.510	1.229
poly(DBH)	2	2215.9	2233.9	13.71	0.001	5.267	1.515
Budburst-early	1	2217.3	2237.3	15.14	< 0.001	1.019	1.010
Fungi-T	1	2215.4	2235.4	13.24	< 0.001	1.223	1.106
DEFw:poly(DBH.2)	2	2213.9	2231.9	11.68	0.003	13.795	1.927
MBAI:poly(DBH)	2	2207	2225	4.78	0.0916 .	10.346	1.793

4 - Alternative model with Height in 2002 as a proxy of size

To test he robustness of the model to the choice of the size predictor, we also a considered a model where size was measured by height instead of DBH:

Pmortality = [DEFw + Fungi + Budburst+ MBAI +

(Nstem OR $Compet_{intra}$ OR $Compet_{tot}$ OR $Compet_{intra+}$)] × H_{2002} (equation A3.4)

The height in 2002 (H_{2002}) varied between 1.5m and 26m and was measured only for a subset of 1199 trees. We applied the same procedure as in the main article for the correlated competition variables. Then, we used the step AIC procedure to select the best model.

The fit of this model revealed less variables with a significant effect than previously. This is probably due to the lower number of individual observations and also to the fact that the measured trees are almost all dominant. The significant effects were consistent with those estimated in the main part of this manuscript.

Table A3.7: Parameter estimates and related statistics for the best model (eq. 3.4). β is the maximum likelihood estimates and SE its estimated error. We give the z value and the associated p-value of the test that β is significantly different from zero. OR is the estimated odds ratios.

Variables	β	SE	z value	p-value	OR
DEFw	6.657	0.481	13.831	< 0.001	778.50
H_2002	-0.215	0.038	-5.642	< 0.001	0.81
MBAI	-0.059	0.018	-3.237	0.0012	0.94
Budburst (Early)	0.791	0.308	2.568	0.0102	2.21

Table A3.8 Variables influences in the best model (eq. A3.4) and model validation. Df is the number of degree of freedom. Dev. is the deviance associated. AIC is the AIC of the model when the variable is removed. LRT is the likelihood ratio test between the complete model and the model with the variable removed, with its associated p-value. GVIF1/2df is the generalized collinearity diagnostic value taking into account the different dimensions of the variables with Df. The Brier score of the model is 0.10 and the goodness of fit computed with the roc curve (area under the curve) is 0.85.

Variables	Df	Dev.	AIC	LRT	p-value	GVIF
DEFw	1	1105.28	1113.28	295.34	< 0.001	1.05
H_{2002}	1	845.77	853.77	35.823	< 0.001	1.04
MBAI	1	823.44	831.44	13.494	< 0.001	1.06
Budburst	1	816.08	824.08	6.129	0.013	1.01

Appendix 4: Survival analysis of the probability of mortality at tree- and year-levels

This appendix aims to present an attempt to fit a survival analysis model to our data set. Survival analysis typically consists in analysing the relationships between the time that elapsed before mortality occurred on the one hand, and the measured covariates that may be associated with that quantity of time on the other hand. This is not exactly similar to measuring the effect of each covariate on the risk of mortality, as presented in the main part of this manuscript.

Method

We created a new data table where each individual is repeated (several lines) as many years as those during which it is noted alive. For the fungi variable, once visible the status changes from 0 to 1. Two types of defoliation variables were considered: Def is the defoliation mark measured for a given year (0= non defoliated; 1=defoliated). Defcum is the sum of defoliation marks up to a given year (Defcum varies between 0 and 9). The model writes as follows:

$$Pmortality = [Defcum + Def + Fungi + Budburst + MBAI + (Nstem\ OR\ Compet_{intra}\ OR\ Compet_{tot}\ OR\ Compet_{intra+})] * (DBH+DBH^2) \quad \text{(equation 4)}$$

We applied the same procedure as in the main article to select the best competition variable. Then, we used the step AIC procedure to select the best model.

Results

The fit of the survival model revealed the same effects as found with the logistic regression model presented in the main text (Table A3.9 and Table 2). In particular, the relative probability of mortality increased with increasing competition (Nstem) and decreased with increasing growth; it was also higher for trees with an earlier budburst as compared to others, and for trees bearing fungi fructifications than for others. Interestingly, we observed different effects of the two variables related to defoliation: On the one hand, increasing cumulated defoliation (Defcum) increased the risk of mortality. On the other hand, increasing single-year defoliation (Def)

decreased the risk of mortality. Almost all years had a positive or negative effect compared to 2003 (except 2010 or the lack of data, did not allow an assessment of the effects).

However, this survival analyses model did not seem fully reliable, because of a major departure from classical assumptions of survival analyses. Indeed, survival analysis following the classical cox model assume proportional hazards, ie the unique effect of a defoliation mark equal to 1 instead of 0 would for instance double the probability of mortality at every year t. However, the effect of defoliation on mortality is likely to vary among years depending on climate, and this cannot easily be taken into account in survival analyses. None of the variable respect the proportional-hazards (PH) assumption (table A3.9).

Table A3.9: Parameter estimates and related statistics for the survival analysis model. β is the maximum likelihood estimates and SE its estimated error. OR the estimated odds ratios. We give the z value and the associated p-value of the test that β is significantly different from zero.

Variables	**β**	**SE**	**OR**	**z**	**p-value**
Fungi	5.057 e-01	9.558 e-02	1.658 e+00	5.291	1.22 e-07 ***
Defcum	6.945 e-01	2.406 e-02	2.003 e+00	28.869	< 2 e-16 ***
DBH_{2002}	-8.615 e+00	1.093 e+01	1.813 e-04	-0.788	0.430595
DBH_{2002}^{2}	4.772 e+01	8.965 e+00	5.328 e+20	5.323	1.02 e-07 ***
Budburst	5.972 e-01	1.214 e-01	1.817 e+00	4.921	8.61 e-07 ***
MBAI	-9.233 e-02	8.846 e-03	9.118 e-01	-10.438	< 2 e-16 ***
Nstem	9.858 e-02	2.313 e-02	1.104 e+00	4.261	2.03 e-05 ***
Def	-1.369 e+00	1.200 e-01	2.543 e-01	-11.412	< 2 e-16 ***
Year 2004	4.702 e-01	1.396 e-01	1.600 e+00	3.368	0.000757 ***

Year 2005	6.228 e-02	1.464 e-01	1.064 e+00	0.425	0.670562
Year 2006	2.633 e-01	1.378 e-01	1.301 e+00	1.911	0.055979 .
Year 2007	-1.533 e-01	1.434 e-01	8.579 e-01	-1.069	0.285131
Year 2008	-1.844 e+00	2.160 e-01	1.581 e-01	-8.541	< 2 e-16 ***
Year 2009	-1.660 e+00	1.984 e-01	1.901 e-01	-8.370	< 2 e-16 ***
Year 2010	NA	0.000 e+00	NA	NA	NA
Year 2011	-1.019 e+00	1.691 e-01	3.609 e-01	-6.025	1.69 e-09 ***
Year 2012	-7.465 e-01	1.566 e-01	4.740 e-01	-4.766	1.88 e-06 ***
Year 2013	-9.312 e-01	1.652 e-01	3.941 e-01	-5.636	1.74 e-08 ***
Year 2014	-1.029 e+00	1.705 e-01	3.574 e-01	-6.037	1.57 e-09 ***
Year 2015	-1.361 e+00	1.862 e-01	2.564 e-01	-7.308	2.71 e-13 ***
Year 2016	-1.923 e+00	2.069 e-01	1.462 e-01	-9.291	< 2 e-16 ***
Defcum:DBH_{2002}^{2}	-1.793 e+01	4.487 e+00	1.628 e-08	-3.996	6.43 e-05 ***
Defcum: DBH_{2002}^{2}	7.488 e+00	3.687 e+00	1.787 e+03	2.031	0.042276 *
DBH2002:Def	-9.782 e+01	3.187 e+01	3.301 e-43	-3.069	0.002148 **
DBH_{2002}^{2}:Def	3.708 e+01	1.975 e+01	1.272 e+16	1.877	0.060478 .

Table A3.10: Table of the result of the proportional-hazards (PH) assumption test. Rho is the correlation coefficient between transformed survival time and the scaled Schoenfeld residuals, chisq the chi-square, and the two-sided p-value.

Variables	**rho**	**chisq**	**p-value**
Fungi (Presence)	0.06380	4.81e+00	2.82e-02
Defcum	-0.23724	5.25e+01	4.32e-13
DBH2002	-0.05881	4.25e+00	3.94e-02
DBH_{2002}^{2}	0.03750	1.41e+00	2.35e-01
Budburst (Early)	0.04496	2.16e+00	1.42e-01
MBAI	0.00513	1.54e-01	6.94e-01
Nstem	0.00117	1.15e-03	9.73e-01
Def	0.13848	2.06e+01	5.63e-06
Year 2004	0.04662	2.34e+00	1.26e-01
Year 2005	0.14269	2.17e+01	3.22e-06
Year 2006	0.24548	5.94e+01	1.29e-14
Year 2007	0.36127	1.29e+02	0.00e+00
Year 2008	0.31053	9.86e+01	0.00e+00
Year 2009	0.35782	1.32e+02	0.00e+00
Year 2010	NA	NaN	NaN
Year 2011	0.43059	1.89e+02	0.00e+00
Year 2012	0.49930	2.76e+02	0.00e+00
Year 2013	0.53221	3.04e+02	0.00e+00
Year 2014	0.56709	3.43e+02	0.00e+00
Year 2015	0.56088	3.29e+02	0.00e+00
Year 2016	0.53854	3.19e+02	0.00e+00
Defcum:DBH_{2002}	0.10397	8.84e+00	2.94e-03
Defcum: DBH_{2002}^{2}	-0.04641	1.81e+00	1.79e-01
DBH2002:Def	0.02150	6.01e-01	4.38e-01
DBH_{2002}^{2}:Def	0.00523	2.21e-02	8.82e-01
GLOBAL	NA	1.06e+03	0.00e+00

References:

Beguería S, Vicente-Serrano SM. **2017**. SPEI: Calculation of the Standardised Precipitation-Evapotranspiration Index.

Cribari-Neto F, Zeileis A. **2010**. Beta Regression in R. *Journal of Statistical Software* **34**.

Fox J, Weisberg S. **2011**. *An {R} Companion to Applied Regression*. Thousand Oaks {CA}: Sage.

Hijmans RJ, Phillips S, Leathwick J, Elith J, Hijmans MRJ. **2017**. Package 'dismo'. *Circles* **9**: 1–68.

Lê S, Josse J, Husson F. **2008**. FactoMineR : An R package for multivariate analysis. *R CRAN Project J Stat Softw* **25**: 1–18.

Oddou-Muratorio, S., & Davi, H. 2014. Simulating local adaptation to climate of forest trees with a Physio-Demo-Genetics model. *Evolutionary Applications*, **7**, 453–467.

Wei T, Simko V. **2016**. corrplot: Visualization of a Correlation Matrix.

5 Résultats et perspectives

Nous avons trouvé qu'il était important de prendre en compte différentes échelles (population et individu) et d'utiliser des outils de modélisation distincts pour identifier et évaluer les causes de mortalité. En effet, à l'échelle de la population le modèle statistique nous a permis de montrer que la sécheresse était le principal facteur climatique causant la mortalité à La Massane. Grâce au modèle basé sur les processus, nous avons ensuite montré que la variation du taux de mortalité dans la population était expliquée par la combinaison de plusieurs mécanismes physiologiques répondant aux stress climatiques de sécheresse et de gelée tardive : la perte de conductance, l'épuisement des réserves de carbone et l'apparition de gelées tardives.

A l'échelle individuelle, les modèles statistiques ont permis de mettre en évidence que la probabilité individuelle de mortalité diminuait avec l'augmentation de la croissance moyenne et augmentait avec l'augmentation de la défoliation, la précocité du débourrement, la présence de champignons et l'augmentation de la concurrence. De plus, ces modèles nous ont permis de mettre en évidence une interaction entre la taille des arbres et la défoliation, indiquant une plus forte augmentation de la mortalité associée à la défoliation chez les arbres plus petits que chez les plus grands. Enfin, le modèle basé sur les processus a permis d'émettre des hypothèses sur l'impact de la défoliation en réponse à un stress hydrique et sur l'impact de la date de débourrement en réponse à un stress de gelée tardive. Le modèle basé sur les processus prédit une perte de conductance plus élevée, ainsi qu'un niveau plus élevé de réserves de carbone pour les arbres dont le débourrement était plus précoce, tandis que la capacité de défolier de l'arbre s'est avérée limiter l'impact du stress hydrique au détriment de l'accumulation des réserves de carbones.

Cette étude nous a permis d'évaluer les limites de chaque approche et leur complémentarité. De plus, elle nous a permis de construire et de valider un indice composite expliquant la fluctuation du risque de mortalité grâce à trois sous-indices : le risque de gelée tardive, le risque de sécheresse et le risque d'épuisement des réserves carbonées. Une perspective de cette partie est de vérifier que les processus écophysiologiques limitant la distribution du Hêtre correspondent aux facteurs climatiques expliquant la mortalité dans les marges et fait l'objet d'un projet avec UMR Biogeco. Ceci permettrait également de valider cet indice composite de mortalité à large échelle, en confrontant des prédictions de risque simulées par CASTANEA aux données de l'ICPforest.

Chapitre III

Le risque de mortalité lié au changement climatique diffère selon les espèces dans le réseau européen de conservation des ressources génétiques forestières

1 Contexte et méthodes

Depuis le début des années 1990, les pays européens engagés dans le programme EUFORGEN ont coordonné leurs stratégies de conservation de la diversité génétique des forêts, qui s'appuie notamment sur un réseau d'unités dynamiques de conservation génétique *in situ* (en anglais, Genetic Conservation Unit, GCU). Ce réseau est constitué de peuplements forestiers potentiellement adaptés à des conditions environnementales spécifiques ou présentant des caractéristiques écologiques distinctes. La gestion des unités vise à maintenir et à améliorer le potentiel d'évolution à long terme des populations d'arbres. Cela signifie que des mesures d'aménagement et des techniques sylvicoles sont appliquées, au besoin, pour favoriser les processus génétiques au sein des populations d'arbres cibles. Cependant les changements climatiques observés et prévus remettent en question la durabilité de ce réseau. Des études antérieures ont prédit que 33 à 65% des GCU seraient à la limite ou hors de la niche bioclimatique actuelle des espèces d'ici 2100 (Schueler et al., 2014). De plus, ces peuplements sont généralement situés dans des forêts gérées à des fins multiples, des zones protégées ou des peuplements semenciers. Il est donc essentiel de prendre en compte la sylviculture comme moyen de prévention et d'atténuation de l'impact du changement climatique. L'objectif principal de cette étude est d'étudier le risque de mortalité d'essences d'arbres majeures au sein des GCUs, de les localiser et de comprendre les processus écophysiologiques en jeu.

Pour cela nous avons utilisé le modèle CASTANEA, qui est un modèle basé sur les processus écophysiologiques, pour simuler la croissance et le risque de mortalité de cinq espèces d'arbres (*Fagus sylvatica, Quercus petraea, Pinus sylvestris, Pinus pinaster et Picea abies*) sur leur aire de répartition européenne, sous le climat actuel et futur, tout en considérant les effets de la gestion forestière. Le risque de mortalité a été évalué grâce à l'indice de risque composite (CRI), précédemment créé et qui a montré dans le chapitre précédent une bonne capacité prédictive du risque de mortalité à l'échelle de la parcelle. Cet indice prend en compte les risques de mortalité dus à la privation de carbone, à la défaillance hydraulique et aux dégâts de gelées tardives. De plus, des pratiques sylvicoles ont été simulées en les adaptant aux habitudes sylvicoles de chaque pays. Pour finir, nous avons étudié l'impact du changement climatique et des pratiques sylvicoles sur les risques d'extinction des GCUs.

Cette étude à été réalisée dans le cadre du WP5.3 du projet européen GenTree et a fait l'objet d'un rapport confidentiel rendu en août 2019. Les objectifs de GenTree sont de fournir au secteur forestier européen une meilleure connaissance, de meilleures méthodes et de nouveaux outils pour optimiser la gestion et l'utilisation durable des ressources génétiques forestières (RGF) des forêts européennes. Les avancées scientifiques, technologiques et de développement de GenTree sont attendues dans trois grands domaines d'application : (i) mise au point de stratégies innovantes pour la conservation dynamique des RGF en Europe; (ii) augmentation de la pa-

lette de RGF utilisée dans les programmes d'amélioration forestiers en Europe; (iii) proposition de nouveaux scénarios de gestion forestière et de nouveaux cadres politiques forestiers intégrant pleinement la conservation des RGF et leur amélioration pour répondre aux nouvelles demandes de la bioéconomie et de la société dans son ensemble. GenTree s'intéresse aux espèces d'arbres forestiers les plus importantes en Europe, aussi bien pour leur rôle écologique qu'économique, couvrant des habitats très variés ainsi que des utilisations et valeurs sociétales très diverses : sept espèces conifères (Abies alba, Picea abies, Pinus cembra, Pinus halepensis, Pinus nigra, Pinus pinaster, Pinus sylvestris, Taxus baccata) et cinq espèces feuillues (*Betula pendula, Fagus sylvatica, Populus nigra, Quercus petraea*).

Dans ce contexte, ma mission était d'évaluer les risques d'extinctions de cinq espèces d'arbres sur 100 sites GenTree fortement suivis. Cependant, dans une optique de comparaison des prédictions de risque de mortalité à large échelle des GCU, qui était l'objet du WP1 dirigé par M. Benito-Garzon avec des outils statistiques, j'ai préféré faire cette étude à l'échelle de la distribution de l'espèce en développant avec l'équipe capsis, une méthode pour lancer CASTANEA à large échelle (Annexe **??**). Cela a nécessité 223390 simulations, soit environ 804204 heures.

2 The risk of mortality under climate change differs among species across the European network of forest gene conservation units

Mots-cléfs : modèle basé sur les processus, changement climatique, pratiques sylvicoles, stratégie de conservation, ressource génétiques.

Title: The risk of mortality under climate change differ among species across the European network of forest gene conservation units

In preparation for : Global Change Biology or Global Ecology and Biogeography

Authors : Cathleen Petit-Cailleux[1], Hendrik Davi[1], François Lefèvre[1], Pieter Johannes Verkerk[2], Bruno Fady[1], Marcus Lindner[3], Sylvie Oddou-Muratorio[1].

[1] INRAE, UR 629 Ecologie des Forêts Méditerranéennes, URFM, Avignon, France

[2] European Forest Institute, Yliopistokatu 6B, 80100 Joensuu, Finland

[3] European Forest Institute, Platz der Vereinten Nationen 7, 53113, Bonn, Germany

Keywords: Process-based model, Climate Change, management practices, conservation strategy, genetic resources.

Abstract

General context: Since the early 1990s, the European countries engaged in the EUFORGEN programme have coordinated their strategies for the conservation of the genetic diversity of their forests, relying notably on a network of dynamic, in-situ gene conservation units (GCU). Observed and projected climate change however question the sustainability of this network, and previous studies have predicted 33–65 % of GCUs to be at the limit or outside species' current bioclimatic niche by 2100.

Objective: The main objective of this study is to investigate the risk of mortality across the European network of major tree species GCUs and to understand the ecophysiological processes underlying this risk under climate change.

Methods: we used the ecophysiological process-based model CASTANEA to simulate the growth and risk of mortality of five tree species (*Fagus sylvatica*, *Quercus petraea*, *Pinus sylvestris*, *Pinus pinaster* and *Picea abies*) over their European distribution range, under current and future climate, while considering forest management effects. The risk of mortality was assessed by a composite risk index (CRI) taking into account the risks of mortality due to carbon starvation, hydraulic failure and late frosts.

Results: Our simulations accurately captured species' current bioclimatic niches, except for *Picea abies*. The physiological processes increasing the risk of mortality differed among species: the risk of hydraulic failure was the main driver of the CRI for broadleaved species and *P. pinaster*, whereas the risk of late frost drove the CRI of *Picea abies* and *Pinus sylvestris*. Under future climates, CASTANEA predicted an increase of the CRI at GCUs locations by 40%, 25%, 18%, and 2%, respectively for *Picea abies*, *Pinus sylvestris, Fagus sylvatica*, and *Pinus pinaster* and a decrease by -4% for *Quercus petraea*. We found that forest management decrease the CRI of all species under current and future climates, by decreasing the average age and density of stands.

Conclusions: Even though the projections of the CRI under future climate obtained here with the process-based model CASTANEA were less pessimistic than those previously provided by bioclimatic niche models, our results call for a rethinking of the design and management of European conservation networks to mitigate their risk of mortality under climate change.

Introduction

Sustainable forest management ultimately aims to attain a balance between society's increasing demands for forest products and services, and the preservation of forest health and biodiversity. However, ongoing climate and global changes pose major challenges to this balance, with for instance 21-50% of economic value loss expected for European forests by 2071-2100 (Hanewinkel *et al.* 2012), and significant predicted changes in forest ecosystem functioning, the composition of communities and the geographic distribution of species worldwide (Lindner *et al.* 2014). Therefore, there is an urgent need for predicting the future ecological dynamics and ecosystem services of forest ecosystems and for guiding sustainable management efforts, including genetic resource conservation strategies, in the possible future trajectories.

Climate change can interact with multiple factors such as forest management, other changes of land-use practices, nitrogen deposition or various pollutions and can have antagonistic or partially compensatory effects on the physiological functioning of trees and ecological dynamics of forests (Walther *et al.* 2002; Thuiller *et al.* 2006; Morin *et al.* 2008; Lindner *et al.* 2014; Anderegg *et al.* 2015; Begon, Townsend, and Harper 2006). In particular, the combination of rising temperatures worldwide, and decreasing summer precipitation in some regions has been associated with increasing frequency and duration of droughts, and consequently, decreasing tree growth and forest productivity (Zhao & Running 2010; Reyer *et al.* 2014; Reyer 2015), increasing risks of tree mortality (Allen *et al.* 2010) and increasing risk of disturbances (wildfire, pests; Seidl *et al.* 2017). Rising temperatures can alternatively result in increasing vegetation length (i.e. period between leaf budburst and leaf fall; Davi *et al.* 2006) and consequently increasing tree growth, seed production and forest productivity. In addition, a single climatic driver can have both positive and negative effects on tree performance; this is exemplified by the role of increasing temperature on the advance of leaf phenology, which is expected to increase vegetation length, but also to expose plants to higher risk of late frosts (Vitasse *et al.* 2014).

Assessing the future physiological functioning and ecological dynamics of forest stands requires not only accounting for multiple effects of climate change, and their variation across species distribution range, but also for the adaptive response of tree populations, and for the possible effects of forest management on this response. The adaptive potential of tree populations to climate change is usually assumed to be non negligible: besides tracking their ecological niche spatially through migration, tree populations could adapt in the short-run

through individual physiological tolerance (plasticity), and/or in the long-run through evolutionary response to climate-induced natural selection. Despite their large and diverse gene pools (Savolainen *et al.* 2007; Alberto *et al.* 2013), the ongoing speed and magnitude of climate change is likely to exceed the natural adaptive potential of most tree species and populations (Kuparinen *et al.* 2010; Schueler *et al.* 2014; Raftery *et al.* 2017). However, innovative forest management practices could increase the resilience of managed forest to climate changes (Lefèvre *et al.* 2014).

In this context, existing networks of dynamic Genetic Conservation Units (GCUs) for forest trees (Koskela et al, 2012) represent a central reservoir of possible future options for adaptation of forests to climate change. In Europe, this network was set up to dynamically conserve forest genetic resources by preserving the ecological and evolutionary processes contributing to the adaptive potential of tree populations to environmental variations. The underlying principle of GCU networks is that genetically diverse groups of mating individuals and populations should be maintained across different environmental gradients to ensure continued evolutionary processes, and not only the preservation of the existing frequencies of alleles and genotypes (Koskela *et al.* 2012). The European transnational network of forest tree GCUs contains 3593 GCUs, representing 4316 tree populations (http://portal.eufgis.org/). Four economically and ecologically important forest tree species (*Fagus sylvatica*, *Picea abies*, *Pinus sylvestris* and *Quercus petraea*) alone account for ~55% of the total area managed for *in situ* genetic conservation, with respectively 256, 451, 508 and 275 GCUs. By contrast, for many other important tree species, only small areas are managed for the same purpose (e.g. *Betula pendula*, *Pinus nigra*, *Pinus pinaster*), with respectively 67, 149 and 62 GCUs.

Projections based on correlative bioclimatic niche models (BNMs) indicate that many GCUs may have a high risk of extirpation under climate change, thus weakening the conservation network as a whole (Schueler *et al.* 2014). Indeed, target species in 33–65 % of conservation units, mostly located in southern Europe, are predicted to be at the limit or outside their current bioclimatic niche by 2100. The highest average increase in the risk of extirpation throughout the network can be expected for coniferous trees (although they are mainly occurring within units in mountainous landscapes, where climate change velocities were the lowest). The correlative BNMs used to obtain these predictions have several strengths: the data needed to calibrate them (e.g. species-specific presence/absence) are available in large numbers and with increasing resolution in open-access databases and a suite of powerful algorithms have been developed based on these data. However, these BNMs, because they are not mechanistic, are usually not able to take into account the physiological

response of trees to new, currently unknown climatic combinations (e. g. the combination of increasing CO_2 concentration and increasing temperatures). Also, the spatial variation in soil properties, not accounted for by Schueler et al. 2014, could have complex effects on species favorability, depending on the interaction between the soil-related water capacity, the climate-related water availability, and the species-specific physiological vulnerability to water stress (Silva *et al.* 2012). These well-known limitations of correlative BNMs may explain the contradictory predictions sometimes generated with different BNMs, as for *Abies alba* along the southern edge of its distribution (Mairota *et al.* 2013; Tinner *et al.* 2013).

The pessimistic BNMs-based projections call for confirmatory predictions of the general risk of forest trees mortality under climate change, and of risk of European GCUs extirpation in particular. The comparison of several complementary models is now widely acknowledged as the best approach for future horizon scanning (Harris *et al.* 2014; Hauck *et al.* 2015). Among the available models to predict the future risk of mortality and distribution ranges of trees species, ecophysiological process-based models (PBM) offer the advantage to simulate vegetation functioning in response to explicit climate and soil variability (as input variables), through their impacts on plant physiology (e.g., Cramer et al. 2001; Dufrêne et al. 2005). Ecophysiological PBMs were initially developed to simulate carbon and water fluxes in forest ecosystems, but can also be used to investigate the environmental drivers and physiological processes triggering tree mortality under climate change. For instance, they are particularly suitable to disentangle the physiological processes contributing to mortality in face of drought (McDowell *et al.* 2008), and the intricate roles of hydraulic failure (the loss of conductance resulting from major xylem embolism) and carbon starvation (the depletion of carbon reserve resulting from stomata closure to avoid hydraulic failure). Ecophysiological PBMs incorporating knowledge on phenological events could also be used to investigate the risk of mortality due to late frosts, which is likely to increase in the future (IPCC 2014; Charrier *et al.* 2018). Indeed, advanced leaf unfolding due to raising temperatures is expected to increase the risk of damage due to spring frost events, while extending the duration of vegetation season (Bigler & Burgman 2018) .

Another main advantage of mechanistic PBMs is their ability to account explicitly for the effect of management on the functioning and dynamics of forest stands. Forest dynamic models have a long tradition of being used to support forest management. Recently, both ecophysiological PBMs or forest dynamic models incorporating ecophysiological processes are being applied to evaluate how management and climate change may interact to influence forest dynamics (Oddou-Muratorio, Davi and Lefèvre, in prep). For instance, several

management practises have been proposed to mitigate the projected increase in drought, from thinning practices aiming at minimizing drought impact on the short-term, to planting of more drought-tolerant species aiming at designing more drought-adapted forests on the long-term. The management of GCUs includes practices aiming at maintaining the evolutionary processes (e.g. gene flow, pollination, regeneration) that are often compatible with common silvicultural practices, although planting is proscribed. Hence, forest managers need to evaluate how thinning practices may mitigate the impacts of climate change on conservation networks.

The objectives of our study were (i) to investigate the risk of GCU extirpation under climate change for major tree species over their European conservation network, (ii) to understand the ecological processes underlying this risk, and (iii) to evaluate how management practices can reduce the risk of mortality. We focused on the risk of mortality associated with droughts and late frosts, two major risks likely to increase in the future (Augspurger 2013; IPCC 2014; Charrier *et al.* 2018). We used the ecophysiological and biophysical PBM CASTANEA (Dufrêne et al. 2005) to simulate the risk of hydraulic failure, carbon starvation and late frost damages of five tree species representative of the main European forest biomes: *Fagus sylvatica* and *Quercus petraea* for temperate deciduous broadleaf forests; *Picea abies* and *Pinus sylvestris* for high-latitude and high-altitude evergreen conifer forests; and *Pinus pinaster*, for low-latitude, evergreen conifer temperate forests (Figure S1). We addressed the following issues: (1) How does the risk of mortality in face of drought and frost vary among species and across species' distribution ranges ? We expected differences between species to emerge from their different sensitivity to the target climatic stress, which is modeled in CASTANEA through species-specific parameters. (2) What is the impact of forest management practises on this risk ? We expected the potential mitigation effect of thinning to vary among species and among climatic scenarios. (3) Will GCUs' risk of extirpation increase under future climates, and are the predictions of our PBM consistent with those based on BNMs ? Overall, we expected ecophysiological PBMs to be less pessimistic than BNMs (as observed by Morin et al. 2008; Cheaib et al. 2012).

Material and methods

CASTANEA model

CASTANEA is an ecophysiological PBM used to simulate carbon and water fluxes in forest ecosystems (Dufrêne et al. 2005). This model has no spatially-explicit representation of individual trees, and represent an average tree by six functional compartments: canopy, branches, stem, coarse roots, fine roots and reserves (an unlocated compartment corresponding to the Non-Structural Carbohydrates, NSC). The canopy is divided into five layers of leaves. Photosynthesis is half-hourly computed for each canopy layer using the model of Farquhar et al. (1980) analytically coupled to the stomatal conductance model proposed by Ball et al. (1987). The effect of temperature on photosynthesis is modelled using a response function of Rubisco-limited photosynthesis (Bernacchi *et al.* 2001). Maintenance respiration is modeled as proportional to the nitrogen content of the considered organs (Ryan 1991). Growth respiration is computed from growth increment combined with a construction cost specific to the type of tissue (De Vries *et al.* 1974). Transpiration is also calculated hourly using the equations of Monteith (1965). The dynamics of Soil Water Content (SWC) is calculated daily using a three-layer bucket model. Soil drought drives stomata closure with a linear decrease when relative SWC is under 40% of field capacity (Sala & Tenhunen 1996; Granier *et al.* 2000). In the carbon allocation sub-model (Davi *et al.* 2009; Davi & Cailleret 2017), the allocation coefficients of biomass between the six compartments are calculated daily, depending on the sink force and on the phenology constraints. CASTANEA was originally developed and validated at stand scale for beech, and then for pine and oaks (Davi *et al.* 2005, 2006).

In this study, we focussed on three output variables simulated by CASTANEA: (1) the NSC content as an indicator of risk of carbon starvation, (2) the percentage of loss of conductance (PLC) as an indicator of risk of hydraulic failure, and (3) the number of late frost days (NLF) as an indicator of risk of frost damage. Note that we did not simulate mortality due to drought and late frost damage with CASTANEA because the thresholds in PLC, NLF and NSC triggering mortality are unknown.

We used the CASTANEA version described in Petit-Cailleux et al. (submitted). This version allows the PLC to be computed based on daily midday water potential and species vulnerability curve to embolism (see equations 5 and 6 in Petit-Cailleux et al. submitted). For budburst, we used aone-phase phenological model, which describes the cumulative effect of forcing temperatures on bud development during the ecodormancy phase (Dufresne et al.

2005). We simulated damages due to late frosts (see Appendix 2 in Petit-Cailleux et al. submitted) and considered that trees were able to reflush after late frosts.

Unlike in Petit-Cailleux et al (submitted), we simulated stand mortality due to competition. We used the relative density index (RDI), derived from the self-thinning rule (Reineke 1933), as a threshold to limit stand density. RDI is classically defined as the ratio of actual stand density (N) to the maximum stand density attainable in a stand with the same average tree volume (Nmax): RDI=N/Nmax, where Nmax is defined as :

$$Nmax = e^{a+bDg} \quad \text{(eq.1)}$$

with Dg the mean quadratic diameter, a=12.912.95 and b=1.941.

When N>Nmax, self-thinning occurs and stand density decreases to Nmax, which directly affects the Leaf Area Index (LAI) of the canopy, as:

$$LAI = N \times BiomassOfLeaves / LMA \quad \text{(eq.2)}$$

where the biomass of leaves depend on tree diameter.

Moreover, the reduction of stand density also decrease the biomass of trunk, branches, reserves and large roots of the average tree.

All these effects (decreasing N, LAI and biomass) also applied where stand density is reduced by thinning (see section Management practises below).

Climate data and scenarios

We considered the European area included within longitudes ranging from -11°W to 40°E and within latitudes ranging from 36°N to 71°N (continental Europe). CASTANEA requires the following daily climatic input variables: the minimum, mean and maximum temperatures (in °C), precipitation (mm), the wind speed ($m.s^{-1}$), the mean relative humidity (%) and the global radiation ($MJ.m^{-2}$). These data were derived for five climate scenarios (one current and four future scenario) as detailed below (Supplementary Table S1, Figure S2).

Current climate: We used the Water and Global Change (WATCH)-Forcing-Data-ERA-Interim data set (WATCH in the following) to obtain current climate data at european scale (Weedon *et al.* 2014). This daily meteorological forcing dataset is available for the period 1979 to 2008 worldwide, with a spatial resolution of 0.5° per 0.5°. This resolution (the coarsest among the climate and soil data set) was used to divide Europe into 3784 raster cells.

Future climates: To take into account the uncertainties on future climate scenarios (McSweeney *et al.* 2015), we used a combination of two regional circulation models (RCMs) from EURO-CORDEX community (Jacob, D *et al.* 2014), and two representative concentration pathways (RCPs) scenarios (IPCC, 2014). We selected the EUR-11.SMHI.CNRM-CERFACS-

CNRM-CM5 (CM5 in the following) as warm and wet RCM (optimistic) and EUR-11.SMHI.MOHC-HadGEM2-ES (Hadgem in the following) as warm and dry RCM (pessimistic). The RCP4.5 scenario considers an increase of CO_2 concentration of 650 ppm with a 1.0–2.6°C increase by 2100, and corresponds to the SRES B1 scenario (Nakićenović & Swart 2000). The RCP8.5 scenario considers an increase of CO_2 concentration of 1,350 ppm CO_2 with a 2.6–4.8°C increase by 2100, and corresponds to the A1F1 SRES scenario (van Vuuren *et al.* 2011; Harris *et al.* 2014; IPCC 2014). The four EURO-CODEX future climate datasets were corrected for bias and downscaled using the R package "meteoland" (De Caceres *et al.* 2018), and considering the WATCH dataset as reference data.

Soil properties data

To account for the variability of soil water capacity across Europe, we used (1) the European Soil Database to obtain data on the soil depth reached by the roots; (2) the SoilGrids250m database to to obtain data on bulk density and clay, silt, sand and coarse fragments contents; and (3) the 3D soil hydraulic database to to obtain data on soil water content at field capacity and at wilting point (Hiederer 2013; Hengl *et al.* 2017; Tóth *et al.* 2017). All these data were aggregated from 1km*1km resolution to 0.5°x0.5° (WGS84) resolution using the R package "raster" (Hijmans 2015). Then, we extracted the mean value of each parameter at each climate grid point (See data accessibility).

A summary table of the values of the climate and soil variables used is available in the annexe (Table S1).

Management practises

Management practices were defined on the basis of thinning rules and regeneration methods proposed in Härkönen *et al.* (2019). We assumed that management practises were constant over the simulated period (130 years from 1979 to 2100). We considered four possible silvicultural systems:

- ➔ "No management": no thinning nor regeneration cuts were applied;
- ➔ "Even-aged forest management with shelter-wood" : only the main target tree species was simulated. The last thinning was defined as a shelter-wood thinning. The age of the final cut for regeneration was specific of each species and each ecoregion.

- ➔ “Even-aged forest management with clear-cut.” After clear-cut, a new stand was planted the following year. Simulation started when the trees reached breast height, which took different lengths of time depending on the ecoregion and the species.
- ➔ “Short rotation”. There were no thinning applied, and an integral final cut was done at an early age, followed by planting.

Thinning rules were adapted from Härkönen et al. (2019) and determined the reduction in stand density according to stand age, and eventually to stand height and/or basal area (Supplementary Table S2). The reduction of stand density decreased the LAI as depicted by equation 2, and the biomass of trunk, branches, reserves and large roots of the average tree. These thinning rules varied among the five species and the four main ecoregions (North, Central East, Central West, South). The shares of each silvicultural system at each grid point was derived from Cardellini *et al.* (2018) (Supplementary Table S3, Figure S3). When country data were not available, the mean of share of every silvicultural management applied in the nearest ecoregion was applied.

Simulation design

We first considered the five climatic scenarios without management (SS1) as references. For each species and each of the five climate scenarios, we ran one CASTANEA simulation at each of the 3784 grid points (i.e. inside and outside the current species distribution range), with fixed soil properties. At each grid point we considered the same average tree per species, with an initial age of 8 years and a diameter at breast height of 5 cm. All specific species parameters are available in (Zenodo)

Secondly, we considered for each species a set of scenarios with management. These scenarios were simulated only at the grid points where a silvicultural scenario other than SS1 was identified (Table S3). In total 94600 CASTANEA simulations were performed. 5 species x 5 climates x 3784 grid points for SS1 and 25040 silvicultural management combination. (Table S4)

Model evaluation

CASTANEA had already been validated at stand scale for the five species in **(Davi et al., 2006; Delpierre 2012)**. To evaluate the validity of CASTANEA large-scale simulations, we used a similar approach as **Cheaib et al (2012).** We investigated its ability to predict species

range, based on the EUFORGEN distribution prediction **(REF)**. We first visually inspected the spatial distribution of net primary production (NPP) and ring widths (rw) inside and outside the current species distribution range. Then, we used two quantitative evaluation methods, classically used in BNMs (Fourcade *et al.* 2018) : the area under the receiver operating curve (AUC) and true skill statistic (TSS). AUC is independent from the threshold value used to convert probabilities of presence per pixel into presence—absence data (Elith & Leathwick 2009) and is one of the most popular criteria to evaluate cSDMs. An AUC value of 1 means a perfect fit, and a value of 0.5 corresponds to random prediction of a species presence in a given cell. To check whether our conclusions are sensitive to the evaluation metrics used, we also used the True Skill Statistic (Allouche *et al.* 2006). The TSS is an alternative metric used in cSDMs studies that is not influenced by the distribution size. It is based on presence–absence data and varies between −1 (poor fit) and 1 (perfect fit). To convert the probabilities of presence into presence–absence data for TSS, we used a threshold value maximizing sensibility and specificity as recommended by Liu *et al.* (2013).

Post-processing for the computation of proxies of the risk of mortality

For each simulation, we computed three proxies of the risk of mortality linked to drought and late frost risks over the simulated period as in Petit-Cailleux et al (submitted).

(i) The relative percent loss of conductivity (rPLC) was computed as a proxy of the risk of mortality due to hydraulic failure following :

$$rPLC = \frac{mean\,PLC_{\square}}{PLC_{speciesthreshold}} \quad \text{(equation 3)}$$

where meanPLC is the mean of yearly PLC-values over the simulated period, and $PLC_{speciesthreshold}$ is the species-specific PLC-value above which mortality occurs (88% for deciduous and 50% for coniferous species; Brodribb 2009; Urli et al. 2013). For all simulated trees with meanPLC>$PLC_{speciesthreshold}$, rPLC was set to 1. Hence rPLC varied from 0 to 1, increasing values indicating increasing risk of hydraulic failure.

(ii) The relative non-structural carbohydrate content (rNSC) was computed as a proxy of the risk of mortality due to carbon starvation, following :

$$rNSC = mean\frac{(NSC_{frac}¿¿n)}{NSC_{threshold}}¿ \quad \text{(equation 4)}$$

where $NSC_{frac\ n}$ is the average fraction of NSC biomass over the biomass of the other compartments at a given year *n*, $mean(NSC_{frac\ n})$ is the average NSC_{frac} over the simulated period, and $NSC_{threshold}$ the threshold in NSC-value above which mortality through carbon starvation is unlikely. $NSC_{threshold}$ was arbitrarily set the mean NSC_{frac}-value (0.09 %) observed in living trees in a database with **177** species entries (Martínez-Vilalta *et al.* 2016). For all simulated trees with $NSC_{frac} > NSC_{threshold}$, *rNSC* was set to 1. Hence *rNSC* varied from 0 to 1, increasing values indicating decreasing risk of carbon starvation.

(iii) The relative number of late frost days over the period (*rNLF*) was computed as a proxy of the risk of late frost damage following :

$$rNLF = \frac{sNLF}{NLF_{threshold}} \qquad \text{(equation 5)}$$

where *sNLF* is the sum of NLF-values over the simulated period, and $NLF_{treshold}$ the *sNLF value* over which frost damage jeopardize the probability of a tree to survive. We arbitrarily set $NLF_{treshold}$ to 1 frost day every 3 years, this value depending on the duration of the simulated period (e.g. $NLF_{treshold}$ = 10 days for 30-years long simulations under current climate). For all simulated trees with $sNLF > NLF_{treshold}$, rNLF was set to 1. Hence rNLF varied from 0 to 1, increasing values indicating increasing risk of late frost damage .

In addition, we computed a composite risk index of mortality (CRI) combining rPLC, rNLF and rNSC with an identical weight :

$$CRI = rPLC + rNLF - rNSC \qquad \text{(equation 6)}$$

CRI is expected to vary between -1 (minimal risk of mortality, when rPLC=rNLF=0 and rNSC=1) and 2 (maximal risk of mortality, when rPLC=rNLF=1 and rNSC=0).

Results

Model evaluation based on the prediction of current distribution

CASTANEA was not able to simulate living trees beyond 66.75 degrees of latitude North. This is due to an inconsistency between the budburst date and the leaf fall date, which resulted in short or negative growing seasons.

The simulated NPP was higher inside than outside the species distribution range for *Fagus sylvatica* (AUC of 0.86 and TSS of 0.63), *Quercus petraea* (AUC of 0.9 and TSS of 0.68), *Pinus pinaster* (AUC of 0.66 and TSS of 0.29) and *Pinus sylvestris* (AUC of 0.63 and TSS of 0.68) but not for *Picea abies* (AUC of 0.57 and TSS of 0.26) (Figure S4). The simulated ring widths were also higher inside than outside the species distribution range for *Fagus sylvatica* (AUC of 0.86 and TSS of 0.59), *Quercus petraea* (AUC of 0.89 and TSS of 0.89) and *Pinus pinaster* (AUC of 0.66 and TSS of 0.29) but not for *Picea abies* (AUC of 0.39 and TSS of 0.53) and *Pinus sylvestris* (AUC of 0.66 and TSS of 0) (Table 1; figure S4).

Table 1: The area under the receiver operating curve (AUC) and true skill statistic (TSS) computed for threshold in CASTANEA output variable optimizing the goodness of fit of species distribution.

Species	Variable	TSS	AUC	Threshold
Fagus sylvatica	rw (mm)	0.59	0.86	2.02
	NPP ($gC.m^{-2}$)	0.63	0.86	453.56
Picea abies	rw (mm)	0.15	0.53	0.15
	NPP ($gC.m^{-2}$)	0.26	0.57	171.8
Pinus pinaster	rw (mm)	0.29	0.66	2.55
	NPP ($gC.m^{-2}$)	0.29	0.66	320.4
Quercus petraea	rw (mm)	0.66	0.89	1.08
	NPP ($gC.m^{-2}$)	0.68	0.9	344.72
Pinus sylvestris	rw (mm)	0	0.67	3.61
	NPP ($gC.m^{-2}$)	0.03	0.63	253.14

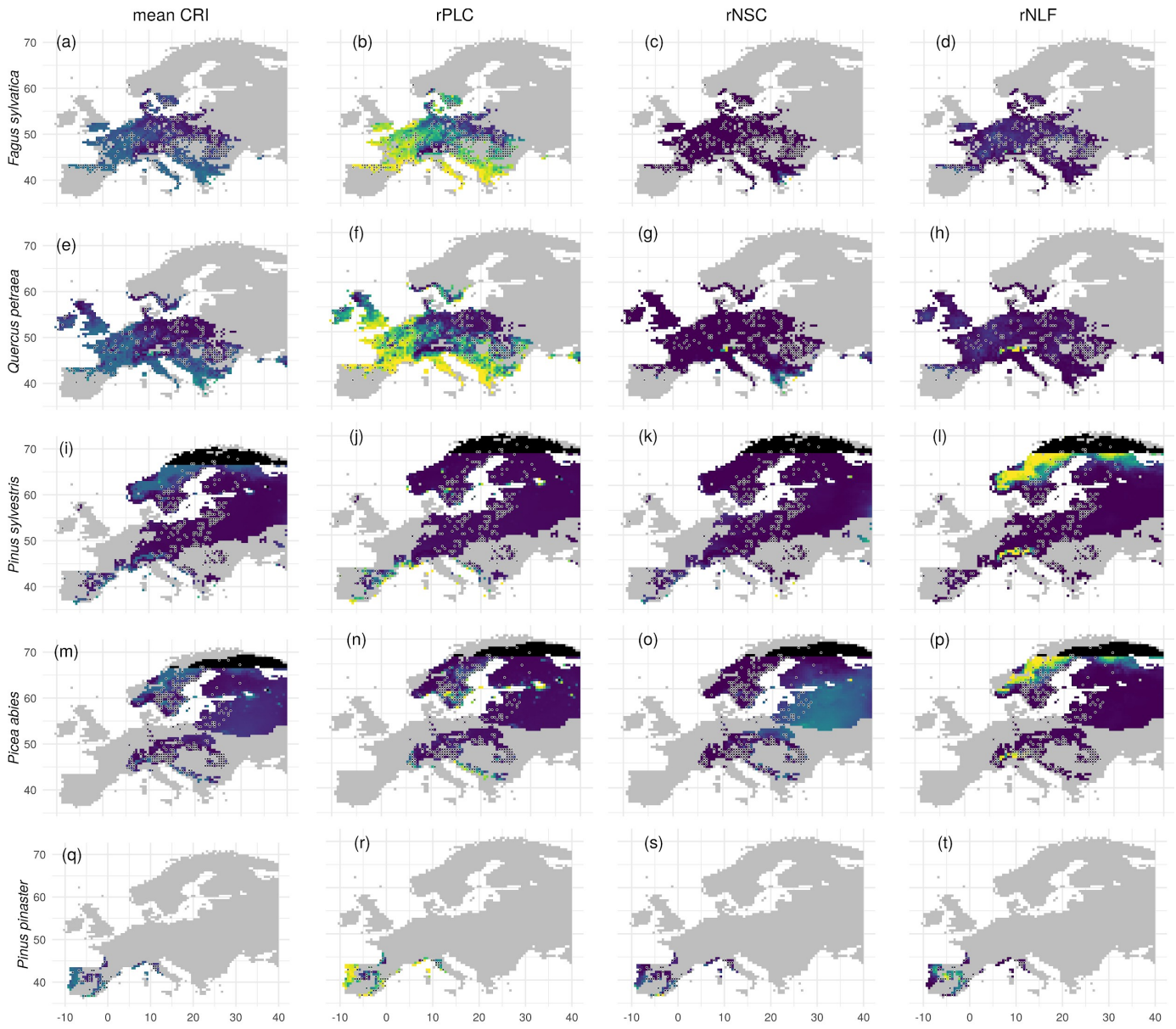

Figure 1: Variation of the risk of mortality between the studied species (on different lines) and over their realized distribution range under current climate.

The first panel on the left (a, e i, m, q) represent the mean value of the composite risk index of mortality (CRI), varying from -1 (purple, low risk) to 2 (yellow, high risk). This CRI is the combination of the three proxies displayed on the other panels: the relative percent loss of conductivity (rPLC) as a proxy of the risk of mortality due to hydraulic failure (from 0, low risk, to 1, high risk, on panels b,f,j,n,r) ; the relative non-structural carbohydrate content (rNSC) as a proxy of the risk of mortality due to carbon starvation (from 0, high risk, to 1, low risk, on panels c,g,k,o,s) ; and the relative number of late frost days over the period (*rNLF*) as a proxy of the risk of mortality due to late frost (from 0, low risk, to 1, high risk, on panels d,h,l,p,t) . Black dots with white circle are the GCUs of the different species.

Variations of the risk of mortality and its components over species realized range under current climate

The cumulative risk index of mortality (CRI) varied from -1 to 1 over the realized distribution range of each species (Figure 1 & 2, Supplementary Table S7 a,b), with a mean CRI of -0.15, -0.35, -0.40, -0.62 and -0.77 respectively for *Pinus pinaster, Fagus sylvatica, Quercus petraea, Picea abies* and *Pinus sylvestris*. Note that the highest possible risk of mortality (CRI= 2) could not be reached with CASTANEA, meaning that the different possible climatic stresses do not combine at the same location (or that tree die before). For broadleaved species, the highest CRI-values were found in the Mediterranean region and in the western part of their distributions. For *Picea abies* and *Pinus sylvestris*, the highest CRI-values were found in northern Scandinavia. For *Pinus pinaster*, the highest CRI-values were found close to the coast line.

Moreover, the processes contributing to CRI varied among species: for broadleaved species and *P. pinaster*, CRI was mainly driven by rPLC, indicating a higher contribution of hydraulic failure to the risk of mortality in these species. By contrast, in *Picea abies* and *Pinus sylvestris*, rNLF highly contributed to CRI, indicating a higher contribution of damages due to late frost to the risk of mortality in these species. The contribution of rNSC to CRI was always low, indicating a weak contribution of carbon starvation to the risk of mortality in the studied species

The highest rPLC-values (indicating a high risk of hydraulic failure) were found in the Mediterranean region for all species. For broadleaved species, high rPLC-values were also found in western Europe. For *Picea abies* and *Pinus sylvestris*, high PLC-values were found in the Baltic sea region. Most of the distribution of *Pinus pinaster* presented high values of rPLC, except at mountainous region and in South-eastern France (Landes forest) **(Figure 1, b,f,j,n,r)**.

For broadleaved species, the lowest rNSC-values (indicating a high risk of carbon starvation) were mainly observed in the south-eastern part of their distribution range. *Picea abies* had low rNSC-values in the continental part of western Europe. *Pinus pinaster* had low rNSC-values at the south of the Iberian coastline. *Pinus sylvestris* had low rNSC-values at the south-eastern part of its distribution **(Figure 1, c,g,k,o,s)**.

High rNLF-values (indicating a high risk of mate frost damages) mainly occurred at high altitudes (Meseta, Alps, Carpathian mountains). For *Picea abies* and *Pinus sylvestris*, high rNLF-values also occurred in northern europe (Kjolen mountains) **(Figure 1, d,h,l,p,t).**

Comparison of the risk of mortality between current and future climates over species realized range

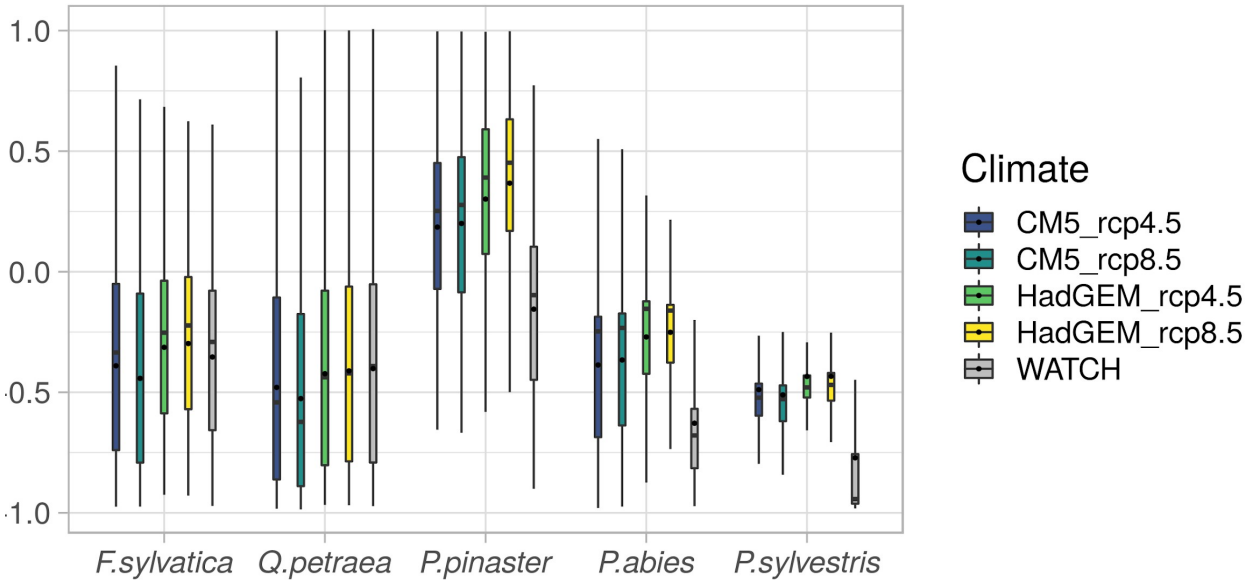

Figure 2 : Variation of the risk of mortality (as measured by CRI) between current and future climates over species realized range. The median CRI value is represented as line, the mean as dot in each boxplot.

As expected, the risk of mortality tended to increase between the "optimistic" CM5 and the "pessimistic" HadGEM RCMs, and between the RCP4.5 and RCP 8.5 scenarios (Figure 2 - figures S5). The three conifer species showed an increase of CRI between current and future climates, with a mean mortality risk increase of 0.42, 0.31, 0.30, respectively for *Pinus pinaster*, *Picea abies* and *Pinus sylvestris* (Figure 2 and Table S7a). By contrast, broadleaved species showed little or no impact of climate change on the risk of mortality. *Fagus sylvatica* showed a small increase of CRI (mean of +0.05) under HadGem scenarios and a decrease of CRI (mean of -0.06) under CM5 scenarios. For *Quercus petraea* , all future predictions showed a decrease in CRI (mean of -0.06), particularly with the CM5 8.5 scenario (-0.12) (Figure 2 and Table S7a, figure S5).

The rNSC-values decreased for all species (increasing mortality risk to carbon starvation) with higher changes for the conifer species (Figure S6a + Table S7a). The rNLF-values (mortality risk to late frost) decreased for all species to reach almost null values (Figure S6b + Table S7a). The rPLC-values (mortality risk to hydraulic failure) increased for all conifer species, with a slight increase for *Picea abies* and *Pinus sylvestris* and a strong increase for the *Pinus pinaster* (0.10). For *Fagus sylvatica*, rPLC increased under the HadGem

GCM, whereas CM5 GCM had not effect or was associated with a decreasing CRI (Figure S6c + Table S7a).

Effect of silviculture on the risk of mortality

Simulations with management had an overall lower risk of mortality than the reference scenarios without management, with variable effect of management between species (Figure S7 + Table S7a) . Under current climate, the median CRI decreased by -0.22 and -0.05 respectively for *Picea abies* and *Fagus sylvatica* between scenario "without" versus "with management", whereas it increased by 0.02 for *Pinus sylvestris*. Management practices had no major effects on the risk of mortality of *Pinus pinaster* and *Quercus petraea*. The impact of silviculture was higher in future scenarios except for *Quercus petraea*, for which the impact remained negligible. For all other species, the median CRI decreased by 0.42, 0.20, 0.09 and 0.07 respectively for *Picea abies*, *Pinus sylvestris*, *Pinus pinaster* and *Fagus sylvatica* between scenario "without" versus "with management".

Comparison of the risk of mortality between current and future climate on species potential distribution range

The increase in CRI between current and future climates was less important when we considered predictions all over Europe, assuming that species niches include locations outside of the current species' distribution range, instead of focussing on the CRI did not increase as much as when we considered only the current species' distribution range for broadleaved species. The median CRI in the whole European space was even lower than in their distribution (Figure S8 + Table S7a and b). Looking at the whole of Europe, future predictions remain the same for each of the species and proxies. The rPLC-values remained high and increased towards the North. A small decrease in rNLF-values was observed, together with increasing rNSC values.

The risk of GCU's extirpation

For all species, the risk of GCUs extirpation increased in all future scenarios and management practices were associated with decreasing CRI. The conservation network suffering the most from climate change was that of *Pinus pinaster,* with all GCUs switching from a low to a high risk of mortality (Table 2).

Table 2: Variation if the risk of extirpation of GCU between species and between current and future climate scenarios. For each species, we computed the percentage of CGUs with a low (< 0.5), medium (> -0.5 & 0.5 <) and high CRI (> 0.5) under four scenarios, including current versus future (HadGem RCP 8.5) climates, and contrasted management scenarios (ie, without or with management). The first columns also gives the total number of GCUs per species (as available in June 2017).

Species	**Scenario**	**CRI under current climate**			**CRI under future climate**		
(#GCU)		**< -0.5**	**> -0.5 & 0.5 <**	**> 0.5**	**< -0.5**	**> -0.5 & 0.5 <**	**> 0.5**
Fagus sylvatica 526	No management	51	49	0	33	64	1
	Management	53	47	0	34	66	0
Quercus petreae 282	No management	45	55	0	53	46	1
	Management	128	154	0	55	44	1
Picea abies 667	No management	78	21	1	46	51	2
	Management	551	116	0	84	16	~0
Pinus sylvestris 421	No management	87	11	2	55	42	3
	Management	88	12	0	88	12	~0
Pinus pinaster 61	No management	23	69	8	0	50	50
	Management	23	69	8	5	60	35

Discussion

The impacts of drought and frost vary between species and across distribution range

In this study, we used the PBM CASTANEA to simulate the spatial and temporal variation in the risk of mortality linked to hydraulic failure, carbon starvation and late frosts of five major European tree species across their entire range, as driven by the variations in climate, soil properties and management practises. We focused on the risk of mortality associated with droughts and late frosts, two major risks likely to increase in the future (Augspurger 2013; IPCC 2014; Charrier *et al.* 2018). CASTANEA was previously used to simulate the risk of mortality at stand scale in *Fagus sylvatica* (Petit-Cailleux et al submitted), and to simulate growth patterns in *Fagus sylvatica*, *Quercus petraea, Quercus ilex, Quercus robur* and *Picea abies* at European scale. The main novelty of this study is to extend CASTANEA simulations of the risk of mortality at European scale.

We first found that the physiological processes increasing the risk of mortality differed between species: hydraulic failure was the main driver of the risk of mortality of broadleaved species and *P. pinaster*, whereas late frost drove the risk of mortality for *Picea abies* and *Pinus sylvestris*. Moreover, the five considered species showed a weak risk of mortality due to carbon starvation. These results are consistent with the narrower safety margin for hydraulic failure reported in deciduous broad-leaved as compared to evergreen conifer trees (Choat *et al.* 2012; Martin-StPaul *et al.* 2017). However, we did not expect to find such high risks of hydraulic failure for *Pinus pinaster* (Figure 2). This surprising result may be due to the fact that CASTANEA underestimates the groundwater that can be accessed by the root system of *Pinus pinaster*. Indeed, CASTANEA accounts only for superficial water capacity (0-150 cm), and neglects the fact that roots can be found even in cracks in the bed rock. The high risk of late frost damages found for the high-latitude and high-altitude conifers was not expected either. This result may be due to the simple phenological model for budburst used here, which is based on accumulation of forcing temperatures only, and neglects the chilling and the progressive increase of vulnerability to late frost along the budburst process. Moreover, the threshold value for late frost damage was considered to be the same for all species (1 frost day every 3 years). Finally, the low risk of carbon starvation observed here is consistent with current ecophysiological knowledge (Martinez-Vilalta et al. 2016), although the fact that simulations were initiated with small trees (diameter 5 cm) also probably contributed to explain this result.

We also found that the physiological processes increasing the risk of mortality differed across species distribution range. The highest risks of hydraulic failure were found under Mediterranean climate, corresponding to long and severe drought, which is consistent with other studies based on PBMs or cSDMs (Morin et al 2008, Garate-Escamilla et al 2019). High risk of hydraulic failure was also found in other regions, in Netherland, odega and nagoda lake in Russia, which might be due to soil properties (Figure 1 + FigureS5). Most regions vulnerable to late frosts were found in high latitude and altitude.

Management practises decreased the risk of mortality due to drought

In our simulations, considering the current management practices usually decreased the risk of mortality as compared to scenario without management. This was found for conifer trees under current climate (except for *Pinus sylvestris*), and for all species under future climates. This is likely because the simulated management practises first reduce the average density of forest stands, which decreases the biomass of the average tree, and thereby its respiration; meanwhile, the leaf area index (LAI) and thus the photosynthesis are also reduced by thinning, but proportionally less than the biomass, which allows increasing the individual growth per stem of the average tree, and hence decrease the risk of carbon starvation. Moreover, silviculture also reduces stand age, which reduces the risk of drought-induced mortality because young, small trees have lower water needs and hence a lower risk of hydraulic failure than old, big trees in CASTANEA. This model behavior is consistent with ecophysiological knowledge and experimental studies, which generally show a higher vulnerability both to carbon starvation and hydraulic failure of old, big trees as compared to young, small trees.

Our findings are thus consistent with previous studies showing that forest thinnings can mitigate drought impacts (Elkin et al. 2015; Sohn et al. 2016). Our simulations suggest that the economic loss could be not that high, (i.e. we found an increase of mean annual growth), as already mentioned by Dolos et al. (2015). These effects of forest thinning are all the more important to account for when predicting the risk of GCU extirpation across GCUs network, since the concept of the dynamic conservation of genetic resources allows and promotes active management to maintain the genetic processes (i.e. gene flow, pollination, regeneration) of the target species (Schueler *et al.* 2014). The management of GCUs may thus include common silvicultural measures, as considered here, or even innovative adaptive management practises, as suggested by Lefèvre *et al.* (2014). Note however that seed transfert, which consist in moving genotypes from populations that are more resistant to

stress towards locations forecast to be exposed to higher stress, are not allowed in conservation network, since it would contradict their obvious objective of conserving local gene pools.

Our study also suggest that PBM are useful tools to evaluate the respective interest of adaptive management practises in the context of CC. Such horizon scanning approaches are especially needed in a context where foresters are willing to change silvicultural practices if growth declines of trees were over 20% and if regeneration failures were over 25% (Seidl *et al.* 2016). Here, we mostly considered even-aged silvicultural systems, which probably allows a faster generation renewal than uneven-aged system (e.g., continuous cover forest management system) or system without management, and could result in a faster genetic evolution of populations at risk, in addition to reducing the risk of mortality of trees (Bussotti *et al.* 2015). However, other models than the one used in this study would be needed to simulate the rate of genetic evolution, which would requires considering additionally the potential of tree adaptation (e.g. Oddou-Muratorio & Davi, 2014).

The risk of GCU extirpation under climate change differs among species.

As expected, the projections of mortality under future climate obtained here with the PBM CATANEA were less pessimistic than those provided by BNMs (Schueler *et al.* 2014; Dyderski *et al.* 2018). We found, for the most pessimistic model and climate scenario (HadGEM rcp 8.5), an increase of GCU risk of extirpation by 40%, 25%, 18%, and 2%, respectively for *Picea abies*, *Pinus sylvestris, Fagus sylvatica*, and *Pinus pinaster* and a decrease of mortality risk of 4% for *Quercus petraea*. By contrast, Schueler et al (2014) reported a stronger increase in GCU risk of extirpation, amounting to 33%-65% depending on the species. Moreover, when the risk of mortality was predicted all over Europe, and not only on the current distribution area, the risk of mortality was predicted to decrease both for *Quercus petraea* and *Fagus sylvatica* (in CM5 scenario), contrary to several studies (Dydersky et al 2018).

However, we found the same trends for the variability of responses between species as Dyderski et al 2017, who described some species as “winners” (with a net gain in distribution range under climate change) or “losers” (with a net loss of range). Contrary to Dyderski et al (2018), we initiated our simulations with the same starter trees (i.e. same DBH, age and competition status all over Europe). Hence, our results suggest that the observed differences between species are rather due to ecophysiological processes and not to the “place of species” in the ecological succession. We found that climate change decreased the risk of mortality of

broadleaved species, *Quercus petraea* (all future prediction) and *Fagus sylvatica* (CM5) and increased the risk of mortality of coniferous species. This increasing risk of mortality of conifers was mainly due to increasing an risk of starvation and late frost occurences.

The decreasing risk of mortality predicted for broadleaf species under climate change can be due to their higher stomatal sensitivity to CO_2. Klein & Ramon (2019) showed that conifers will need as much water as they currently do to complete their photosynthesis under future climate, while angiosperms will need less water for the same amount of CO_2 to complete their photosynthetic cycles. In our simulations, the decreasing risk of carbon starvation for *Q. petraea* and *F. sylvatica* under climate change resulted from the increase in growing season duration, which compensated the increasing risk of hydraulic failure and late frosts. The positive effect of increasing growing season duration is perhaps overestimated because the phenological model used here does not take into account the breaking of dormancy, which could be delayed under climate change (Gaüzere et al., 2017). On the other hand, if the positive effect of CO_2 on the photosynthesis simulated by CASTANEA is in the range of the effects observed on the FACE experiments, a similar effect on the growth and ecosystem carbon accumulation is far from being evident as shown many studies (see Norby et al. 2011 for a synthesis).

Future directions

We stimulated the growth and risk of mortality of an average tree across Europe with CASTANEA under current and future climate, with a fair match between current species range and the prediction of NPP (except for *Pinus abies* and latitudes over 67.5) and an accurate prediction of growth for broadleaved species and *Pinus pinaster*. In our simulations, budburst was modeled with a simple forcing model which does not take into account the dormancy and photoperiod effects on budburst (Gauzere et al. 2017). This can explain why budburst failed to be simulated over a certain latitude. Three hypotheses can explain a lower NPP and growth in the distribution area for *Pinus sylvestris* and *Picea abies* than in the whole of Europe: (1) these two species are not limited by climate, neither by soil but their distribution are dependant of biotic interaction/agent. (2) The coarse climate used does not represent local climate conditions (i.e extreme values of climate were not taken into account) (3) the current distribution is not limited by survival at adult stage, but by reproduction or survival at seedling stages (Niinemets & Valladares 2006). (4) Even if CASTANEA is validated at stand

scale for these species, these stands could be not representative of the species conditions across Europe.

The methods to evaluate CASTANEA model at large scale could be improved. Here, we used a method relying on the optimisation of the correlation between NPP and ring width predicted by CASTANEA and the observed presence of the species. However, the flux predictions under current climate could also be compared to observations of ICOS (Integrated Carbon Observation System) sites for each target species (Reyer *et al.* 2019).

Finally, this study only partially accounted for interspecific variability in thresholds to mortality (e.g. the PLC value leading to mortality differed among broadleaved and conifer trees), and not at all for intra-specific variability in vulnerability. Yet, local adaptation is widespread in tree populations throughout their distribution ranges (Benito Garzón *et al.* 2011; Alberto *et al.* 2013). For example, the study of Anderegg et al. (2016) demonstrated genetic differentiation of xylem resistance traits in several species. For *Fagus sylvatica*, Kreyling et al. (2014) found genetic differentiation of frost resistance parameters, particularly in marginal populations. These patterns of intra-specific variability and differentiation of adaptive traits involved in response to drought and frost would be interesting to consider in future simulations.

Data accessibility

The data set analysed in this preprint will be available online under the zenodo repository (10.5281/zenodo.3691774).
Due to their weight, climatic data are available on request.

Supplementary material

The process-based model CASTANEA is an open-source software available on capsis website: http://capsis.cirad.fr/

REFERENCES

Alberto, F.J., Aitken, S.N., Alía, R., González-Martínez, S.C., Hänninen, H., Kremer, A., *et al.* (2013). Potential for evolutionary responses to climate change - evidence from tree populations. *Glob. Chang. Biol.*, 19, 1645–1661.

Allen, C.D., Macalady, A.K., Chenchouni, H., Bachelet, D., McDowell, N., Vennetier, M., *et al.* (2010). A global overview of drought and heat-induced tree mortality reveals emerging climate change risks for forests. *For. Ecol. Manage.*, 259, 660–684.

Allouche, O., Tsoar, A. & Kadmon, R. (2006). Assessing the accuracy of species distribution models: Prevalence, kappa and the true skill statistic (TSS). *J. Appl. Ecol.*, 43, 1223–1232.

Anderegg, W.R.L., Hicke, J.A., Fisher, R.A., Allen, C.D., Aukema, J., Bentz, B., *et al.* (2015). Tree mortality from drought, insects, and their interactions in a changing climate. *New Phytol.*, 208, 674–683.

Anderegg, W.R.L., Klein, T., Bartlett, M., Sack, L., Pellegrini, A.F.A., Choat, B., *et al.* (2016). Meta-analysis reveals that hydraulic traits explain cross-species patterns of drought-induced tree mortality across the globe. *Proc. Natl. Acad. Sci. U. S. A.*, 113, 5024–5029.

Augspurger, C.K. (2013). Reconstructing Patterns of Temperature, Phenology, and Frost Damage over 124 Years: {{Spring}} Damage Risk Is Increasing. *Ecology*, 94, 41–50.

Ball, J.T., Woodrow, I.E. & Berry, J.A. (1987). A Model Predicting Stomatal Conductance and its Contribution to the Control of Photosynthesis under Different Environmental Conditions. In: *Progress in Photosynthesis Research*. Springer, pp. 221–224.

Begon, Michael, Townsend, Colin R., et Harper, John L. *Ecology: from individuals to ecosystems*. 2006.

Benito Garzón, M., Alía, R., Robson, T.M. & Zavala, M.A. (2011). Intra-specific variability and plasticity influence potential tree species distributions under climate change. *Glob. Ecol. Biogeogr.*, 20, 766–778.

Bernacchi, C.J., Singsaas, E.L., Pimentel, C., Portis Jr, A.R. & Long, S.P. (2001). Improved temperature response functions for models of Rubisco-limited photosynthesis. *Plant, Cell Environ.*, 24, 253–259.

Bigler, Christof and Harald Bugmann. 2018. “Climate-induced shifts in leaf unfolding and frost risk of European trees and shrubs.” Scientific Reports 8(1):1–10.

Brodribb, T.J. (2009). Xylem hydraulic physiology: The functional backbone of terrestrial plant productivity. *Plant Sci.*, 177, 245–251.

Bussotti, F., Pollastrini, M., Holland, V. & Brüggemann, W. (2015). Functional traits and adaptive capacity of European forests to climate change. *Environ. Exp. Bot.*, 111, 91–113.

De Caceres, M., Martin-StPaul, N., Turco, M., Cabon, A. & Granda, V. (2018). Estimating daily meteorological data and downscaling climate models over landscapes. *Environ. Model.*

Softw., 186–196.

Cardellini, G., Valada, T., Cornillier, C., Vial, E., Dragoi, M., Goudiaby, V., *et al.* (2018). EFO-LCI: A New Life Cycle Inventory Database of Forestry Operations in Europe. *Environ. Manage.*, 61, 1031–1047.

Charrier, G., Chuine, I., Bonhomme, M. & Améglio, T. (2018). Assessing frost damages using dynamic models in walnut trees: exposure rather than vulnerability controls frost risks. *Plant Cell Environ.*, 41, 1008–1021.

Cheaib, A., Badeau, V., Boe, J., Chuine, I., Delire, C., Dufrêne, E., *et al.* (2012). Climate Change Impacts on Tree Ranges: Model Intercomparison Facilitates Understanding and Quantification of Uncertainty: {{Understanding}} and Quantification of Uncertainties of Climate Change Impacts on Tree Range. *Ecol. Lett.*, 15, 533–544.

Choat, B., Jansen, S., Brodribb, T.J., Cochard, H., Delzon, S., Bhaskar, R., *et al.* (2012). Global convergence in the vulnerability of forests to drought. *Nature*, 491, 752–755.

Cramer, W., Bondeau, A., Woodward, F.I., Prentice, I.C., Betts, R.A., Brovkin, V., *et al.* (2001). Global response of terrestrial ecosystem structure and function to CO2 and climate change: Results from six dynamic global vegetation models. *Glob. Chang. Biol.*, 7, 357–373.

Davi, H., Barbaroux, C., Francois, C. & Dufrêne, E. (2009). The fundamental role of reserves and hydraulic constraints in predicting LAI and carbon allocation in forests. *Agric. For. Meteorol.*, 149, 349–361.

Davi, H. & Cailleret, M. (2017). Assessing Drought-Driven Mortality Trees with Physiological Process-Based Models. *Agric. For. Meteorol.*, 232, 279–290.

Davi, H., Dufrêne, E., Francois, C., Le Maire, G., Loustau, D., Bosc, A., *et al.* (2006). Sensitivity of water and carbon fluxes to climate changes from 1960 to 2100 in European forest ecosystems. *Agric. For. Meteorol.*, 141, 35–56.

Davi, H., Dufrêne, E., Granier, A., Le Dantec, V., Barbaroux, C., François, C., *et al.* (2005). Modelling carbon and water cycles in a beech forest. Part II.: Validation of the main processes from organ to stand scale. *Ecol. Modell.*, 185, 387–405.

Dolos, K., Bauer, A. & Albrecht, S. (2015). Site suitability for tree species: Is there a positive relation between a tree species' occurrence and its growth? *Eur. J. For. Res.*, 134, 609–621.

Dufrêne, E., Davi, H., François, C., Le Maire, G., Le Dantec, V. & Granier, A. (2005). Modelling carbon and water cycles in a beech forest. Part I: Model description and uncertainty analysis on modelled NEE. *Ecol. Modell.*, 185, 407–436.

Dyderski, M.K., Paź, S., Frelich, L.E. & Jagodziński, A.M. (2018). How Much Does Climate Change Threaten {{European}} Forest Tree Species Distributions? *Glob. Chang. Biol.*, 24, 1150–1163.

E Silva, D., Rezende Mazzella, P., Legay, M., Corcket, E. & Dupouey, J.L. (2012). Does natural

regeneration determine the limit of European beech distribution under climatic stress? *For. Ecol. Manage.*, 266, 263–272.

Elith, J. & Leathwick, J.R. (2009). Species Distribution Models: Ecological Explanation and Prediction Across Space and Time. *Annu. Rev. Ecol. Evol. Syst.*, 40, 677–697.

Farquhar, G.D., Caemmerer, S. Von & Berry, J. a. (1980). A Biochemical Model of Photosynthetic CO. *Planta*, 149, 78–90.

Fourcade, Y., Besnard, A.G. & Secondi, J. (2018). Paintings predict the distribution of species, or the challenge of selecting environmental predictors and evaluation statistics. *Glob. Ecol. Biogeogr.*, 27, 245–256.

Gauzere, J., Delzon, S., Davi, H., Bonhomme, M., Garcia de Cortazar-Atauri, I. & Chuine, I. (2017). Integrating Interactive Effects of Chilling and Photoperiod in Phenological Process-Based Models. {{A}} Case Study with Two {{European}} Tree Species: {{Fagus}} Sylvatica and {{Quercus}} Petraea. *Agric. For. Meteorol.*, 244–245, 9–20.

Gárate-Escamilla, Homero, Arndt Hampe, Natalia Vizcaíno-Palomar, T. Matthew Robson, and Marta Benito Garzón. 2019. "Range-Wide Variation in Local Adaptation and Phenotypic Plasticity of Fitness-Related Traits in Fagus Sylvatica and Their Implications under Climate Change." *Global Ecology and Biogeography* 28(9):1336–50.

Granier, A., Biron, P. & Lemoine, D. (2000). Water balance, transpiration and canopy conductance in two beech stands. *Agric. For. Meteorol.*, 100, 291–308.

Hanewinkel, M., Cullmann, D., Schelhaas, M., Nabuurs, G. & Zimmermann, N. (2012). Climate change may cause severe loss in the economic value of European forest land. *Nat. Clim. Chang.*, 3, 203–207.

Härkönen, S., Neumann, M., Mues, V., Berninger, F., Bronisz, K., Cardellini, G., *et al.* (2019). A climate-sensitive forest model for assessing impacts of forest management in Europe. *Environ. Model. Softw.*, 115, 128–143.

Harris, R.M.B., Grose, M.R., Lee, G., Bindoff, N.L., Porfirio, L.L. & Fox-Hughes, P. (2014). Climate projections for ecologists. *Wiley Interdiscip. Rev. Clim. Chang.*, 5, 621–637.

Hauck, J., Völker, C., Wolf-Gladrow, D.A., Laufkötter, C., Vogt, M., Aumont, O., *et al.* (2015). On the Southern Ocean CO2 uptake and the role of the biological carbon pump in the 21st century. *Global Biogeochem. Cycles*, 29, 1451–1470.

Hengl, T., De Jesus, J.M., Heuvelink, G.B.M., Gonzalez, M.R., Kilibarda, M., Blagotić, A., *et al.* (2017). SoilGrids250m: Global gridded soil information based on machine learning. *PLoS One*, 12, e0169748.

Hiederer, R. (2013). *Mapping Soil Properties for Europe - Spatial Representation of Soil Database Attributes*. *JRC Tech. Reports*.

Hijmans, R.J. (2015). raster: Geographic Data Analysis and Modeling.

IPCC. (2014). Climate Change 2014: climate change impacts, adaptation and vulnerablility. Working Group II contribution to the Intergovernmental Panel on Climate Change Fifth Assessment Report. Summary for Policymakers, 19.

Jacob, D, Petersen, J., Eggert, B, Alias, A, Christensen,O & et al. (2014). {EURO}-{CORDEX}: {New} high-resolution climate change projections for {European} impact research. *Reg. Environ. Chang.*, 14, 563–578.

Klein, T. & Ramon, U. (2019). Stomatal sensitivity to CO2 diverges between angiosperm and gymnosperm tree species. *Funct. Ecol.*, 33, 1411–1424.

Koskela J., Lefevre F., Schueler S., Kraigher H., Olrik D.C., Hubert J., *et al.* (2012). Translating conservation genetics into management: Pan-European minimum requirements for dynamic conservation units of forest tree genetic diversity. *Biol. Conserv.*, 157, 39–49.

Kreyling, J., Buhk, C., Backhaus, S., Hallinger, M., Huber, G., Huber, L., *et al.* (2014). Local adaptations to frost in marginal and central populations of the dominant forest tree Fagus sylvatica L. as affected by temperature and extreme drought in common garden experiments. *Ecol. Evol.*, 4, 594–605.

Kuparinen, A., Savolainen, O. & Schurr, F.M. (2010). Increased mortality can promote evolutionary adaptation of forest trees to climate change. *For. Ecol. Manage.*, 259, 1003–1008.

Lefèvre, F., Boivin, T., Bontemps, A., Courbet, F., Davi, H., Durand-Gillmann, M., *et al.* (2013). Considering evolutionary processes in adaptive forestry. *Ann. For. Sci.*

Lindner, M., Fitzgerald, J.B., Zimmermann, N.E., Reyer, C., Delzon, S., van der Maaten, E., *et al.* (2014). Climate change and European forests: What do we know, what are the uncertainties, and what are the implications for forest management? *J. Environ. Manage.*

Liu, C., White, M. & Newell, G. (2013). Selecting thresholds for the prediction of species occurrence with presence-only data. *J. Biogeogr.*, 40, 778–789.

Mairota, P., Cafarelli, B., Boccaccio, L., Leronni, V., Labadessa, R., Kosmidou, V., *et al.* (2013). Using landscape structure to develop quantitative baselines for protected area monitoring. *Ecol. Indic.*, 33, 82–95.

Martin-StPaul, N., Delzon, S. & Cochard, H. (2017). Plant resistance to drought depends on timely stomatal closure. *Ecol. Lett.*

Martínez-Vilalta, J., Sala, A., Asensio, D., Galiano, L., Hoch, G., Palacio, S., *et al.* (2016). Dynamics of non-structural carbohydrates in terrestrial plants: a global synthesis. *Ecol. Monogr.*, 86, 495–516.

McDowell, N., Pockman, W.T., Allen, C.D., Breshears, D.D., Cobb, N., Kolb, T., *et al.* (2008). Mechanisms of plant survival and mortality during drought: Why do some plants survive while others succumb to drought? *New Phytol.*, 178, 719–739.

McSweeney, C.F., Jones, R.G., Lee, R.W. & Rowell, D.P. (2015). Selecting CMIP5 GCMs for downscaling over multiple regions. *Clim. Dyn.*, 44, 3237–3260.

Monteith, J.L. (1965). Evaporation and environment. The state and movement of water in living organisms. *Symp. Soc. Exp. Biol. Vol. 19*, 205–234.

Morin, X., Viner, D. & Chuine, I. (2008). Tree species range shifts at a continental scale: New predictive insights from a process-based model. *J. Ecol.*, 96, 784–794.

Nakićenović, N. & Swart, R. (2000). *Special Report on Emission Scenarios.* Cambridge University Press, Cambridge.

Niinemets, Ü. & Valladares, F. (2006). Tolerance to shade, drought, and waterlogging of temperate northern hemisphere trees and shrubs. *Ecol. Monogr.*, 76, 521–547.

Nogués-Bravo, D., Pulido, F., Araújo, M.B., Diniz-Filho, J.A.F., García-Valdés, R., Kollmann, J., *et al.* (2014). Phenotypic correlates of potential range size and range filling in European trees. *Perspect. Plant Ecol. Evol. Syst.*, 16, 219–227.

Norby, Richard J. and Donald R. Zak. 2011. "Ecological Lessons from Free-Air CO2 Enrichment (FACE) Experiments." *Annual Review of Ecology, Evolution, and Systematics* 42(1):181–203.

Oddou-Muratorio S., Davi H. & Lefèvre F. (submitted) Integrating evolutionary, demographic and ecophysiological processes to predict the adaptive dynamics of forest tree populations under global change. Submitted to Tree Genetics and Genome.

Paillet, Y., Bergès, L., HjÄltén, J., Ódor, P., Avon, C., Bernhardt-Römermann, M., *et al.* (2010). Biodiversity differences between managed and unmanaged forests: Meta-analysis of species richness in Europe. *Conserv. Biol.*, 24, 101–112.

Petit-Cailleux, C., Davi, H., Lefèvre, F., Garrigue, J., Magdalou, J.-A., Hurson, C., *et al.* (2019). Combining Statistical and Mechanistic Models to Identify the Drivers of Mortality within a Rear-Edge Beech Population. *bioRxiv*.

Raftery, A.E., Zimmer, A., Frierson, D.M.W., Startz, R. & Liu, P. (2017). Less than 2 °c warming by 2100 unlikely. *Nat. Clim. Chang.*, 7, 637–641.

Reineke, L.H. (1933). Perfecting a stand-density index for even-aged forests. *J. Agric. Res.*, 46, 627–638.

Reyer, C. (2015). Forest productivity under environmental change—A review of stand-scale modeling studies. *Curr. For. Reports*, 1, 53–68.

Reyer, C., Lasch-Born, P., Suckow, F., Gutsch, M., Murawski, A. & Pilz, T. (2014). Projections of regional changes in forest net primary productivity for different tree species in Europe driven by climate change and carbon dioxide. *Ann. For. Sci.*, 71, 211–225.

Reyer, C.P., Silveyra Gonzalez, R., Dolos, K., Hartig, F., Hauf, Y., Noack, M., *et al.* (2019). The PROFOUND database for evaluating vegetation models and simulating climate impacts on forests. *Earth Syst. Sci. Data*.

Ryan, M.G. (1991). Effects of climate change on plant respiration. *Ecol. Appl.*, 1, 157–167.

Sala, A. & Tenhunen, J.D. (1996). Simulations of canopy net photosynthesis and transpiration in Quercus ilex L. under the influence of seasonal drought. *Agric. For. Meteorol.*, 78, 203–222.

Savolainen, O., Pyhäjärvi, T. & Knürr, T. (2007). Gene Flow and Local Adaptation in Trees. *Annu. Rev. Ecol. Evol. Syst.*, 38, 595–619.

Schueler, S., Falk, W., Koskela, J., Lefèvre, F., Bozzano, M., Hubert, J., *et al.* (2014). Vulnerability of dynamic genetic conservation units of forest trees in Europe to climate change. *Glob. Chang. Biol.*, 20, 1498–1511.

Seidl, R., Aggestam, F., Rammer, W., Blennow, K. & Wolfslehner, B. (2016). The sensitivity of current and future forest managers to climate-induced changes in ecological processes. *Ambio*, 45, 430–441.

Seidl, R., Thom, D., Kautz, M., Martin-Benito, D., Peltoniemi, M., Vacchiano, G., *et al.* (2017). Forest disturbances under climate change. *Nat. Clim. Chang.*, 7, 395–402.

Thuiller, W., Lavorel, S., Sykes, M.T. & Araújo, M.B. (2006). Using niche-based modelling to assess the impact of climate change on tree functional diversity in Europe. *Divers. Distrib.*, 12, 49–60.

Tinner, W., Colombaroli, D., Heiri, O., Henne, P.D., Steinacher, M., Untenecker, J., *et al.* (2013). The past ecology of Abies alba provides new perspectives on future responses of silver fir forests to global warming. *Ecol. Monogr.*, 83, 419–439.

Tóth, B., Weynants, M., Pásztor, L. & Hengl, T. (2017). 3D soil hydraulic database of Europe at 250 m resolution. *Hydrol. Process.*, 31, 2662–2666.

Urli, M., Porté, A.J., Cochard, H., Guengant, Y., Burlett, R. & Delzon, S. (2013). Xylem embolism threshold for catastrophic hydraulic failure in angiosperm trees. *Tree Physiol.*, 33, 672–683.

Vitasse, Y., Lenz, A. & Kramer, C. (2014). The interaction between freezing tolerance and phenology in temperate deciduous trees. *Front. Plant Sci.*, 5, 1–12.

De Vries, F.W.T.P., Brunsting, A.H.M. & Van Laar, H.H. (1974). Products, requirements and efficiency of biosynthesis a quantitative approach. *J. Theor. Biol.*, 45, 339–377.

van Vuuren, D.P., Edmonds, J., Kainuma, M., Riahi, K., Thomson, A., Hibbard, K., *et al.* (2011). The representative concentration pathways: An overview. *Clim. Change*, 109, 5–31.

Walther, G.R., Post, E., Convey, P., Menzel, A., Parmesan, C., Beebee, T.J.C., *et al.* (2002). Ecological responses to recent climate change. *Nature*, 416, 389–395.

Weedon, G.P., Balsamo, G., Bellouin, N., Gomes, S., Best, M.J. & Viterbo, P. (2014). The WFDEI meteorological forcing data set: WATCH Forcing data methodology applied to ERA-Interim reanalysis data. *Water Resour. Res.*, 50, 7505–7514.

Winter, S. & Möller, G.C. (2008). Microhabitats in lowland beech forests as monitoring tool for nature conservation. *For. Ecol. Manage.*, 255, 1251–1261.

Zhao, M. & Running, S.W. (2010). Drought-induced reduction in global terrestrial net primary production from 2000 through 2009. *Science (80-.).*, 329, 940–943.

3 Supplementary online material

Figure S1: Species actual distribution and their genetic conservation unit. Green shape is the species distribution and purple dot the CGUs. (a) Fagus sylvatica, (b) Quercus petraea, (c) Pinus pinaster, (d) Pinus sylvestris, (e) Picea abies.

(a)Fagus sylvatica

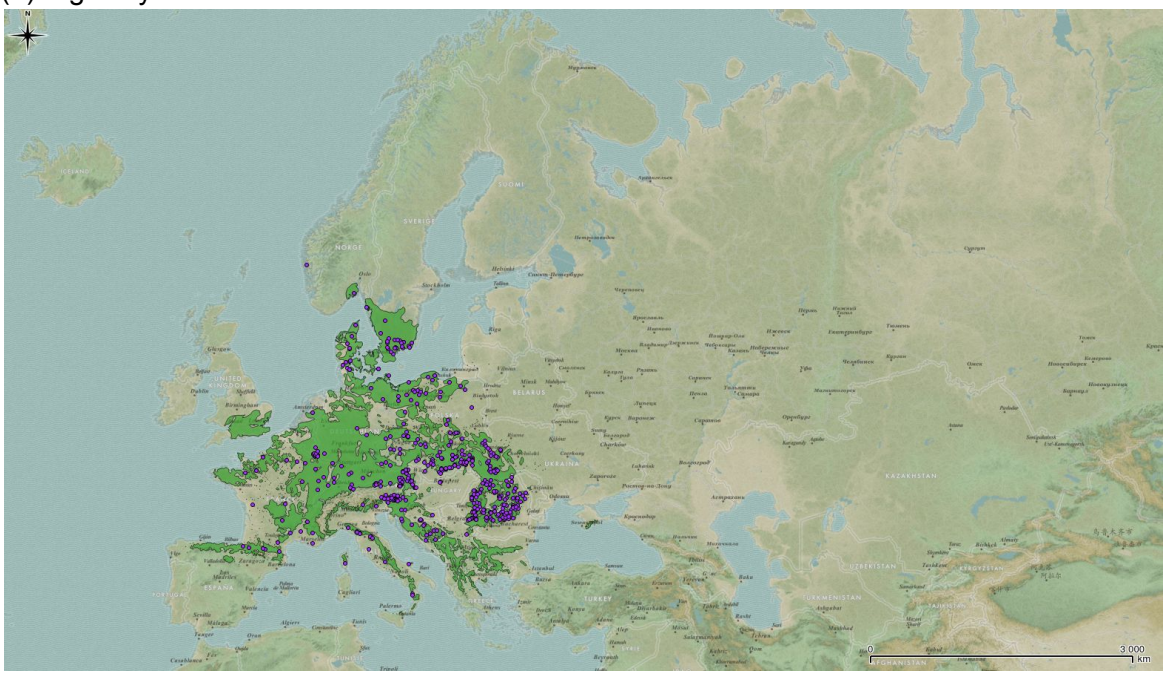

(b) Quercus petraea

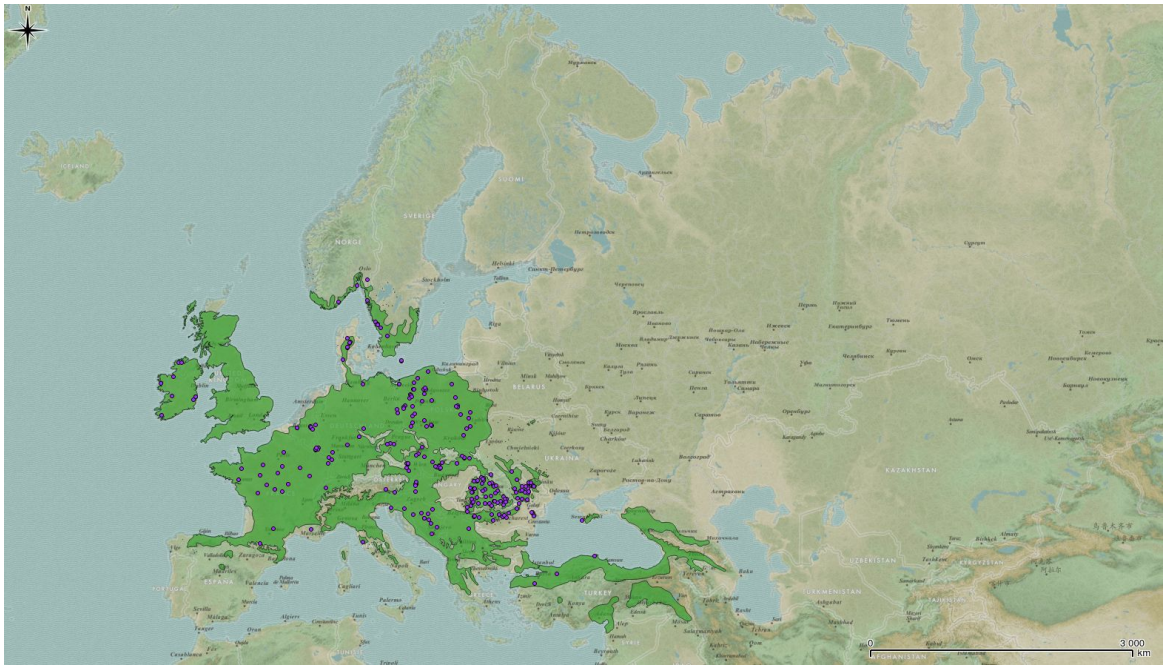

(c) Pinus pinaster

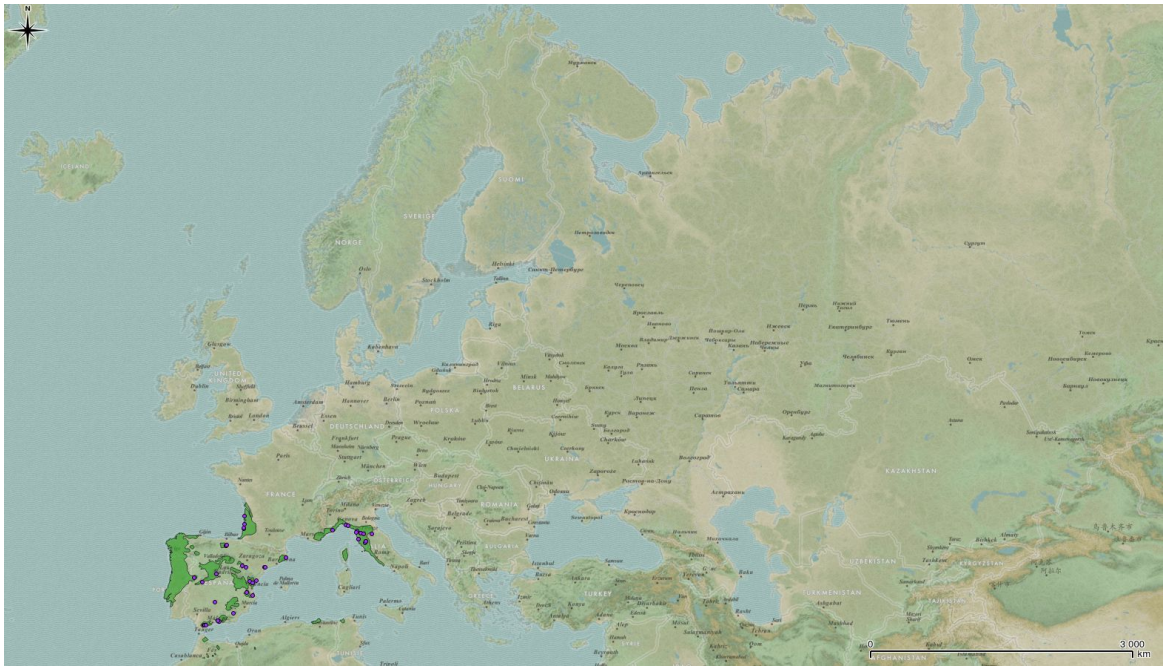

(d) Pinus sylvestris

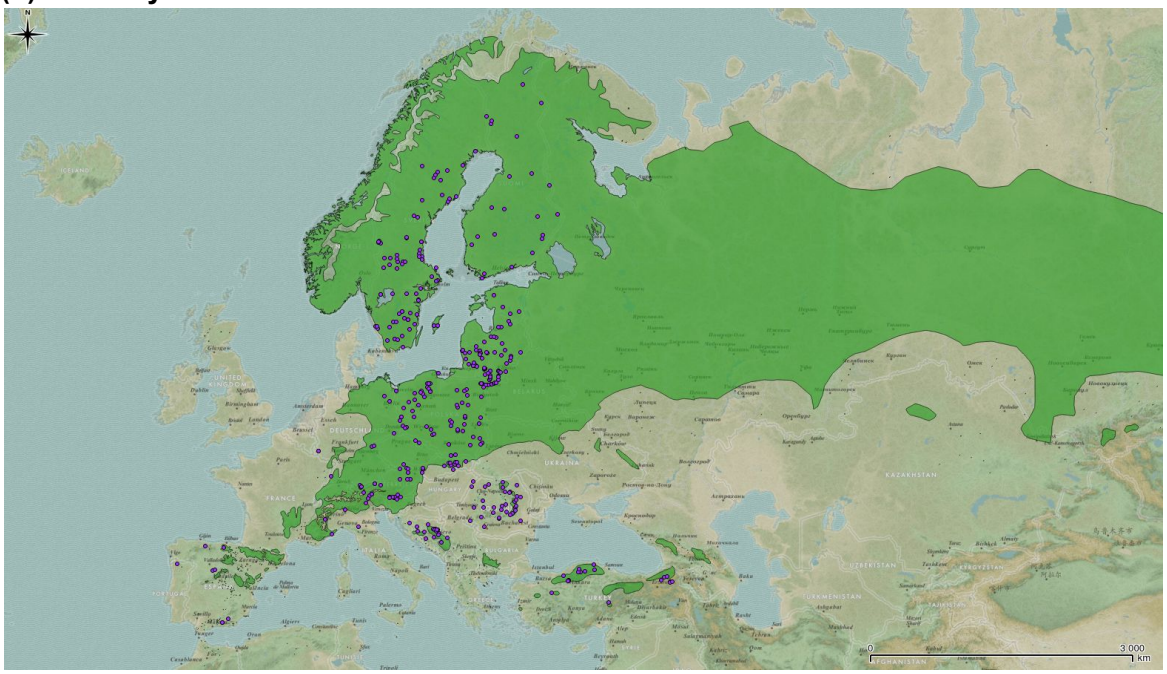

(e) Picea abies

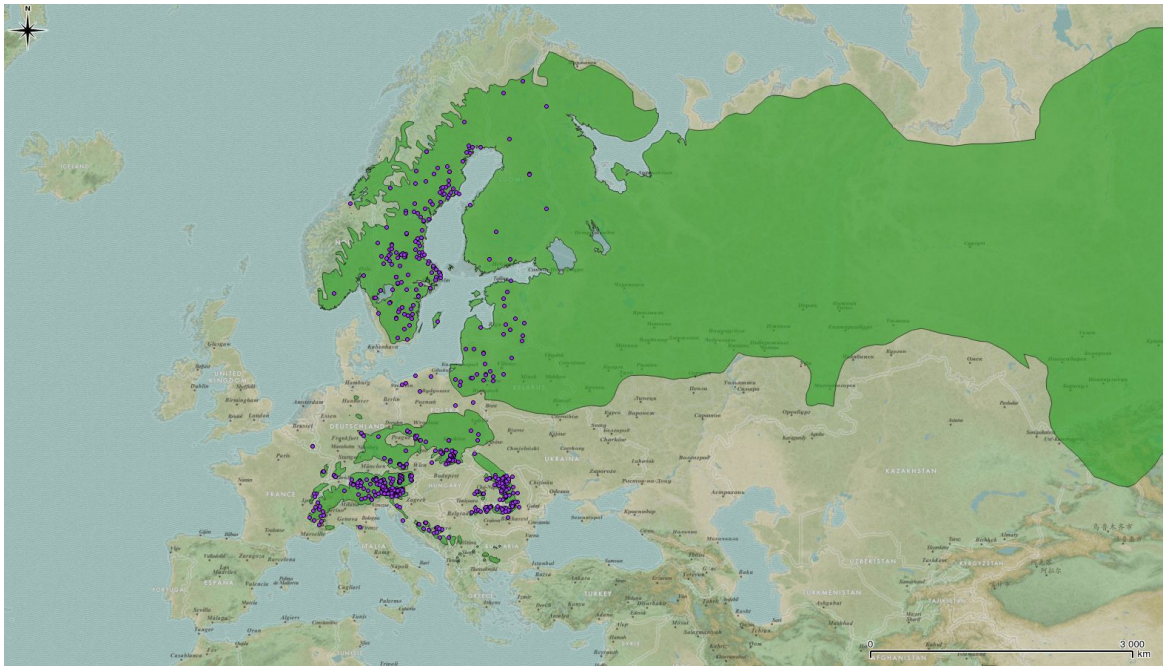

Figure S2: Graphique du Groupe d'experts intergouvernemental sur l'évolution du climat (GIEC) sur l'évolution future de la température dans le cadre d'autres scénarios d'émissions de gaz à effet de serre (adapté par McCarl [2015] de Knutti et Sedíaček [2013]; la mesure du réchauffement de la surface du globe est la température projetée dans le cadre des scénarios de la phase 5 du Projet de comparaison inter-modèles couplés (CMIP5) du GIEC [2013], car elle diffère de la moyenne des températures du globe entre 1986 et 2005 ; RCP, voie de concentration représentative de C02) . Adapté de MacCarl 2016

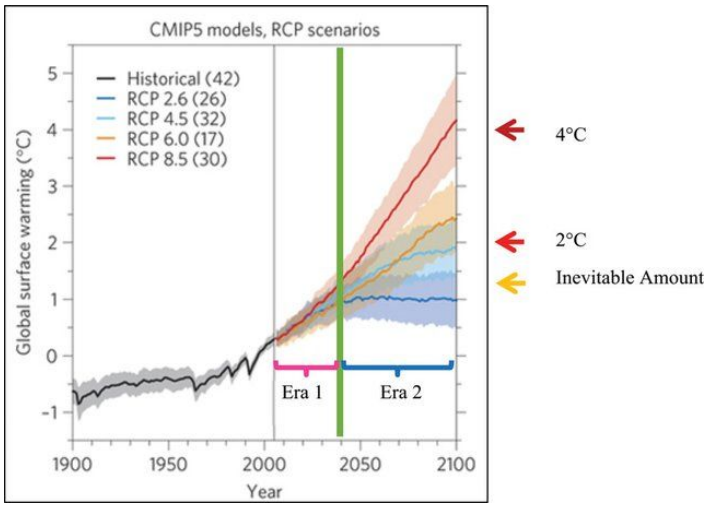

Figure S3 : Ecoregion used to define thinning rules. Ecoregion were adapted from Härkönen et al. (2019), South is yellow (lighter grey), North is green (light grey), CentralEast is blue (grey) and CentralWest is dark purple (dark grey).

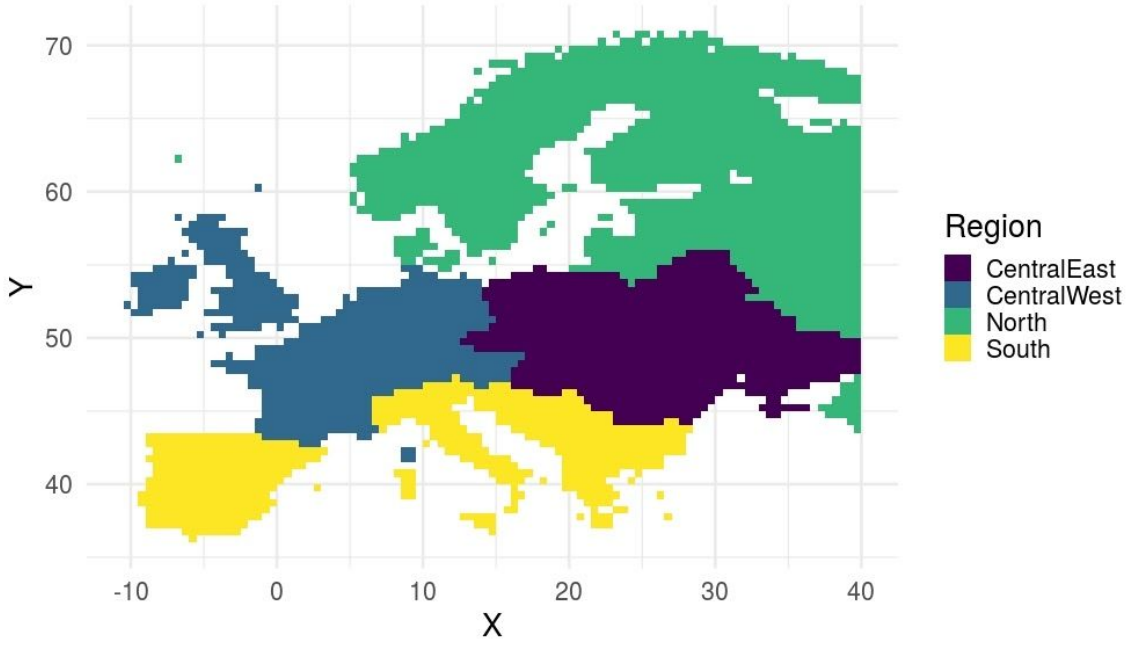

FigureS4: Validation of CASTANEA, through the comparison of key output variables inside (in) vs outside (out) the species distribution: (a) NPP, (b) ring width, (c) budburst. a)

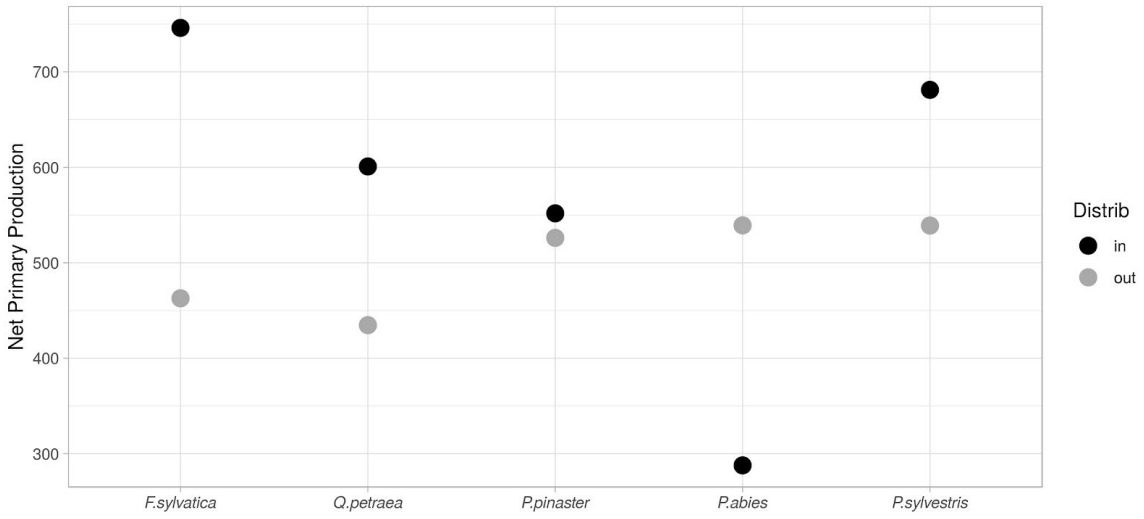

b)

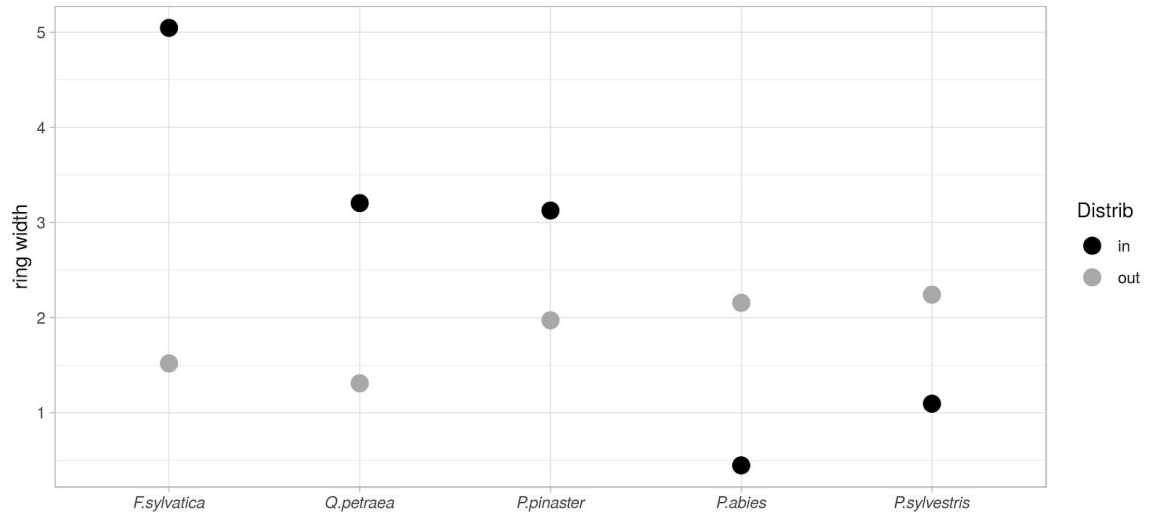

c)

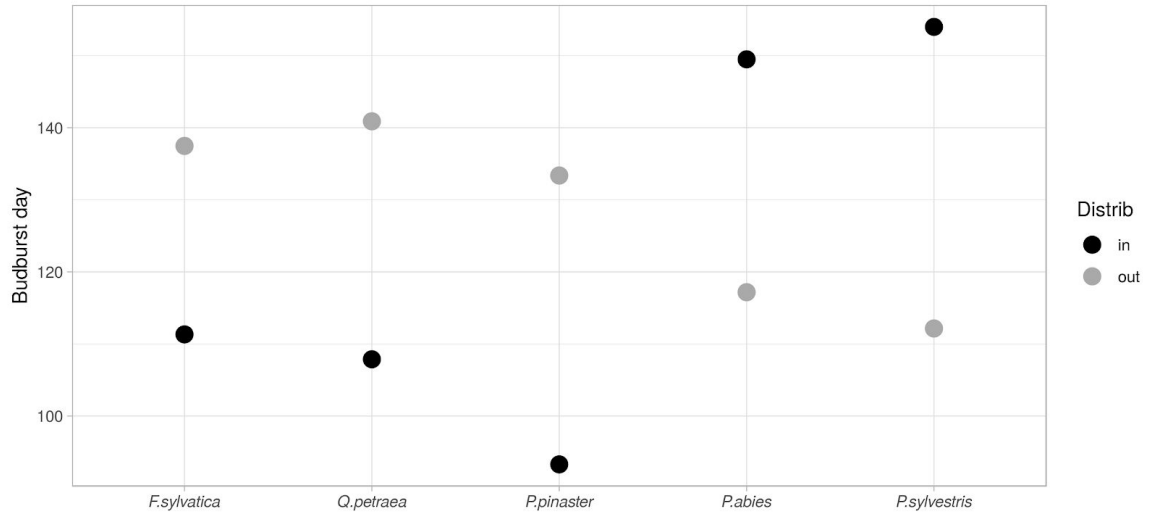

Figure S5: Variation of the risk of mortality between the studied species (on different lines) and over their realized distribution range under future climate. (A) CM5 RCP 4.5, (B) CM5 RCP 8.5, (C) HadGEM RCP 4.5, (D) HadGEM RCP 4.5.
The first panel on the left (a, e i, m, q) represent the mean value of the composite risk index of mortality (CRI), varying from -1 (purple, low risk) to 2 (yellow, high risk). This CRI is the combination of the three proxies displayed on the other panels: the relative percent loss of conductivity (rPLC) as a proxy of the risk of mortality due to hydraulic failure (from 0, low risk, to 1, high risk, on panels b,f,j,n,r) ; the relative non-structural carbohydrate content (rNSC) as a proxy of the risk of mortality due to carbon starvation (from 0, high risk, to 1, low risk, on panels c,g,k,o,s) ; and the relative number of late frost days over the period (*rNLF*) as a proxy of the risk of mortality due to late frost (from 0, low risk, to 1, high risk, on panels d,h,l,p,t) . Black dots with white circle are the GCUs of the different species.

(A)

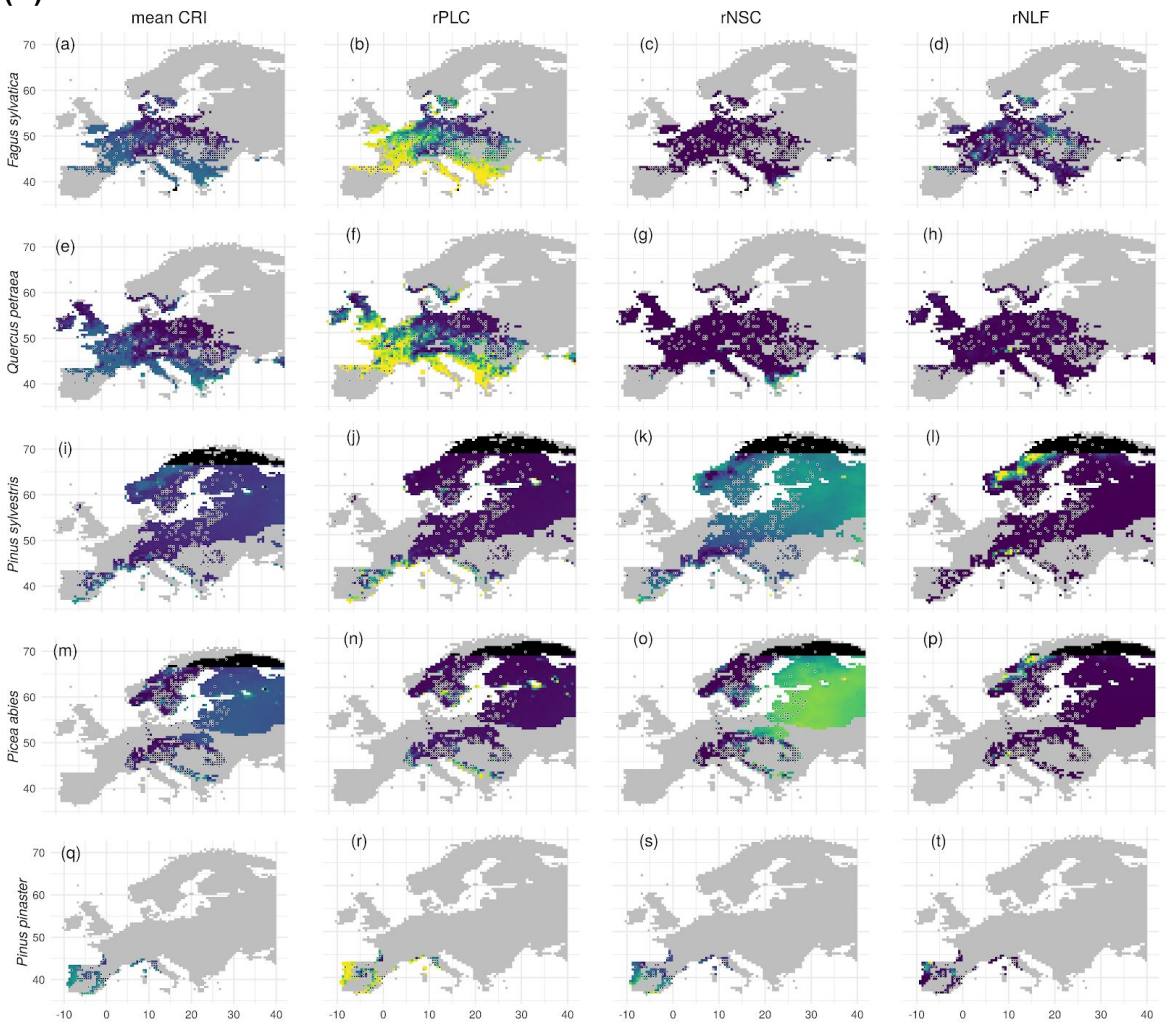
mean CRI
rPLC
rNSC
rNLF
(a)
(b)
(c)
(d)
(e)
(f)
(g)
(h)
(i)
(j)
(k)
(l)
(m)
(n)
(o)
(p)
(q)
(r)
(s)
(t)
Fagus sylvatica
Quercus petraea
Pinus sylvestris
Picea abies
Pinus pinaster
70
60
50
40
-10
0
10
20
30
40

(B)

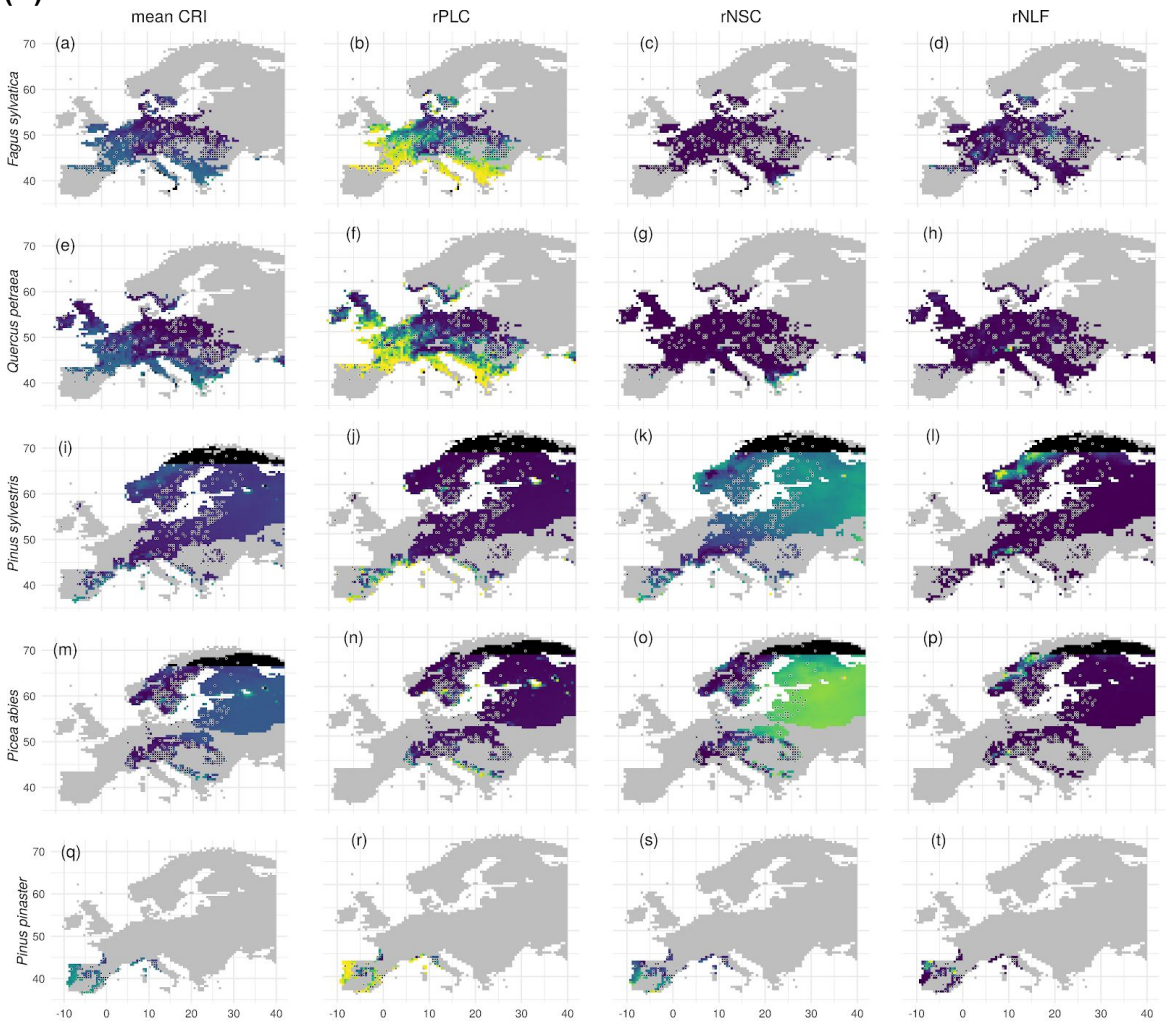
mean CRI
rPLC
rNSC
rNLF
(a)
(b)
(c)
(d)
(e)
(f)
(g)
(h)
(i)
(j)
(k)
(l)
(m)
(n)
(o)
(p)
(q)
(r)
(s)
(t)
Fagus sylvatica
Quercus petraea
Pinus sylvestris
Picea abies
Pinus pinaster
70
60
50
40
-10
0
10
20
30
40

(C)

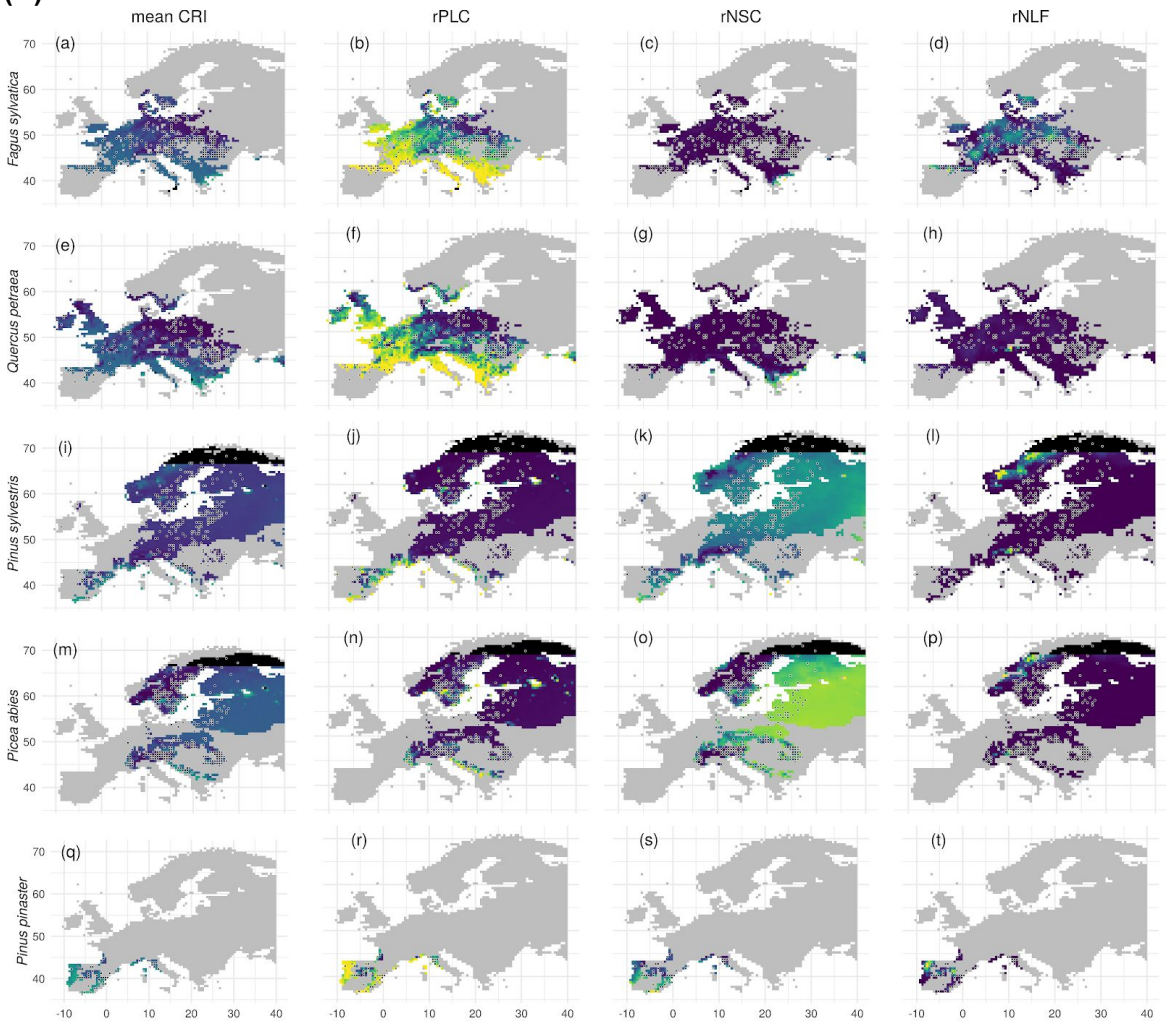
mean CRI
rPLC
rNSC
rNLF
Fagus sylvatica
Quercus petraea
Pinus sylvestris
Picea abies
Pinus pinaster
(a)
(b)
(c)
(d)
(e)
(f)
(g)
(h)
(i)
(j)
(k)
(l)
(m)
(n)
(o)
(p)
(q)
(r)
(s)
(t)
70
60
50
40
-10
0
10
20
30
40

(D)

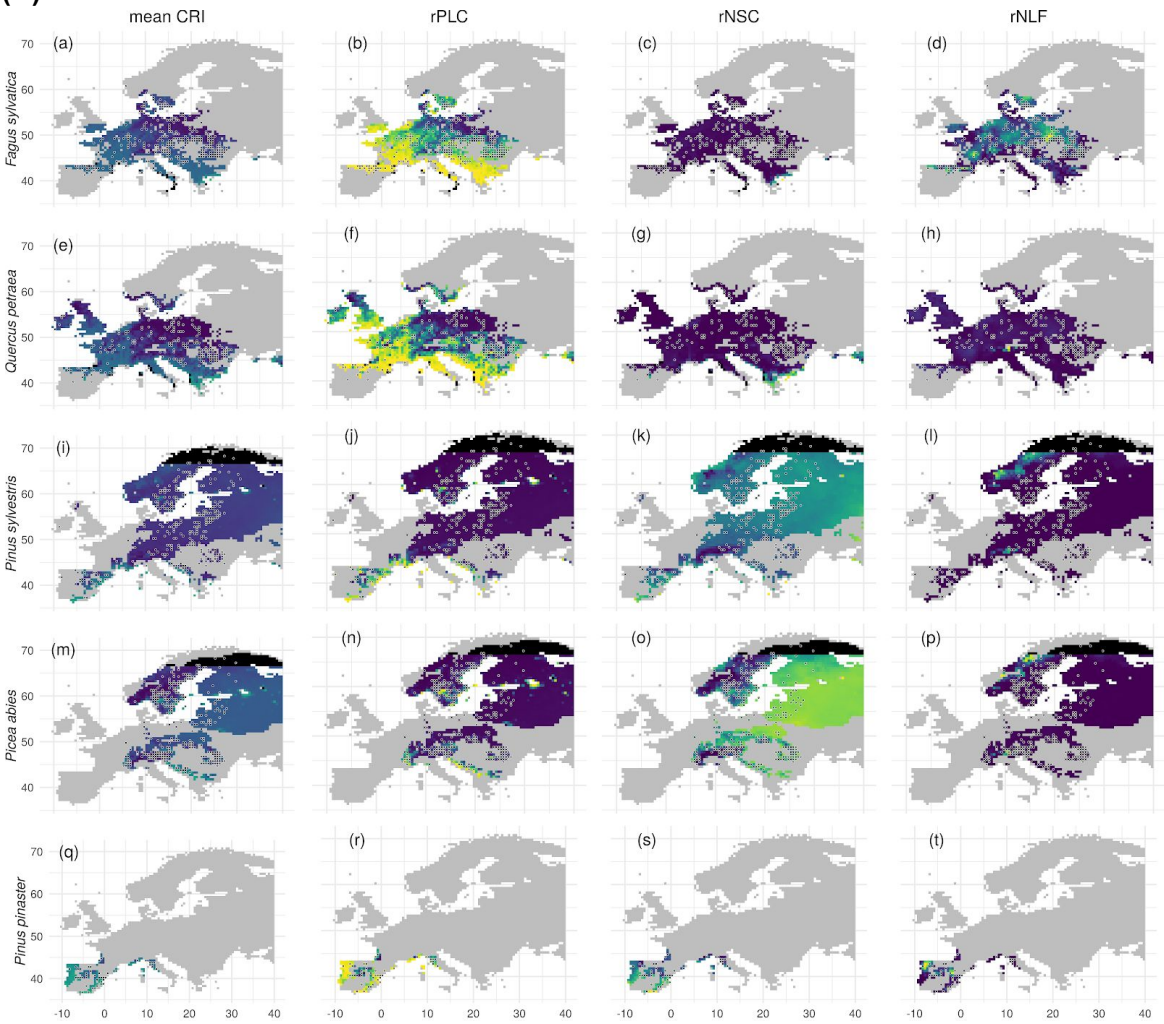

Figure S6 Variation of the risk of mortality (as measured by rNSC, rNFL and rPLC) between current and future climates over species realized range. The median value is represented as line, the mean as dot in each boxplot.

a

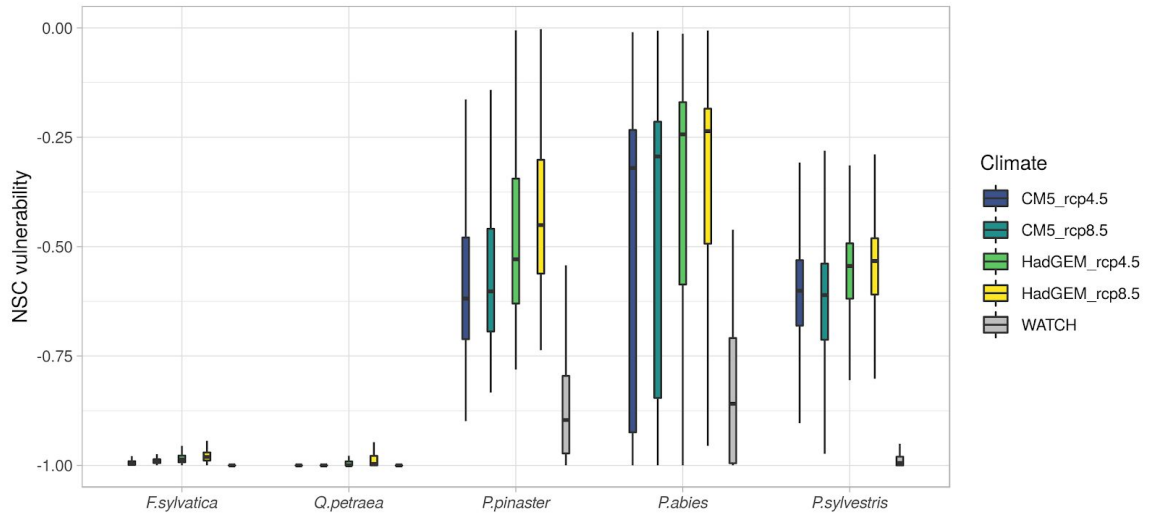

b)

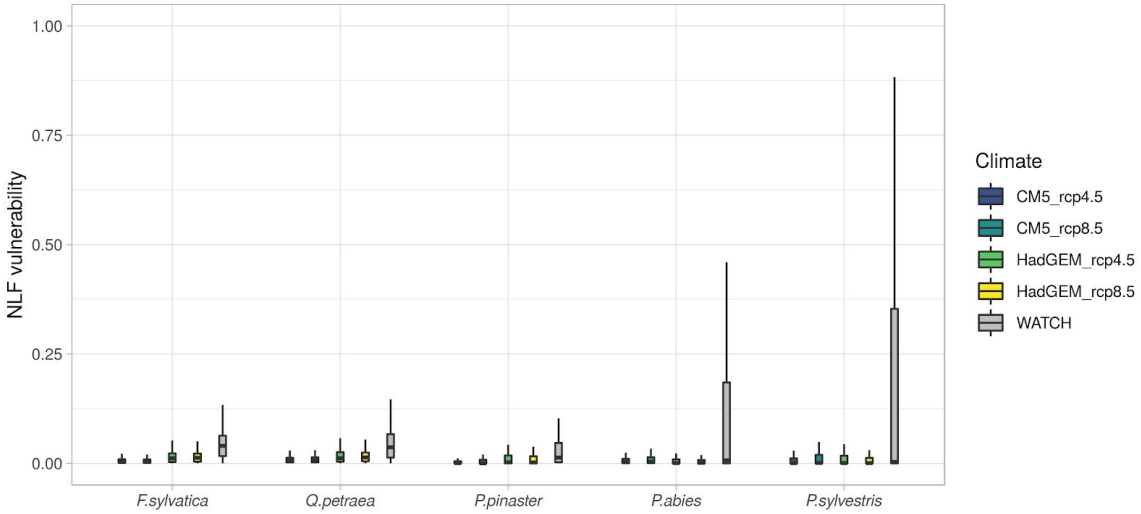
NLF vulnerability
1.00
0.75
0.50
0.25
0.00
F.sylvatica
Q.petraea
P.pinaster
P.abies
P.sylvestris
Climate
CM5_rcp4.5
CM5_rcp8.5
HadGEM_rcp4.5
HadGEM_rcp8.5
WATCH

c)

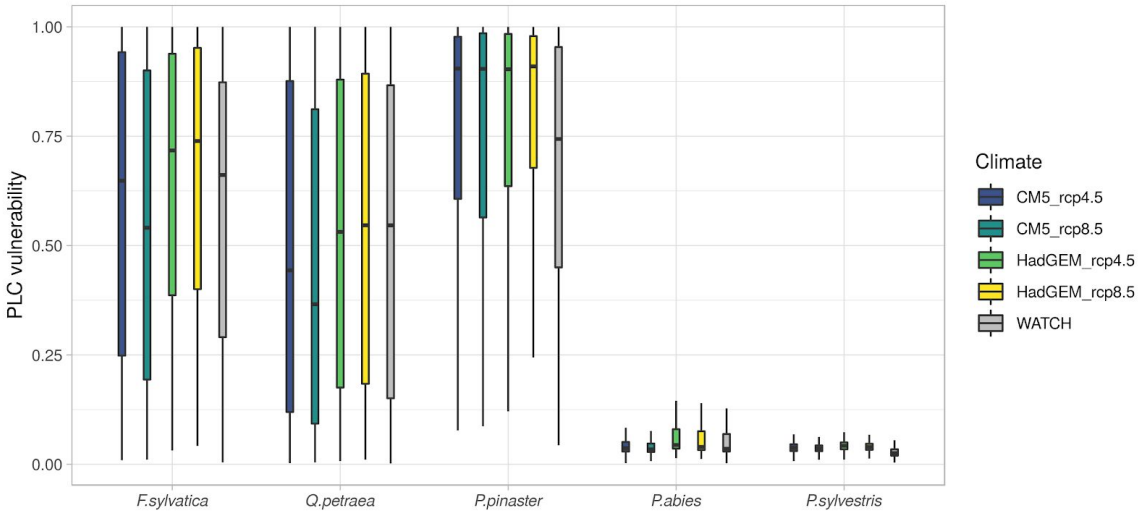
PLC vulnerability
1.00
0.75
0.50
0.25
0.00
F.sylvatica
Q.petraea
P.pinaster
P.abies
P.sylvestris
Climate
CM5_rcp4.5
CM5_rcp8.5
HadGEM_rcp4.5
HadGEM_rcp8.5
WATCH

Figure S7 : Variation of the risk of mortality (as measured by CRI, rNSC, rNFL and rPLC) between between scenario with or without management (_null vs sylv) under current climate (grey) and future climate (yellow).

a)

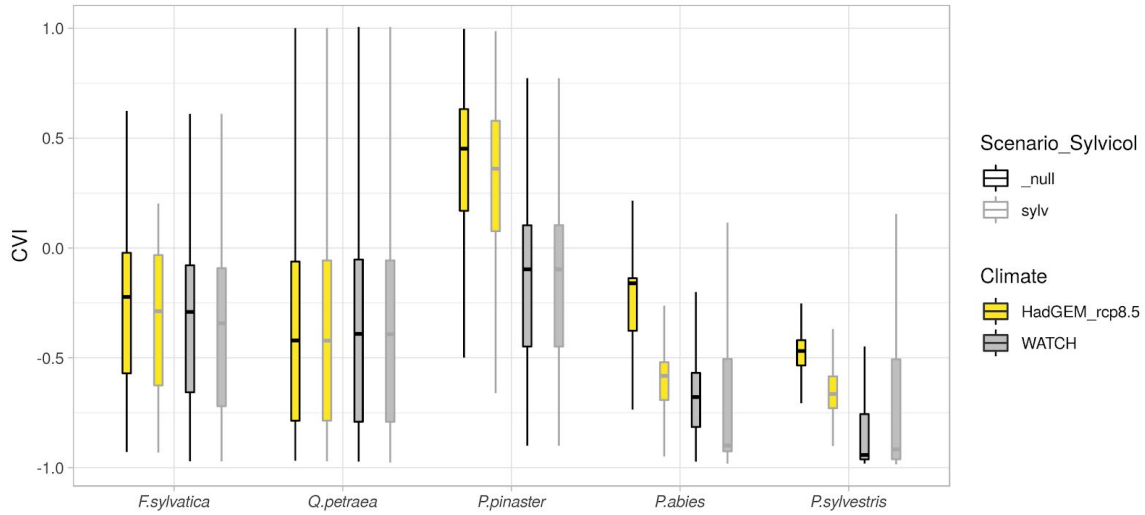

b)

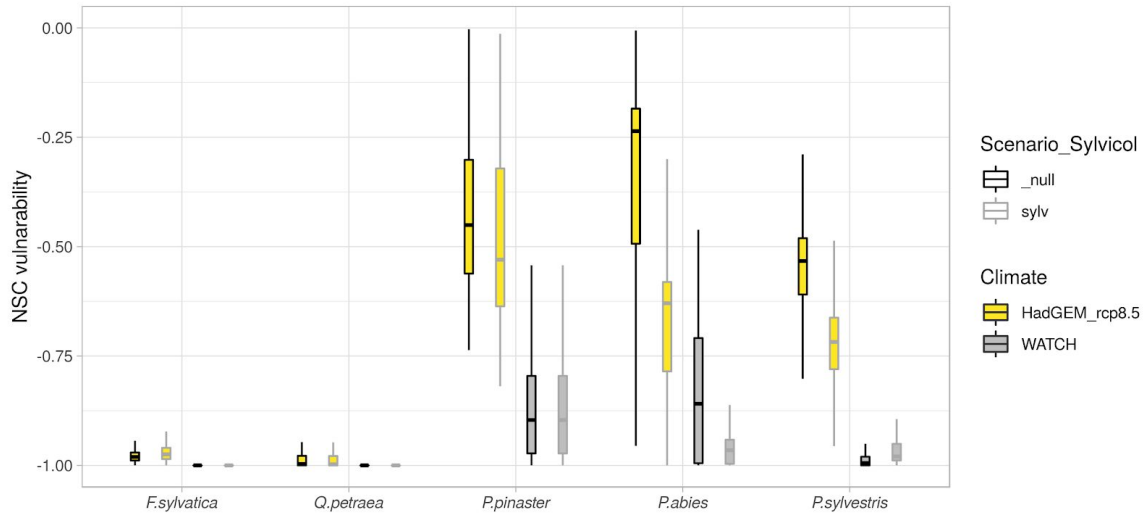

c)

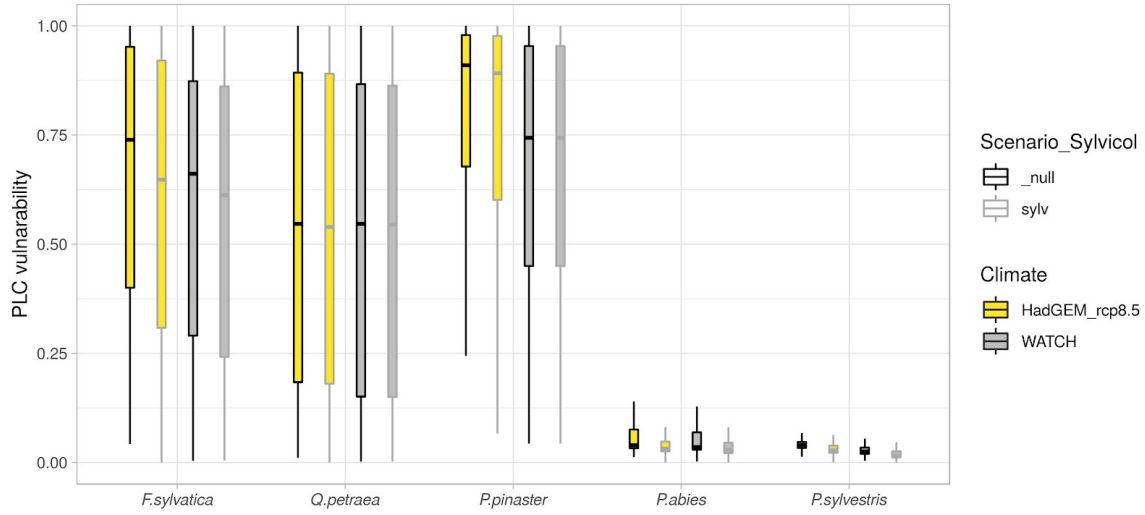

FigureS8: Variation of the risk of mortality (as measured by rNSC) within and outside the distribution

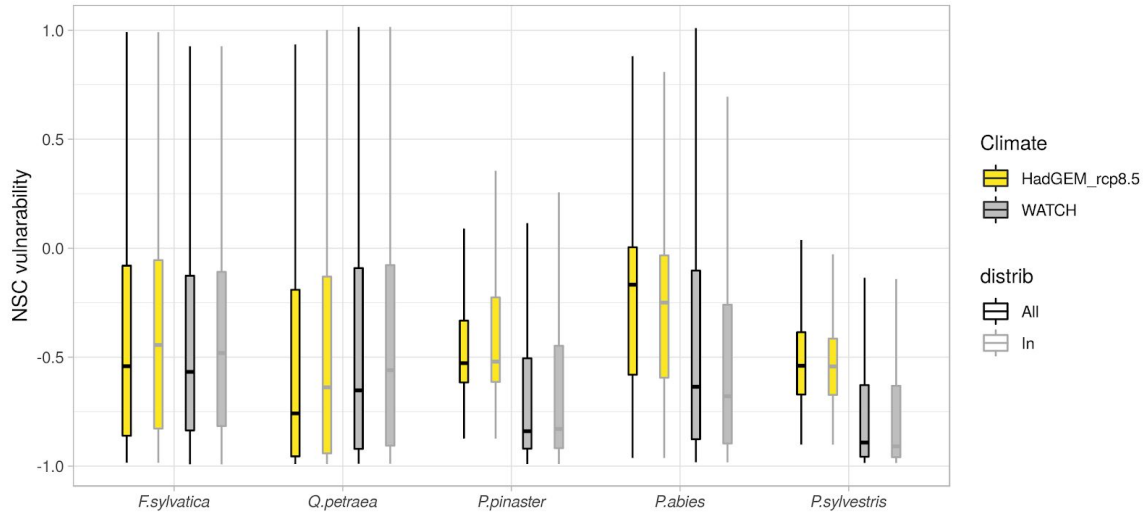

Table S1 : Climate and soil input variables used for simulations

		Range of mean values across Europe				
Daily climate variables	Final units	Current 1970 to 2008	CM5 rcp4.5 2070 to 2099	CM5 rcp8.5 2070 to 2099	HadGEM rcp4.5 2070 to 2099	HadGEM rcp8.5 2070 to 2099
Mean Temperature	°C	7.0 to 9.2	8.1 to 10.2	10.4 to 12.8	9.3 to 11.4	10.8 to 14.0
Max Temperature	°C	11.3 to 13.5	11.9 to 14.3	14.3 to 16.7	13.3 to 15.6	14.7 to 18.4
Min Temperature	°C	2.8 to 5.0	4.3 to 6.2	6.5 to 9	5.1 to 7.2	6.9 to 9.6
Wind speed	$m.s^{-1}$	3.2 to 3.4	3.2 to 3.4	3.2 to 3.4	3.1 to 3.4	3.1 to 3.4
Relative humidity	%	73.5 to 76.8	73.9 to 77.1	73.0 to 76.1	71.3 to 80.0	73.5 to 79.3
Precipitation	mm					
Radiation	$MJ.m^{-2}$	11.4 to 12.3	10.3 to 10.9	10.6 to 11.4	10.5 to 12.0	10.7 to 11.8
soil hydraulic variables						
Water content at field capacity	$cm^3.cm^{-3}$	0.22 to 0.37				
Water content at wilting point	$cm^3.cm^{-3}$	0.08 to 0.22				
soil grid variables						
Bulk density	$g.cm^{-3}$	0.41 to 1.53				
Clay content	weight %	0.03 to 0.38				
Silt content	weight %	0.15 to 0.86				
Sand content	weight %	0.14 to 0.85				
Coarse fragments	Volumetric %	0 to 0.29				
Depth available to roots	mm	36 to 1405				

Table S2. Harvesting rules for the different ecoregions and species under the four considered silvicultural systems. SS1= “No management”; SS2=” “Even-aged forest management with shelter-wood”; SS3=” “Even-aged forest management with clear-cut.”; SS4=” “Short rotation”

A. Northern Europe

SS	Species	
	Pinus sylvestris & Picea abies	**Quercus petraea & Fagus sylvatica**
SS1	No management	

SS2	Not applied	**Thinnings: (Age 10,30, 50)**
		if (H<20 & BA> -0.0179*H^2 + 1.2214*H + 3.7714) :
		BA = - 0.0536*H^2 + 2.4643*H - 12.886
		if BA> 21: BA = 15
		Final cutting:
		if (age =90): BA = 0

SS3	**Thinnings: (Age 10,25,65)**
	if SWC > 100:
	if (H<20 & BA> -0.0893*H^2 + 4.0071*H - 11.343):
	BA = -0.0536*H^2 + 2.7643*H - 9.6857
	else if BA> 33: BA = 24
	if 100 > SWC > 60
	if (H<20 & BA> -0.125*H^2 + 4.95*H - 20.9):
	BA = -0.1071*H^2 + 3.9286*H - 15.771
	else if BA>28: BA = 20
	
	if SWC < 60
	if (H<20 & BA> -0.1071*H^2 + 4.2286*H - 15.571):
	BA = -0.0714*H^2 + 2.7857*H - 9.1143
	else if BA>26: BA = 18
	Final cutting:
	if (age = 85): BA = 0
		Thinnings: (Age 10,30, 50)
		if (H<20 & BA> -0.0179*H^2 + 1.2214*H + 3.7714) :
		BA = - 0.0536*H^2 + 2.4643*H - 12.886
		
		if BA> 21:
		BA = 15
		
		Final cutting:
		if (age =70): BA = 0

SS4	-	

B. East Central Europe

SS	Species group			
	Pinus sylvestris	***Picea abies***	***Quercus petraea***	***Fagus sylvatica***
SS1	No management			
SS2	**Thinnings: (Age 10, 25, 65, 80)** **if BA>10:** BA = 0.01432*H^3 - 0.6149*H^2 + 9.0863*H^1 -22.5383 **if H>22:** BA=30 **Final cutting:** **if Age=100:** old forest is cut, new trees of age 10 remain	**Thinnings: : (Age 10, 25, 65, 80)** **if BA>10:** BA = -0.0004495*H^3 - 0.06473*H^2 + 3.5777*H^1 -8.629 **if H>22:** BA = 33 **Final cutting:** **if Age=100:** old forest is cut, new trees of age 10 remain	**Thinnings: (Age 10, 30,60)** **if BA>10:** BA = 0.002678*H^3 - 0.1426*H^2 + 3.075*H^1 -1.927, BA))) **if H>22:** BA = 26 **Final cutting:** **if Age=80:** old forest is cut, new trees of age 10 remain	**Thinnings: (Age 10, 30,60)** **if BA>10:** BA = 0.0003842*H^3 - 0.02163*H^2 + 1.258*H^1 + 3.508, BA))) **if H>29:** BA = 30 **Final cutting:** **if Age=80:** old forest is cut, new trees of age 10 remain
SS3	**Thinnings: (Age 10, 25, 65)** **if BA>10:** BA = 0.01432*H^3 - 0.6149*H^2 + 9.0863*H^1 -22.53 **if H>22:** BA=30 **Final cutting:** **if Age=80:** BA=0. New seedlings assumed to be planted next year.	**Thinnings: (Age 10, 25, 65)** **if BA>10:** BA = -0.0004495*H^3 - 0.06473*H^2 + 3.5777*H^1 -8.629 **if H>22:** BA = 33 **Final cutting:** **if Age=80:** BA=0. New seedlings assumed to be planted next year.	**Thinnings: (Age 10, 30, 50)** **if BA>10:** BA = 0.002678*H^3 - 0.1426*H^2 + 3.075*H^1 -1.927, BA))) **if H>22:** BA = 26 **Final cutting:** **if Age=60:** BA=0. New seedlings assumed to be planted next year.	**Thinnings: (Age 10, 30, 50)** **if BA>10:** BA = 0.0003842*H^3 - 0.02163*H^2 + 1.258*H^1 + 3.508, BA))) **if H>29:** BA = 30 **Final cutting:** **if Age=60:** BA=0. New seedlings assumed to be planted next year.
SS4	**Final cutting:** if Age=25, BA = 0			

C. West Central Europe

SS	Species				
	Pinus sylvestris	***Picea abies***	***Pinus pinaster***	***Quercus petraea***	***Fagus sylvatica***
SS1	No management				
SS2	**Thinnings: (Age 30,50,60)** **if age>=30**:BA = 15.7 **if age>=35 | D>11.9:** BA = 20 **if age>=50 |D>17:** BA = 23 **if age>=60 | D>19.9:** BA = 23 **Final cutting:** **if age>=85:** old forest is cut, new trees of age 10 remain	**Thinnings: (Age 30,50, 70)** **if age>=25:** BA = 20.15 **if age>=40 | D>23.4**:BA = 25 **if age>=60 | D>31.6:** BA = 30 **if age>=80 | D>36.8**:BA = 35 **Final cutting:** **if age>=85:** old forest is cut, new trees of age 10 remain	**Final cutting:** **if age>=60 | D>50:** BA = 0	**Thinnings: (Age 30,60,80)** **if age>=25:**BA = 10.02 **if age>=35 | D>11.5:**BA = 13 **if age>=55 | D>19.5:B**A = 17 **if age>=80 | D>30.3:** BA = 19 **Final cutting:** **if age>=95:**old forest is cut, new trees of age 10 remain	**Thinnings: (Age 30,60,80)** **if age>=30:** BA = 12.66 **if age>=35 | D>23.4:** BA = 16 **if age>=60 | D>31.6:**BA = 21 **if age>=100 | D>36.8:** BA = 24 **Final cutting:** **if age>=105:** old forest is cut, new trees of age 10 remain
SS3	**Thinnings: (Age 30,50,60)** **if age>=30:** BA = 15.7 **if age>=35 | D>11.9:** BA = 20 **if age>=50 | D>17:** BA = 23 **if age>=60 | D>19.9:** BA = 23 **Final cutting:** **if age>=85:** BA=0. New seedlings assumed to be planted next year.	**Thinnings: (Age 30,50, 70)** **if age>=25:** BA = 20.15 **if age>=40 | D>23.4:** BA = 25 **if age>=60 | D>31.6:** BA = 30 **if age>=80 | D>36.8:** BA = 35 **Final cutting:** **if age>=85:** BA=0. New seedlings assumed to be planted next year.	**Final cutting:** **if age>=60 | D>50:** BA=0. New seedlings assumed to be planted next year.	**Thinnings:** **if age>=25:** BA = 10.02 **if age>=35 | D>11.5:** BA = 13 **if age>=55 | D>19.5:** BA = 17 **if age>=80 | D>30.3:** BA = 19 **Final cutting:** **if age>=95:** BA=0. New seedlings assumed to be planted next year.	**Thinnings:** **if age>=30:** BA = 12.66 **if age>=35 | D>23.4:** BA = 16 **if age>=60 | D>31.6:** BA = 21 **if age>=100 | D>36.8:** BA = 24 **Final cutting:** if **age>=105** BA=0. New seedlings assumed to be planted next year.
SS4	**Final cutting:** if age>25, BA = 0				

D. **Southern Europe**

	Species				
	Pinus sylvestris	***Picea abies***	***Pinus pinaster***	***Quercus petraea***	***Fagus sylvatica***
1	No management				

2		**Thinnings: (Age 30,70,90,100)**
		if (age>=30| BA>30): N = 700
		if age>=70| BA>40): N = 400
		
		Final cutting:
		if (age>120 | BA>50): N = 0
			Thinnings: (Age 20,40,60)
			if (age>=15): N = 1000
			if (age>=20 | D>20): N = 850
			if (age>=40 | D>24): N = 700
			if (age>=60 | D>30): N = 500
			
			Final cutting:
			if ((age>=60 & D>=30) | BA>50): N = 0
				Thinnings: (Age 40,60,80,100)
				if (age>=40 |D>=21): N = 500
				if (age>=60 |D>=35): N = 370
				if (age>=80 |D>=37): N = 290
				if (age>=100 |D>=40: N = 255
				
				Final cutting:
				if (age>=120 |D>=42 | BA>50): N = 0
					Thinnings: (Age 40,60,80,100)
					if (age>=40 |D>=20: N = 550
					if (age>=60 |D>=30: N = 400
					if (age>=80 |D>=39: N = 360
					if (age>=100 |D>=46: N = 300
					
					Final cutting:
					if (age>=120 |D>53 | BA>50): N = 0

3	**Thinnings: (Age 20, 40,60,80)**
	if (H>=11: N = 550
	
	if (H>=25: N = 300
	Final cutting:
	if (age>100 | BA>50): N = 0				

4	if (age >= 15): N = 0	if (age >= 15): N = 0	if (age >= 15): N = 0	if (age >= 15): N = 0	if (age >= 15): N = 0

Table S4 : percentage of each silvicultural system per country and species, as provided by Cardellini et al. (2018)

Country	Species	Unmanaged forests	Even-aged with shelterwood	Even-aged with clearcut	Copice	Short Rotation	Continuous cover forest management
Austria							
	Fagus sylvatica	0	100				
	Picea abies	0	74	20			6
	Pinus sylvestris	0		100			
	Quercus petraea	0	70		30		
Belgium							
	Fagus sylvatica	5.6	94.4				
	Picea abies		11	89			
	Pinus sylvestris		100				
	Quercus petraea	7		48	45		
Bulgaria							
	Fagus sylvatica	2	98				
	Picea abies		100				
	Pinus sylvestris	2	98				
	Quercus petraea	2	98				
Croatia							
	Fagus sylvatica		100				
	Quercus petraea		100				
CzechRepublic							
	Fagus sylvatica	0.1	99.9				
	Picea abies	0.1	24.9	75			
	Pinus sylvestris			100			
	Quercus petraea	0.1		99.9			
Denmark							
	Fagus sylvatica	1	50				49
	Picea abies	1		23			76
	Pinus sylvestris	1		80			19
	Quercus petraea	1	50				49
Estonia							
	Picea abies	8		92			
	Pinus sylvestris	14	12	74			
Finland							
	Picea abies	13		86			1
	Pinus sylvestris	13		87			
France							
	Fagus sylvatica		100				
	Pinus sylvestris			100			
Germany							
	Fagus sylvatica	3	57				40

	Picea abies	3	57				40
	Pinus sylvestris	3	30	67			
	Quercus petraea	3	95		2		
Hungary							
	Fagus sylvatica	0.1	99.9				
	Pinus sylvestris			100			
	Quercus petraea	0.1		99.9			
Ireland							
	Fagus sylvatica	1	5	90			4
	Picea abies	1	5	90			4
	Pinus sylvestris	1	5	90			4
	Quercus petraea	1	3	90		4	2
Italy							
	Fagus sylvatica	1	25		49		25
	Picea abies	1	44				55
	Pinus pinaster	5		95			
	Pinus sylvestris	1		99			
	Quercus petraea	7	40		53		
Latvia							
	Picea abies	10	20	60			10
	Pinus sylvestris	10	30	60			
	Quercus petraea	10	90				
Lithuania							
	Picea abies	1	8	90			1
	Pinus sylvestris	1	19	80			
	Quercus petraea	1	99				
Moldova							
	Quercus petraea		100				
Netherlands							
	Fagus sylvatica		100				
	Picea abies		100				
	Pinus sylvestris			100			
	Quercus petraea		100				
Norway							
	Picea abies			100			
	Pinus sylvestris		100				
Poland							
	Fagus sylvatica	8	92				
	Picea abies	6	45	15			34
	Pinus sylvestris	1	29	70			
	Quercus petraea	1	99				
Portugal							
	Pinus pinaster	2		98			
Romania							
	Fagus sylvatica	2	50				48
	Picea abies	2	98				
	Pinus sylvestris			100			
	Quercus petraea		100				

Serbia							
	Fagus sylvatica	1	99				
	Pinus sylvestris	1		99			
	Quercus petraea	2	98				
Slovakia							
	Fagus sylvatica	0.5	60	39.5			
	Picea abies	1	99				
	Pinus sylvestris			100			
	Quercus petraea		100				
Slovenia							
	Fagus sylvatica	1	11				
	Picea abies	3	7				
	Pinus sylvestris	2		98			
	Quercus petraea	1	99				
Spain							
	Fagus sylvatica		100				
	Picea abies						
	Pinus pinaster		100				
	Pinus sylvestris		87				13
	Quercus petraea				100		
Sweden							
	Picea abies			100			
	Pinus sylvestris		50	50			
Switzerland							
	Fagus sylvatica	0	100				
	Picea abies	0	81	8			
	Pinus sylvestris	0		100			
	Quercus petraea	0	30		70		
UK							
	Fagus sylvatica	1	49				
	Picea abies	1	5	90			
	Pinus sylvestris	1	6	90			
	Quercus petraea	1	30				39

Table S4: Simulation design

No management scenario (SS1) simulated over the whole European grid					
GCM_Scenario	*Fagus sylvatica*	*Pinus sylvestris*	*Pinus pinaster*	*Quercus petraea*	*Picea abies*
WATCH_Current	3784	3784	3784	3784	3784
HadGem_4.5	3784	3784	3784	3784	3784
HadGem_8.5	3784	3784	3784	3784	3784
CM5_4.5	3784	3784	3784	3784	3784
CM5_8.5	3784	3784	3784	3784	3784
Management SS2 to SS4 over a selected grid points					
	Fagus sylvatica	*Pinus sylvestris*	*Pinus pinaster*	*Quercus petraea*	*Picea abies*
WATCH_Current	3323	4473	311	3093	4035
HadGem_4.5	3323	4473	311	3093	4035
HadGem_8.5	3323	4473	311	3093	4035
CM5_4.5	3323	4473	311	3093	4035
CM5_8.5	3323	4473	311	3093	4035

4 Résultats

Nos simulations avec CASTANEA à l'échelle Européenne ont permis de prédire de façon satisfaisante les niches bioclimatiques actuelles des espèces étudiées, à l'exception de *Picea abies*. Les processus physiologiques augmentant le risque de mortalité diffèrent selon les espèces. Le risque de défaillance hydraulique est le principal facteur de mortalité des feuillus et de *Pinus pinaster*, alors que le risque de gel tardif est le principal facteur de mortalité de *Picea abies* et de *Pinus sylvestris*. Sous les climats futurs, CASTANEA prédit un risque d'extinction des GCU de 40%, 25%, 18% et 2%, respectivement pour *Picea abies, Pinus sylvestris, Fagus sylvatica et Pinus pinaster* et une diminution de -4% pour *Quercus petraea*. Nous avons constaté que les pratiques sylvicoles diminuaient le risque de mortalité de toutes les espèces sous les climats actuel et futurs, en diminuant l'âge moyen, la densité des peuplements, la biomasse et la surface foliaire.

Même si les projections de l'indice du risque de mortalité sous le climat futur obtenues sont moins pessimistes que celles fournies précédemment par les modèles de niche bioclimatiques, nos résultats appellent à repenser la conception et la gestion des réseaux de conservation européens afin d'atténuer leur risque d'extinction sous le changement climatique. De plus, nos résultats encouragent fortement de différencier les stratégies de conservations en fonction de la zone de distribution considérée et de prendre en compte les réponses physiologiques et plastiques d'ampleur différente entre les feuillus et les résineux.

Chapitre IV

La variabilité intra-spécifique permet d'atténuer le risque de mortalité dû à la sécheresse et aux gelées tardives chez le Hêtre

1 Contexte et méthodes

La variabilité intraspécifique, qui comprend les variations de plasticité et la diversité génétique (Figure IV.1), joue un rôle clé dans la réponse des espèces au changement climatique et dans leur capacité à s'adapter localement par le biais de la plasticité physiologique et/ou de la réponse à la sélection. Cependant, pour les organismes à longue durée de vie et sessiles comme les arbres, la vitesse du changement climatique est susceptible de dépasser les gammes de variations d'adaptation par la seule plasticité physiologique et d'être trop rapide pour permettre l'adaptation génétique des populations (Alberto et al., 2013; Savolainen et al., 2007).

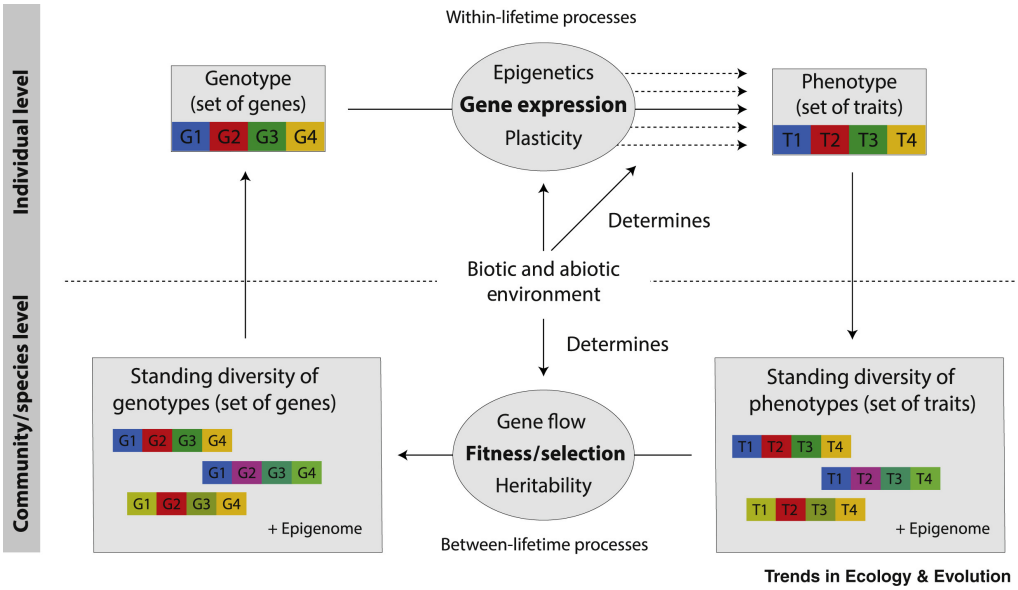

Figure IV.1: Schéma de la variabilité intra-sépcifique. Les rectangles représentent les états (génotype ou phénotype) et les ovales représentent les processus qui déterminent la variabilité. La moitié supérieure représente les processus au niveau individuel qui déterminent la variabilité des caractères au cours d'une vie. La moitié inférieure représente les processus au niveau de la communauté ou de la population qui influencent la variabilité entre les générations. Les flèches en pointillés représentent la façon dont la génétique et la plasticité peuvent déclencher des changements dans le phénotype au cours de la vie d'un individu. Tiré de Berzaghi et al (2019).

Dans cette étude, nous avons évalué comment la prise en compte de la variabilité intraspécifique existante (due à l'adaptation locale et à la plasticité) affecte le risque de mortalité du Hêtre sous différents climats actuels et futurs. Pour cela, nous avons utilisé CASTANEA, un modèle basé sur les processus, pour simuler les flux de carbone et d'eau. Ce modèle permet d'évaluer les risques de défaillance hydraulique, d'épuisement de réserves carbonées et de dommages dus au gel tardif, tout en prenant en

compte la gestion sylvicole. L'originalité de cette étude est de prendre en compte, en chaque point du continent européen, la diversité génétique de trois caractères adaptatifs majeures : (1) la date du débourrement, liée au risque de gelées tardives, (2) le pourcentage de perte de conductance, lié au risque d'embolie hydrique et (3) l'efficacité de l'utilisation de l'eau, liée au risque d'épuisement des réserves carbonées et au risque d'embolies hydriquse.

Nous avons pris en compte un scénario climatique actuel et un modèle climatique futur (le plus pessimiste du chapitre 2) et deux modèles RCP (4.5 et 8.5). Ensuite, pour chaque climat, des simulations ont été réalisées avec ou sans variabilité des caractères dans chaque population. De plus, pour mettre en lumière l'effet de la diversité génétique disponible pour la sélection sur le risque futur de mortalité, nous avons effectué des simulations où toute la gamme de valeur des caractères est disponible à chaque point de l'aire (scénario théorique de transfert de gènes). Le risque de mortalité induit par le changement climatique a été évalué en utilisant l'indice de risque de mortalité composite (CRI) défini dans les chapitres précédents et combinant les risques : de gelée tardives, d'épuisement des réserves carbonées et de défaillance hydraulique.

Cette étude fait partie de l'objectif de mise au point de stratégies innovantes pour la conservation dynamique des ressources génétiques forestières en Europe du projet GenTree. Dans ce projet, avec l'équipe de Capsis, j'ai développé la prise en compte des caractères variables à larges échelle. J'ai fais les tests abaques des traits ciblés et élaboré le design des simulations de matériel de transfert génétique. Cela a nécessité 879174 simulations, soit environ 2 930 580 d'heures.

2 Intra-specific variability can mitigate the risks of drought and late frost in forests under climate change

Mots-cléfs : *Fagus sylvatica L.*, modèle basé sur les processus, CASTANEA, variabilité génétique, changement climatique, pratiques sylvicoles, stratégie de conservation, ressources génétiques.

Intra-specific variability can mitigate the risks of drought and late frost in forests under climate change.

Manuscript en préparation pour Journal of Ecology, Functional Ecology ou Evolutionary applications.

Authors : Cathleen Petit-Cailleux[1], Hendrik Davi[1], François Lefèvre[1], Sylvie Oddou-Muratorio[1].

[1] INRAE, UR 629 Ecologie des Forêts Méditerranéennes, URFM, Avignon, France

Abstract

Context: The intra-specific variability of functional traits, which includes plastic and genetic variability, plays a key role in species' response to climate change and their ability to adapt locally through physiological tolerance and/or response to selection. However, for long-lived and sessile organisms like trees, the climate change velocity is likely to exceed physiological thresholds and the speed of natural adaptation of local populations without gene flow.

Objective: We investigate how the consideration of existing intra-specific variability (due to local adaptation and plasticity) affects the risk of mortality under current and future climates in European beech across its distribution range.

Methods: We used CASTANEA, a process-based model, to simulate carbon and water fluxes and assess the risks of hydraulic failure, carbon starvation and late frost damage of beech stands across Europe under different CC scenarios. At each location, we accounted for standing genetic diversity in three major functional traits: (1) the timing of budburst (TBB), related to vulnerability to late frosts, (2) the water use efficiency (WUE), related to vulnerability to carbon starvation and hydraulic failure and (3) the percent loss of conductance (PLC), related to vulnerability to hydraulic failure. The simulation design included several current and future climatic scenarios, with or without within-stand trait variability, and one scenario with unrestricted transfer of provenances (allowing the whole range of variation everywhere). We assessed CC-induced risks for forests using an original composite risk index combining the risks of late frost, carbon starvation and hydraulic failure.

***Results*:** We found that the risk of mortality is lower for forests with within-stand variation of traits than for forests without variation because some genotypes are less sensitive to the CC-induced risks. In addition, with within-stand variability, the current species distribution range is larger than simulated without variability, especially in the south of Europe. Finally, in the future scenarios under CC, silviculture practices tend to reduce the local risk of mortality, and transferred provenances are able to grow under conditions further North of their native area.

Introduction

Sustainable forest management ultimately aims to attain a balance between society's increasing demands for forest products and benefits, and the preservation of forest health and biodiversity. The ongoing climate and global changes may compromise this balance, through their observed and predicted effects on tree species distribution, forest ecosystem functioning and the composition of forest communities (Walther et al., 2002; Thuiller et al., 2006; Morin et al., 2008). The interplay between biodiversity and ecosystem functioning may itself become a component of species and ecosystem response to environmental change. For instance, functional biodiversity has been widely reported to support ecosystem functioning (wardle 2000, Debra 2002), stability and productivity (Paquette 2010) and resilience against disturbances and environmental variability (Sakschewski et al. 2016). In a manipulative field experiment, increasing the genotypic diversity of a seagrass was shown to enhance biomass production, plant density, and faunal abundance (Reush et al. 2005). By contrast, the links between **intraspecific variability (iVa)**, ecosystem functioning and productivity remain largely to explore in forest ecosystems.

The observed iVa in plant functional traits can result from plastic response to environment (phenotypic plasticity), and from heritable genetic difference among individuals or populations (genetic variability, gVa). As evidenced by multi-site common garden experiments (using foresters' provenance tests), tree populations generally show important levels of phenotypic plasticity. This makes them sensitive to climate variation, especially as the average temperature is high or water availability is low (Rehfeldt *et al.*, 2002). These experiments and other genetic trials have also demonstrated that most forest trees populations usually harbor much genetic variation (Alberto et al., 2013; Savolainen et al. 2007), while simultaneously displaying patterns of local adaptation (Sáenz-Romero et al. 2017; Gárate-Escamilla et al. 2019). Moreover, common garden experiments and population genomics studies overall highlight that genetic diversity for stress responses is strongly organized along environmental gradients, such as gradients of water availability (Eckert et al. 2010; Hajek et al. 2016) or temperatures (Yeaman et al. 2016; Kramer et al 2017). Such patterns of local adaptation and genetic differentiation suggest that forest tree populations successfully adapted to past climatic variations over the course of post-glacial recolonization. Therefore, given their large size, high levels of within-population diversity and gene flow capacities, it is generally assumed that tree populations also have a high evolutionary

potential in the face of climate change (Alberto et al., 2013; Savolainen et al., 2007). However, tree population abilities of genetic evolution over a short timescale (i.e., microevolution) remain largely unresolved, especially since the speed of ongoing CC is likely to exceed the natural adaptive response potential of local populations for many tree species (Kuparinen et al. 2010).

In this context, there is an urgent need to better assess the potential impacts of the plastic and genetic variation of functional traits between individuals and populations on the ecosystem carbon stocks and fluxes, vegetation dynamics and temporal stability of populations and species distributions. Correlative species distribution models (cSDMs) recently begun to account for existing patterns of plastic and genetic iVa, with measures in multi-site common gardens (Benito-Garzon et al. 2011, 2019; Gárate-Escamilla et al. 2019). Traditional cSDMss consider that the climate variability over the observed species distribution range reflects the range of possible adaptation of the species to the environment. However, this hypothesis is challenged by the capacity of exotic species to establish far beyond the limits of their native bioclimatic range (Broennimann et al, 2007). By contrast, deltaTraitSDM include the variation of traits of different populations to explore the clinal response of critical traits (Benito Garzón, Robson, and Hampe 2019). Other approaches were proposed to account for the potential of evolutionary responses in cSDMs. For instance, by coupling a cSDM with an evolutionary dynamics model, Cotto et al. (2017) showed that perennial alpine plants persist in unsuitable habitats, but produce maladapted offspring, whereas classical cSDMs predicted extinction. Process-based, dynamic vegetation models (DVMs) have also begun to incorporate iVa in functional traits through three main approaches (Berzaghi et al. 2019). First, almost all existing DVMs incorporate the plastic component of iVa through equations describing the physiological response to changing environmental conditions; secondly, some DVMs additionally incorporate the **genetic component of iVa (hereafter, gVa)** by sampling trait values in measured distributions, and assigning these values to different individual plants at the same location. For instance, Sakschewski et al. (2015) included gVa in five functional traits for DVM simulations in a tropical tree species. They found that sites with high climatic variability promoted trait divergence, while sites with low climatic variability were associated with lower plant trait diversity. Finally, eco-evolutionary models (part of DVMs) allows the gVa to evolve dynamically through selection processes which result from the model itself, thereby accounting for the potential of

evolutionary response to climate change. Using such a model, Oddou-Muratorio & Davi (2014) showed that five generations where enough for a *Fagus sylvatica* population to evolve diverging budburst values that promote local adaptation along an altitudinal gradient. To summarize, both cSDMs and process-based DVMs are now able to incorporate existing patterns of iVa due to phenotypic plasticity or local adaptation in response to past selection. Due to higher computational costs, the consideration of evolutionary potential, i.e. with dynamic evolution of gVa patterns, is presently limited to a selected number of traits, and a local or regional spatial scale in eco-evolutionary cSDMs or DVMs .

In the forestry sector, iVa also represent a central component of adaptive management strategies to global and climate changes. Options to enhance forest adaptation to CC based on iVa can be classified along a gradient spanning from "hard" to "soft" options, depending on the intensity of human impact. On the hard option side, a full-control strategy consists in replacing the local population by a presumably better-fit provenance (i.e., transferred population). This can be achieved through plantation of forest reproductive material originating from a breeding program or from a selected seed stand. This strategy allows for drastic stepwise evolutions, but the resources presumably better fit in the long term may be less fit in the short term, thus raising trade-off issues between short-term and long-term risks. Furthermore, this strategy requires minimizing uncertainties about the ecological integration of the alien resource in the new site under future climates. On the soft option side, evolution-oriented forestry consists in guiding, i.e. supporting and accelerating, natural evolutionary processes using the local genetic resource, ecologically integrated within its current environment. This is achieved through natural regeneration. This strategy produces progressive changes only, limited by the evolutionary potential of the local resource, but it is flexible and relaxes the ecological uncertainty related to introduction of alien material (Lefèvre et al., 2014). The "hard" strategy based on large-scale movement of genetic material and the "soft" strategy based on the exploitation of local adaptive potential, which are not mutually exclusive, have their respective advantages and constraints that still need to be more precisely quantified. Process-based DVMs are useful tools to investigate these issues, considering their ability to account both for climate effects on vegetation dynamics, forest functioning and for management practices.

This study investigates the effects of iVa on the growth and risk of mortality in an important tree species of pan-European forests, the European beech (*Fagus sylvatica* L.).

Beech combines a widespread distribution (from northern Spain to southern Sweden and from England to Greece) with a high sensitivity to climate variations. For example, more frequent extreme droughts have been associated with slower growth (Dittmar, Zech, and Elling 2003; Jump, Hunt, and Penuelas 2006; Knutzen et al. 2017), altered physiological performances (Bréda et al. 2006) and increased defoliation (Penuelas and Boada 2003). Accordingly, cSDMs predict a future reduction of the distribution of this species at the rear edge of its range over the next few decades (particularly in the southern part of its distribution), in response to reduced rainfall (Cheaib et al. 2012; Kramer et al. 2010). Accounting for iVa in cSDMs, Gárate-Escamilla et al. (2019) showed that different factors constrain beech's distribution in different parts of its range: the northernmost edge is mainly constrained by flushing phenology, the southern edge constrained by drought-induced mortality, and the eastern edge is characterized by decreasing radial growth. However, the low mortality rate observed so far in beech has led some authors to propose that this species presents a higher drought stress tolerance and metabolic plasticity as compared to other tree species (García-Plazaola et al. 2008, Cavin 2016, Dorado-Linan 2018). This apparent paradox between a low mortality and a high sensitivity to climate makes beech an interesting model species to study.

In addition, patterns of iVa are documented for many of the adaptive traits potentially involved in beech response to climate variation (Robson et al. 2012). However, the adaptive value of the variability itself remains a complex issue (i.e. the adaptive value of a trait depends on the environment and the genetic variability is advantageous only in a changing environment). The contribution of plasticity to iVa is generally higher than gVa (Gárate-Escamilla et al. 2019). However, genetic clines for timing of budburst (TBB) were observed across altitudinal or latitudinal gradients such that provenances of high latitude/altitude show earlier budburst in common gardens (Teissier du Cros et Thiebaut, 1988; Gomory et Paule 2011; Kramer et al., 2017). These patterns suggest that populations evolved forcing requirement for TBB optimizing the avoidance of late frost on the one side and maximizing the duration of the vegetation period on the other side. Kreyling et al (2014) also found a high genetic variability in response to winter frosts, with a higher frost-resistance of populations at high altitude or latitude. Wood anatomy and physiological traits involved in response to drought showed more contrasted patterns of genetic differentiation. Provenances originating from drought-prone sites would be expected to have evolved higher embolism

resistance and water use efficiency (WUE), in order to optimize hydraulic efficiency and carbon acquisition under water stress. Dounavi et al . (2016) and Stojnić et al. (2012) support these expectations, but Hajek et al. (2016) rather found that embolism resistance is unrelated to climatic aridity at the place of provenance origin, while WUE decreases with increasing climatic aridity. Moreover, all these studies showed a high within-population variability for WUE and embolism resistance. However, these results should be considered with caution, considering that the expression of adaptation to drought stress is very sensitive to experimental conditions (imposing strong control), and to life-stage (i.e. seedlings response may differ from adult response).

Here, we used a DVM accounting for prescribed patterns of gVa to simulate carbon and water fluxes and assess the risks of carbon starvation, hydraulic failure, and late frost damage of beech stands across Europe under different CC scenarios. We considered three major adaptive traits involved in the response to climate (1) the timing of budburst (TBB), related to the risk of late frosts, (2) the water use efficiency (WUE), related to the risk of carbon starvation and hydraulic failure and (3) the percent loss of conductance (PLC), related to the risk of hydraulic failure to embolism. We used CASTANEA DVM, which accounts for the dynamic plastic response of functional traits to climate and soil variability. The originality of this study is that we considered explicitly the genetic component of iVa. To that aim, we modelled patterns of variation of the parameters controlling the three focal functional traits , based on their measured range of within-population genetic diversity and current patterns of between-population genetic differentiation.

We addressed the following issues: (1) Does accounting for gVa affect the prediction of beech risk of mortality ? To that aim, we compared CASTANEA simulations accounting or not for gVa at the three focal adaptive traits, under past and future representative concentration pathway (RCP 4.5 and 8.5) climate scenarios. Based on cSDMs studies, we expected iVa to increase the species distribution range by decreasing the risk of mortality for beech. (2) Is there a trade-off between the risk of mortality and growth, and how local silviculture practices affect this possible trade-off ? To that aim, we investigated the relationship between the risk of mortality and growth, using CASTANEA simulations accounting for gVa, and including or not traditional management practises, under current and representative concentration pathway (RCP 4.5 and 8.5) climates. Based on our previous study, we expected management practises to reduce the risk of mortality for beech. (3) How does the transfer of

genetic material affects the prediction of beech distribution and risk of mortality ? To that aim, we simulated an additional CASTANEA scenario allowing the largest possible range of gVa everywhere across beech range (as would allow intensive transfer of genetic material).

Materials and methods

CASTANEA model accounting for trait genetic variation

CASTANEA is a process-based model used to simulate carbon and water fluxes in forest ecosystems without a spatially explicit representation of individual trees (Dufrêne et al. 2005). An average tree is represented by six functional compartments : canopy, branches, stem, coarse roots, fine roots and reserve (an unlocated compartment corresponding to the Non-Structural Carbohydrates, NSC). The canopy is divided into five layers of leaves. Photosynthesis is half-hourly computed for each canopy layer using the Farquhar et al. (1980) model analytically coupled to the stomatal conductance model proposed by Ball et al. (1987). The effect of temperature on photosynthesis is modelled using response function of Rubisco-limited photosynthesis (Bernacchi et al., 2001). Maintenance respiration is modeled as proportional to the nitrogen content of the considered organs (Ryan 1991). Growth respiration is computed from growth increment combined with a construction cost specific to the type of tissue (De Vries, Brunsting, and Van Laar 1974). Transpiration is also hourly calculated using the Monteith (1965) equations. The dynamics of soil water content (SWC; in mm) is daily calculated using a three-layers bucket model. Soil drought drives stomata closure via a linear decrease when relative SWC is under 40% of field capacity (Granier, Biron, and Lemoine 2000; Sala and Tenhunen 1996). In the carbon allocation sub-model (Davi et al., 2009; Davi & Cailleret 2017), the allocation coefficients of biomass between the six compartments are daily calculated, depending on the sink force and the phenology constraints. CASTANEA was originally developed and validated at stand-scale for beech (Davi et al. 2005, 2006).

We focussed on three functional traits, for which CASTANEA allowed us to simulate both the plastic response to environmental variation, and the genetic variation within and between populations. Here, a population is a set of average trees simulated at the same location (i.e., in the same environment, see below) and a genotype is the combination of parameters' values.

Table 1: Focal functional traits and their source of iVa modeled in this study*. The column "Environment" indicates which environmental variable drives traits' plastic variation in CASTANEA. The column "genetic parameter" indicates which CASTANEA parameter controls trait genetic variation, with its unit. The next column gives the mean known value for beech, and the range of values simulated in this study. The column "BP variation" indicates which variable determined the between-population genetic differentiation of the parameter. The column "WP" indicates the 95% variation interval of the trait around its mean value within the population.*

Variable adaptive trait	**ABB.**	**Environmental driver**	**Genetically variable parameter (unit)**	**Mean parameter value** [WP]	**Drivers of BP trait variation**
Timing of budburst	TBB	Temperature	F_{CRITBB}, the sum of temperature required for budburst	245°C [-75 °C; +75°C]	Latitude, longitude, altitude
Water use efficiency	WUE	Temperature and precipitations	g1max, the slope of the relationship between assimilation and conductance.	11.8 [-3.8; +3.8]	Climate, altitude
Percent loss of conductance	PLC	Temperature and precipitations	The Slope of the relationship between soil water potential and PLC	50 [-10;+10]	-

Model for the timing of budburst (TBB): TBB was modeled using a one-phase model, which describes the cumulative effect of forcing temperatures on bud development during the ecodormancy phase following (eq. 9- 11 in Dufrêne et al. 2005):

$$R_{frcBB} = \{T \text{ if } T > T2 \text{ and } N > Nstart1\}\ \{0 \text{ if } T < T2 \text{ or } N < Nstart1\} \qquad \text{(Equation 1)}$$

where R_{frcBB} is the rate of forcing for bud break, T the mean daily temperature, T_2 the base temperature, N the day of the year and N_{START1} the date of onset of rest.

$$S_{frcBB} = \sum_{NSTART1}^{N} R_{frcBB} \; if \; S_{frcBB} F_{critBB} \qquad \text{(Equation 2)}$$

$$TBB = N if S_{frcBB} \geq F_{critBB} \qquad \text{(Equation 3)}$$

with S_{frcBB} the state of forcing, F_{critBB} the critical value of state of forcing for the transition from quiescence to the active period and TBB the day when bud break occurred. Note that T_2, Nstart1 and F_{critBB} are parameters, while R_{frcBB}, S_{frcBB} and TBB are dynamic variables computed by CASTANEA.

To model genetic variation in TBB, we considered that the parameter F_{critBB} could vary genetically within and among populations. Based on the studies of (Kramer et al., 2017), the genetic variation in TBB was modeled as a function of latitude, longitude and altitude (Appendix 1). Then, F_{critBB}-values were considered to vary linearly among populations following the same model, with the mean F_{critBB} at location i computed as follows:

$$MeanF_{CRITBBi} = 245 + -0.78 \times latitude_i + -2.16 \times longitude_i + -0.06 \times altitude_i \qquad \text{(Equation 4)}$$

where 245°C is the mean F_{critBB} fitted for beech on Renecofor dataset.

Moreover, Gauzere et al. (2016) allowed to estimate the genetic variance of TBB within population (σ^2_{TBB} =25), which converts (using CASTANEA, see Appendix 1) into a 67% interval of variation of [-75°C; +75°C] around $MeanF_{CRITBBi}$.

To summarize, we used CASTANEA to simulate both plastic variation (through equation 1-3) and genetic variation (equation 4) in TBB (Table 1, Online Appendix 1). TBB determines the number of late frost days (NLF) of a given average tree for each simulated year, and therefore affects the level of frost induced damage (see Appendix 2 in Petit-Cailleux et al. **Submitted**). Note that we considered that trees were always able to reflush after late frosts.

Model for Water Use Efficiency (WUE): WUE can be defined at leaf level as the ratio of assimilation (A) to stomatal conductance (g_{sH2O}):

$$WUE_i = \frac{A}{g_{sH_2O}} \qquad \text{(Equation 5)}$$

In CASTANEA, three main equations determine A and g_{sH2O} (eq 1,2 and 4 in Dufrêne *et al.* 2005), following the model from Ball *et al.* (1987).

First the carbon dioxide demand is:

$$A = V_C - R_d \text{ . (Equation 6)}$$

where V_C is the carboxylation rate and R_d the respiration during the night.

Second, the carbon dioxide supply is:

$$A = g_{sCO_2}(C_S - C_I) \text{ (Equation 7)}$$

where g_{sCO2} is the stomatal conductance for CO_2 and (C_S-C_I) the gradient of CO_2 concentration between evaporative site and leaf surface.

Third, the carbon dioxide control which allows the calculation of g_{sH2O} is:

$$g_{sH_2O} = \frac{g_0 + g_1 \times A \times RH}{C_S} \text{ (Equation 8)}$$

where is RH the relative humidity in the surrounding air, g1 depends on soil water stress and g0 correspond to cuticle conductance of the leaf.

Rearranging Equation 8 shows that g1, the slope of the relation between photosynthesis and stomatal conductance, is inversely related to WUE :

$$\frac{A}{g_{sH_2O} - \frac{g_0}{C_S}} = \frac{C_S}{g_1 \times RH} \text{ (Equation 9)}$$

As $g_{sH_2O} \gg \frac{g_0}{C_S}$, the higher g1 is, the lower is WUE.

In CASTANEA, g_1 is assumed to decrease linearly when soil water storage decreases. The effect of soil water stress on photosynthesis is mediated through g1:

$$g_1 = (g_{1max} - g_{1min}) \times reduc + g_{1min} \text{ . (Equation 10)}$$

where g_{1max} and g_{1min} are the maximal and minimal values taken by g1, and "reduc" is a soil water stress index varying between 0 (maximal soil water stress) and 1 (no water stress).

To model the gVa of WUE, we considered that the parameter g_{1max} could vary within and among populations. To calibrate g_{1max} variation among populations, we used the study of Hajek et al. (2016), investigated the among- provenances variation of several physiological traits, including δ13C, an indicator of WUE also simulated in CASTANEA. We used a linear regression model to model the variation in δ13C in response to the first four Principal Components (PC) of the climate variables measured at provenance sites, then from CASTANEA relationship between δ13C and g_{1max} we derived the following model for the mean value of g_{1max} at each location *i*:

$$\text{Mean}g_{1max\,i} = -0.3973 + \delta 13C \times -0.418602 \text{ (equation 10)}$$

with 11.8 the mean $g1_{max}$ value for beech, and PC combinations of climatic variables detailed in Appendix 1.

Moreover, Hajek et al. (2016) estimated the standard deviation of δ 13C within population ($\sigma_{\delta 13C}$ =0.263), which converts (using CASTANEA, see Appendix 1) into a 67% variation interval of [-3.8; +3.8] around Mean$g_{1max\,i}$.

To summarize, we used CASTANEA to simulate both plastic variation (through equation 9) and genetic variation (equation 10) in WUE (Table 1, Appendix 1). WUE determines the ability of a given tree to assimilate carbon without losing too much water, and thereby the risk of carbon starvation and hydraulic failure.

Model for Percent Loss of Conductance (PLC) : in CASTANEA**,** PLC is computed based on daily midday water potential (P) and species vulnerability curve to embolism with Ψ_{leaf} (MPa) the simulated midday leaf water potential (equation 11), Ψ_{50} (MPa) the species-specific potential below which 50% of the vessels are embolized, and *slope* a constant fixed to 50.

The leaf water potential Ψ_{leaf} was calculated as:

$$\Psi_{leaf}(t+1) = \Psi_{soil}(t+1) - \frac{TR}{3600} \times R_{SoilToLeaves} + \frac{\Psi_{leaf}(t)}{\Psi_{soil}(t+1) + TR \times R_{SoilToLeaves}} \times e^{\frac{deltaT}{R_{SoilToleaves} \times Cap_{SoilToleaves}}} \quad \text{(equation 11)}$$

where the soil water potential (Ψ_{soil} MPa) was calculated from daily SWCo (Campbell 1974). Ψ_{leaf} was calculated hourly (deltaT = 3600s) based on the sap flow (TR in mmol.m^{-2}.leaf^{-1}) simulated following the soil-to-leaves hydraulic pathway model of Loustau et al. (1990). We used a single resistance ($R_{SoilToleaves}$ in MPa.m^{-2}.s^{-1}.kg^{-1}, following Campbell 1974) and a single capacitance ($Cap_{SoilToleaves}$ in kg.m^{-2}.MPa^{-1}) along the pathway. $R_{SoilToleaves}$ was assessed using midday and predawn water potentials found in the literature.

Moreover, PLC depends on xylem pressure through a sigmoid function :

$$PLC = \frac{100}{1+exp\left(\frac{PLC_{slope}}{25} x (P - P_{50})\right)} \quad \text{(equation 12)}$$

where P50 (MPa) is the xylem pressure inducing a 50% loss of hydraulic conductivity and PLC_{slope} (% MPa^{-1}) is the slope of the curve.

Because Hajek et al. (2016) showed that P50 was not significantly differentiated between provenances, we chose to model iVa in PLC by considering that the PLC_{slope} parameter could vary genetically within and among populations and we used the studies of Stojnić et al., (2018) and Hajek et al. (2016) to model the variation in PLC_{slope} values across Europe. First, Hajek et al. (2016) showed that parameters related to embolism resistance do not significantly depend on the climate of the provenance. Therefore, we considered that $meanPLC_{slope}$= 50 all over Europe (ie. no local adaptation for PLC_{slope}). Moreover, we assumed that PLC_{slope} had a coefficient of variation of 20%, that is a 67% interval of variation of [-10; +10] around $meanPLC_{slope}$, randomly distributed among populations.

To summarize, we used CASTANEA to simulate both plastic variation (through equation 11,12,13) and genetic variation (values of 40,50 and 60 of the PLC_{slope}) in PLC (Table 1, Online Appendix 1). PLC determines the risk of hydraulic failure of a given tree under water stress. Appendix 1 details the relationships between CASTANEA parameters ($g1_{max}$, TBB, PLC_{slope}) and traits related to vulnerability (respectively, WUE, TBB, PLC).

Climate data and scenarios

We considered the European area included within longitudes ranging from -11°W to 40°E and within latitudes ranging from 36°N to 71°N. CASTANEA requires the following daily climatic input variables: the minimum, mean and maximum temperatures (in °C), precipitation (mm), the wind speed ($m.s^{-1}$), the mean relative humidity (%) and the global radiation ($MJ.m^{-2}$) (Table s2b and Figure S2 in Petit-Cailleux et al (in prep1)). These climatic data were derived for three scenarios (one current and two future scenarios) as detailed below.

Current climate: We used the Water and Global Change (WATCH)-Forcing-Data-ERA-Interim data set (WATCH in the following) to obtain current climate data at european scale (Weedon et. al, 2014). This daily meteorological forcing dataset is available for the period 1979 to 2008 worldwide, with a spatial resolution of 0.5° per 0.5°. This resolution (the coarsest among climate and soil data set) was used to divide the European grid into 3784 raster cells.

Future climates: To take into account the uncertainties on future climate scenarios (McSweeney *et al.* 2015)**,** we used a combination of one regional circulation models (RCM)

from EURO-CORDEX community (Jacob *et al.* 2014), and two representative concentration pathways (RCPs) scenarios (IPCC 2014). We selected the EUR-11.SMHI.MOHC-HadGEM2-ES (Hadgem in the following). The RCP4.5 scenario considers an increase of CO_2 concentration of 650 ppm with a 1.0–2.6°C increase by 2100, and corresponds to the SRES B1 scenario (Nakićenović & Swart 2000). The RCP8.5 scenario considers an increase of CO_2 concentration of 1,350 ppm CO2 with a 2.6–4.8°C increase by 2100, and corresponds to the A1F1 SRES scenario (van Vuuren *et al.* 2011; Harris *et al.* 2014; IPCC 2014). The four EURO-CODEX future climate datasets were corrected for bias and downscaled using the R package "meteoland"(De Caceres *et al.* 2018). The WATCH dataset was used as reference data.

Soil properties data

To account for the variability of soil water capacity across Europe, we used (1) the European Soil Database to obtain data on the soil depth reached by the roots; (2) the SoilGrids250m database to to obtain data on bulk density and clay, silt, sand and coarse fragments contents; and (3) the 3D soil hydraulic database to to obtain data on soil water content at field capacity and at wilting point (Hiederer 2013; Hengl *et al.* 2017; Tóth *et al.* 2017). All these data were aggregated from 1km*1km resolution to 0.5°x0.5° (WGS84) resolution using the R package "raster" (Hijmans 2015). Then, we extracted the mean value of each parameter at each climate grid point (Supplementary Table S2 in Petit-Cailleux et al in prep1).

Management practises

Management practices were defined on the basis of thinning rules and regeneration methods proposed in Härkönen *et al.* (2019). We assumed that management practises were constant over the simulated period (130 years from 1979 to 2100). We considered four possible silvicultural systems:

- ➔ "No management": no thinning nor regeneration cuts were applied;
- ➔ "Even-aged forest management with shelter-wood" : only the main target tree species was simulated. The last thinning was defined as a shelter-wood thinning. The age of the final cut for regeneration was specific of each species and each ecoregion.
- ➔ "Even-aged forest management with clear-cut." After clear-cut, a new stand was planted the following year. Simulation started when the trees reached breast height, which took different lengths of time depending on the ecoregion and the species.

➔ "Short rotation". There were no thinning applied, and an integral final cut was done at an early age, followed by planting.

Thinning rules were adapted from Härkönen et al. (2019) and determined the reduction in stand density according to stand age, and eventually to stand height and/or basal area (Supplementary Table S3 in Petit-Cailleux et al (in prep1)). The reduction of stand density decreased the LAI as depicted by equation 2, and the biomass of trunk, branches, reserves and large roots of the average tree. These thinning rules varied among the five species and the four main ecoregions (North, Central East, Central West, South). The shares of each silvicultural system at each grid point was derived from Cardellini *et al.* (2018) (Supplementary Table S4 in Petit-Cailleux et al (in prep1)). When country data were not available, the mean of share of every silvicultural management applied in the nearest ecoregion was applied.

Simulation design

Europe was simulated as a grid of 3784 raster cells, each characterized by specific climate and soil properties. We first ran a set of "reference" scenarios without genetic variability (neither between nor within population) and without forest management. To that aim, a single average tree was simulated at all grid locations, and the values of the three genetically variable parameters were set to their mean values for beech all over Europe (Table 1). At initialization, the average tree was eight years old and had a diameter at breast height of 5 cm. In total, we performed 11,352 CASTANEA simulations for three "reference" scenarios (3 climates x 1 average tree x 3784 grid points).

Secondly, we considered a set of three scenarios with gVa and without forest management ("Current gVA-without management"). To account for between- and within-population variation of parameter value across Europe, but keep the number of simulations tractable, we simulated only three possible values for each parameter (g1max, FcritBB, PLCslope) at each location: the mean, mean plus one standard deviation and mean minus one standard deviation. These mean, maximum and minimum parameter values were those predicted at each location by linear models accounting for local adaptation (see details below), and could thus differ among locations. Hence, at each grid point, we simulated a population of 27 average trees, which represented the 3^3 possible combinations between the three traits. In total, we performed 306,504 CASTANEA simulations for three "Current gVA-without

management" scenarios (3 climates x 27 average trees x 3784 grid points)

Thirdly, we considered a set of three scenarios with gVa and forest management ("Current gVA-with management"). These scenarios were simulated only at the 2819 grid points, where at one least silvicultural scenario other than "No management" was identified (Table S2-Petit-Cailleux et al in prep1). As for the "gVA-without management", we considered a population of 27 trees at each of these locations. In total, we performed 578,340 simulations for 3 "Current gVA-with management" scenarios (3 climates x 27 average trees x 3784 grid points x up to 3 management scenario)

Finally, we considered a set of scenarios with gVa based on genotype transfer ("gVaTransfer- with management"). As for the "Current gVA" scenarios, we considered a population of 27 trees at each of the locations. But unlike the "Current gVA" scenarios, we considered that all the genetic variability of the beech European gene pool was available at each location; this means that for each parameter (g1max, FcritBB, PLCslope), the mean, mean plus one standard deviation (max, here after) and mean minus one standard deviation (min, here after) parameter values were the same all over Europe, and corresponded to values displayed in Table 1. In total, we performed 385,560 simulations for three "gVaTransfer-with/without management" scenarios (3 climates x 27 average trees x 3784 grid points x up to 4 management scenarios) (Table 2).

Table 2: Simulation design . In total 1 474 740 simulations were performed

Climate	Current reference-without management	Current reference-with management	Current gVA-without management	Current t gVA-with management	gVaTransfer-without management	gVaTransfer-with management
Current	3784	3323	102168	192780	0	0
HadGem_4.5	3784	3323	102168	192780	102168	192780
HadGem_8.5	3784	3323	102168	192780	102168	192780

Post-processing for the computation of proxies of the risk of mortality

For each genotype *i* at each location *j*, we computed three proxies of the risks associated to drought and late frost over the simulated period. The relative PLC of genotype *i* at location *j* ($rPLC_{ij}$) was computed as a proxy of the risk of hydraulic failure following :

$$rPLCij = \frac{meanPLCij}{PLC_{species\ threshold}} \quad \text{(equation 14)}$$

where meanPLCij is the mean of yearly PLC-values simulated for genotype i at location j over the simulated period, and $PLC_{speciesthreshold}$ is the species-specific PLC-value above which mortality occurs (here, 88% Urli 2013, Brodribb 2009). For all simulated trees with $meanPLC_{ij}$>88%, $rPLC_{ij}$ was set to 1, and the genotype *i* was considered as non viable at location *j*. Hence rPLC varied from 0 to 1, increasing values indicating increasing risk of hydraulic failure.

The relative **non-structural carbohydrate** content of genotype *i* at location *j* ($rNSC_{ij}$) was computed as a proxy of the risk of carbon starvation, following :

$$rNSC_{ij} = \frac{meanNSC_{fracij}}{NSC_{threshold}}$$

$$NSC_{frac\ n} = \frac{Biomass(NSC)}{Biomass(Stem)+Biomass(CoarseRoot)+Biomass(Branch)+Biomass(Leaves)+Biomass(FineRoots)} \quad \text{(equation 15)}$$

Where $NSC_{frac\ n}$ is the average fraction of NSC biomass over the biomass of the other compartments at a given year *n*, mean$NSC_{frac\ ij}$ is the average NSC_{frac}over the simulated period for genotype *i* at location *j*, and $NSC_{threshold}$ the threshold in NSC-value above which mortality through carbon starvation is unlikely. $NSC_{threshold}$ was arbitrarily set the mean NSC_{frac}-value (0.09 %) observed in alive trees in a database with **177** species entries (Martinez-Vilalta et al. 2016). For all simulated trees with $meanNSC_{fracij}$> $NSC_{threshold}$, $rNSC_{ij}$ was set to 1. The genotype *i* was considered as non viable at location *j* when $meanNSC_{fracij}$=0. Hence *rNSC* varied from 0 to 1, increasing values indicating decreasing risk of carbon starvation.

The relative number of late frost days over the period for genotype *i* at location *j* ($rNLF_{ij}$) was computed as a proxy of the risk of late frost following :

$$rNLFij = \frac{sNLFij}{NLF_{threshold}} \quad \text{(equation 16)}$$

where *sNLFij* is the sum of NLF-values for genotype i at location j over the simulated period, and *NLFtreshold* the *sNLF value* over which frost damage jeopardize the probability of a tree to survive. We arbitrarily set *NLFtreshold* to 1 frost day every 3 years, this value depending

on the duration of the simulated period (e.g. NLFtreshold = 10 days for 30-years long simulations under current climate). For all simulated trees with $sNLF_{ij}$>$NLFtreshold$, rNLF was set to 1 and the genotype *i* was considered as non viable at location *j*. Hence rNLF varied from 0 to 1, increasing values indicating increasing risk of late frost damage.

In addition, we computed a composite risk index of mortality (CRI) combining rPLC, rNLF and rNSC with an identical weight for each genotype i at location j:

$$CRI_{ij} = rPLC_{ij} + rNLF_{ij} - rNSC_{ij} \quad \text{(equation 17)}$$

CRI is expected to vary between -1 (minimal risk of mortality, when rPLC=rNLF=0 and rNSC=1) and 2 (maximal risk of mortality, when rPLC=rNLF=1 and rNSC=0).
In the CRI index, sources of mortality may compensate for each other. Therefore, we also converted the continuous risk of mortality index into a binary prediction of viability for geno type *i* at location *j* as :

$viability_{ij}$ = 0 if $rPLC_{ij}$=1 OR $rNLF_{ij}$=1 OR if $rNSC_{ij}$=0

$viability_{ij}$= 1 if $rPLC_{ij}$<1 AND $rNLF_{ij}$<1 AND $rNSC_{ij}$>0

Model evaluation

CASTANEA had already been validated at stand scale for the *Fagus sylvatica* species in Davi et al., (2006) and Delpierre et al., (2012) and evaluated at large scale for the reference genotype (Petit-Cailleux et al in prep1)

Table 3: The area under the receiver operating curve (AUC) and true skill statistic (TSS) computed for threshold in CASTANEA output variable optimizing the goodness of fit for the reference genotype with mean parameter values.

variable	TSS	AUC	threshold
rw	0.59	0.86	2.02
NPP	0.63	0.86	453.56

Results

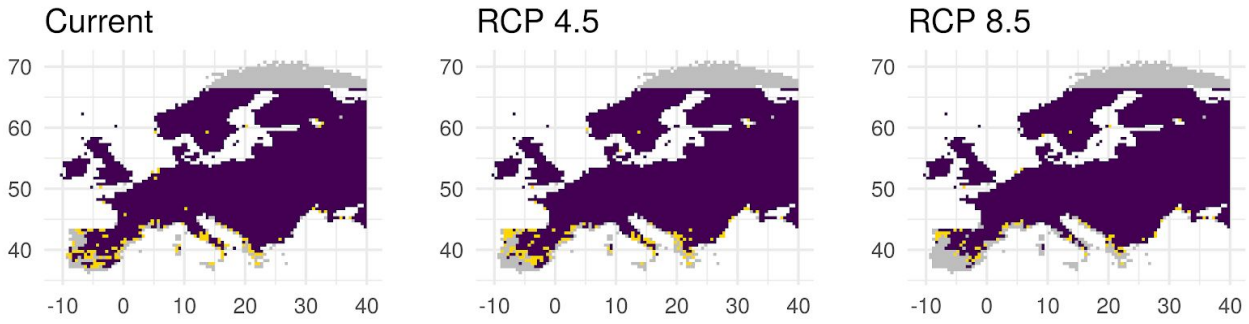

Figure 1: Decreasing risk of mortality for beech over its distribution range when accounting for gVa, under current (a), RCP4.5 (b), and RCP 8.5 (c) scenarios*. Purple pixels indicate viable locations both with and without gVa, meaning, that at least one genotype is above the mortality threshold for all risk tested (late frost, carbon starvation or hydraulic failure). Yellow pixels indicate viable locations with gVa, but not viable without gVa, grey pixels are not viable in both cases.*

Effect of gVa on beech risk of mortality under current climate (comparison of "Current gVA-without management" vs reference scenario)

Under current climate, the risk of mortality strongly varied across beech range in both simulations without gVa (-0.98<CRI<0.99) and with gVa (-0.99<CRI<0.90). The median CRI of the mean genotype over all positions in the reference scenario (CRI= -0.54) was lower than the median CRI of all genotypes over all positions in the "Current gVA-without management" scenario (CRI=-0.40), but higher than the median CRI of the best genotypes over all positions in the "Current gVA-without management" (CRI= -0.63).

We mapped the viability of Beech populations to identify the locations where all the sources of mortality (late frost, carbon starvation or hydraulic failure) were above the viability threshold for at least one genotype at this location (Figure 1 and S1). Taking into account gVa, the number of locations where at least one Beech genotype was predicted as viable increased by 123 (3%) compared to the reference scenario without gVa (Figure 1). These locations where the critical level of risk changed with gVa were the southern margins, the coasts of the Netherlands and of the Baltic Sea. All genotypes were viable throughout the reference distribution range in Europe, except in these grid points (Figure 1), where only 23 genotypes

out of 27 were viable. The four non viable genotypes had high F_{critBB} values (i.e. $Maxg1_{Max}\_MaxPLC_{slope}\_maxF_{critBB}$, $Maxg1_{Max}\_MoyPLC_{slope}\_maxF_{critBB}$, $Moyg1_{Max}\_MaxPLC_{slope}\_maxF_{critBB}$, $Moyg1_{Max}\_MeanPLC_{slope}\_maxF_{critBB}$, TableS1). In addition, $MinG1_{max}$ parameter was widely spread in these areas (Figure 2, Table S1, Table S2).

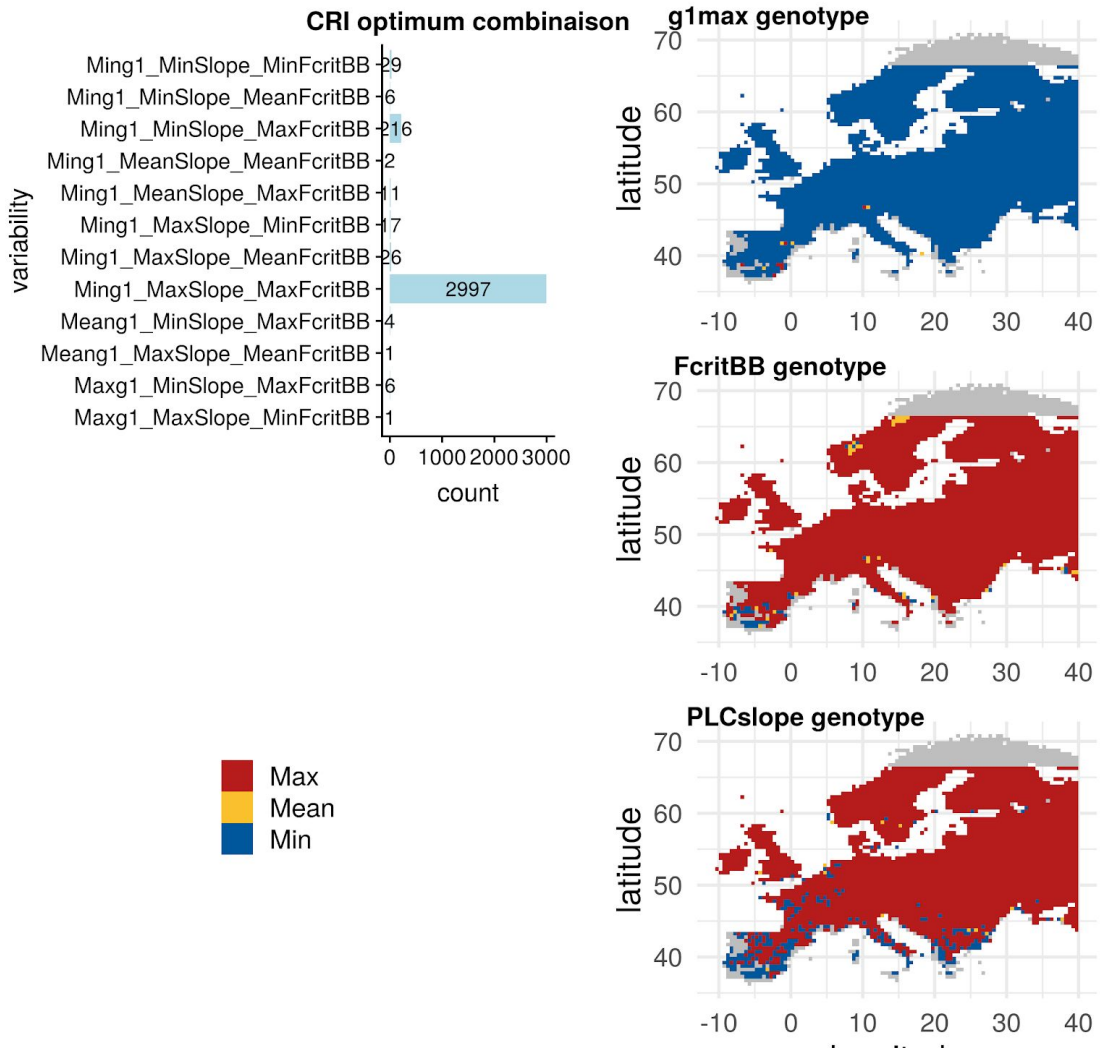

Figure 2: Distribution (a-c) and count (d) of genotypes minimizing the risk of mortality (CRI) under current climate. *(a) Map of the $g1_{max}$ genotypes minimizing the CRI. (b) Map of the F_{critBB} genotypes minimizing the CRI. (c) Map of the PLC_{slope} genotypes minimizing the CRI. Red, orange and blue pixel mean that the "best" genotype has respectively the maximum, the*

mean or the minimal local value of the focal parameter. Grey pixel indicate non viable location.(d) Histogram representing the number of times each genotype gives the lowest CRI.

Between-genotype variation of the risk of mortality under current climate ("Current gVA-without management" scenario)

Under current climate, similar genotypic combinations ("Ming1$_{max}$_MaxPLC$_{slope}$_MaxF$_{critBB}$") minimized the risk of mortality (as depicted by the median CRI) over 80% of Beech range (**Figure 2.d**). In general, g1$_{max}$ was the parameter with the stronger effect on the risk of mortality followed by F$_{critBB}$ and then PLC$_{slope}$. Genotypes with high g1$_{max}$ values (low WUE) were subjected to a higher risk of mortality (median CRI= -0.11), whereas genotypes with low g1$_{max}$ values (high WUE) displayed the lowest risk of mortality (median CRI= -0.64). The risk of mortality was the highest for genotypes with low F$_{critBB}$-value, i.e. tree with early budburst, (median CRI= -0.20), and the lowest for the genotypes with high F$_{critBB}$values displaying a later budburst (median CRI= -0.51). Finally, the risk of mortality was the highest for the genotypes with low PLC$_{slope}$ values, which cavitate later (median CRI =-0.34) and the lowest for genotypes with high PLC$_{slope}$ (median CRI =-0.36) (Figure 3, Table S3b).

We analysed in detail how each parameter affected each kind of risk. The parameter F$_{critBB}$ strongly influenced the risk of late frost (as depicted by rNLF): the median rNLF decreased by 0.22 between genotypes including the highest vs lowest F$_{critBB}$ values. The parameter g1$_{max}$ strongly influenced the risk to embolism : the median rPLC decreased by 0.43 between genotype with the lowest (high WUE) versus the highest (low WUE) g1$_{max}$ values. By contrast, the influence of PLC$_{slope}$ parameter on risk to embolism (as depicted by rPLC) was weak: the median rPLC decreased only by 0.02 between genotypes including the highest vs lowest PLC$_{slope}$ values. Surprisingly, the influence of g1$_{max}$ on carbon starvation risk was also weak: rNSC increased only by 0.01 between the genotypes with minimal (high WUE) versus minimal (low WUE) g1$_{max}$ values (Figure S3a,b,c ; Table S3a,b).

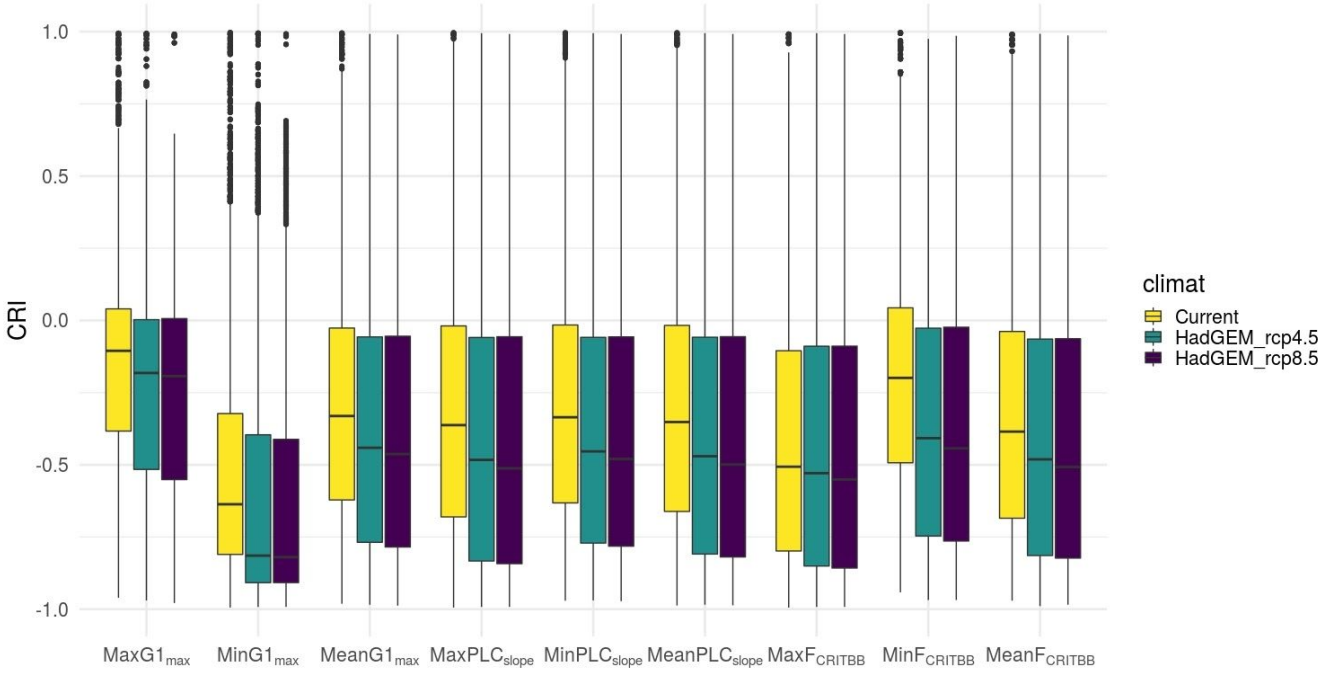

Figure 3: Among-genotypes variations of the risk of mortality, as depicted by CRI *The yellow (light grey), green (medium grey) and purple (dark grey) correspond to CRI simulated respectively under the current, rcp 4.5 and rcp 8.5 climate scenarios. Each boxplot describes the variation over all spatial positions in the CRI in the genotypes combining the fixed value of the parameter displayed on the X-axis with all values of the two other parameters.*

Effect of gVa on beech risk of mortality under future climates (comparison of "Current gVA-without management" under current and future climates)

Simulations under future climate scenarios with gVa showed a decreasing CRI as compared to the CRI under current climate (-0.05), with similar median CRI in the two RCP scenarios (i.e. $CRI_{RCP4.5}$ = -0.30; $CRI_{RCP8.5}$ = -0.30) (Figure 3, Figure S2, Table S4a,b). This decrease in CRI was due to a strong decrease of rNLF (by -0.28 on average) and a slight increase in rNSC (by 0.08) which compensated the slight increase of rPLC (by 0.05) (Figure S3abc, Table S4a,b). As for simulations under current climate, the median CRI of the mean genotype over all positions in the reference scenario ($CRI_{RCP4.5}$= -0.30; $CRI_{RCP8.5}$= -0.30) was

higher than the median CRI of the best genotype over all positions ($CRI_{RCP4.5}$= -0.57; $CRI_{RCP8.5}$= -0.55) in the "Current gVA-without management" scenario (Table S2).

The same genotypic combinations ("$Ming1_{max}$_$MaxPLC_{slope}$_$MaxF_{critBB}$") also minimized the risk of mortality allover beech range, including the southern margin. Moreover, the decrease in CRI under future scenarios differed among genotypes. Genotypes with minimal $g1_{max}$ (high WUE) and minimal F_{critBB} (early budburst) values showed the highest decrease of CRI (-0.12), while genotypes with the maximal $g1_{max}$ (low WUE) and maximal F_{critBB} (late budburst) values had the lowest decrease of CRI (-0.02) (Figure 3 , Table S2a,b, Figure S2).

Effect of local silviculture on the risk of mortality and growth under current climate (comparison of scenario with and without management)

Current management practices decreased the risk of mortality in simulations with gVa or without gVa (CRI decreased by -0.05 in both cases). This decrease was due to an increase in rNSC and a decrease in rPLC (respectively of 0.03 and -0.06) while rNFL was not impacted (Table S3ab, Figure S2, Figures S4, Petit-Cailleux et al in prep 1). The CRI was overall more homogeneous among genotypes with management.

The impact of management varied among genotypes, the more sensitive genotypes overall benefitting the most from the effect of management. For instance, genotypes with the highest $g1_{max}$ value showed the highest management-induced decrease in CRI (with -0.06 decrease of CRI between scenario with and without silviculture). Other genotypes were not affected by management, such as those with the lowest $g1_{max}$ value, which showed only a weak -0.01 decrease of CRI between scenario with and without silviculture (Figure S2, Table S3ab).

Variation in the relationship between growth and risk of mortality among genotypes

The relationship between growth and risk of mortality was overall positive under current climate without management ($r=0.10$, p-val<0.001), indicating a trade-off between survival and growth. This relationship also holded within each genotype (see the ellipses on Figure 4), and between genotypes (see the dots on Figure 4). The trade-off disappear in simulation under future climate without management ($r = 0.22$, NS) (Figure 4). The trade-off was stronger with management under current climate ($r= 0.14$, p-val<0.001) and under future climate ($r=0.19$, p-val<0.001).

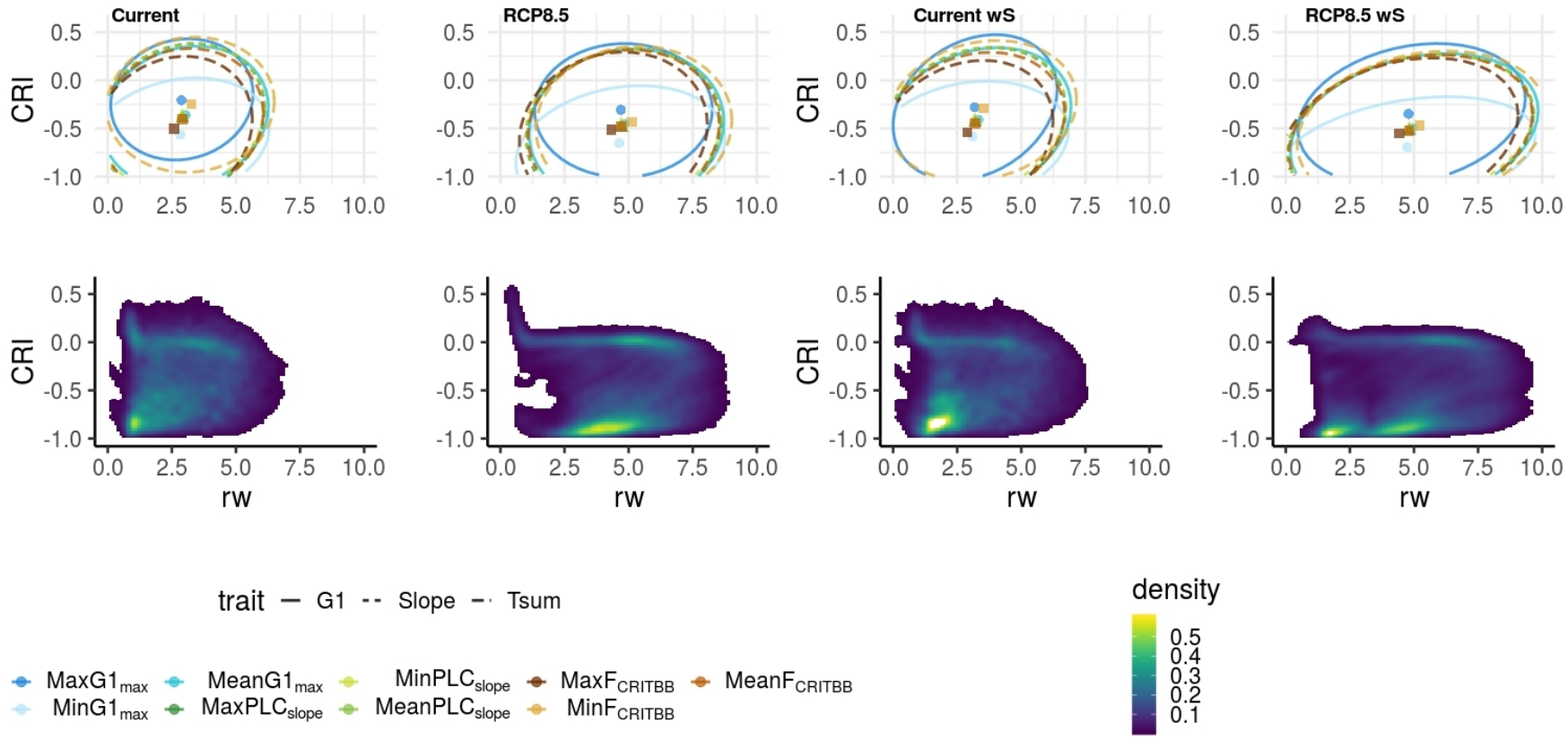

Figure 4: Relationship between growth (rw) and risk of mortality (CRI) across species range and genotypes for scenarios under current and future climate, and without/ with management. *The ellipses on the figure at the top contain 95% of the points for each genotype combination with the focal parameter values, while the dots show the mean genotype values across space. The figure at the bottom shows the overall density of pairs of CRI and ring width values across genotypes and space.*

Effect of a gene transfer scenario (comparison of "Current gVA-with management" vs "gVaTransfer- with management" scenario)

With the transfer scenario, we observed the same trend in selection pressure for a decreasing risk of mortality as with simple gVA-simulation. The CRI of the genotype minimizing the risk over all positions in the "gVaTransfer- with management" scenario (CRIrcp4.5= -0.23, CRIrcp8.5= -0.28) was higher than the median CRI of the genotypes minimizing the risk over all positions in the "Current gVA-without management" scenario (CRI= -0.40) (Table S5). The selection pressure favoured the genotypes combining the higher WUE and the later TBB, no matter cavitation resistance (Figure 5). Almost the same value of CRI were found between both future scenario with a median of 0.056 and 0.027 respectively for rcp 4.5 and rcp 8.5 (Table S5).

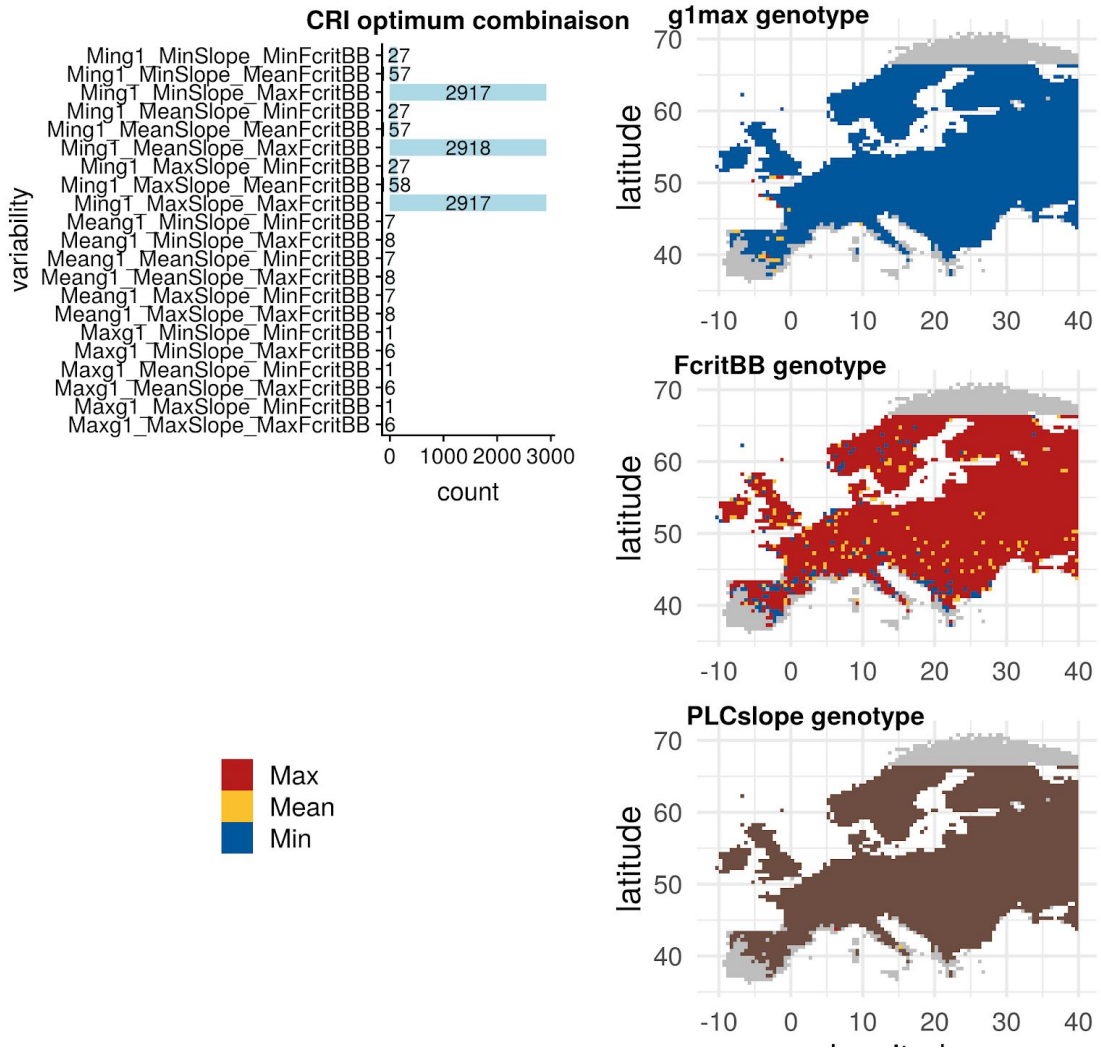

Figure 5: Distribution and count of genotypes minimizing the risk of mortality (CRI)

under pseudo transferred genetic material. *(a) Map of the $g1_{max}$ genotype with the lowest CRI. (b) Map of the F_{critBB} genotype with the lowest CRI. (c) Map of the PLC_{slope} genotype with the lowest CRI. (d) Histogram representing the number of times each genotype gives the lowest CRI. Red, orange and blue pixels mean that the "best" genotype has respectively the maximum, the mean or the minimal local value of the focal parameter. Brown pixels indicate that the three different values of the focal parameter perform equally. Grey pixels indicate non viable location.*

Discussion

(1) Accounting for genetic variability mitigates the risk of mortality due to drought and late frost under current and future climatic conditions

Taking into account the genetic variability between and within populations of functional traits involved in the response to climate stress has led to an overall lower risk of mortality. This also predicted a wider distribution of beech than when genetic variability was neglected in the process-based simulation model. Genetic variability allowed in particular the south, xeric margin of beech range to become viable. These effects of gVA were consistent between simulations under current and future climate, with an overall decrease in the risk of mortality under future climate, from CRI=-0.36 (current climate) to CRI=-0.50 (future climate). By contrast, in simulation without gVa**,** the median CRI did not vary significantly between current and future climatic scenarios.

We modeled both the within- and between-population gVA in three focal functional traits values (the timing of budburst, TBB; the water use efficiency, WUE ; the percent loss of conductance, PLC), by allowing three parameters of CASTANEA, each directly related to one focal trait, to vary: the sum of forcing requirement for budburst (F_{critBB}), the maximal slope of the relation between photosynthesis and stomatal conductance ($g1_{max}$) ; the slope of the curve of vulnerability to cavitation (PLC_{slope}). Thus, for these two traits, when the "same" parameter modality minimizes the risk of mortality in two different localities (for example, the minimum value g1max), it means that the genotype panels favoured by the selection include the minimum possible local values of this parameter. Compared to simulations without gVa , simulations with gVa predicted a lower mortality risk for the "best" genotypes, i.e. the combination of parameters {g1max; FcritBB; PLCslope} minimizing CRI.

In particular, there was a strong selection all over Europe for the genotypes with WUE (i.e., low $g1_{max}$-values) all over Europe. These genotypes became even more advantageous under future climates. The decreasing sensitivity of these genotypes with a higher WUE was due to their lower transpiration of under water stress, which allowed them to avoid the risk of hydraulic failure in response to drought. This result is consistent with the experimental results in common garden studies, where genotypes with higher WUE perform better under water stress (Robson et al., 2012). By contrast, there was only a weak selection for increased resistance to water stress, as measured by the ability to support more negative water potential before reaching the critical value of 88% of PLC. Indeed, differences in PLC_{slope} values did not markedly affect the variation in the risk of mortality.

The south, xeric margin of beech distribution become viable in simulation with gVa, but only for a subset of genotypes. Indeed, in most part of Europe, selection favoured genotypes with late budburst (i.e., high F_{critBB} values), which have a lower risk of late frost damage and a lower cost of re-flushing (Zohner, Rockinger, and Renner 2019). By contrast, in the southern area, genotypes with earlier budburst (i.e., lower F_{critBB} values) had a lower risk of mortality, likely because the risk of late frost was lower in this region, and a longer growing season minimized the risk of carbon starvation. This is consistent with the study of Kreyling et al (2014), who reported a higher frost-resistance of populations at high altitude or latitude, which may have evolved because these populations are more exposed to late frosts than populations from the southern margin. Interestingly, the sensitivity of genotypes with earlier budburst decreased under future climate in most part of Europe, as a consequence of the warming temperatures. Hence, the safety margins for budburst damage rather increased under climate change, unlike the pessimistic scenario discussed in Bigler and Burgman (**2018**).

Moreover, in the southern xeric margin, genotypes with a low PLC_{slope}-value, which more slowly reach the critical value of 88% of loss of conductance, had a lower risk of mortality. By contrast, in the rest of beech range, (i.e. under lower risk of drought occurrence), genotypes with a high PLC_{slope}-value, which reach more quickly 88% of loss of conductance, had a lower risk of mortality. This non-expected pattern can be due to the shape of the PLC curve used to model vulnerability to cavitation in CASTANEA : increasing the slope of this curve simultaneously increases the xylem pressure leading to 88% of loss of conductance and decreases the xylem pressure leading to 12% of loss of conductance. Hence, genotypes with a high PLC_{slope} are associated to a lower resistance to severe drought, but also to a higher

resistance to weak drought as compared to genotypes with a low PLC_{slope}. Moreover, as detailed above, our model tend to favor water-saver genotypes, which avoid drought, rather than drought-resistant genotypes. It is possible that in our model, the variation in PLC_{slope} parameter fails to capture the genetic variation in vulnerability to cavitation, and that other parameters, such as the P50, should be prefered (Stojnić 2018). Finally, other functional trait can determine vulnerability to cavitation, such as wood anatomic trait (e.g., the number of vessels; Hajek 2016), which would require a strong modification of CASTANEA to be accounted for.

Finally, the risk of carbon starvation was very low all over Europe and whatever the scenario, because almost all genotypes had NSCs values well above the threshold. This is in line with the low observed mortality due to carbon starvation in experiments (Adams et al 2017). We cannot rule out that the threshold value considered here for mortality due to carbon starvation (rNSC = 0) is too low, and that carbon starvation could occur for higher rNSC. Moreover, to model the genetic variation in the sensitivity to carbon starvation, maybe another parameter than g1max would better capture the dynamics of NSCs.

(2) Trade-off between growth and risk of mortality, and management effects

As previously found for *Fagus sylvatica* in **Petit-Cailleux et al (in prep1),** management practices decreased the risk of mortality, although they do not predict a larger viable distribution range. This is due to the decrease of biomass and density of the simulated plot after thinning, and to the overall decrease in stand age as silviculture shortens tree lifetime. In our model, younger and smaller trees in less dense stands have lower respiration costs, and hence more resource.

In simulations without forest management, different genotypes were found to minimize the risk of mortality across beech range. In addition, we found that management homogenized the risk of mortality between genotypes, because it reduced more strongly the risk of mortality of the genotypes that were the most sensitive without management. For instance, the risk of mortality of genotypes with a low WUE, which was high in simulations without management, decreased in simulation with management. This homogenization of the risk of mortality means that management favor a higher genetic variability.

In most of our simulations with gVA, we also observed a trade-off between growth and risk of mortality, such that (1) genotypes maximising growth also had a higher risk of mortality and (2) for a same panel of genotypes across species range, the location where a higher growth was observed also had a higher risk of mortality. Moreover, this trade-off between growth and survival tended to weaken between current and future climates, but to strengthen when accounting for forest management. This stronger trade-off under forest management was not necessarily expected, as management practices decreased the risk of mortality. However, management practises also increased growth, which is likely to favor the expression of the trade-off between growth and survival.

Overall, our results support the importance of local genetic diversity in managed forests, since different genotypes maximize different functions or ecosystem services at the same and across locations.

(3) How does the transfer of genetic material affect the prediction of beech distribution and risk of mortality ?

The simulation scenario with gene transfer mimicked a situation where all the possible range of genetic values of each parameter was available at each point of European beech range. The results were very similar to the corresponding scenario with gVA, i.e. with a more restricted range of genetic variation at each point of the European grid. Overall, the same type of genetic combinations minimise the risk of mortality, i.e. genotypes with higher WUE (low g1max) all over the range, genotypes with late budburst (high F_{critBB}) in the northern part of the range versus genotypes with early budburst (low F_{critBB}) in the southern part of the range. The risk of mortality of the best genotype combination was even a bit higher in the scenario with gene transfer as compared to the scenario with current gVa, illustrating that the risk of transfering maladapted genotype may not be negligible.

Because this scenario with gene transfer simulates the same 27 genotypes all over Europe, it is also particularly interesting to study the environmental effects on selection, as measured by the relationship between the parameter value (the genetic component of the trait), the trait value (the phenotype including environmental effect) and the risk of mortality (as a proxy of fitness). Overall, the results may suggest that environmental effects on selection are weak. However, more detailed analyses of the variation of the risk of mortality among genotypes

(instead on focussing on the genotypes minimising the risk) are probably required to dissect these effects.

What could also be done in a next step is to simulate transfer of genetic material from the southern genotypes across Europe. Indeed, several points need to be improved in the modelling of genotype transfert. First, we chose to take the extreme values of the parameters, without taking into account if their combination was possible because no data were available on the physiological or genetic trade-off between the focal adaptive traits.

Conclusion

The strength of our study has been to use the genetic variability measured in common gardens to account for local adaptation and within-population diversity in process-based simulations of the risk of mortality and growth in beech at the distribution range scale. This partitioning of intraspecific variation into genetic and plastic components is an improvement of previous studies; for instance **Sakschewski (2015)** used a used database confounding all sources of variability. In future work however, we will need to validate the prediction of traits values, and to take into account if the trade-off between traits simulated is possible.

Data accessibility

The data set analysed in Petit-cailleux et al in prep 1. will be available online under the zenodo repository (XXX) :

Supplementary Table S1 : Climates data

Supplementary Table S2b : summary of climates and soil data

Supplementary Table S2 : Soil data

Supplementary Table S5: Correspondence table between scenarios and grid points

The data set analysed in this preprint will be available online under the zenodo repository (XXX)

Supplementary material

The process-based model CASTANEA is an open-source software available on capsis website: http://capsis.cirad.fr/

The larger supplementary table in this preprint will be available online under the zenodo repository (XXX) .

Supplementary Table S2: Summary of gVa simulation by genotype

Supplementary Table S3: Summary of gVa simulation by value of trait (min, mean, max of FcritBB, PLCSlope and G1max)

Supplementary Table S4: Summary of gVa simulation by simulation.

Supplementary Table S5 : Summary of transfer simulation by genotype

Bibliography

Adams, Henry D., Melanie J. B. Zeppel, William R. L. Anderegg, Henrik Hartmann, Simon M. Landhäusser, David T. Tissue, Travis E. Huxman, Patrick J. Hudson, Trenton E. Franz, Craig D. Allen, Leander D. L. Anderegg, Greg A. Barron-Gafford, David J. Beerling, David D.

Breshears, Timothy J. Brodribb, Harald Bugmann, Richard C. Cobb, Adam D. Collins, L. Turin Dickman, Honglang Duan, Brent E. Ewers, Lucía Galiano, David A. Galvez, Núria Garcia-Forner, Monica L. Gaylord, Matthew J. Germino, Arthur Gessler, Uwe G. Hacke, Rodrigo Hakamada, Andy Hector, Michael W. Jenkins, Jeffrey M. Kane, Thomas E. Kolb, Darin J. Law, James D. Lewis, Jean Marc Limousin, David M. Love, Alison K. Macalady, Jordi Martínez-Vilalta, Maurizio Mencuccini, Patrick J. Mitchell, Jordan D. Muss, Michael J. O'Brien, Anthony P. O'Grady, Robert E. Pangle, Elizabeth A. Pinkard, Frida I. Piper, Jennifer A. Plaut, William T. Pockman, Joe Quirk, Keith Reinhardt, Francesco Ripullone, Michael G. Ryan, Anna Sala, Sanna Sevanto, John S. Sperry, Rodrigo Vargas, Michel Vennetier, Danielle A. Way, Chonggang Xu, Enrico A. Yepez, and Nate G. McDowell. 2017. "A Multi-Species Synthesis of Physiological Mechanisms in Drought-Induced Tree Mortality." *Nature Ecology and Evolution* 1(9):1285–91.

Alberto, Florian J., Sally N. Aitken, Ricardo Alía, Santiago C. González-Martínez, Heikki Hänninen, Antoine Kremer, François Lefèvre, Thomas Lenormand, Sam Yeaman, Ross Whetten, and Outi Savolainen. 2013. "Potential for Evolutionary Responses to Climate Change - Evidence from Tree Populations." *Global Change Biology* 19(6):1645–61.

Ball, J. Timothy, Ian E. Woodrow, and Joseph A. Berry. 1987. "A Model Predicting Stomatal Conductance and Its Contribution to the Control of Photosynthesis under Different Environmental Conditions." Pp. 221–24 in *Progress in Photosynthesis Research*. Springer.

Benito Garzón, Marta, Ricardo Alía, T. Matthew Robson, and Miguel A. Zavala. 2011. "Intra-Specific Variability and Plasticity Influence Potential Tree Species Distributions under Climate Change." *Global Ecology and Biogeography* 20(5):766–78.

Benito Garzón, Marta, T. Matthew Robson, and Arndt Hampe. 2019. "ΔTraitSDMs: Species Distribution Models That Account for Local Adaptation and Phenotypic Plasticity." *New Phytologist* 222(4):1757–65.

Bernacchi, C. J., E. L. Singsaas, C. Pimentel, A. R. Portis Jr, and S. P. Long. 2001. "Improved Temperature Response Functions for Models of Rubisco-Limited Photosynthesis." *Plant, Cell and Environment* 24(2):253–59.

Berzaghi, Fabio, Ian J. Wright, Koen Kramer, Sylvie Oddou-Muratorio, Friedrich J. Bohn, Christopher P. O. Reyer, Santiago Sabaté, Tanja G. M. Sanders, and Florian Hartig. 2019. "Towards a New Generation of Trait-Flexible Vegetation Models." *Trends in Ecology and Evolution*.

Bigler, Christof and Harald Bugmann. 2018. "Climate-Induced Shifts in Leaf Unfolding and Frost Risk of European Trees and Shrubs." *Scientific Reports* 8(1):1–10.

Bréda, Nathalie, Roland Huc, André Granier, and Erwin Dreyer. 2006. "Temperate Forest Trees and Stands under Severe Drought : A Review of Ecophysiological Responses ,

Adaptation Processes and Long-Term Consequences." *Annals of Forest Science* 63(6):625–44.

Brodribb, Timothy J. 2009. "Xylem Hydraulic Physiology: The Functional Backbone of Terrestrial Plant Productivity." *Plant Science* 177(4):245–51.

Broennimann, O., U. a. Treier, H. Müller-Schärer, W. Thuiller, a. T. Peterson, and a. Guisan. 2007. "Evidence of Climatic Niche Shift during Biological Invasion." *Ecology Letters* 10(8):701–9.

De Caceres, Miquel, Nicolas Martin-StPaul, Marco Turco, Antoine Cabon, and Victor Granda. 2018. "Estimating Daily Meteorological Data and Downscaling Climate Models over Landscapes." *Environmental Modelling and Software* 186–96.

Campbell, Gaylon S. 1974. "A Simple Method for Determining Unsaturated Conductivity from Moisture Retention Data." *Soil Science* 117(6):311–14.

Cardellini, Giuseppe, Tatiana Valada, Claire Cornillier, Estelle Vial, Marian Dragoi, Venceslas Goudiaby, Volker Mues, Bruno Lasserre, Arkadiusz Gruchala, Per Kristian Rørstad, Mathias Neumann, Miroslav Svoboda, Risto Sirgmets, Olli Pekka Näsärö, Frits Mohren, Wouter M. J. Achten, Liesbet Vranken, and Bart Muys. 2018. "EFO-LCI: A New Life Cycle Inventory Database of Forestry Operations in Europe." *Environmental Management* 61(6):1031–47.

Cheaib, Alissar, Vincent Badeau, Julien Boe, Isabelle Chuine, Christine Delire, Eric Dufrêne, Christophe François, Emmanuel S. Gritti, Myriam Legay, Christian Pagé, Wilfried Thuiller, Nicolas Viovy, and Paul Leadley. 2012. "Climate Change Impacts on Tree Ranges: Model Intercomparison Facilitates Understanding and Quantification of Uncertainty: {{Understanding}} and Quantification of Uncertainties of Climate Change Impacts on Tree Range." *Ecology Letters* 15(6):533–44.

Cotto, Olivier, Johannes Wessely, Damien Georges, Günther Klonner, Max Schmid, Stefan Dullinger, Wilfried Thuiller, and Frédéric Guillaume. 2017. "A Dynamic Eco-Evolutionary Model Predicts Slow Response of Alpine Plants to Climate Warming." *Nature Communications* 8(May).

Davi, H., C. Barbaroux, C. Francois, and E. Dufrêne. 2009. "The Fundamental Role of Reserves and Hydraulic Constraints in Predicting LAI and Carbon Allocation in Forests." *Agricultural and Forest Meteorology* 149(2):349–61.

Davi, H. and M. Cailleret. 2017. "Assessing Drought-Driven Mortality Trees with Physiological Process-Based Models." *Agricultural and Forest Meteorology* 232:279–90.

Davi, H., E. Dufrêne, C. Francois, G. Le Maire, D. Loustau, A. Bosc, S. Rambal, A. Granier, and E. Moors. 2006a. "Sensitivity of Water and Carbon Fluxes to Climate Changes from

1960 to 2100 in European Forest Ecosystems." *Agricultural and Forest Meteorology* 141(1):35–56.

Davi, H., E. Dufrêne, C. Francois, G. Le Maire, D. Loustau, A. Bosc, S. Rambal, A. Granier, and E. Moors. 2006b. "Sensitivity of Water and Carbon Fluxes to Climate Changes from 1960 to 2100 in European Forest Ecosystems." *Agricultural and Forest Meteorology* 141(1):35–56.

Davi, H., E. Dufrêne, A. Granier, V. Le Dantec, C. Barbaroux, C. François, and N. Bréda. 2005. "Modelling Carbon and Water Cycles in a Beech Forest. Part II.: Validation of the Main Processes from Organ to Stand Scale." *Ecological Modelling* 185(2–4):387–405.

Delpierre, N., K. Soudani, C. François, G. Le Maire, C. Bernhofer, W. Kutsch, L. Misson, S. Rambal, T. Vesala, and E. Dufrêne. 2012. "Quantifying the Influence of Climate and Biological Drivers on the Interannual Variability of Carbon Exchanges in European Forests through Process-Based Modelling." *Agricultural and Forest Meteorology* 154–155:99–112.

Dittmar, Christoph, Wolfgang Zech, and Wolfram Elling. 2003. "Growth Variations of Common Beech (Fagus Sylvatica L.) under Different Climatic and Environmental Conditions in Europe - A Dendroecological Study." *Forest Ecology and Management* 173(1–3):63–78.

Dorado-Liñán, I., L. Akhmetzyanov, and A. Menzel. 2017. "Climate Threats on Growth of Rear-Edge European Beech Peripheral Populations in Spain." *International Journal of Biometeorology* 61(12):2097–2110.

Dounavi, A., F. Netzer, N. Celepirovic, M. Ivanković, J. Burger, A. G. Figueroa, S. Schön, J. Simon, E. Cremer, B. Fussi, M. Konnert, and H. Rennenberg. 2016. "Genetic and Physiological Differences of European Beech Provenances (F. Sylvatica L.) Exposed to Drought Stress." *Forest Ecology and Management* 361:226–36.

Dufrêne, E., H. Davi, C. François, G. Le Maire, V. Le Dantec, and A. Granier. 2005. "Modelling Carbon and Water Cycles in a Beech Forest. Part I: Model Description and Uncertainty Analysis on Modelled NEE." *Ecological Modelling* 185(2–4):407–36.

Eckert, Andrew J., Joost Van Heerwaarden, Jill L. Wegrzyn, C. Dana Nelson, Jeffrey Ross-Ibarra, Santíago C. González-Martínez, and David B. Neale. 2010. "Patterns of Population Structure and Environmental Associations to Aridity across the Range of Loblolly Pine (Pinus Taeda L., Pinaceae)." *Genetics* 185(3):969–82.

Farquhar, G. D., S. Von Caemmerer, and J. a Berry. 1980. "A Biochemical Model of Photosynthetic CO." *Planta* 149:78–90.

Gárate-Escamilla, Homero, Arndt Hampe, Natalia Vizcaíno-Palomar, T. Matthew Robson, and Marta Benito Garzón. 2019. "Range-wide Variation in Local Adaptation and Phenotypic Plasticity of Fitness-related Traits in *Fagus Sylvatica* and Their Implications under Climate Change" edited by B. Blonder. *Global Ecology and Biogeography* 28(9):1336–50.

García-Plazaola, José Ignacio, Raquel Esteban, Koldobika Hormaetxe, Beatriz Fernández-Marín, and José María Becerril. 2008. "Photoprotective Responses of Mediterranean and Atlantic Trees to the Extreme Heat-Wave of Summer 2003 in Southwestern Europe." *Trees - Structure and Function* 22(3):385–92.

Gauzere, J., E. K. Klein, O. Brendel, H. Davi, and S. Oddou-Muratorio. 2016. "Using Partial Genotyping to Estimate the Genetic and Maternal Determinants of Adaptive Traits in a Progeny Trial of Fagus Sylvatica." *Tree Genetics and Genomes* 12(6).

Gömöry, Dušan and Ladislav Paule. 2011. "Trade-off between Height Growth and Spring Flushing in Common Beech (Fagus Sylvatica L.)." *Annals of Forest Science* 68(5):975–84.

Granier, A., P. Biron, and D. Lemoine. 2000. "Water Balance, Transpiration and Canopy Conductance in Two Beech Stands." *Agricultural and Forest Meteorology* 100(4):291–308.

Hacket-Pain, A. J., L. Cavin, A. D. Friend, and A. S. Jump. 2016. "Consistent Limitation of Growth by High Temperature and Low Precipitation from Range Core to Southern Edge of European Beech Indicates Widespread Vulnerability to Changing Climate." *European Journal of Forest Research* 135(5):897–909.

Hajek, Peter, Daniel Kurjak, Georg Von Wühlisch, Sylvain Delzon, and Bernhard Schuldt. 2016. "Intraspecific Variation in Wood Anatomical, Hydraulic, and Foliar Traits in Ten European Beech Provenances Differing in Growth Yield." *Frontiers in Plant Science* 7(JUNE2016):791.

Härkönen, S., M. Neumann, V. Mues, F. Berninger, K. Bronisz, G. Cardellini, G. Chirici, H. Hasenauer, M. Koehl, M. Lang, K. Merganicova, F. Mohren, A. Moiseyev, A. Moreno, M. Mura, B. Muys, K. Olschofsky, B. Del Perugia, P. K. Rørstad, B. Solberg, A. Thivolle-Cazat, V. Trotsiuk, and A. Mäkelä. 2019. "A Climate-Sensitive Forest Model for Assessing Impacts of Forest Management in Europe." *Environmental Modelling and Software* 115:128–43.

Harris, Rebecca Mary B., Michael R. Grose, Greg Lee, Nathaniel L. Bindoff, Luciana L. Porfirio, and Paul Fox-Hughes. 2014. "Climate Projections for Ecologists." *Wiley Interdisciplinary Reviews: Climate Change* 5(5):621–37.

Hengl, Tomislav, Jorge Mendes De Jesus, Gerard B. M. Heuvelink, Maria Ruiperez Gonzalez, Milan Kilibarda, Aleksandar Blagotić, Wei Shangguan, Marvin N. Wright, Xiaoyuan Geng, Bernhard Bauer-Marschallinger, Mario Antonio Guevara, Rodrigo Vargas,

Robert A. MacMillan, Niels H. Batjes, Johan G. B. Leenaars, Eloi Ribeiro, Ichsani Wheeler, Stephan Mantel, and Bas Kempen. 2017. "SoilGrids250m: Global Gridded Soil Information Based on Machine Learning" edited by B. Bond-Lamberty. *PLoS ONE* 12(2):e0169748.

Hiederer, Roland. 2013. *Mapping Soil Properties for Europe - Spatial Representation of Soil Database Attributes*.

Hijmans, Robert J. 2016. *Raster: Geographic Data Analysis and Modeling*. Vol. 1.

IPCC. 2014. "Climate Change 2014: Climate Change Impacts, Adaptation and Vulnerablility. Working Group II Contribution to the Intergovernmental Panel on Climate Change Fifth Assessment Report. Summary for Policymakers." P. 19 in Vol. 2.

Jacob, D, Petersen, J., Eggert, B, Alias, A, Christensen,O, and et al. 2014. "{EURO}-{CORDEX}: {New} High-Resolution Climate Change Projections for {European} Impact Research." *Regional Environmental Change* 14:563–78.

Jump, Alistair S., Jenny M. Hunt, and Josep Pen¨uelas. 2006. "Rapid Climate Change-Related Growth Decline at the Southern Range Edge of Fagus Sylvatica." *Global Change Biology* 12(11):2163–74.

Knutzen, Florian, Choimaa Dulamsuren, Ina Christin Meier, and Christoph Leuschner. 2017. "Recent Climate Warming-Related Growth Decline Impairs European Beech in the Center of Its Distribution Range." *Ecosystems* 20(8):1494–1511.

Kramer, Koen, Bernd Degen, Jutta Buschbom, Thomas Hickler, Wilfried Thuiller, Martin T. Sykes, and Wim de Winter. 2010. "Modelling Exploration of the Future of European Beech (Fagus Sylvatica L.) under Climate Change-Range, Abundance, Genetic Diversity and Adaptive Response." *Forest Ecology and Management* 259(11):2213–22.

Kramer, Koen, Alexis Ducousso, Dušan Gömöry, Jon Kehlet Hansen, Lucia Ionita, Mirko Liesebach, Adrian Lorenţ, Silvio Schüler, Malgorzata Sulkowska, Sven de Vries, and Georg von Wühlisch. 2017. "Chilling and Forcing Requirements for Foliage Bud Burst of European Beech (Fagus Sylvatica L.) Differ between Provenances and Are Phenotypically Plastic." *Agricultural and Forest Meteorology* 234–235:172–81.

Kreyling, Juergen, Constanze Buhk, Sabrina Backhaus, Martin Hallinger, Gerhard Huber, Lukas Huber, Anke Jentsch, Monika Konnert, Daniel Thiel, Martin Wilmking, and Carl Beierkuhnlein. 2014. "Local Adaptations to Frost in Marginal and Central Populations of the Dominant Forest Tree Fagus Sylvatica L. as Affected by Temperature and Extreme Drought in Common Garden Experiments." *Ecology and Evolution* 4(5):594–605.

Kuparinen, Anna, Outi Savolainen, and Frank M. Schurr. 2010. “Increased Mortality Can Promote Evolutionary Adaptation of Forest Trees to Climate Change.” *Forest Ecology and Management* 259(5):1003–8.

Lefèvre, François, Thomas Boivin, Aurore Bontemps, François Courbet, Hendrik Davi, Marion Durand-Gillmann, Bruno Fady, Julie Gauzere, Cindy Gidoin, Marie Joe Karam, Hadrien Lalagüe, Sylvie Oddou-Muratorio, and Christian Pichot. 2014. “Considering Evolutionary Processes in Adaptive Forestry.” *Annals of Forest Science* 71(7):723–39.

Loustau, D., A. Granier, F. El Hadj Moussa, M. Sartore, and M. Guedon. 1990. “Evolution Saisonnière Du Flux de Sève Dans Un Peuplement de Pins Maritimes.” *Annales Des Sciences Forestières* 47(6):599–618.

Martínez-Vilalta, Jordi, Anna Sala, Dolores Asensio, Lucía Galiano, Günter Hoch, Sara Palacio, Frida I. Piper, and Francisco Lloret. 2016. “Dynamics of Non-Structural Carbohydrates in Terrestrial Plants: A Global Synthesis.” *Ecological Monographs* 86(4):495–516.

McSweeney, C. F., R. G. Jones, R. W. Lee, and D. P. Rowell. 2015. “Selecting CMIP5 GCMs for Downscaling over Multiple Regions.” *Climate Dynamics* 44(11–12):3237–60.

Monteith, J. L. 1965. “Evaporation and Environment. The State and Movement of Water in Living Organisms.” *Symposium of the Society of Experimental Biology, Vol. 19* 205–34.

Morin, Xavier, David Viner, and Isabelle Chuine. 2008. “Tree Species Range Shifts at a Continental Scale: New Predictive Insights from a Process-Based Model.” *Journal of Ecology* 96(4):784–94.

Nakićenović, N. and R. Swart. 2000. *Special Report on Emission Scenarios.* Cambridge: Cambridge University Press.

Oddou-Muratorio, Sylvie and Hendrik Davi. 2014. “Simulating Local Adaptation to Climate of Forest Trees with a Physio-Demo-Genetics Model.” *Evolutionary Applications* 7(4):453–67.

Paquette, Alain and Christian Messier. 2011. “The Effect of Biodiversity on Tree Productivity: From Temperate to Boreal Forests.” *Global Ecology and Biogeography* 20(1):170–80.

Penuelas, Josep and Martí Boada. 2003. “A Global Change-Induced Biome Shift in the Montseny Mountains (NE Spain).” *Global Change Biology* 9(2):131–40.

Petit-Cailleux, Cathleen, Hendrik Davi, François Lefevre, Joseph Garrigue, Jean-André Magdalou, Christophe Hurson, Elodie Magnanou, and Sylvie Oddou-Muratorio. 2019.

"Combining Statistical and Mechanistic Models to Unravel the Drivers of Mortality within a Rear-Edge Beech Population." *PCIEcology* under revi.

Rehfeldt, Gerald E., Nadejda M. Tchebakova, Yelena I. Parfenova, William R. Wykoff, Nina A. Kuzmina, and Leonid I. Milyutin. 2002. "Intraspecific Responses to Climate in Pinus Sylvestris." *Global Change Biology* 8(9):912–29.

Reusch, Thorsten B. H., Anneli Ehlers, August Hämmerli, and Boris Worm. 2005. "Ecosystem Recovery after Climatic Extremes Enhanced by Genotypic Diversity." *Proceedings of the National Academy of Sciences of the United States of America*.

Robson, T. Matthew, David Sánchez-Gómez, F. Javier Cano, and Ismael Aranda. 2012. "Variation in Functional Leaf Traits among Beech Provenances during a Spanish Summer Reflects the Differences in Their Origin." *Tree Genetics and Genomes* 8(5):1111–21.

Ryan, M. G. 1991. "Effects of Climate Change on Plant Respiration." *Ecological Applications* 1(2):157–67.

Sáenz-Romero, Cuauhtémoc, Jean-Baptiste Lamy, Alexis Ducousso, Brigitte Musch, François Ehrenmann, Sylvain Delzon, Stephen Cavers, Władysław Chałupka, Said Dağdaș, Jon Kehlet Hansen, Steve J. Lee, Mirko Liesebach, Hans-Martin Rau, Achilleas Psomas, Volker Schneck, Wilfried Steiner, Niklaus E. Zimmermann, and Antoine Kremer. 2016. "Adaptive and Plastic Responses of Quercus Petraea Populations to Climate across Europe." *Global Change Biology*.

Sakschewski, Boris, Werner Von Bloh, Alice Boit, Lourens Poorter, Marielos Peña-Claros, Jens Heinke, Jasmin Joshi, and Kirsten Thonicke. 2016. "Resilience of Amazon Forests Emerges from Plant Trait Diversity." *Nature Climate Change*.

Sakschewski, Boris, Werner von Bloh, Alice Boit, Anja Rammig, Jens Kattge, Lourens Poorter, Josep Peñuelas, and Kirsten Thonicke. 2015. "Leaf and Stem Economics Spectra Drive Diversity of Functional Plant Traits in a Dynamic Global Vegetation Model." *Global Change Biology* 21(7):2711–25.

Sala, A. and J. D. Tenhunen. 1996. "Simulations of Canopy Net Photosynthesis and Transpiration in Quercus Ilex L. under the Influence of Seasonal Drought." *Agricultural and Forest Meteorology* 78(3–4):203–22.

Savolainen, Outi, Tanja Pyhäjärvi, and Timo Knürr. 2007. "Gene {{Flow}} and {{Local Adaptation}} in {{Trees}}." *Annual Review of Ecology, Evolution, and Systematics* 38(1):595–619.

Stojnić, Srdan, Saša Orlović, Andrej Pilipović, Dragica Vilotić, Mirjana Šijačić-Nikolić, and Danijela Miljković. 2012. "Variation in Leaf Physiology among Three Provenances of

European Beech (Fagus Sylvatica L.)in Provenance Trial in Serbia." *Genetika* 44(2):341–53.

Teissier du cros, E., B. Thiebaut, and H. Duval. 1988. "Variability in Beech : Budding, Height Growth and Tree Form." *Annales Des Sciences Forestières* 45(4):383–98.

Thuiller, Wilfried, Sandra Lavorel, Martin T. Sykes, and Miguel B. Araújo. 2006. "Using Niche-Based Modelling to Assess the Impact of Climate Change on Tree Functional Diversity in Europe." *Diversity and Distributions* 12(1):49–60.

Tóth, Brigitta, Melanie Weynants, László Pásztor, and Tomislav Hengl. 2017. "3D Soil Hydraulic Database of Europe at 250 m Resolution." *Hydrological Processes* 31(14):2662–66.

Urli, Morgane, Annabel J. Porté, Herve Cochard, Yann Guengant, Regis Burlett, and Sylvain Delzon. 2013. "Xylem Embolism Threshold for Catastrophic Hydraulic Failure in Angiosperm Trees." *Tree Physiology* 33(7):672–83.

De Vries, F. W. T. Pennin., A. H. M. Brunsting, and H. H. Van Laar. 1974. "Products, Requirements and Efficiency of Biosynthesis a Quantitative Approach." *Journal of Theoretical Biology* 45(2):339–77.

van Vuuren, Detlef P., Jae Edmonds, Mikiko Kainuma, Keywan Riahi, Allison Thomson, Kathy Hibbard, George C. Hurtt, Tom Kram, Volker Krey, Jean Francois Lamarque, Toshihiko Masui, Malte Meinshausen, Nebojsa Nakicenovic, Steven J. Smith, and Steven K. Rose. 2011. "The Representative Concentration Pathways: An Overview." *Climatic Change* 109(1):5–31.

Walther, Gian Reto, Eric Post, Peter Convey, Annette Menzel, Camille Parmesan, Trevor J. C. Beebee, Jean Marc Fromentin, Ove Hoegh-Guldberg, and Franz Bairlein. 2002. "Ecological Responses to Recent Climate Change." *Nature* 416(6879):389–95.

Wardle, Da, Ma Huston, Jp Grime, Thomas Bell, Jonathan a Newman, Bernard W. Silverman, Sarah L. Turner, Andrew K. Lilley, Silke Langenheder, Eva S. Lindström, Lars J. Tranvik, Hannes Peter, Sara Beier, Stefan Bertilsson, Eva S. Lindström, Silke Langenheder, and Lars J. Tranvik. 2005. "Biodiversity and Ecosystem Function: An Issue in Ecology." *Nature* 5(3):957–67.

Weedon, Graham P., Gianpaolo Balsamo, Nicolas Bellouin, Sandra Gomes, Martin J. Best, and Pedro Viterbo. 2014. "The WFDEI Meteorological Forcing Data Set: WATCH Forcing Data Methodology Applied to ERA-Interim Reanalysis Data." *Water Resources Research* 50(9):7505–14.

Yeaman. 2016. “Convergent Local Adaptation to Climate in Distantly Related Conifers Supplementary.” *Science* 353(6306):23–26.

Zohner, Constantin M., Alexander Rockinger, and Susanne S. Renner. 2019. “Increased Autumn Productivity Permits Temperate Trees to Compensate for Spring Frost Damage.” *New Phytologist* 221(2):789–95.

3 Supplementary online material

Figure S1: Number of viable genetic combination under current (a), RCP4.5 (b), and RCP 8.5 (c) scenarios.

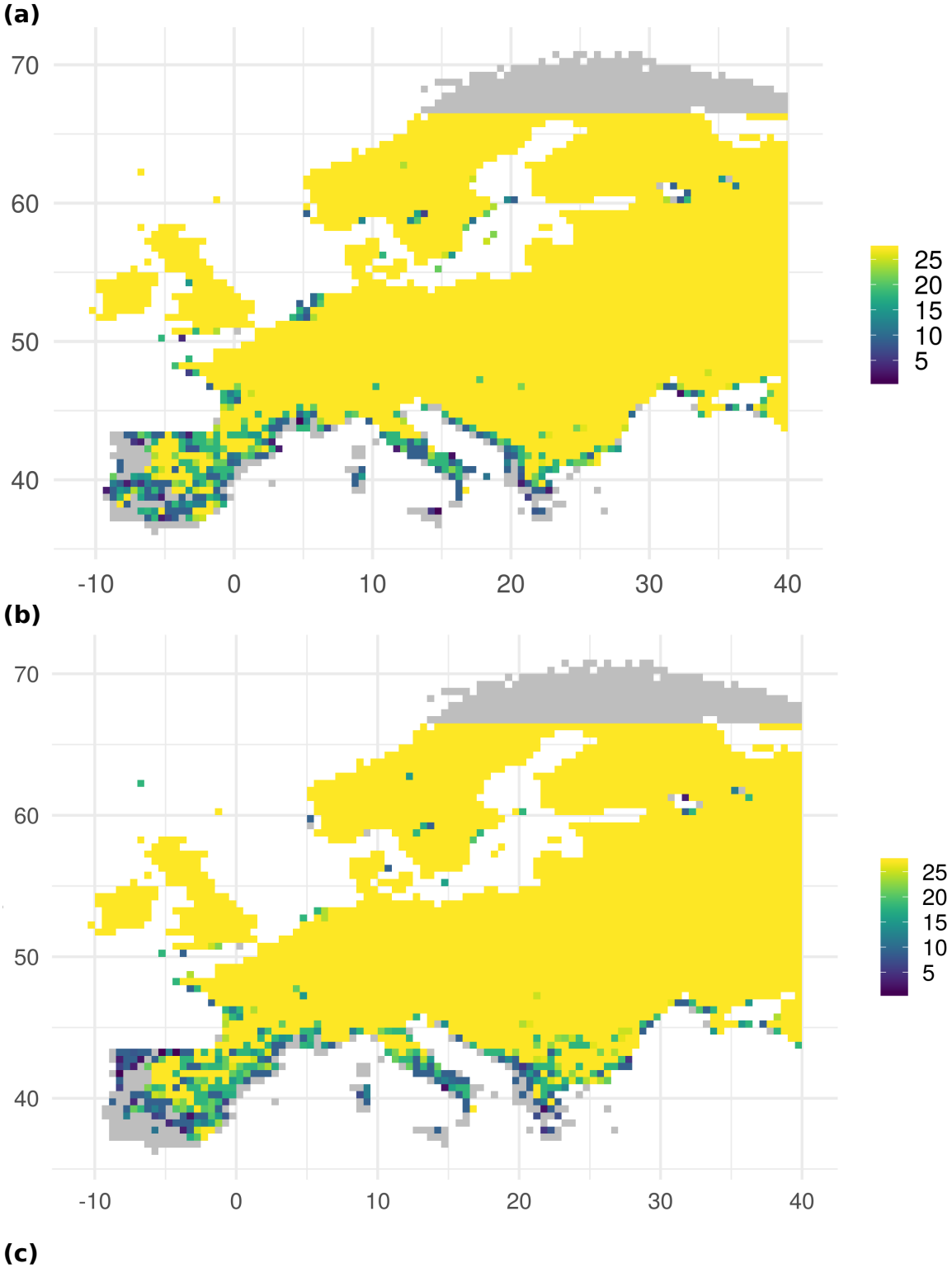

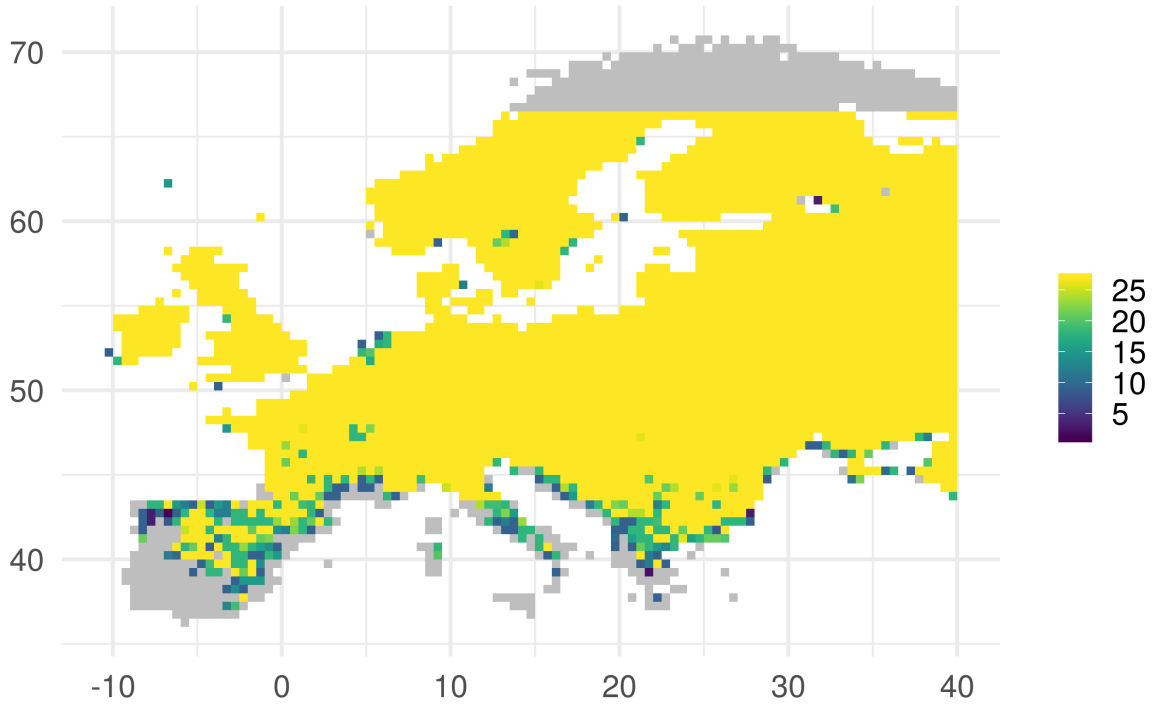

Figure S2: Among-genotypes variations of the risk of mortality, as depicted by CRI under current (a), RCP4.5 (b), and RCP 8.5 (c) scenarios and under SS1 (no management) or SS2 to SS4 (classical management) . The yellow (light grey), green (medium grey) and purple (dark grey) correspond to CRI simulated respectively under the current, rcp 4.5 and rcp 8.5 climate scenarios. Black and grey outline correspond respectively to simulation with and without management. Each boxplot describes the variation over all spatial positions in the CRI in the genotypes combining the fixed value of the parameter displayed on the X-axis with all values of the two other parameters.

climat
Current
HadGEM_rcp4.5
HadGEM_rcp8.5
management
No
Sylv
g1Moy_SlopMoy_TsumMoy
g1Moy_SlopMoy_TsumMin
g1Moy_SlopMoy_TsumMax
g1Moy_SlopMin_TsumMoy
g1Moy_SlopMin_TsumMin
g1Moy_SlopMin_TsumMax
g1Moy_SlopMax_TsumMoy
g1Moy_SlopMax_TsumMin
g1Moy_SlopMax_TsumMax
g1Min_SlopMoy_TsumMoy
g1Min_SlopMoy_TsumMin
g1Min_SlopMoy_TsumMax
g1Min_SlopMin_TsumMoy
g1Min_SlopMin_TsumMin
g1Min_SlopMin_TsumMax
g1Min_SlopMax_TsumMoy
g1Min_SlopMax_TsumMin
g1Min_SlopMax_TsumMax
g1Max_SlopMoy_TsumMoy
g1Max_SlopMoy_TsumMin
g1Max_SlopMoy_TsumMax
g1Max_SlopMin_TsumMoy
g1Max_SlopMin_TsumMin
g1Max_SlopMin_TsumMax
g1Max_SlopMax_TsumMoy
g1Max_SlopMax_TsumMin
g1Max_SlopMax_TsumMax
variability
1.0
0.5
0.0
-0.5
-1.0
CVI

Figure S3: Boxplot representing the (a) rPLC, (b) rNSC and (c)rNLF of the simulated trees bearing each traits under SS1 (no management). The yellow (light grey), green (medium grey) and purple (dark grey) boxplots are respectively, simulations made with the current climate, HadGEM rcp 4.5 and HadGEM rcp 8.5.

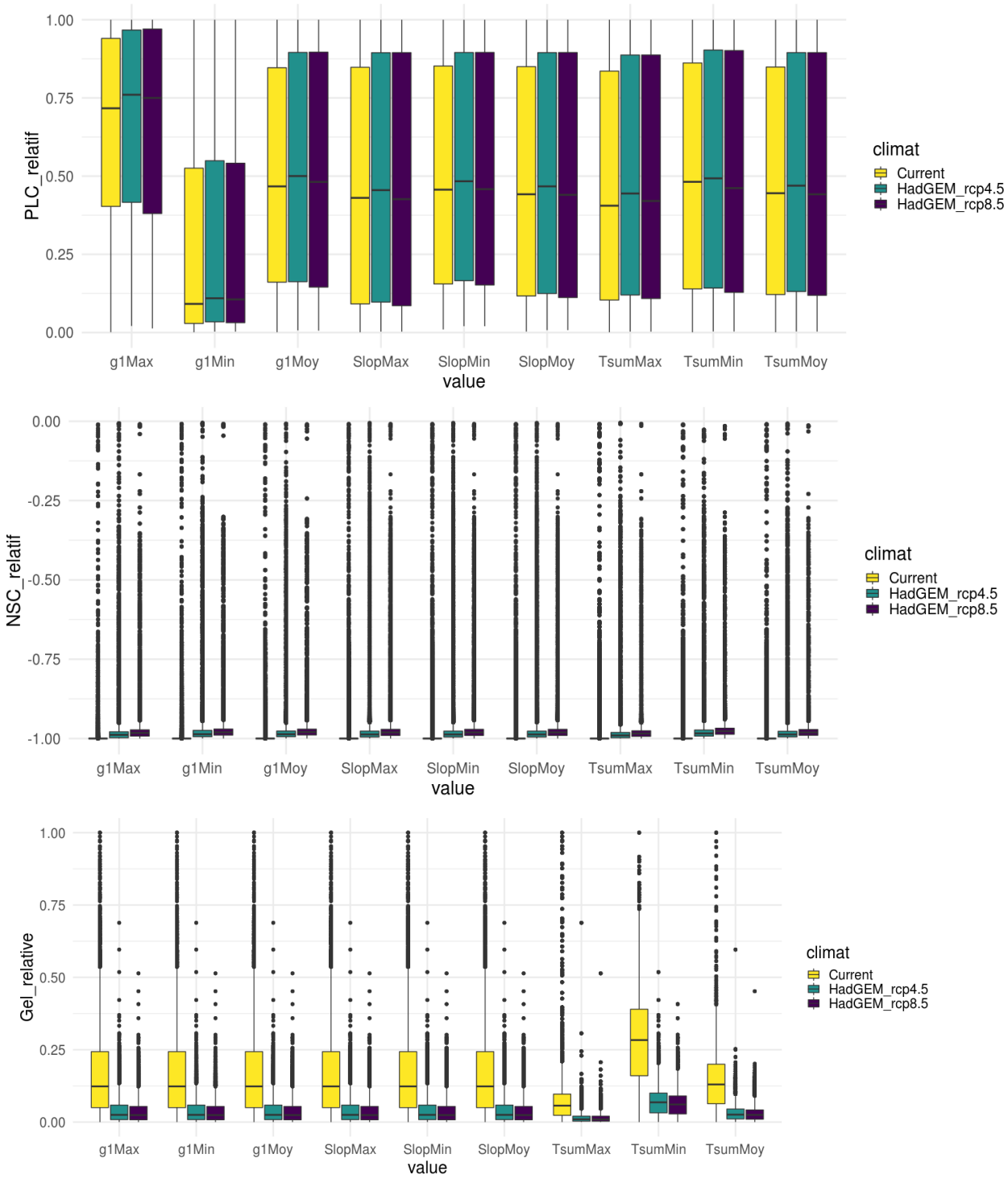

Figures S4: **Boxplot representing the (a) CVI, (b) rPLC and (c) rNSC of the simulated trees bearing each traits under SS1 to SS4 (no + classical management).** The yellow (light grey), green (medium grey) and purple (dark grey) boxplots are respectively, simulations made with the current climate, HadGEM rcp 4.5 and HadGEM rcp 8.5.

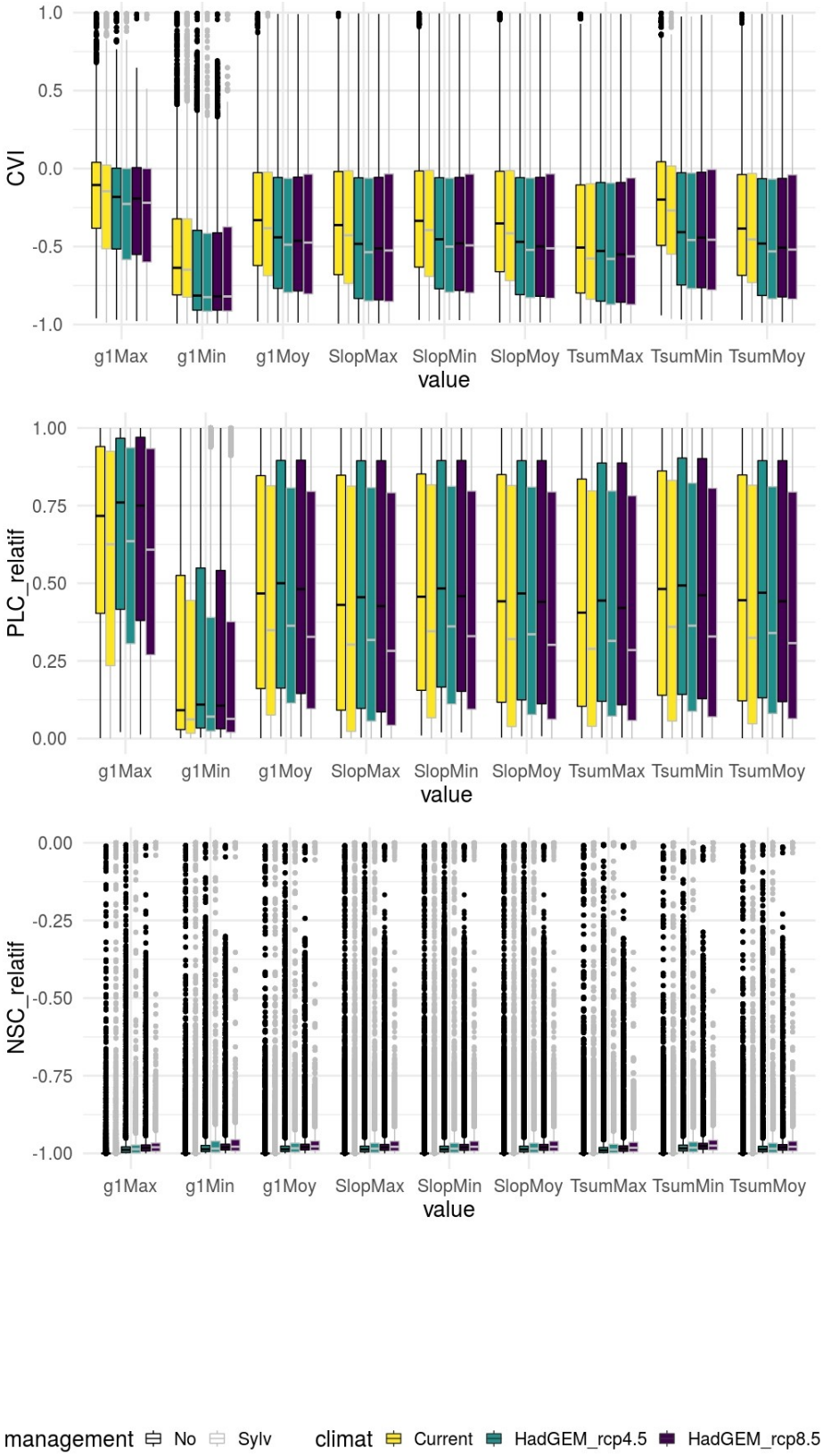

TableS1: Number of occurrence of genotypes in the extension area. 123 grid point increased. There are 123 more viable grid points when variability is taken into account.

Genotypes	Number of presence
MaxG1max_MaxPLCslope_MinFcritBB	1
MaxG1max_MaxPLCslope_MeanFcritBB	1
MaxG1max_MinPLCslope_MaxFcritBB	1
MaxG1max_MinPLCslope_MinFcritBB	2
MaxG1max_MinPLCslope_MeanFcritBB	2
MaxG1max_MeanPLCslope_MinFcritBB	1
MaxG1max_MeanPLCslope_MeanFcritBB	1
MinG1max_MaxPLCslope_MaxFcritBB	103
MinG1max_MaxPLCslope_MinFcritBB	92
MinG1max_MaxPLCslope_MeanFcritBB	101
MinG1max_MinPLCslope_MaxFcritBB	122
MinG1max_MinPLCslope_MinFcritBB	115
MinG1max_MinPLCslope_MeanFcritBB	120
MinG1max_MeanPLCslope_MaxFcritBB	109
MinG1max_MeanPLCslope_MinFcritBB	102
MinG1max_MeanPLCslope_MeanFcritBB	106
MeanG1Max_MaxPLCslope_MinFcritBB	1
MeanG1Max_MaxPLCslope_MeanFcritBB	1
MeanG1Max_MinPLCslope_MaxFcritBB	8
MeanG1Max_MinPLCslope_MinFcritBB	6
MeanG1Max_MinPLCslope_MeanFcritBB	6
MeanG1Max_MeanPLCslope_MinFcritBB	1
MeanG1Max_MeanPLCslope_MeanFcritBB	1
MaxG1max_MaxPLCslope_MaxFcritBB	0
MaxG1max_MeanPLCslope_MaxFcritBB	0
MeanG1Max_MaxPLCslope_MaxFcritBB	0
MeanG1Max_MeanPLCslope_MaxFcritBB	0

4 Appendices

Appendix

Appendix (A1)- Link between climate and traits/parameters

To simulate the spatial variability of the target traits, we used data from provenance tests. We also constructed the climate variables from WATCH (Weedon et. al, 2014) that explained significant differences of traits variability in the two main studies (Kramer et al 2017 and Hajek et al 2016). This allowed us to have our own equations explaining the variability of CASTANEA parameters ($g1_{max}$, TBB, PLC_{slope}) and traits related to vulnerability (respectively, WUE, TBB, PLC).

1- Link between FcritBB and the environment

We used the studies of (Kramer et al., 2017) to calibrate FCRITBB variation across Europe. Based on four beech provenance tests across Europe, this study investigated the variation of several phenological parameters, including state of forcing among provenances. We used their phenological score to model the effect of on latitude, longitude and altitude (equation 1).

$$Score \sim Trial + NbObs + yearPheno + lonProv + latProv + ALTI \quad \text{(equation 1)}$$

With Score, the phenological score (i.e. higher the score is, later is the BDD); As the "backgroundnoise" :Trial, the trials; NbObs, the number of observations across years; yearPheno, years of phenological observation. As the environmental driver: lonProv, the longitude of the provenance; latProv, the latitude of the provenance; ALTI, the altitude of the provenance. We found a significant effect of the latitude, longitude and altitude of provenances (Table A1.1). Then we did a simple cross-multiplication to adapt the environmental driver variables (equations 2).

$$lonProv = ((meanFcritBB \times 3.265e\text{-}02)/meanScore)*-1 \quad \text{(equation 2.a)}$$

$$latProv = ((meanFcritBB \times 1.186e\text{-}02)/meanScore)*-1 \quad \text{(equation 2.b)}$$

$$lALTI = ((meanFcritBB \times 6.910e\text{-}04)/meanScore)*-1 \quad \text{(equation 2.c)}$$

With 3.71 as the mean phenological score measured in the trials and 245 for the mean FcritBB value for the beech tree. Minus one is applied because the phenological score increased mean earlier BBD, while the FcritBB is decreasing for an ealier BBD (they are in the opposite direction). Then to simulate the traits variability we corrected the intercept of the relation between FcritBB and environmental variables (equations 3).

MeanFcritBB = 245 – (intercept_eq1) (equations 3.a)

MinFcritBB = 170 – (intercept_eq1) (equations 3.b)

MaxFcritBB = 320 – (intercept_eq1) (equations 3.c)

With intercept_eq1, the value of the equation 1 intercept (Table A1-1). The INRA experiments on Mont Ventoux (France) allowed to estimate the variance of TBB within population (σ^2BBday =25), which converts into a 95% interval of variation of [-75°C; +75°C] around MeanFCRITBBi. Hence 245, 170 and 320 are respectively, the value représenting the mean and the standard deviation observed for the TBB traits.

MeanFCRITBBi = Mean/Min/MaxFcritBB + -0.78*latitudei +-2.16* longitudei + -0.06*altitudei ; (equation 4)

With [99°C to 260°C] the variation of predicted minFcritBB, [249 °C to 409°C] the variation of predicted maxFcritBBThe predicted and [174.4°C to 334.1°C] the variation of predicted meanFcritBB. meanFcritBB prediction are reprensented figure A2-1.

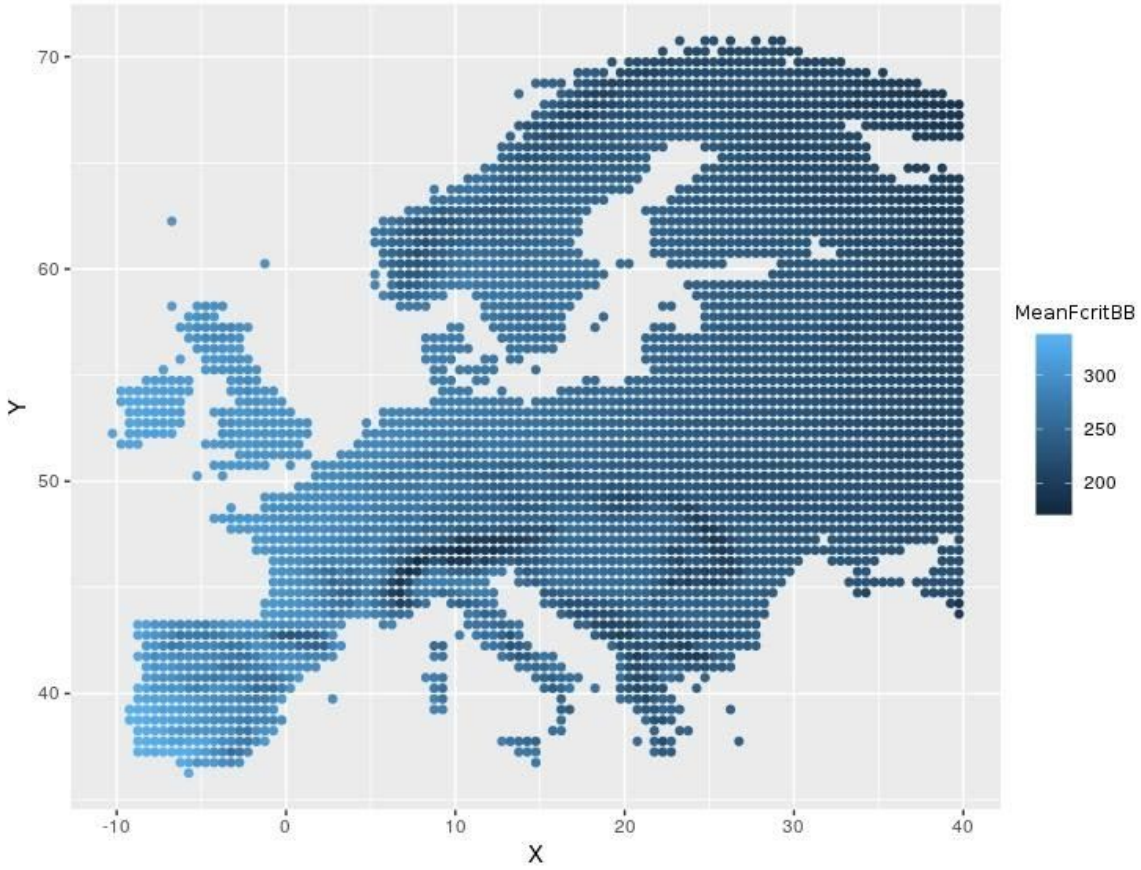

Figure A1-1. Mean FcritBB predictions across Europe.

Table A1.1: Parameter estimates and related statistics for the model equation 1. β is the maximum likelihood estimate, with its estimated error (SE), z-value, and associated p-value (Pr(>|z|)).

Variables	β	SE	z value	Pr(>|z|)
(Intercept)	-6.25E+01	3.75E+00	-1.67E+01	< 2e-16 ***
TrialBU1905	-7.40E-01	3.73E-02	-1.98E+01	< 2e-16 ***
TrialBU1908	-1.98E-01	4.23E-02	-4.67E+00	2.96e-06 ***
TrialBU1909	1.36E-02	3.51E-02	3.87E-01	6.99E-01
TrialBU1915	3.86E-01	3.63E-02	1.06E+01	< 2e-16 ***
TrialBU1917	-2.22E+00	3.85E-02	-5.77E+01	< 2e-16 ***

TrialBU1921	1.42E+00	4.54E-02	3.12E+01	< 2e-16 ***
TrialBU1922	-6.05E-01	4.36E-02	-1.39E+01	< 2e-16 ***
TrialBU2001	-2.67E-02	3.58E-02	-7.45E-01	4.56E-01
TrialBU2004	-7.24E-01	3.96E-02	-1.83E+01	< 2e-16 ***
TrialBU2005	9.85E-02	4.26E-02	2.31E+00	0.020745 *
TrialBU2008	-1.63E+00	3.83E-02	-4.27E+01	< 2e-16 ***
TrialBU2009	-2.17E+00	4.03E-02	-5.38E+01	< 2e-16 ***
TrialBU2010	-5.03E-01	3.94E-02	-1.28E+01	< 2e-16 ***
TrialBU2012	1.46E-01	3.72E-02	3.93E+00	8.68e-05 ***
TrialBU2014	-5.07E-01	4.18E-02	-1.21E+01	< 2e-16 ***
TrialBU2018	-1.10E+00	3.68E-02	-2.97E+01	< 2e-16 ***
TrialBU2019	-1.67E+00	4.51E-02	-3.71E+01	< 2e-16 ***
TrialBU2020	-1.02E+00	4.67E-02	-2.18E+01	< 2e-16 ***
TrialBU2021	-1.91E+00	4.48E-02	-4.26E+01	< 2e-16 ***
TrialBU2023	-7.50E-01	3.52E-02	-2.13E+01	< 2e-16 ***
TrialBU2024	-1.11E+00	3.83E-02	-2.89E+01	< 2e-16 ***
NbObs	1.46E-02	4.17E-03	3.51E+00	0.000457 ***
yearPheno	3.27E-02	1.87E-03	1.75E+01	< 2e-16 ***
lonProv	3.27E-02	6.89E-04	4.74E+01	< 2e-16 ***
latProv	1.19E-02	1.88E-03	6.31E+00	2.80e-10 ***
ALTI	6.91E-04	1.77E-05	3.90E+01	< 2e-16 ***

2- Link between $g1_{max}$ and the environment

We used the studies of (Hajek et al 2016) to calibrate $g1_{max}$ variation across Europe. This study used Ten 20-year old European beech (*Fagus sylvatica L.*) provenances representing the entire distribution range throughout Europe to investigate intraspecific variation in wood anatomical, hydraulic, and foliar traits. We used a linear regression model to model the variation in δ13C in response to the first four Principal Components (PC) of the climate variables measured at provenance sites [Table supp N].

$$\text{Mean } \delta 13C = -3.065^{e+01} + 7.747^{e-04} \text{x altitude} - 1.947^{e-01} \text{x axe1} - 2.162^{e-01} \text{x axe2} + 3.160^{e-01} \text{x axe3} - 1.712e^{-01} \text{x axe4} \quad \text{(equation5)}$$

Then with the relationship between δ13C and $g1_{max}$ calculated with the abaqus test was used to predict the mean $g1_{max}$ all over Europe.

$$\text{Mean} g_{1max\,i} = -0.3973 + \delta 13C \times -0.418602 \quad \text{(equation 6)}$$

with 11.8 the mean $g1_{max}$ value for beech. Moreover, Hajek et al. (2016) estimated the standard deviation of δ13C within population ($\sigma_{\delta 13C}$ =0.263), which converts (using CASTANEA, see Appendix 1) into a 67% variation interval of [-3.8; +3.8] around Mean$g_{1max\,i}$

With [7.0 to 9.7] the variation of predicted min$g1_{max}$,[14.7 to 17.2] the variation of predicted max$g1_{max}$ and [10.9 to 13.5] the variation of predicted mean$g1_{max}$. Mean$g1_{max}$ prediction are reprensented figure A2-2.

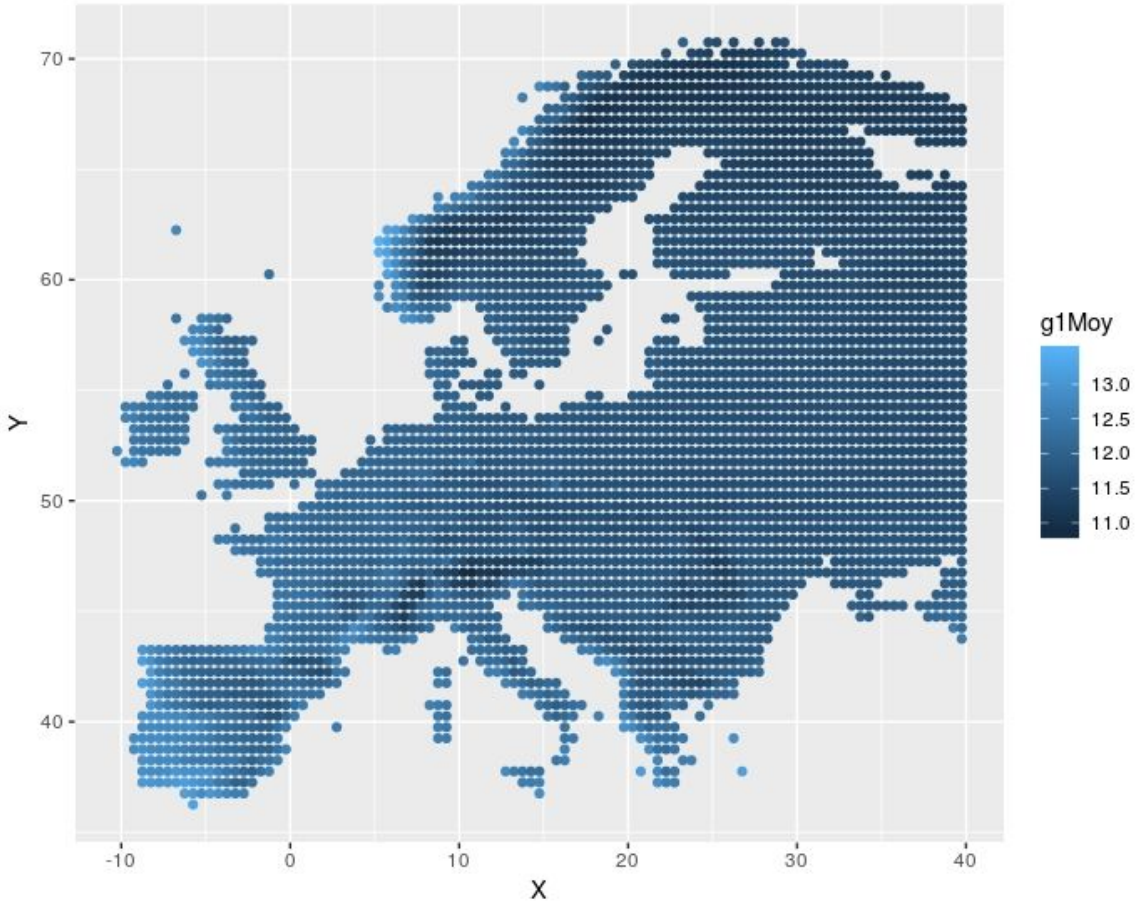

Figure A1.2. Mean $g1_{max}$ predictions across Europe.

Table A1.2: Parameter estimates and related statistics for the model equation 2. β is the maximum likelihood estimate, with its estimated error (SE), z-value, and associated p-value (Pr(>|z|)).

Variables	β	SE	z value	Pr(>|z|)
(Intercept)	-3.07E+01	1.77E-01	-1.74E+02	6.6e-09 ***
alt_watch	7.75E-04	1.88E-04	4.12E+00	0.01466 *
axe1	-1.95E-01	3.73E-02	-5.22E+00	0.00644 **
axe2	-2.16E-01	4.22E-02	-5.13E+00	0.00685 **
axe3	3.16E-01	5.92E-02	5.34E+00	0.00591 **
axe4	-1.71E-01	6.13E-02	-2.79E+00	0.04920 *

Appendix A2

Relationship between parameter and trait values for each focal functional traits

This appendix illustrate the response of each target trait (i.e timing of budburst, TBB; , percentage of loss of conductance (PLC) and water use efficiency, WUE, assessed by isotopic discrimination, δ 13C) to the variation in the considered parameters (respectively: FcritBB, PLCslope and G1max) on 9 grid points scattered in Europe (Figure A2.1 and A2.2a,b,c).

TBBincreases with increasing FcritBB, as summarized by each regression line (Figure A2.2a). The average PLC, which described the response to weak drought, decreases with increasing PLCslope, until a ceiling around 50 (Figure A2.2ab). Δ 13C becomes more negative, meaning that WUE increases with increasing G1max (Figure A2.2c). The variation along each regression line corresponds to among-year variation in trait value for each given parameters values and values vary among grid points because of the average environment variation among grid points.

Figure A2.1: Localisation of target grid points.

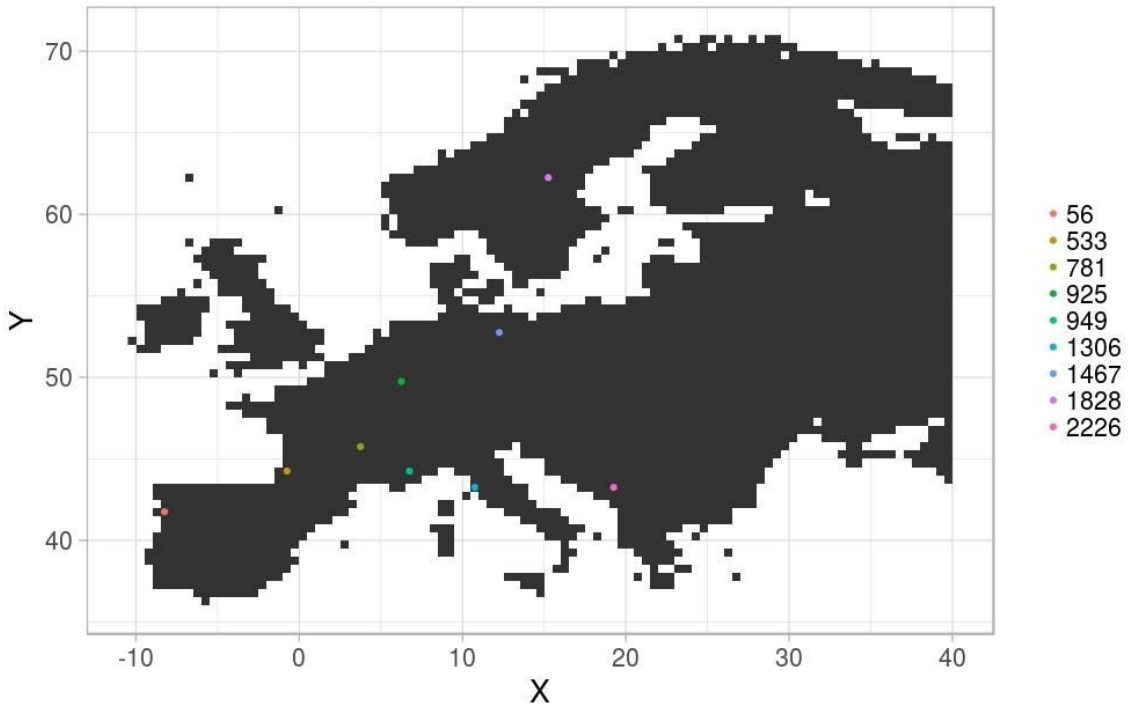

Figure A2.2: Response of each target trait according to the modified parameters on 9 grid points. (a) Relation between FcritBB and TBB, (b) relation between PLCslope and PLC, (c) relation between G1max and δ13C.

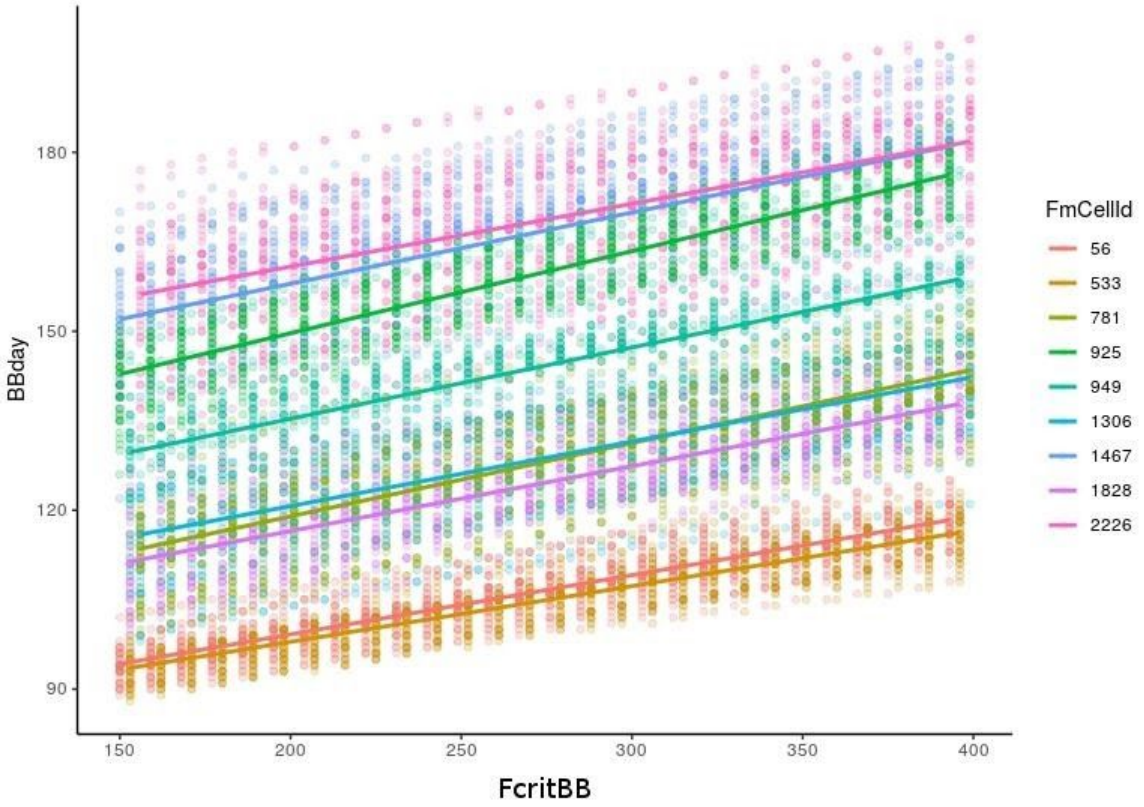

b

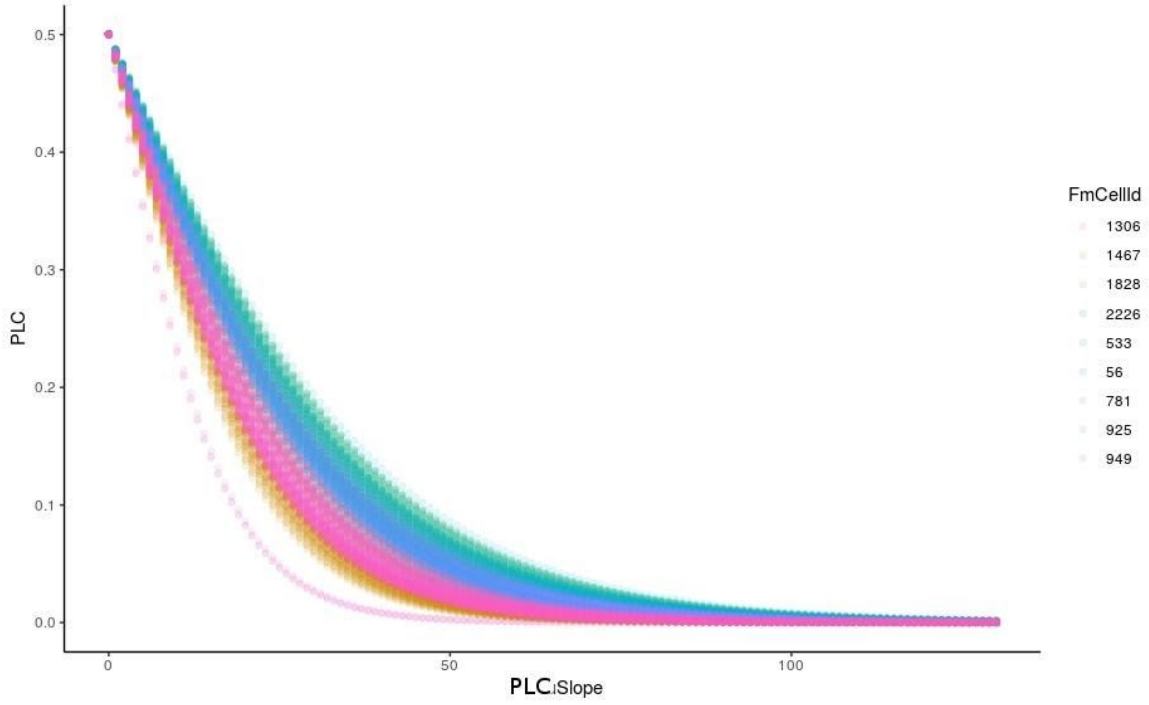
PLC
0.5
0.4
0.3
0.2
0.1
0.0
0
50
100
PLCiSlope
FmCellId
1306
1467
1828
2226
533
56
781
925
949

c

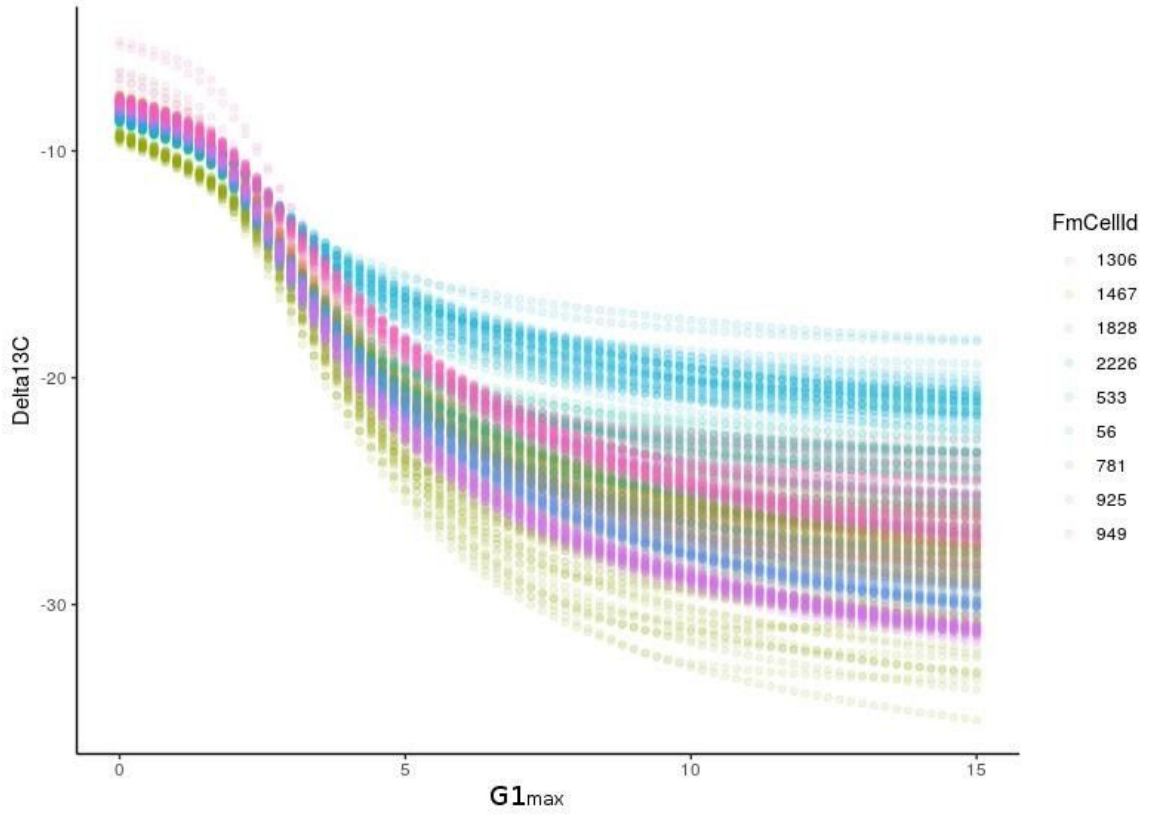
Delta13C
-10
-20
-30
0
5
10
15
G1max
FmCellId
1306
1467
1828
2226
533
56
781
925
949

5 Résultats et perspectives

Cette étude nous a permis de constater que les simulations de risques de mortalité sont plus faibles pour les forêts avec de la variabilité génétique que pour les forêts sans variabilité génétique. De plus, en prenant en compte la variabilité génétique au sein des peuplements, l'aire de distribution actuelle simulée du Hêtre est plus grande que celle simulée sans variabilité génétique, en particulier dans le sud de l'Europe. En effet, certains génotypes sont moins sensibles aux risques induits par le changement climatique. Enfin, cette étude confirme notre résultat précédent, montrant que dans les scénarios futurs sous changement climatique, les pratiques sylvicoles tendent à réduire le risque local de mortalité.

Le scénario théorique de transfert de gènes nous a permis de constater que le sens de la sélection sur le risque de mortalité allait vers des génotypes avec une forte efficience d'utilisation de l'eau et un débourrement plus tardif dans le coeur et au nord de l'Europe, alors que dans le sud de l'Europe, les génotypes avec un débourrement plus précoce ont une sensibilité plus faible aux stress climatiques. D'autre part, les génotypes minimisant le risque de mortalité ont généralement une croissance plus faible. Ces différents résultats illustrent l'intérêt de conserver une diversité de génotypes pour minimiser le risque de mortalité du Hêtre à l'échelle de son aire de répartition, tout en ne sacrifiant pas la productivité. Une prochaine étape sera de simuler des transferts de matériel génétiques des zones ayant un fort risque de mortalité actuel et future vers des zones plus favorables dans le futur.

Chapitre V

Discussion générale

1 Discussion sur la méthodologie

Dans cette thèse, différents modèles statistiques ainsi qu'un modèle basé sur les processus (PBM), CASTANEA, ont été utilisés. L'utilisation des modèles statistiques s'est limitée à la première partie de la thèse ainsi qu'à un projet sur les causes de mortalité aux marges de distribution du Hêtre (en cours avec l'UMR Biogeco). Les modèles statistiques, tout comme CASTANEA ont été utilisés à différentes échelles spatiales (individu, population, aire de distribution) et temporelles (passée et future). L'utilisation de CASTANEA étant centrale dans cette thèse, je me concentre par la suite sur ses améliorations et ses limites. Pour répondre aux questions scientifiques posées, nous avons implémenté plusieurs options dans CASTANEA comme par exemple la simulation de l'indice de densité relative, la défoliation, la gestion sylvicole et la prise en compte de la variabilité génétique. De plus nous avons développé une méthode efficace permettant de lancer CASTANEA à l'échelle Européenne et faire plusieurs millions de simulation en quelques jours.

1.1 Nouveaux développements dans CASTANEA

Les options dans CASTANEA permettent d'ajuster un ou des processus physiologique.s en particulier, comme par exemple, choisir le modèle de débourrement ou encore le type de réponse physiologique de la respiration en été.

Compétition : CASTANEA est un modèle arbre-moyen, qui simule un peuplement et ne peut donc pas prendre explicitement en compte la compétition entre individus. Pour tenir compte indirectement de la compétition, nous avons calculé l'indice de densité relative (RDI) basé sur la loi d'auto-éclaircie (Charru, 2012). La loi d'auto-éclaircie est une relation allométrique entre le diamètre quadratique moyen et le nombre maximal de tiges de même diamètre qu'un peuplement pourrait tolérer avant que ne se manifeste une mortalité spontanée (Reineke, 1933). Le RDI est défini comme le rapport entre le nombre de tiges d'un peuplement et le nombre de tiges maximales de même diamètre qu'il pourrait contenir, et varie donc dans l'intervalle [0,1] 3. Pour toutes les espèces, la densité maximale en nombre de tiges a été estimé à partir des équations et des paramètres donnés dans la thèse de Marie Charru (2014). Cela permet de simuler les effets d'une baisse de densité au niveau de la parcelle sur la projection du houppier et le risque de mortalité. La simulation de la baisse de la compétition passe aussi par le fait que la coupe induit une baisse seulement transitoire de l'indice foliaire simulé, alors que la réduction du nombre de tiges est durable. La coupe induit donc une augmentation du ratio entre la photosynthèse et la respiration et donc le carbone disponible pour chaque arbre.

Limite des simulations qui ne tiennent pas compte du statut de l'arbre : CASTANEA ne tient pas compte, non plus, du statut de dominance individuelle, qui peut affecter le bilan carbone d'un arbre et donc la capacité à atténuer

un stress. Dans les populations d'arbres, les plus grands arbres sont généralement dominants, avec un meilleur accès aux ressources en lumière favorisant l'accumulation de carbone par rapport aux petits arbres, qui sont plus susceptibles d'être sur-cimés. Une autre raison est que la taille des arbres peut varier en fonction de la qualité de l'environnement dans la population étudiée. En effet, les grands arbres ont plus de chance d'apparaître sur de meilleurs sols. Par conséquent, l'effet taille sur la mortalité observée avec l'approche statistique (avec une mortalité plus importante des petits arbres) peut être dû à un effet confondant de l'hétérogénéité spatiale des sols, non pris en compte dans l'approche statistique, ce qui explique les différences de prédiction de mortalité entre le modèle statistique et PBM (qui ne simule pas de mortalité plus forte chez arbres de petites tailles). Une mesure de la disponibilité de l'eau au niveau de chaque arbre serait nécessaire pour mieux distinguer les effets purement "taille" des effets "microstation". Cela signifie aussi que les prédictions de risques à large échelle sous-estiment peut-être le risque de mortalité des petits arbres, et donc sur-estiment le recrutement des individus pour former les futures populations. Cette sous-estimation pourrait expliquer les différences locales de risques de mortalité entre notre étude et celle de Garaté et al 2019, basée sur des modèles ΔtraitSDMs qui mettent en évidence un risque de mortalité plus élevé chez les jeunes arbres dans l'est de la distribution du Hêtre.

Effet du stress sur la défoliation : Le chapitre 2 confirme l'importance de la défoliation dans la mortalité du Hêtre en situation de stress, mise en évidence également par d'autres études (**?**). Dans CASTANEA, il existe un modèle prenant en compte l'impact des gelées tardives sur le LAI. Dans le même esprit, nous avons implémenté une option pour tenir compte du stress hydrique et de la cavitation sur le LAI, de telle sorte que le pourcentage de perte de conductance se traduise directement aussi par un pourcentage de perte de surface foliaire (via le LAI). Nous n'avons pas pu valider ce module de défoliation induit par le stress hydrique à La Massane, les données qualitatives ne s'y prêtant pas. Pour valider ce module, il serait envisageable d'utiliser les données de suivi de défoliation du Hêtre du réseau RENECOFOR/ICPforest. Une fois validé, ce module pourrait être utilisé pour tenir compte de façon plus réaliste de la réponse de l'arbre à un stress hydrique et notamment de son impact sur la dynamique des réserves.

Sylviculture : La sylviculture a été modélisée selon les scénarios sylvicoles et les règles de coupes et de rotation synthétisées par (Härkönen et al., 2019). De plus, pour savoir quel scénario sylvicole appliquer à quel point de la grille européenne, nous avons utilisé une base de données EFI donnant le pourcentage de ces sylvicultures appliqué à chaque pays issu des travaux du projet GenTree. Dans ce travail, certains modes de gestion sylvicole n'ont pas été considérés, notamment les modes de "gestion sous couvert continu" (sylviculture irrégulière) ou ceux de gestion en taillis. En effet, CASTANEA peut difficilement simuler de la gestion irrégulière sans tenir compte explicitement de la compétition entre individus. Il serait également préférable d'affiner les règles de coupes selon les pays et leurs régions. De plus, nous avons consi-

déré les mêmes gestions sylvicoles pour le futur, alors que les pratiques de gestion peuvent évoluer. Ces évolutions sont d'autant plus envisageables que les forestiers seraient prêts à changer les pratiques sylvicoles, si le déclin de la croissance des arbres était supérieur à 20% et si les échecs de régénération étaient supérieurs à 25% (Seidl et al., 2016). La gestion sylvicole pourrait également préserver la biodiversité génétique et aider à réduire le risque de mortalité des arbres liés aux changements climatiques.

1.2 CASTANEA à large échelle

Un défi majeur de cette thèse a été d'utiliser CASTANEA à large échelle. Cela a posé différents défis techniques, en terme de puissance de calcul (résolu grâce à un serveur et à de la parallélisation), de manipulation de fichiers volumineux (climats, sol) et de stockage de données (les sorties des modèles). Un code permettant de lancer CASTANEA sur un ensemble de cellules, en modifiant pour chaque cellule automatiquement les paramètres d'entrée (i.e fichiers climats, sylvicultures appliqués, paramètres du sol, variabilité des caractères génétiques), a été développé (Manuel CASTANEA pour plus de précisions). Dans l'ensemble, les défis techniques ont été surmontés, et la principale limitation a été la disponibilité des données. Par exemple, la résolution spatiale des simulations [0.5°x0.5°] a été déterminée par celle des données climatiques journalières correspondant au climat actuel. Cette résolution ne permet pas de bien caractériser les zones montagneuses (les cellules avec une forte hétérogénéité climatique), et présente le risque de mal représenter les valeurs extrêmes des variables de sorties d'intérêt. Par comparaison, des données climatiques annuelles sont disponibles dans les bases de données à une résolution plus fine, ce qui rend par exemple les prédictions des modèles de niches réalisées généralement beaucoup plus précises spatialement. Pour améliorer la précision des prédictions à large échelle et déterminer plus finement les zones à risques, les nouvelles données ERA5, qui constituent une amélioration des données de ré-analyse climatique WATCH, pourraient être utilisées dans de prochains projets.
En revanche, nous avons pu utiliser pour ce travail des bases de données de caractéristiques du sol permettant d'estimer quasiment tous les paramètres sol nécessaires à CASTANEA (Hiederer, 2013; Hengl et al., 2017; Tóth et al., 2017). Cela a permis de simuler plus précisément les risques de mortalité, en intégrant le contexte pédologique au contexte climatique. En effet, pour le Hêtre lorsque l'on considère les caractéristiques du sol, l'aire de distribution actuelle est mieux prédite (meilleure AUC) qu'en considérant un sol moyen homogène (même avec une résolution grossière) (Annexe sol - simulation avec et sans variabilité du sol). D'ailleurs, ces résultats éclairent en partie les problèmes de prédiction de l'aire de distribution actuelle du Hêtre dans les précédentes études avec CASTANEA (Cheaib et al., 2012; Guillemot et al., 2015).
Malgré le progrès que représente la prise en compte des données de sol, la faible résolution (0.5°x0.5°) explique peut-être en partie les valeurs élevées de PLC simulées sous le climat actuel. De plus, CASTANEA sous-estime l'eau souterraine à laquelle les arbres du système racinaire ont accès. En effet, CASTANEA ne représente que

la capacité en eau superficielle (0-150 cm), et néglige le fait que les racines peuvent se trouver même dans les fissures du lit rocheux (Carrière et al., 2020). Un plus grand risque de gel tardif a été simulé pour les conifères à aiguilles persistantes des hautes latitudes et des hautes altitudes. Ce résultat peut être dû (1) au modèle phénologique, relativement simple, de débourrement utilisé ici, basé sur l'accumulation des températures de forçage uniquement et qui ne tient pas compte de la levée de dormance, (2) à la valeur seuil pour les dommages causés par le gel tardif, considérée ici comme identique entre toutes les espèces. De plus, il n'a pas été identifié de marge "précise" dans le nord de l'Europe, ni dans les zones de haute altitude. Cela peut être dû à la non prise en compte des phénomènes de stress hivernaux (i.e cavitation pendant l'hiver, gelure hivernale). En plus de l'intégration des phénomènes de stress hivernaux, la prise en compte de modèles phénologiques adaptés à chaque espèce pourrait être envisagé pour mieux évaluer l'influence des gelées tardives et leur impact, même si aucun modèle de phénologie ne fait consensus actuellement (Hänninen et al., 2018; Hufkens et al., 2018).

Evaluation de CASTANEA à large échelle : Dans les seconde et troisième parties de cette thèse, nous avons utilisé CASTANEA pour prédire la distribution des espèces à l'échelle européenne. Pour valider nos prédictions, nous avons utilisé la NPP et les croissances de cernes simulées par CASTANEA pour prédire la présence de l'espèce, en fixant le seuil de NPP critique à partir de la comparaison des absences et présences prédites et de celles observées, comme dans Cheaib et al. 2012. Cette approche de validation pourrait être complétée par une approche plus détaillée, en utilisant les données mesurées par les tours à flux dans différentes conditions environnementales à travers l'Europe aux flux simulés par CASTANEA. Ces données sont disponibles au sein du réseau européen FLUXNET [(1)], mais cette validation supplémentaire représente un travail considérable qui n'était pas envisageable dans le cadre de cette thèse.

Les indices que nous avons utilisé pour déterminer les risques face aux stress climatiques ont été construits à partir de seuils physiologiques connus des espèces pour rPLC et rNSC ou de façon arbitraire pour rNFL. Une façon d'évaluer nos indices de risque et de déterminer au mieux les seuils à utiliser dans CASTANEA, serait d'utiliser les données de mortalité à large échelle, dans une approche similaire à celle utilisée dans le Chapitre 1. Cette évaluation est au coeur d'un projet que j'ai initié pendant ma thèse, en collaboration avec une équipe de l'UMR Biogeco. Ce projet a notamment pour but d'étudier les mécanismes physiologiques permettant d'expliquer la distribution des espèces, en caractérisant les limites physiologiques aux marges climatiques des espèces grâce à des approches PBM et modèles de niche corrélatifs (cSDM) et en utilisant des données de mortalité relevées par le réseau ICPforest pour valider les modèles.

(1). https ://fluxnet.fluxdata.org/

1.3 Complémentarité des approches permettant une meilleure compréhension des phénomènes de mortalités

Grâce à une double approche, l'une avec des modèles statistiques, l'autre avec un PBM à l'échelle d'un arbre moyen, à deux échelles (individuelle et populationnelle), nous avons évalué les facteurs de risque climatique pour le Hêtre. Comme suggéré par Hawkes 2000; O'Brien et al. 2017; Seidl et al. 2011, croiser les approches nous a permis de réduire l'incertitude des conclusions faites sur les résultats. Dans le (chapitre 2) avec le modèle statistique à l'échelle individuelle, nous avons montré que les individus plus précoces présentaient de plus forts taux de mortalité, que nous avons attribués aux nombres de jours de gelées tardives subit par ces individus grâce à CASTANEA. Le modèle statistique à l'échelle de la population a pu capter une corrélation entre les sécheresses et la mortalité, alors qu'avec CASTANEA, nous n'avions pas de relation significative entre la perte de conductance plus forte observée les années de forte sécheresse et de mortalité. Ainsi, les modèles statistiques nous ont permis d'orienter les hypothèses à tester avec le modèle mécaniste CASTANEA. Le fait d'avoir observé que dans cette population la compétition avait un faible rôle dans le risque de mortalité a conforté les simulations du modèle PBM, qui ne tient pas compte explicitement des interactions biotiques. En retour, le modèle CASTANEA nous a permis de comprendre les mécanismes d'action des facteurs identifiés par les approches statistiques sur les causes de mortalités observées. En effet, nous avons compris que le mécanisme de défoliation joue un rôle majeur dans le risque de mortalité et la réponse du hêtre à la sécheresse, ce qui nous a poussé à modéliser le mécanisme de défoliation dans CASTANEA. De ce fait, les modèles statistiques d'une part et ceux basés sur les processus d'autre part sont étroitement complémentaires et leur combinaison permet de déchiffrer les rôles respectifs des mécanismes contribuant à la mort des arbres et la compréhension de leur variabilité entre les individus ou les années (Hawkes, 2000; O'Brien et al., 2017; Seidl et al., 2011). Les deux approches peuvent être simplement comparées comme dans notre première partie au niveau individuel ou populationnel (Chapitre 2), ou bien elles peuvent être plus finement intégrées comme dans l'analyse de la corrélation entre le taux de mortalité observé et les variables simulées liées à la réponse au stress, ce qui permettrait de déduire les seuils physiologique déclenchant la mortalité (Davi & Cailleret, 2017).

1.4 Complémentarité entre les cSDM et PBM concernant la prédiction du risque de mortalité

Les prévisions issues des modèles cSDMs sont connues pour prédire de plus larges zones de risque de mortalité que celles basées sur les PBMs (Cheaib et al., 2012). En effet, les prédictions des modèles cSDMs reposent sur la corrélation des données de présences actuelles avec des variables climatiques actuelles (le plus souvent), puis sur

la projection de la présence future à partir des données climatiques futures. Ces approches prennent en compte implicitement les interactions biotiques (i.e. simulent la niche réalisée de Hutchinson), la gestion forestière (Van Meir et al., 2010), et prédisent généralement un déplacement de la niche réalisée future vers des latitudes/altitudes plus élevées. Cependant, elles ne prennent pas en compte les processus d'acclimatation physiologique liés à l'augmentation du CO_2. La capacité des espèces, particulièrement les arbres, à suivre ce déplacement peut être limitée par leur vitesse de migration (i.e. colonisation de nouveaux espaces via la dispersion de leur graines/pollen) (Schueler et al., 2014; Morin et al., 2008; Kremer et al., 2012). Cependant, même si ces modèles cSDMs ont l'avantage de prendre en compte la niche réalisée, ils ne prennent pas en compte la niche fondamentale, ni les composantes plastiques de réponse à l'environnement des espèces.
Une nouvelle approche, appelée ΔTraitSDM est plus optimiste dans ses prédictions de distributions future des populations. Ces modèles tentent de prendre en compte la variabilité intra-spécifique des réponses physiologiques aux stress, via des mesures de variabilité intra- et inter-population de la réponse au climat, évaluée dans des environnements communs (Benito Garzón et al., 2019). Cependant, ces modèles ne prennent pas en compte la plasticité physiologique à un changement de conditions environnementales inédit (i.e concentration de CO_2 dans l'atmosphère jamais observée).

Quant aux PBMs, qui prennent en compte les réponses écophysiologiques des arbres à l'environnement, ils peuvent être trop optimistes sur les capacités adaptatives des arbres par rapport aux prédictions futures des modèles statistiques. En effet, CASTANEA, ne prend pas en compte les interactions biotiques négatives (compétition intraspécifique, interspécifique, les ravageurs et maladie), ou positives (mycorhize, pollinisateurs, etc...). Les approches PBMs, en simulant les contraintes environnementales sans l'interaction, prédisent la niche fondamentale de l'espèce. De plus, CASTANEA, simule uniquement les individus dominants. Des modèles intermédiaires comme ORCHIDEE, qui prennent en compte certains processus et explicitement la compétition (Krinner et al., 2005), prédisent des risques de mortalité sur des surfaces intermédiaires entre les cSDMs et les autres PBMs (Cheaib et al., 2012). Pour augmenter les capacités prédictives de CASTANEA quant aux impacts du changement climatique sur les zones d'extinction, nous travaillons sur un projet ayant pour but de déterminer la distribution spatiale du Hêtre en Europe et d'expliquer les limites en prenant en compte la capacité de reproduction en plus des risques de mortalité (Projet en cours avec V. Journé). En plus d'inclure la variabilité plastique et génétique dans les modèles, il serait intéressant d'utiliser un modèle prenant en compte la physiologie (plasticité phénotypique), la variabilité génétique, la dynamique démographique (interactions biotiques) et l'évolution au fil du temps des traits à larges échelles pour expliquer en partie la distribution actuelle et future sous changement climatique, comme le préconise Berzaghi et al. 2019. Comme pour notre première étude, nous allons comparer les prédictions entre les modèles cSDMs, ΔtraitSDM et

PBM, car l'incertitude issue de leur prédiction du risque d'extinction/vulnérabilité, devrait simuler la gamme des possibilités futures de distributions/vulnérabilités.

Ces développements ont permis de répondre aux différentes questions scientifique de ma thèse et des livrables GenTree (à savoir quels sont les mécanismes causant la mortalité des arbres ? Quelle est l'influence de la sylviculture et de la variabilité génétique sur le risque de mortalité ? Le Hêtre a été utilisé comme espèce modèle grâce aux nombreuses connaissances éco-physiologique accumulées et données disponibles pour cette espèce.

2 Réponse du Hêtre aux stress induits par les sécheresses et les gelées tardives

La première partie de cette thèse a permis de mieux comprendre les mécanismes impliqués dans la mortalité du Hêtre en réponse à la sécheresse et aux gelées tardives, et leur variabilité entre individus. Cette étude s'est appuyée sur une population de Hêtre en situation marginale dans laquelle une mortalité importante est observée (2% par an, alors que les valeurs moyennes à l'échelle de l'espèces se situent entre 0% et 2.2% Hülsmann et al. 2016; Archambeau et al. 2020, IFN 2016) [(2)]. Nos résultats montrent que la mortalité est due à la combinaison des effets de la sécheresse et des gelées tardives : en effet, les variations interannuelles du taux de mortalité observé sont significativement associées aux variations de l'indice composite de risque (CRI), intégrant le nombre de jours de gelées tardives (NLF), le pourcentage de perte de conductance (PLC) et la biomasse de réserves carbonées (BoR) simulés par un modèle basé sur les processus (PBM), CASTANEA. En revanche, aucune de ces variables considérées séparément n'explique à elle seule les patrons de mortalité. Ceci est cohérent avec l'étude de Vanoni et al (2016) qui a aussi montré, avec des modèles statistiques prenant en compte un effet temporel, que la sécheresse et le gel contribuaient à la mortalité des hêtres. Ces résultats sont également cohérents avec le consensus selon lequel la mortalité aux marges chaudes et sèches n'est pas due seulement à l'épuisement des ressources en carbone, ou seulement à une embolie du xylème, mais résulte plutôt d'une interaction entre ces mécanismes (McDowell et al., 2011; Sevanto et al., 2014).

Nous avons montré également que la sensibilité aux stress dépend de "l'histoire de vie" individuelle. En effet, après l'exclusion des individus les plus petits (< 10 cm de diamètre), nous avons trouvé un effet non linéaire de la taille sur la probabilité de

(2). Ce chiffre se situe dans la fourchette supérieure des quelques estimations de mortalité disponibles pour le hêtre. Hülsmann et al., (2016) ont observé des taux annuels moyens de mortalité de 1,4%, 0,7% et 1,5% dans les forêts non gérées de Suisse, d'Allemagne et d'Ukraine, avec un taux maximal de mortalité de 2,2%. Archambeau et al (2019) ont estimé des taux de mortalité encore plus faibles (valeur annuelle moyenne = 3,8×10e-3%, fourchette = 3,7×10e-3% à 3,5×10%) à partir des données de l'inventaire forestier européen (y compris les forêts gérées et non gérées).

mortalité, avec un risque de mortalité plus fort pour les arbres les plus petits et les plus gros en comparaison des arbres de taille intermédiaire. Cette première partie nous a ainsi permis de valider trois indices (le pourcentage de perte de conductance, le niveau de réserve et le nombre de jours de gels) pour simuler avec CASTANEA le risque de mortalité en réponse aux stress induits par les sécheresses et les gelées tardives. Ces mêmes indices ont ensuite été mobilisés dans la seconde partie et ont permis d'explorer le risque de mortalité en réponse aux stress climatiques à l'échelle de l'aire de distribution du Hêtre. Nos résultats obtenus par simulation avec un modèle mécaniste sont conformes à ceux des modèles corrélatifs de niche bioclimatique (cSDM) et basé sur la variabilité des caractères (ΔtraitSDM), qui montrent que le risque de mortalité du Hêtre augmente à cause de la sécheresse dans ses marges sud de distribution (Gárate-Escamilla et al., 2019; Saltré et al., 2015), et à cause des gelées tardives dans les zones de plus hautes latitudes/altitudes (Kreyling et al., 2014; Vitasse et al., 2018). Notre étude met en évidence un rôle majeur de la défaillance hydraulique dans la mortalité, et un rôle moindre des dégâts de gelées ou de l'épuisement des réserves, ce qui est conforme aux connaissances écophysiologiques actuelles (Martínez-Vilalta et al., 2016). En effet la marge de sécurité vis-à-vis de la défaillance hydraulique est plus étroite chez les feuillus à feuilles caduques (Choat et al., 2018; Martin-StPaul et al., 2017).

La troisième et dernière partie de cette thèse a porté sur le rôle de la variabilité génétique de la sensibilité au climat dans la réponse aux stress climatiques. Grâce aux connaissances issues des expériences en jardins communs, nous avons pu modéliser la variabilité génétique existante intra- et inter-populations pour trois caractères adaptatifs liés à la réponse aux stress climatiques : (1) la date de débourrement, liée aux risques de gelées tardives, (2) l'efficience de l'utilisation de l'eau, liée au risque d'épuisement des réserves carbonées et au stress hydrique, et (3) le pourcentage de perte de conductance, lié au risque d'embolie du xylème. En incluant la variabilité génétique dans le modèle CASTANEA, nous avons simulé une aire actuelle de distribution du Hêtre plus grande que celle prédite par le même modèle sans variabilité génétique. Les génotypes ayant une date de débourrement plus précoce et donc une plus longue saison de végétation, ainsi que ceux ayant une meilleure efficience d'utilisation de l'eau permettent ainsi d'étendre la zone de viabilité dans les marges sud de distribution du Hêtre. Une plus longue saison de végétation permettrait au Hêtre d'accumuler plus de réserves par photosynthèse à la période de l'année au printemps où la sécheresse, n'est pas encore trop marquée (Bontemps et al., 2017). De plus, ces zones sont caractérisées par des climats où les gelées tardives sont rares : un débourrement précoce n'y entraîne donc pas un risque accrue de mortalité (Kreyling et al., 2014). Dans le reste de l'aire de distribution simulée du Hêtre, les génotypes minimisant le risque de mortalité sont toujours caractérisés par l'efficience d'utilisation d'eau la plus élevée et une date de débourrement la plus tardive, ce qui permet à ces individus d'être à la fois moins sensible à la sécheresse et d'éviter les gelées tardives. Ainsi, différents génotypes minimisent le risque de mortalité au travers de l'aire de distribution du Hêtre.

En outre, nos résultats suggèrent un compromis entre survie et croissance.

Dans nos simulations, la sylviculture diminue toujours le risque de mortalité en limitant les risques d'épuisement des réserves carbonées et d'embolie. En effet, la plupart des scénarios de gestion simulés (gestion en futaie régulière) diminuent la densité et donc la compétition pour les ressources, ce qui permet une plus grande accessibilité de l'eau et plus de photosynthèse pour les arbres subsistant après coupe. De plus, en augmentant la fréquence des coupes, le diamètre et la taille des arbres diminuent, ce qui diminue leurs besoins en ressources. Dans cette thèse, il est observé que le risque de mortalité globale est globalement réduit et que la croissance annuelle moyenne est plus élevée dans les peuplements sous gestion sylvicole. Cependant la sylviculture appliquée n'est pas la plus répandue pour le Hêtre, qui se gère principalement en taillis.

Tout au long de cette thèse, nous avons également simulé sous différents scénarios futurs les risques de mortalité du Hêtre dans le contexte du changement climatique. La prédiction la plus pessimiste suggère une légère augmentation du risque de mortalité sur l'aire de distribution globale, tandis que la plus optimiste prédit une diminution (importante) du risque de mortalité du Hêtre sur son aire totale. Cet optimisme face au futur est habituel avec les modèles basés sur les processus (Cheaib et al., 2012). La baisse du risque de mortalité globale simulée est due à l'augmentation du CO_2 qui permet une augmentation de la photosynthèse et une meilleure efficience d'utilisation de l'eau. Mais malgré la baisse globale du risque de mortalité, l'aire de distribution en marge sud diminue en raison de la forte augmentation du risque de sécheresse, ce qui a déjà été montré dans d'autres études de modélisation corrélative (Gárate-Escamilla et al., 2019; Cheaib et al., 2012). Ce risque de mortalité accru localement peut avoir des impacts sur la gestion sylvicole dans ces régions : il peut être envisagé de changer les pratiques sylvicoles ou de remplacer le Hêtre par une autre essence. Ce risque accru en marge sud a également des conséquences pour la conservation des ressources génétiques de l'espèce. En effet, pour sauvegarder cette diversité génétique menacée, des mesures de transfert assisté pourraient être nécessaires.

Le Hêtre nous as servi d'espèce modèle pour tester, valider et comprendre les causes de mortalité liées aux changements climatiques. La validation de CASTANEA sur d'autres espèces, nous a permis d'extrapoler les indices de mortalité développer pour identifier et évaluer les processus écophysiologiques sensibles à l'impact du changement climatique sur les sites de ressources génétiques forestières.

3 Risques sur les réseaux de conservation de la diversité génétique des arbres

Les unités de conservation génétique (GCU) et leur devenir ont fait l'objet de plusieurs études, afin de déterminer leur risque d'extinction sous changement climatique

(Schueler et al. 2014, Rapport Gentree). Schueler et al. 2014, avec des cSDM, ont signalé une forte augmentation du risque d'extinction des GCU, s'élevant à 33%-65% selon les espèces. Dans le rapport [D1.4] du projet Gentree, utilisant les ΔtraitSDMs prédisant la survie de 24 GCU et choisis selon un gradient nord-sud et altitudinal pour 5 espèces (*Fagus sylvatica, Picea abies, Pinus sylvestris, Quercus petraea, Abies Alba*), un risque d'extinction fort a été prédit pour 25% des CGU. Un ΔtraitSDM prédisant la croissance de 32 GCU sur ces même espèces est plus pessimiste, et prédit un risque d'extinction fort pour 41% des GCU. Avec CASTANEA, nous avons trouvé, pour le modèle et le scénario le plus pessimiste (HadGEM RCP8.5), une augmentation du risque de mortalité massive des GCU de 40%, 25%, 18% et 2%, respectivement pour *Picea abies, Pinus sylvestris, Fagus sylvatica* et *Pinus pinaster* et une diminution du risque de mortalité de 4 % pour *Quercus petraea*.

En revanche, une diminution du risque de mortalité a été prédite pour *Quercus petraea* et *Fagus sylvatica* (dans le scénario CM5) (annexe chapitre 2), contrairement à une autre étude (Dyderski et al., 2018). En effet, grâce au PBM, nous avons pu mettre en lumière que les feuillus compensent l'augmentation du stress hydrique par un meilleur stock de carbone accumulé, non seulement grâce à l'augmentation du CO_2 mais aussi grâce à l'augmentation de la durée de la saison de végétation. En revanche, les conifères sont moins sensibles à l'augmentation de CO_2 en raison d'une plus faible conductance stomatique, qui serait due à l'épaisseur des aiguilles (Klein & Ramon, 2019). Les conifères ont aussi un seuil de mortalité à la cavitation plus faible (50% de cavitation déclenche la mortalité, versus 88% pour les feuillus) [ref].

A l'échelle de l'aire de distribution, nous avons trouvé les mêmes tendances pour la variabilité des réponses entre espèces que Dyderski et al (2018), qui ont décrit certaines espèces comme des "gagnantes" (avec une extension nette de l'aire de répartition sous changement climatique) ou des "perdantes" (avec une contraction nette de l'aire de répartition). Contrairement à Dyderski et al (2017), nous avons commencé nos simulations avec les mêmes arbres de départ (c'est-à-dire avec les mêmes DBH, âge et statut de compétition partout en Europe). Ainsi, nos résultats suggèrent que les différences observées entre espèces sont plutôt dues à l'écophysiologie de l'espèce et non à la "place des espèces" dans la succession écologique. Nous avons constaté que le changement climatique diminuait le risque de mortalité des espèces de feuillus, *Quercus petraea* (toutes les prédictions futures) et *Fagus sylvatica* (CM5) et augmentait le risque de mortalité face au changement climatique des espèces de conifères. L'augmentation du risque de mortalité des espèces de conifères est principalement due à une augmentation accrue du risque de cavitation, ce qui est conforme à plusieurs études (Niinemets & Valladares, 2006; Fordham et al., 2014). Nogues-Bravo et al. (2014) ont montré que les espèces dont la distribution se situe à des latitudes plus élevées ont une moindre tolérance à la sécheresse. Ces différences de réponse physiologique entre les angiospermes et les conifères doivent être prise en compte dans les politiques de conserva-

tion des GCU.

Une piste à considérer est la prise en compte la variabilité génétique pour augmenter la résilience et permettre l'adaptabilité des CGU. Benito et al 2011 ont montré que la prise en compte de la variabilité de réponse physiologique entre populations permet d'augmenter la zone de viabilité de l'espèce. Dans notre cas, la prise en compte de la variabilité génétique, en plus de la variabilité plastique, de trois caractères impliqués dans la réponse au stress hydrique et au gel tardif ont permis une augmentation de la zone de viabilité potentielle de l'espèce (Figure 1 - chapitre 3). Ce résultat est encourageant pour des pratiques de transfert de matériel génétique. En effet, transférer du matériel génétique des zones d'extensions vers d'autres sites permettrait (1) de conserver leur patrimoine génétique et (2) de mettre des génotypes avec des adaptations aux stress que la population future subira. En effet, le changement climatique pousserait à une sélection des individus avec un génotype ayant une température cumulée avant débourrement plus forte, car cela compenserait les hivers plus doux (et donc un débourrement trop précoce) et éviterait les gelées tardives. Le changement climatique pousserait à une sélection des génotypes ayant une efficience de l'utilisation de l'eau plus forte, permettant d'accumuler plus de réserve pour un pas de temps donné. De plus, avec l'augmentation du CO_2, l'accumulation de carbone (réserve) en un pas de temps donné serait plus important.

Cependant nos prédictions demeurent très optimistes (voir chapitre IV partie 1.1) et devrait être mis en regard d'autres modèles. En effet, les observations des dernières décennies indiquent que la croissance des arbres dans les régions tempérées du Nord décline (Charru et al., 2010; Silva, 2010). Il y a également de nombreux signes de changements d'aires de répartition liés au changement climatique chez les arbres européens (Jump et al., 2006; Carnicer et al., 2011; Van Mantgem et al., 2009). Dans les montagnes du Montseny en Espagne, la forêt de hêtres s'est déplacée vers le haut de l'altitude d'environ 70 m au cours des 50 dernières années et est en train d'être remplacée par le chêne vert à des altitudes plus basses (Penuelas & Boada, 2003). Une autre étude montre l'impact négatif des hivers chauds sur la croissance du Hêtre en Espagne (Dorado-Liñán et al., 2017). La modélisation et l'incertitude créées par tous ces modèles peut permettre d'évaluer et de localiser les risques de perte de diversité génétique des arbres.

4 Conclusion

Cette thèse a permis de mettre en regard des techniques de modélisation différentes (statistique et basé sur les processus), pour tirer des conclusions et avoir une indication de l'incertitude quant aux impacts possibles du changement climatique, des modèles les plus pessimistes cSDM au modèles les plus optimistes PBM sur l'avenir des forêts européennes. Les prochaines étapes de ce travail consistent (1) en la vali-

dation et la mise en regard des seuils de mortalité à l'échelle européenne ; (2) en la prise en compte d'autres processus du cycle de vie des arbres (i.e. reproduction) ; (3) en la modélisation de la pérennité des populations d'arbres dans un futur plus lointain, en considérant leur capacité d'évolution.

Bibliographie

Adams, H. D., Zeppel, M. J., Anderegg, W. R., Hartmann, H., Landhäusser, S. M., Tissue, D. T., Huxman, T. E., Hudson, P. J., Franz, T. E., Allen, C. D., Anderegg, L. D., Barron-Gafford, G. A., Beerling, D. J., Breshears, D. D., Brodribb, T. J., Bugmann, H., Cobb, R. C., Collins, A. D., Dickman, L. T., Duan, H., Ewers, B. E., Galiano, L., Galvez, D. A., Garcia-Forner, N., Gaylord, M. L., Germino, M. J., Gessler, A., Hacke, U. G., Hakamada, R., Hector, A., Jenkins, M. W., Kane, J. M., Kolb, T. E., Law, D. J., Lewis, J. D., Limousin, J. M., Love, D. M., Macalady, A. K., Martínez-Vilalta, J., Mencuccini, M., Mitchell, P. J., Muss, J. D., O'Brien, M. J., O'Grady, A. P., Pangle, R. E., Pinkard, E. A., Piper, F. I., Plaut, J. A., Pockman, W. T., Quirk, J., Reinhardt, K., Ripullone, F., Ryan, M. G., Sala, A., Sevanto, S., Sperry, J. S., Vargas, R., Vennetier, M., Way, D. A., Xu, C., Yepez, E. A., and McDowell, N. G. (2017). A multi-species synthesis of physiological mechanisms in drought-induced tree mortality. *Nature Ecology and Evolution*, 1(9) :1285–1291.

Alberto, F. J., Aitken, S. N., Alía, R., González-Martínez, S. C., Hänninen, H., Kremer, A., Lefèvre, F., Lenormand, T., Yeaman, S., Whetten, R., and Savolainen, O. (2013). Potential for evolutionary responses to climate change - evidence from tree populations.

Allen, C. D., Macalady, A. K., Chenchouni, H., Bachelet, D., McDowell, N., Vennetier, M., Kitzberger, T., Rigling, A., Breshears, D. D., Hogg, E. H., Gonzalez, P., Fensham, R., Zhang, Z., Castro, J., Demidova, N., Lim, J. H., Allard, G., Running, S. W., Semerci, A., and Cobb, N. (2010). A global overview of drought and heat-induced tree mortality reveals emerging climate change risks for forests. *Forest Ecology and Management*, 259(4) :660–684.

Anderegg, W. R., Berry, J. A., Smith, D. D., Sperry, J. S., Anderegg, L. D., and Field, C. B. (2012). The roles of hydraulic and carbon stress in a widespread climate-induced forest die-off. *Proceedings of the National Academy of Sciences of the United States of America*, 109(1) :233–237.

Anderegg, W. R., Hicke, J. A., Fisher, R. A., Allen, C. D., Aukema, J., Bentz, B., Hood, S., Lichstein, J. W., Macalady, A. K., Mcdowell, N., Pan, Y., Raffa, K., Sala, A., Shaw, J. D., Stephenson, N. L., Tague, C., and Zeppel, M. (2015). Tree mor-

tality from drought, insects, and their interactions in a changing climate. *New Phytologist*, 208(3) :674–683.

Archambeau, J., Ruiz-Benito, P., Ratcliffe, S., Fréjaville, T., Changenet, A., Muñoz Castañeda, J. M., Lehtonen, A., Dahlgren, J., Zavala, M. A., and Benito Garzón, M. (2020). Similar patterns of background mortality across Europe are mostly driven by drought in European beech and a combination of drought and competition in Scots pine. *Agricultural and Forest Meteorology*, 280(265171).

Augspurger, C. K. (2009). Spring 2007 warmth and frost : Phenology, damage and refoliation in a temperate deciduous forest. *Functional Ecology*, 23(6) :1031–1039.

Benito Garzón, M., González Muñoz, N., Wigneron, J. P., Moisy, C., Fernández-Manjarrés, J., and Delzon, S. (2018). The legacy of water deficit on populations having experienced negative hydraulic safety margin. *Global Ecology and Biogeography*, 27(3) :346–356.

Benito Garzón, M., Robson, T. M., and Hampe, A. (2019). ΔTraitSDMs : species distribution models that account for local adaptation and phenotypic plasticity.

Berzaghi, F., Wright, I. J., Kramer, K., Oddou-Muratorio, S., Bohn, F. J., Reyer, C. P., Sabaté, S., Sanders, T. G., and Hartig, F. (2019). Towards a New Generation of Trait-Flexible Vegetation Models. *Trends in Ecology and Evolution*.

Bigler, C. and Bugmann, H. (2018). Climate-induced shifts in leaf unfolding and frost risk of European trees and shrubs. *Scientific Reports*, 8(1) :1–10.

Bontemps, A., Davi, H., Lefèvre, F., Rozenberg, P., and Oddou-Muratorio, S. (2017). How do functional traits syndromes covary with growth and reproductive performance in a water-stressed population of Fagus sylvatica ? *Oikos*, 126(10) :1472–1483.

Brando, P. M., Balch, J. K., Nepstad, D. C., Morton, D. C., Putz, F. E., Coe, M. T., Silvério, D., Macedo, M. N., Davidson, E. A., Nóbrega, C. C., Alencar, A., and Soares-Filho, B. S. (2014). Abrupt increases in Amazonian tree mortality due to drought-fire interactions. *Proceedings of the National Academy of Sciences of the United States of America*, 111(17) :6347–6352.

Bréda, N., Huc, R., Granier, A., and Dreyer, E. (2006). Temperate forest trees and stands under severe drought : a review of ecophysiological responses , adaptation processes and long-term consequences. *Annals of Forest Science*, 63(6) :625–644.

Carnicer, J., Coll, M., Ninyerola, M., Pons, X., Sánchez, G., and Peñuelas, J. (2011). Widespread crown condition decline, food web disruption, and amplified tree mortality with increased climate change-type drought. *Proceedings of the National Academy of Sciences of the United States of America*, 108(4) :1474–1478.

Carrière, S. D., Ruffault, J., Pimont, F., Doussan, C., Simioni, G., Chalikakis, K., Limousin, J. M., Scotti, I., Courdier, F., Cakpo, C. B., Davi, H., and Martin-StPaul, N. K. (2020). Impact of local soil and subsoil conditions on inter-individual variations in tree responses to drought : insights from Electrical Resistivity Tomography. *Science of the Total Environment*, 698.

Ceglar, A., Zampieri, M., Toreti, A., and Dentener, F. (2019). Observed Northward Migration of Agro-Climate Zones in Europe Will Further Accelerate Under Climate Change. *Earth's Future*, 7(9) :1088–1101.

Charrier, G., Ngao, J., Saudreau, M., and Ameglio, T. (2015). Effects of environmental factors and management practices on microclimate, winter physiology, and frost resistance in trees. *Frontiers in plant science*, 6 :259.

Charru, M. (2012). *La productivité forestière dans un environnement changeant : caractérisation multi-échelle de ses variations récentes à partir des données de l'Inventaire Forestier National (IFN) et interprétation environnementale.* PhD thesis.

Charru, M., Seynave, I., Morneau, F., and Bontemps, J. D. (2010). Recent changes in forest productivity : An analysis of national forest inventory data for common beech (Fagus sylvatica L.) in north-eastern France. *Forest Ecology and Management*, 260(5) :864–874.

Cheaib, A., Badeau, V., Boe, J., Chuine, I., Delire, C., Dufrêne, E., François, C., Gritti, E. S., Legay, M., Pagé, C., Thuiller, W., Viovy, N., and Leadley, P. (2012). Climate change impacts on tree ranges : Model intercomparison facilitates understanding and quantification of uncertainty. *Ecology Letters*, 15(6) :533–544.

Chevin, L.-M., Lande, R., and Mace, G. M. (2010). Adaptation, plasticity, and extinction in a changing environment : towards a predictive theory. *PLoS biology*, 8(4) :e1000357.

Choat, B., Brodribb, T. J., Brodersen, C. R., Duursma, R. A., López, R., and Medlyn, B. E. (2018). Triggers of tree mortality under drought. *Nature*, 558(7711) :531–539.

Cowan, I. R. and Farquhar, G. D. (1977). Stomatal function in relation to leaf metabolism and environment. *Symposia of the Society for Experimental Biology*, 31 :471–505.

Daily, G. C. et al. (1997). Introduction : what are ecosystem services.

Dantec, C. F., Ducasse, H., Capdevielle, X., Fabreguettes, O., Delzon, S., and Desprez-Loustau, M. L. (2015). Escape of spring frost and disease through phenological variations in oak populations along elevation gradients. *Journal of Ecology*, 103(4) :1044–1056.

Davi, H. and Cailleret, M. (2017). Assessing drought-driven mortality trees with physiological process-based models - appendix.

Dawson, T. P., Jackson, S. T., House, J. I., Prentice, I. C., and Mace, G. M. (2011). Beyond predictions : Biodiversity conservation in a changing climate.

Dorado-Liñán, I., Akhmetzyanov, L., and Menzel, A. (2017). Climate threats on growth of rear-edge European beech peripheral populations in Spain. *International Journal of Biometeorology*, 61(12) :2097–2110.

Dufour-Kowalski, S., Courbaud, B., Dreyfus, P., Meredieu, C., and de Coligny, F. (2012). Capsis : An open software framework and community for forest growth modelling. *Annals of Forest Science*, 69(2) :221–233.

Dufrêne, E., Davi, H., François, C., Le Maire, G., Le Dantec, V., and Granier, A. (2005). Modelling carbon and water cycles in a beech forest. Part I : Model description and uncertainty analysis on modelled NEE. *Ecological Modelling*, 185(2-4) :407–436.

Durand-Gillmann, M., Cailleret, M., Boivin, T., Nageleisen, L. M., and Davi, H. (2014). Individual vulnerability factors of Silver fir (Abies alba Mill.) to parasitism by two contrasting biotic agents : Mistletoe (Viscum album L. ssp. Abietis) and bark beetles (Coleoptera : Curculionidae : Scolytinae) during a decline process. *Annals of Forest Science*, 71(6) :659–673.

Dyderski, M. K., Paź, S., Frelich, L. E., and Jagodziński, A. M. (2018). How much does climate change threaten European forest tree species distributions ? *Global Change Biology*, 24(3) :1150–1163.

Feng, X., Ackerly, D. D., Dawson, T. E., Manzoni, S., Skelton, R. P., Vico, G., and Thompson, S. E. (2018). The ecohydrological context of drought and classification of plant responses.

Fordham, D. A., Brook, B. W., Moritz, C., and Nogués-Bravo, D. (2014). Better forecasts of range dynamics using genetic data. *Trends in ecology & evolution*, 29(8) :436–443.

Futuyma, D. J. (2010). Evolutionary constraint and ecological consequences.

Gárate-Escamilla, H., Hampe, A., Vizcaíno-Palomar, N., Robson, T. M., and Benito Garzón, M. (2019). Range-wide variation in local adaptation and phenotypic plasticity of fitness-related traits in Fagus sylvatica and their implications under climate change. *Global Ecology and Biogeography*, 28(9) :1336–1350.

Ghalambor, C. K., McKay, J. K., Carroll, S. P., and Reznick, D. N. (2007). Adaptive versus non-adaptive phenotypic plasticity and the potential for contemporary adaptation in new environments. *Functional ecology*, 21(3) :394–407.

Greenwood, S., Ruiz-Benito, P., Martínez-Vilalta, J., Lloret, F., Kitzberger, T., Allen, C. D., Fensham, R., Laughlin, D. C., Kattge, J., Bönisch, G., Kraft, N. J., and Jump, A. S. (2017). Tree mortality across biomes is promoted by drought intensity, lower wood density and higher specific leaf area. *Ecology Letters*, 20(4) :539–553.

Guillemot, J., Martin-Stpaul, N. K., Dufrêne, E., François, C., Soudani, K., Ourcival, J. M., and Delpierre, N. (2015). The dynamic of the annual carbon allocation to wood in European tree species is consistent with a combined source-sink limitation of growth : Implications for modelling. *Biogeosciences*, 12(9) :2773–2790.

Hajek, P., Kurjak, D., Von Wühlisch, G., Delzon, S., and Schuldt, B. (2016). Intraspecific variation in wood anatomical, hydraulic, and foliar traits in ten European beech provenances differing in growth yield. *Frontiers in Plant Science*, 7(JUNE2016) :791.

Hanewinkel, M., Cullmann, D. A., Schelhaas, M.-J., Nabuurs, G.-J., and Zimmermann, N. E. (2012). Climate change may cause severe loss in the economic value of European forest land. *Nature Climate Change*, 3(3) :203–207.

Hänninen, H. and Tanino, K. (2011). Tree seasonality in a warming climate.

Hänninen, R., Hurmekoski, E., Mutanen, A., and Viitanen, J. (2018). Complexity of assessing future forest bioenergy markets—review of bioenergy potential estimates in the european union. *Current Forestry Reports*, 4(1) :13–22.

Harfoot, M., Tittensor, D. P., Newbold, T., McInerny, G., Smith, M. J., and Scharlemann, J. P. W. (2014). Integrated assessment models for ecologists : the present and the future. *Global Ecology and Biogeography*, 23(2) :124–143.

Härkönen, S., Neumann, M., Mues, V., Berninger, F., Bronisz, K., Cardellini, G., Chirici, G., Hasenauer, H., Koehl, M., Lang, M., Merganicova, K., Mohren, F., Moiseyev, A., Moreno, A., Mura, M., Muys, B., Olschofsky, K., Del Perugia, B., Rørstad, P. K., Solberg, B., Thivolle-Cazat, A., Trotsiuk, V., and Mäkelä, A. (2019). A climate-sensitive forest model for assessing impacts of forest management in Europe. *Environmental Modelling and Software*, 115 :128–143.

Hauck, J., Völker, C., Wolf-Gladrow, D. A., Laufkötter, C., Vogt, M., Aumont, O., Bopp, L., Buitenhuis, E. T., Doney, S. C., Dunne, J., Gruber, N., Hashioka, T., John, J., Quéré, C. L., Lima, I. D., Nakano, H., Séférian, R., and Totterdell, I. (2015). On the Southern Ocean CO2 uptake and the role of the biological carbon pump in the 21st century. *Global Biogeochemical Cycles*, 29(9) :1451–1470.

Hawkes, C. (2000). Woody plant mortality algorithms : Description, problems and progress. *Ecological Modelling*, 126(2-3) :225–248.

Hengl, T., De Jesus, J. M., Heuvelink, G. B., Gonzalez, M. R., Kilibarda, M., Blagotić, A., Shangguan, W., Wright, M. N., Geng, X., Bauer-Marschallinger, B., Guevara, M. A., Vargas, R., MacMillan, R. A., Batjes, N. H., Leenaars, J. G., Ribeiro, E., Wheeler, I., Mantel, S., and Kempen, B. (2017). SoilGrids250m : Global gridded soil information based on machine learning. *PLoS ONE*, 12(2) :e0169748.

Hiederer, R. (2013). *Mapping Soil Typologies-Spatial Decision Support Applied to the European Soil Database*.

Hufkens, K., Basler, D., Milliman, T., Melaas, E. K., and Richardson, A. D. (2018). An integrated phenology modelling framework in r. *Methods in Ecology and Evolution*, 9(5) :1276–1285.

Hülsmann, L., Bugmann, H., and Brang, P. (2017). How to predict tree death from inventory data - lessons from a systematic assessment of European tree mortality models. *Canadian Journal of Forest Research*, 47(7) :890–900.

Hülsmann, L., Bugmann, H. K., Commarmot, B., Meyer, P., Zimmermann, S., and Brang, P. (2016). Does one model fit all? Patterns of beech mortality in natural forests of three European regions. *Ecological Applications*, 26(8) :2463–2477.

Journé, V., Barnagaud, J.-Y., Bernard, C., Crochet, P.-A., and Morin, X. (2019). Correlative climatic niche models predict real and virtual species distributions equally well. *Ecology*, page e02912.

Jump, A. S., Hunt, J. M., and Penuelas, J. (2006). Rapid climate change-related growth decline at the southern range edge of Fagus sylvatica. *Global Change Biology*, 12(11) :2163–2174.

Klein, T. and Ramon, U. (2019). Stomatal sensitivity to CO2 diverges between angiosperm and gymnosperm tree species. *Functional Ecology*, 33(8) :1411–1424.

Kramer, K., Ducousso, A., Gömöry, D., Hansen, J. K., Ionita, L., Liesebach, M., Lorenţ, A., Schüler, S., Sulkowska, M., de Vries, S., and von Wühlisch, G. (2017). Chilling and forcing requirements for foliage bud burst of European beech (Fagus sylvatica L.) differ between provenances and are phenotypically plastic. *Agricultural and Forest Meteorology*, 234-235 :172–181.

Kremer, A., Ronce, O., Robledo-Arnuncio, J. J., Guillaume, F., Bohrer, G., Nathan, R., Bridle, J. R., Gomulkiewicz, R., Klein, E. K., Ritland, K., Kuparinen, A., Gerber, S., and Schueler, S. (2012). Long-distance gene flow and adaptation of forest trees to rapid climate change. *Ecology Letters*, 15(4) :378–392.

Kreyling, J., Buhk, C., Backhaus, S., Hallinger, M., Huber, G., Huber, L., Jentsch, A., Konnert, M., Thiel, D., Wilmking, M., and Beierkuhnlein, C. (2014). Local adaptations to frost in marginal and central populations of the dominant forest

tree Fagus sylvatica L. as affected by temperature and extreme drought in common garden experiments. *Ecology and Evolution*, 4(5) :594–605.

Krinner, G., Viovy, N., de Noblet-Ducoudré, N., Ogée, J., Polcher, J., Friedlingstein, P., Ciais, P., Sitch, S., and Prentice, I. C. (2005). A dynamic global vegetation model for studies of the coupled atmosphere-biosphere system. *Global Biogeochemical Cycles*, 19(1).

Kuparinen, A., Savolainen, O., and Schurr, F. M. (2010). Increased mortality can promote evolutionary adaptation of forest trees to climate change. *Forest Ecology and Management*, 259(5) :1003–1008.

Lefèvre, F., Boivin, T., Bontemps, A., Courbet, F., Davi, H., Durand-Gillmann, M., Fady, B., Gauzere, J., Gidoin, C., Karam, M. J., Lalagüe, H., Oddou-Muratorio, S., and Pichot, C. (2014). Considering evolutionary processes in adaptive forestry.

Lenz, A., Hoch, G., Vitasse, Y., and Körner, C. (2013). European deciduous trees exhibit similar safety margins against damage by spring freeze events along elevational gradients. *New Phytologist*, 200(4) :1166–1175.

Lorenz, M. and Becher, G. (2012). Forest condition in Europe. Technical Report January, Technical Report of ICP Forests. Work report of Thunen Institute for Word˜.

Maraun, M., Salamon, J. A., Schneider, K., Schaefer, M., and Scheu, S. (2003). Oribatid mite and collembolan diversity, density and community structure in a moder beech forest (Fagus sylvatica) : Effects of mechanical perturbations. *Soil Biology and Biochemistry*, 35(10) :1387–1394.

Martin-StPaul, N., Delzon, S., and Cochard, H. (2017). Plant resistance to drought depends on timely stomatal closure.

Martínez-Vilalta, J., Sala, A., Asensio, D., Galiano, L., Hoch, G., Palacio, S., Piper, F. I., and Lloret, F. (2016). Dynamics of non-structural carbohydrates in terrestrial plants : a global synthesis. *Ecological Monographs*, 86(4) :495–516.

McDowell, N. G., Beerling, D. J., Breshears, D. D., Fisher, R. A., Raffa, K. F., and Stitt, M. (2011). The interdependence of mechanisms underlying climate-driven vegetation mortality. *Trends in Ecology & Evolution*, 26(10) :523–532.

Mcdowell, N. G., Fisher, R. A., Xu, C., Domec, J. C., Hölttä, T., Mackay, D. S., Sperry, J. S., Boutz, A., Dickman, L., Gehres, N., Limousin, J. M., Macalady, A., Martínez-Vilalta, J., Mencuccini, M., Plaut, J. A., Ogée, J., Pangle, R. E., Rasse, D. P., Ryan, M. G., Sevanto, S., Waring, R. H., Williams, A. P., Yepez, E. A., and Pockman, W. T. (2013). Evaluating theories of drought-induced vegetation mortality using a multimodel-experiment framework.

McDowell, N. G. and Sevanto, S. (2010). The mechanisms of carbon starvation : How, when, or does it even occur at all ? *New Phytologist*, 186(2) :264–266.

Meir, P., Mencuccini, M., and Dewar, R. C. (2015). Drought-related tree mortality : addressing the gaps in understanding and prediction. *New Phytologist*, 207(1) :1443–1447.

Menzel, A., Helm, R., and Zang, C. (2015). Patterns of late spring frost leaf damage and recovery in a European beech (Fagus sylvatica L.) stand in south-eastern Germany based on repeated digital photographs. *Frontiers in Plant Science*, 6 :110.

Monserud, R. A. (1976). Simulation of forest tree mortality. *Forest Science*, 22(4) :438–444.

Morin, X., Viner, D., and Chuine, I. (2008). Tree species range shifts at a continental scale : New predictive insights from a process-based model. *Journal of Ecology*, 96(4) :784–794.

Mouquet, N., Lagadeuc, Y., Devictor, V., Doyen, L., Duputié, A., Eveillard, D., Faure, D., Garnier, E., Gimenez, O., Huneman, P., Jabot, F., Jarne, P., Joly, D., Julliard, R., Kéfi, S., Kergoat, G. J., Lavorel, S., Le Gall, L., Meslin, L., Morand, S., Morin, X., Morlon, H., Pinay, G., Pradel, R., Schurr, F. M., Thuiller, W., and Loreau, M. (2015). Predictive ecology in a changing world. *Journal of Applied Ecology*, 52(5) :1293–1310.

Mueller, R. C., Scudder, C. M., Porter, M. E., Talbot Trotter, R., Gehring, C. A., and Whitham, T. G. (2005). Differential tree mortality in response to severe drought : Evidence for long-term vegetation shifts. *Journal of Ecology*, 93(6) :1085–1093.

Nicotra, A. B., Atkin, O. K., Bonser, S. P., Davidson, A. M., Finnegan, E. J., Mathesius, U., Poot, P., Purugganan, M. D., Richards, C. L., Valladares, F., et al. (2010). Plant phenotypic plasticity in a changing climate. *Trends in plant science*, 15(12) :684–692.

Niinemets, Ü. and Valladares, F. (2006). Tolerance to shade, drought, and waterlogging of temperate northern hemisphere trees and shrubs. *Ecological monographs*, 76(4) :521–547.

Nourtier, M., Chanzy, A., Cailleret, M., Yingge, X., Huc, R., and Davi, H. (2014). Transpiration of silver Fir (Abies alba mill.) during and after drought in relation to soil properties in a Mediterranean mountain area. *Annals of Forest Science*, 71(6) :683–695.

O'Brien, M. J., Engelbrecht, B. M., Joswig, J., Pereyra, G., Schuldt, B., Jansen, S., Kattge, J., Landhäusser, S. M., Levick, S. R., Preisler, Y., Väänänen, P., and Macinnis-Ng, C. (2017). A synthesis of tree functional traits related to drought-induced mortality in forests across climatic zones.

O'Brien, M. J., Leuzinger, S., Philipson, C. D., Tay, J., and Hector, A. (2014). Drought survival of tropical tree seedlings enhanced by non-structural carbohydrate levels. *Nature Climate Change*, 4(8) :710–714.

Penuelas, J. and Boada, M. (2003). A global change-induced biome shift in the Montseny mountains (NE Spain). *Global Change Biology*, 9(2) :131–140.

Pividori, M., Giannetti, F., Barbati, A., and Chirici, G. (2016). European forest types : tree species matrix. *European Atlas of Forest Tree Species. Publ. Off. EU, Luxembourg, pp. e01f162+. https ://w3id. org/mtv/FISE-Comm/v01/e01f162*.

Rehfeldt, G. E., Tchebakova, N. M., Parfenova, Y. I., Wykoff, W. R., Kuzmina, N. A., and Milyutin, L. I. (2002). Intraspecific responses to climate in Pinus sylvestris. *Global Change Biology*, 8(9) :912–929.

Reineke, L. H. (1933). Perfecting a stand-density index for even-aged forests. *J. Agric. Res.*, 46(7) :627–638.

Saltré, F., Duputié, A., Gaucherel, C., and Chuine, I. (2015). How climate, migration ability and habitat fragmentation affect the projected future distribution of European beech. *Global Change Biology*, 21(2) :897–910.

Sánchez-Salguero, R., Camarero, J. J., Gutiérrez, E., González Rouco, F., Gazol, A., Sangüesa-Barreda, G., Andreu-Hayles, L., Linares, J. C., and Seftigen, K. (2017). Assessing forest vulnerability to climate warming using a process-based model of tree growth : bad prospects for rear-edges. *Global Change Biology*, 23(7) :2705–2719.

Savolainen, O., Pyhäjärvi, T., and Knürr, T. (2007). Gene Flow and Local Adaptation in Trees. *Annual Review of Ecology, Evolution, and Systematics*, 38(1) :595–619.

Schueler, S., Falk, W., Koskela, J., Lefèvre, F., Bozzano, M., Hubert, J., Kraigher, H., Longauer, R., and Olrik, D. C. (2014). Vulnerability of dynamic genetic conservation units of forest trees in Europe to climate change. *Global Change Biology*, 20(5) :1498–1511.

Seidl, R., Aggestam, F., Rammer, W., Blennow, K., and Wolfslehner, B. (2016). The sensitivity of current and future forest managers to climate-induced changes in ecological processes. *Ambio*, 45(4) :430–441.

Seidl, R., Fernandes, P. M., Fonseca, T. F., Gillet, F., Jönsson, A. M., Merganičová, K., Netherer, S., Arpaci, A., Bontemps, J. D., Bugmann, H., González-Olabarria, J. R., Lasch, P., Meredieu, C., Moreira, F., Schelhaas, M. J., and Mohren, F. (2011). Modelling natural disturbances in forest ecosystems : A review.

Sevanto, S., Mcdowell, N. G., Dickman, L. T., Pangle, R., and Pockman, W. T. (2014). How do trees die ? A test of the hydraulic failure and carbon starvation hypotheses. *Plant, Cell and Environment*, 37(1) :153–161.

Silva, D. E. (2010). *Ecologie du hêtre (Fagus sylvatica L) en marge sud-ouest de son aire de distribution.* PhD thesis.

Sperry, J. S., Venturas, M. D., Todd, H. N., Trugman, A. T., Anderegg, W. R., Wang, Y., and Tai, X. (2019). The impact of rising CO2 and acclimation on the response of US forests to global warming. *Proceedings of the National Academy of Sciences*, in press :201913072.

Taccoen, A., Piedallu, C., Seynave, I., Perez, V., Gégout-Petit, A., Nageleisen, L. M., Bontemps, J. D., and Gégout, J. C. (2019). Background mortality drivers of European tree species : Climate change matters. *Proceedings of the Royal Society B : Biological Sciences*, 286(1900).

Tóth, B., Weynants, M., Pásztor, L., and Hengl, T. (2017). 3D soil hydraulic database of Europe at 250 m resolution. *Hydrological Processes*, 31(14) :2662–2666.

Tyree, M. T. and Sperry, J. S. (1989). Vulnerability of Xylem to Cavitation and Embolism. *Annual Review of Plant Physiology and Plant Molecular Biology*, 40(1) :19–36.

Van Mantgem, P. J., Stephenson, N. L., Byrne, J. C., Daniels, L. D., Franklin, J. F., Fulé, P. Z., Harmon, M. E., Larson, A. J., Smith, J. M., Taylor, A. H., and Veblen, T. T. (2009). Widespread increase of tree mortality rates in the Western United States. *Science*, 323(5913) :521–524.

Van Meir, E. G., Hadjipanayis, C. G., Norden, A. D., Shu, H.-K., Wen, P. Y., and Olson, J. J. (2010). Exciting new advances in neuro-oncology : the avenue to a cure for malignant glioma. *CA : a cancer journal for clinicians*, 60(3) :166–193.

Vanoni, M., Bugmann, H., Nötzli, M., and Bigler, C. (2016). Drought and frost contribute to abrupt growth decreases before tree mortality in nine temperate tree species. *Forest Ecology and Management*, 382 :51–63.

Vitasse, Y., Delzon, S., Dufrêne, E., Pontailler, J. Y., Louvet, J. M., Kremer, A., and Michalet, R. (2009). Leaf phenology sensitivity to temperature in European trees : Do within-species populations exhibit similar responses ? *Agricultural and Forest Meteorology*, 149(5) :735–744.

Vitasse, Y., Schneider, L., Rixen, C., Christen, D., and Rebetez, M. (2018). Increase in the risk of exposure of forest and fruit trees to spring frosts at higher elevations in Switzerland over the last four decades. *Agricultural and Forest Meteorology*, 248(May 2017) :60–69.

Williams, S. E., Shoo, L. P., Isaac, J. L., Hoffmann, A. A., and Langham, G. (2008). Towards an integrated framework for assessing the vulnerability of species to climate change. *PLoS biology*, 6(12) :e325.

Yu, H., Luedeling, E., and Xu, J. (2010). Winter and spring warming result in delayed spring phenology on the Tibetan Plateau. *Proceedings of the National Academy of Sciences of the United States of America*, 107(51) :22151–22156.

Annexes

1 Présentation générale du modèle écophysiologique CASTANEA

CASTANEA est un modèle basé sur les procesussus écophysiologique utilisée pour simuler les flux de carbone et d'eau dans les écosystèmes forestiers (Dufrêne et al. 2005). Ce modèle n'a pas de représentation spatialement explicite des arbres individuels, et représente un arbre moyen par six compartiments fonctionnels : canopée, branches, tige, racines grossières, racines fines et réserves (un compartiment non localisé correspondant aux glucides non structurels, NSC). La canopée est divisée en cinq couches de feuilles. Les simulations du fonctionnement et de la croissance des peuplements forestiers sont représentées à l'échelle de l'arbre moyen. Les données d'entrée du modèle sont des variables météorologiques à l'échelle journalière et les caractéristiques du sol. L'ensemble de ces processus sont représentés dans la Figure 1. Ce modèle comporte un grand nombre de paramètres physiques et physiologiques décrivant (i) les caractéristiques de l'espèce, (ii) les caractéristiques du site étudié, (iii) les constantes des équations décrivant les processus (Dufrêne et al., 2005). Le modèle simule différentes variables de sortie : la photosynthèse de la canopée, les coûts de respiration liés à l'entretien et à la croissance de l'arbre, la transpiration et l'évaporation, les stocks carbones, des indices de stress, en plus du bilan hydrique du sol. Actuellement, le carbone est alloué d'abord aux fonctions de croissance des feuilles et de respiration, puis le carbone restant est alloué aux compartiments de biomasse aérienne, de racines et réserves. Il existe actuellement deux versions de ce modèle. Une version est développée au laboratoire de ESE (version FORTRAN) et une autre version est développée à l'INRA URFM (version CAPSIS, <`http://capsis.cirad.fr/capsis/help_en/castaneaonly`>). Contrairement à la version FORTRAN, la version présente sur la plateforme de modélisation CAPSIS (Dufour-Kowalski et al., 2012), correspond à une librairie qui peut être connectée avec d'autres modèles présents également sur cette même plate-forme. Le manuel est en cours de réalisation en collabaration avec Hendrik Davi et Valentin Journée `https://www.overleaf.com/read/nmyvszjkfxxh`, 3

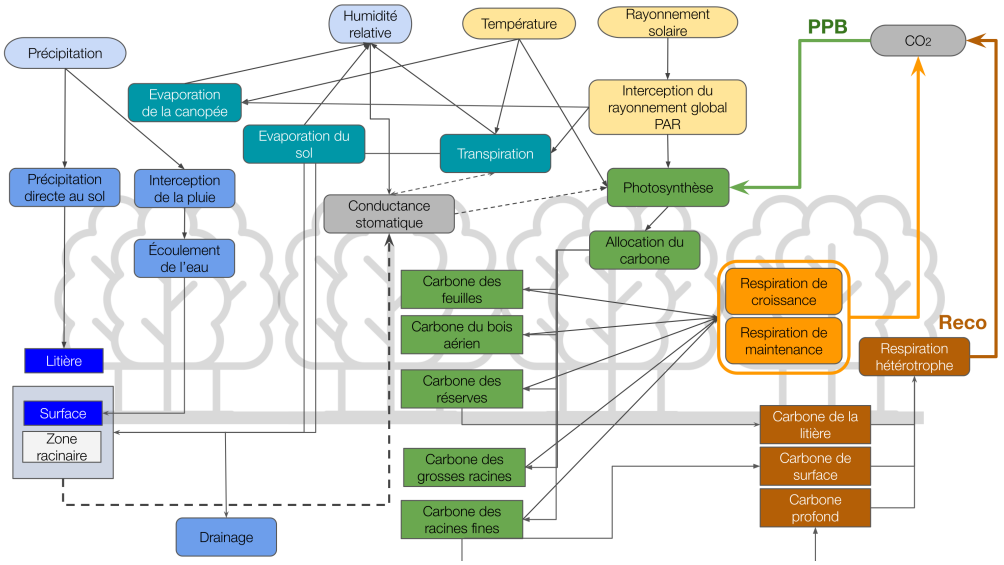

Figure 1: Schéma général du modèle CASTANEA (version CAPSIS). Les ellipses représentent les variables d'entrées. Les rectangles représentent les stocks et les rectangles arrondis représentent les processus simulés. Adapté par V.Journé

2 Impact de la défoliation des arbres sur la croissance et la reproduction

Dans cette étude, les auteurs se sont intéressés à l'effet de la défoliation foliaire sur la croissance et la reproduction pour une population marginale Sud du Hêtre commun. La fécondité mâle et femelle ont été estimées pour chaque individus grâce à des analyses de parentés. La fécondité femelle diminue et la croissance des arbres diminue avec le niveau de défoliation et la compétition. La fécondité mâle diminue lorsque la compétition augmente. De plus il a été observé que pour des arbres défoliés, certains individus ont une fécondité femelle plus élevé au détriment de leurs croissance, et d'autres individus avec une croissance plus élevée et une fécondité femelle plus faible. Dans cette étude, j'ai préparé et analysé les données brutes (carottes d'arbres). J'ai aussi contribué plus particulièrement à la discussion sur les en jeux de défoliation et mortalité.

Peer Community In Ecology

RESEARCH ARTICLE

Open Access
Open Data
Open Code
Open Peer-Review

Cite as: Oddou-Muratorio., S., Petit-Cailleux, C., Journe, V., Lingrand, M., Magdalou, J.-A., Hurson, C., Garrigue, J., Davi, H. and Magnanou, E. Crown defoliation decreases reproduction and wood growth in a marginal European beech population. bioRxiv 474874, ver. 4 peer-reviewed and recommended by PCI Ecology (2019).

Posted: 4th November 2019

Recommender:
Georges Kunstler

Reviewers:
Three anonymous reviewers

Correspondence:
sylvie.muratorio@inra.fr

Crown defoliation decreases reproduction and wood growth in a marginal European beech population

Sylvie Oddou-Muratorio[1*], Cathleen Petit-Cailleux[1], Valentin Journé[1], Matthieu Lingrand[1], Jean-André Magdalou[2], Christophe Hurson[3], Joseph Garrigue[2], Hendrik Davi[1], Elodie Magnanou[2,4]

[1] URFM, INRA, 84000 Avignon, France
[2] Réserve Naturelle Nationale de la forêt de la Massane - France
[3] Fédération des Réserves Naturelles Catalanes - France
[4] Sorbonne Université, CNRS, Biologie Intégrative des Organismes Marins (BIOM), Observatoire Océanologique, F-66650, Banyuls/Mer, France

This article has been peer-reviewed and recommended by *Peer Community in Ecology*

Keywords: Mediterranean forest, dieback, drought, female fecundity, male fecundity, radial growth, *Fagus sylvatica*, Mixed Effect Mating Model, parentage analyses, microsatellite, margin of species distribution

ABSTRACT

1. Abiotic and biotic stresses related to climate change have been associated to increased crown defoliation, decreased growth and a higher risk of mortality in many forest tree species, but the impact of stresses on tree reproduction and forest regeneration remains understudied. At dry, warm margin of species distributions, flowering, pollination and seed maturation processes are expected to be affected by drought, late frost and other stresses, eventually resulting in reproduction failure. Moreover, inter-individual variations in reproductive performances versus other performances (growth, survival) could have important consequences on population's dynamics.

2. We investigated the relationships between individual crown defoliation, growth and reproduction in a drought-prone population of European beech, *Fagus sylvatica*. We used a spatially explicit mating model and marker-based parentage analyses to estimate effective female and male fecundities of 432 reproductive trees, which were also monitored for basal area increment and crown defoliation over nine years.

3. Female and male fecundities markedly varied among individuals, more than did growth. Both female fecundity and growth decreased with increasing crown defoliation and competition and increased with size. Male fecundity only responded to competition, and decreased with increasing competition. Moreover, the negative effect of defoliation on female fecundity was size-dependent, with a slower decline in female fecundity with increasing defoliation for the large individuals. Finally, a trade-off between growth and female fecundity was observed in response to defoliation: some large trees maintained significant female fecundity at the expense of reduced growth in response to defoliation, while some other defoliated trees rather maintained high growth at the expense of reduced female fecundity.

4. *Synthesis*. Our results suggest that while decreasing their growth, some large defoliated trees still contribute to reproduction through seed production and pollination. This non-coordinated decline of growth and fecundity at individual-level in response to stress may compromise the evolution of stress-resistance traits at population level, and increase forest tree vulnerability.

Introduction

The increasing impact of stresses associated with climate and global change are likely to cause widespread forest decline, eventually leading to massive tree mortality due to inability to recover from stresses (Allen et al., 2010; McDowell et al., 2011). Depending on their frequency, duration, or intensity, abiotic stresses (e.g. drought, wind throw, flood, heavy snow, late frosts, fire) and biotic stresses (predation, competition) have the potential to alter tree structure (e.g. branch breakage, leaf fall), physiological processes (e.g. hydraulic failure, reduced photosynthesis) and overall vigour (e.g., crown defoliation) and performances (e.g. reduced growth, reproduction and survival). Moreover, as stresses often co-occur and interact, it is notoriously difficult to disentangle the drivers of tree decline observed in a given environment. Hence, the diversity of both stresses and decline components needs to be accounted for in order to better predict forest decline in response to environmental change.

The warm and dry margins of tree species distributions are expected and already observed to suffer massive forest decline, driven by increasing temperatures, drought, late frost and other stresses. Most importantly, prolonged droughts and high temperatures have been extensively associated to decreasing tree growth and forest productivity (Zhao & Running, 2010; Zimmermann, Hauck, Dulamsuren, & Leuschner, 2015), increasing crown defoliation and leaf fall (Dobbertin, 2005; Galiano, Martínez-Vilalta, & Lloret, 2011) and higher risks of tree mortality (Adams et al., 2017; Allen et al., 2010; Anderegg, Kane, & Anderegg, 2013). There is also an increasing concern that the advance in spring phenology currently observed in many species expose them to a higher risk of late frost, with damaging effects on crown development (Bigler & Bugmann, 2018; Charrier, Ngao,

Saudreau, & Améglio, 2015). Overall, the response of tree sexual reproduction and forest regeneration to abiotic and biotic stresses remain largely under-documented, despite the critical importance of reproduction for the maintenance, demography and adaptation of populations at the rear-edge of species distribution (Hampe & Petit, 2005). Here, we consider sexual reproduction globally, including all the stages from floral initiation to the production of mature seeds.

Based on species physiology, abiotic stresses such as droughts or late frosts are expected to directly reduce plant sexual reproduction through altered reproductive phenology (i.e. the timing of flowering and fruiting), a higher risk of pollen abortion or pollination failure, a shorter seed maturation cycle and/or a higher risk of seed abortion (Bykova, Chuine, Morin, & Higgins, 2012; Hedhly, Hormaza, & Herrero, 2009; Zinn, Tunc-Ozdemir, & Harper, 2010). Moreover, indirect negative effects are also expected: for instance, by decreasing photosynthetic activity, leaf fall may reduce the amount of stored resources to invest in reproduction of the next year (Obeso, 1988). The few results available so far from experiments manipulating stresses *in situ* overall support these expectation of negative impacts of stresses on reproduction and growth. By manipulating temperature during pollen dispersal and germination, Flores-Rentería *et al.* (2018) demonstrated negative impacts of high temperatures on male reproduction, particularly on pollen viability of *Pinus edulis*. Bykova *et al.* (2018) also showed that water deficit increases pollen abortion and thus decreases pollen production in *Quercus ilex*. In *Quercus ilex*, Pérez-Ramos *et al.* (2010) showed that reduced water availability increased the rate of acorn abortion, while Sanchez-Humanes & Espelta (2011) showed that increased drought reduces acorn production in coppice. In parallel, these drought-manipulation experiments demonstrated that growth generally decreases (e.g. Delaporte, Bazot, & Damesin, 2016; Lempereur et al., 2015) and crown defoliation increases (e.g. Galiano et al., 2011) in response to increasing water stress.

On the other hand, stresses have been hypothesised to shift patterns of resource allocation and act like a cue stimulating higher reproductive effort and reduced growth (Bréda, Huc, Granier, & Dreyer, 2006; Lee, 1988; Pulido et al., 2014; Wiley, Casper, & Helliker, 2017). However, results from experiments manipulating stresses *in situ* hardy support this expectation, even though they highlight flexible allocation rules to reproduction and growth in response to stress. Using experimental warming, Sherry *et al.* (2007) demonstrated divergent responses of reproductive phenology to water stress for grass species: some species advanced their flowering and fruiting phenology before the peak of summer heat while other species started flowering after the peak temperature and delayed their reproduction. In *Quercus ilex*, Pulido et al. (2014) did not find evidence that drought enhances resource allocation to reproduction but suggested that the negative individual correlation between growth and female reproduction observed in controlled conditions disappears under limited resources (including water stress). The clearest experimental evidence of the positive impact of biotic and abiotic stresses on reproduction can be found in the literature on (fruit) tree orchards. Among the cultural practices allowing early and abundant flowering, water stress is used to enhance flower initiation in conifers, while hot, dry summers are reported to induce abundant seed crops in both conifers and broadleaved species (Meilan, 1997). Another practice relies on circumferential girdles (the removal of a swath of the bark, down to the phloem, around the entire stem), which are associated to reduced vegetative growth and increased fruiting (Bonnet-Masimbert & Webber, 2012). Finally, pruning (the reduction of crown leaf area) is also recommended to favour reproductive development while reducing vegetative growth in fruit trees (Karimi et al., 2017).

Taken together, these results suggest that stress impacts on reproduction and the relationship between reproduction and growth in response to stress both need further investigations (Figure 1). Environment-manipulation experiments typically use a limited number of individuals in controlled conditions to characterize the fine impacts of stresses on the physiological mechanisms driving plant performances (eventually testing for

individual effects, e.g. Camarero, Gazol, Sangüesa-Barreda, Oliva, & Vicente-Serrano, 2015). Besides these ecophysiological approaches, we also need population ecology approaches to investigate the among-individual variations in reproductive and vegetative performances in response to stress, and their consequences on population dynamics. Here, we propose to use crown defoliation taken as an indicator of stress, and to analyse the relationship between crown defoliation, reproduction and growth in order to test two hypotheses. First (H1), crown defoliation is associated to a proportional decrease in growth and reproduction through the impact of stresses on the resources allocated to these performances, so that the relationship between reproduction and growth does not change with increasing crown defoliation. Alternatively (H2), if defoliation or stresses act like a cue stimulating reproductive performances at the expense of reduced growth, then the relationship between reproduction and growth should change with increasing crown defoliation.

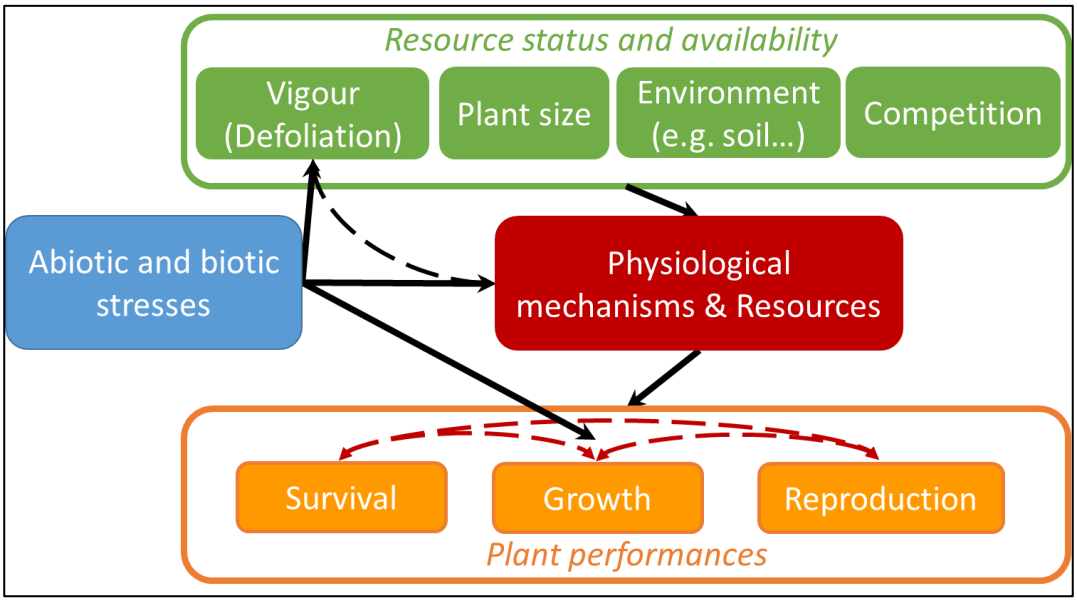

Figure 1: Conceptual framework for the impacts of abiotic and biotic stresses on individual plant performances (survival, growth, and reproduction). Stresses are expected to affect performances through their effect on the physiological mechanisms and the level of resources of the plant. Usually not easily measurable in natural populations, this level of resources also varies among individuals as a function of (i) plant resource status, a combination of plant size and vigour, and (ii) resource availability, which depend on the quality of the local environment and on competition. Vigour (eg crown defoliation) can in turn rapidly change in response to stress or to the level of resources (i.e. potential feedback loops, dashed arrows), and therefore it is itself an indicator of stress. Finally, stresses can act like cues changing resources allocation to survival, growth and reproduction, thereby affecting their correlations at individual level (eg., tradeoffs, dashed red arrows).

We focus here on the European beech (*Fagus sylvatica* L.), a major broadleaf tree species considered to be vulnerable to summer drought. Beech is a monoecious, wind-dispersed species, and shows an intermittent production of large seed crops synchronized across a population (i.e., masting), triggered both by weather and plant resource status (Vacchiano et al., 2017). Hacket-Pain, Lageard, & Thomas (2017) showed that drought years were associated to both reduced reproduction and growth, while during non-drought years, both masting and high growth could be observed. By contrast, Bréda *et al.* (2006) reported increased seed production associated to leaf fall in high drought years, even though this relationship between crown defoliation and fruit production may not be directly causal. This study investigates the relationships between tree defoliation, growth

and fecundity in 432 individuals within a single, rear-edge natural population of *F. sylvatica* in Southern France, where crown defoliation and mortality are being surveyed since 2003 (Petit-Cailleux et al., submitted). We used molecular markers and parentage analyses to estimate effective, relative female and male fecundities, which integrate the success of pollination and germination processes cumulated from 2002 to 2012. Growth over the same period was assessed through inventory data, completed by ring-width measurements. We analysed the relationships between crown defoliation, growth and fecundity at the among-individual scale in order to (i) characterize the decline in fecundity and growth associated with defoliation and (ii) investigate the correlation between growth and fecundity in response to defoliation.

Our study is based on the well-accepted hypothesis that recurrent defoliation is related to physiological stresses and symptomatic of a declining health in beech (Bréda et al., 2006; Peñuelas & Boada, 2003). Using statistical models and 4327 trees individually surveyed, a companion study in the same population showed that crown defoliation increases the risk of mortality (Petit-Cailleux et al., submitted). Moreover, simulations with a process-based physiological model indicated that the mortality rate in this population is driven by a combination of drought-related processes (conductance loss, carbon reserve depletion) and late frost damages (Petit-Cailleux et al., submitted). Crown defoliation thus appears as an appropriate indicator of a higher intrinsic sensitivity to these stresses, and/or a higher impact of these stresses due to a lower availability of resources in a heterogeneous environment.

Material and methods

Study site

Located in southern France and bordering Spanish Cataluña, the Massane forest is situated on the foothills of Eastern Pyrenees (Figure 2B). This coastal range, called Albera massif, covers about 19,000 ha on the French territory. The Massane forest National Nature Reserve (42° 28' 41" N, 3° 1' 26" E) was created in 1973. It covers 336 ha on the highest part of the Massane valley, from 600 to 1,127 m a.s.l., and is only around 5 km far from the Mediterranean Sea. The site is under a meso Mediterranean climate influence (Quézel & Médail, 2003: mean annual temperature = 11.95°C; annual precipitations = 1164.9 mm, monitored on site since respectively 1976 and 1960; Figure S1A). This site is one of the French beech location the most prone to water stress (Figure S1B).

More than half of the Reserve is constituted of an old grown forest, where no logging operation has been performed since at least 1886. The canopy is dominated by European beech in mixture with downy oak (*Quercus pubescens* Willd.), maples (*Acer opalus* Mill., *Acer campestris* L., *Acer monspessulanum* L.) and holly (*Ilex aquifolium* L.). A 10 ha fenced plot was remote from any cow grazing since 1956. All trees from this protected plot are monitored since 2002.

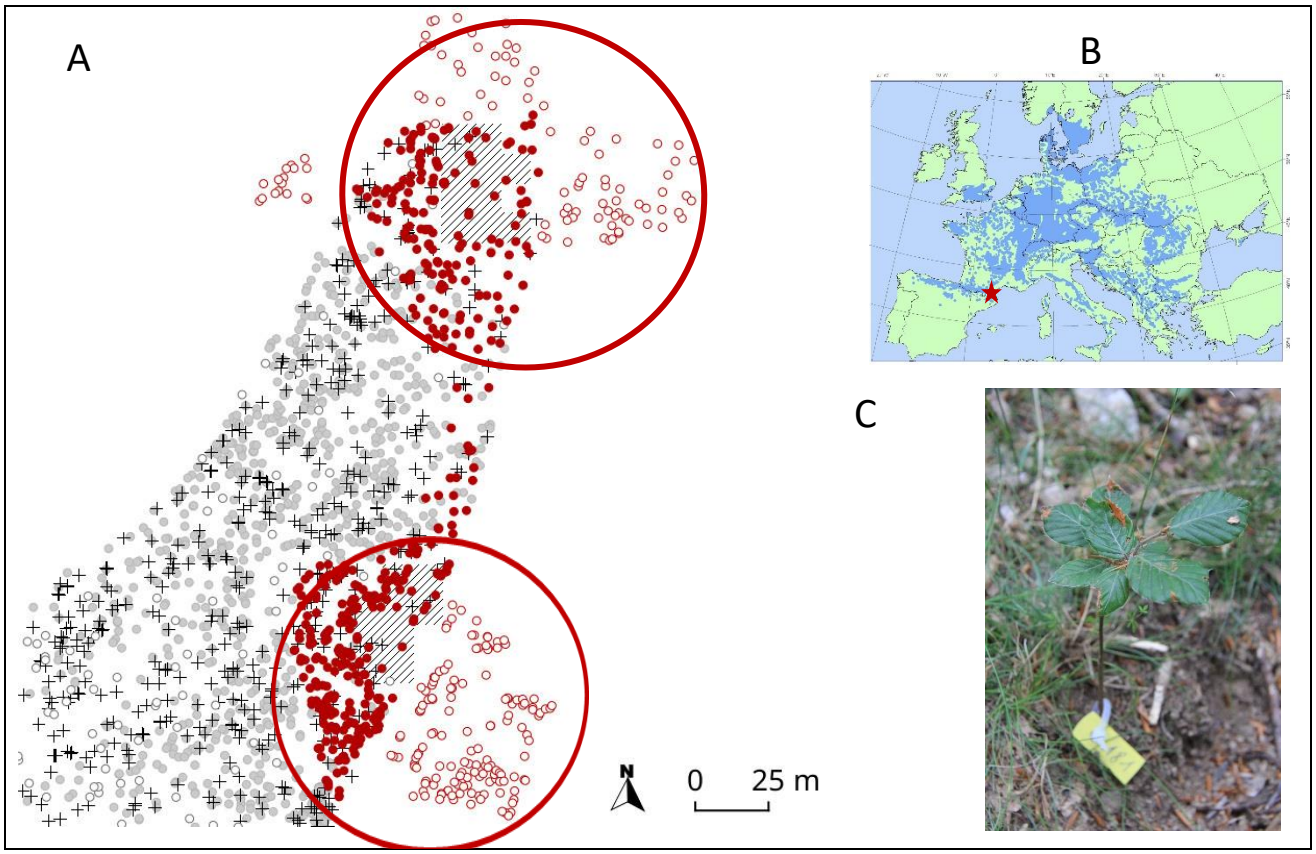

Figure 2: Study site and (A) sampling design: red filled dots (●) represent the 432 beech trees for which individual fecundity, growth and defoliation were assessed. Hatched squares represent the seedlings patches used to estimate fecundity through parentage analyses and mixed-effect mating models (MEMM). The two red circles encompass all the individuals (seedlings and adult) used for MEMM analyses. Red empty dots (○) represent the 244 beech trees outside of the protected area and included in the fecundity analyses (but not phenotyped for growth and defoliation). Grey dots (●) and crosses (+) represent other beeches within the protected area not included in the fecundity analyses either because they were far from sampled seedlings (●) or because they were dead in 2012 (+). Empty dots (○) represent other species within the protected area. (B) Study site location (red star) on European Beech distribution map (source Euforgen). (C) Picture of a sampled seedlings.

Adult seed-tree inventory and phenotyping

This study was conducted on two circular-shaped plots (as classically used in parentage analyses) covering 0.17 ha in total, where all the 683 alive adult beeches were mapped and collected for genetic analyses in 2012 (red dots on Figure 2). Although beech reproduction is mostly sexual, vegetative reproduction may occasionally occur, with the production of stump shoots resulting in multiple stems (i.e. several ramets for a single genet). In obvious cases of vegetative reproduction (ie root-connected stems), we sampled only the biggest ramet of each genet for genetic analyses.

Only 439 among the 683 collected beeches were included within the protected plot and monitored since 2002 (filled dots on Figure 2). The monitoring consisted first in measuring tree size as the diameter at breast height (DBH) in 2002 and 2012, which allowed us to derive the basal area ($BA=\pi*DBH^2/4$). Individual growth was

measured by the basal area increment (herein BAI) between 2002 and 2012, as estimated by: $BAI=\pi(DBH^2_{2012}-DBH^2_{2002})/4$.

The presence of dead branches and leaves was recorded each year between 2004 and 2012 as a qualitative measure (1=presence; 0=absence). We used the sum of these nine annual defoliation scores (herein DEF) as an integrative, qualitative ordered measure, combining the recurrence of defoliation and the ability to recover from defoliation.

The conspecific local density (herein $Dens_{dmax}$) was estimated as the number of beech neighbors found within a radius of *dmax* around each mother-tree. We also used the Martin-Ek index (Martin & Ek, 1984) to quantify the intensity of competition on a focal individual *i*. This index (herein $Compet_{dmax}$) accounts simultaneously for the diameter and the distance of each beech competitor *j* to the competed individual *i*:

$$\text{Compet}_{i,d_{\max}} = \frac{1}{\text{DBH}_i}\sum_{\text{j=1}}^{n_{dmax}} \text{dbh}_j e^{\frac{-16d_{\text{ij}}}{DBH_i+DBH_j}} \quad \text{(equation 1)}$$

where DBH_i and DBH_j are the diameter at breast height (in cm) of the competed individual *i* and of competitor *j* (any adult tree of any species with $DBH_j>DBH_i$), n_{dmax} the total number of competitors in a given radius d_{max} (in m) around each individual *i*, and d_{ij} the distance between individuals i and j. We computed a total of 20 $Dens_{dmax}$ variables and 20 $Compet_{dmax}$ variables, by considering d_{max} values between 1 and 20 m with a 1m-step. The $Dens_{dmax}$ variables were strongly and positively correlated with each other's, and so were the $Compet_{dmax}$ variables, but $Dens_{dmax}$ variables were not correlated with $Compet_{dmax}$ variables (Figure S2).

Offspring sampling and genotyping

To estimate adult fecundity, we sampled 365 seedlings established amidst the 683 genotyped adult beeches (shaded quadrats on Figure 2). Two cohorts of seedlings were sampled exhaustively within a selected number of quadrats at the center of each circular plot: 165 "young" seedlings germinated in spring 2012 (masting year 2011), and 200 "old seedlings" germinated from spring 2011 back to spring 2001 (age was estimated using annual bud scars). Qualitative surveys indicated that masting occurred in years 2002, 2004, 2006 and 2009. In this study, the two seedlings cohorts were mixed, in order to estimate cumulated reproduction from 2001 to 2012.

The genotypes of the 683 alive adult beeches and 365 seedlings were scored at a combination of 18 microsatellite loci (Table S1). DNA extraction, PCR amplifications and genotype scoring with a MegaBACE 1000 sequencer were performed using the conditions described by Oddou-Muratorio, *et al.* (2018). The total number of alleles observed in each cohort was greater than 95 (Table S1). Adult genotypes revealed seven pairs of clones among the adult beeches. We checked that these clones were always spatially clustered, and kept only one ramet for each genet in the MEMM analyses (i.e. 676 adult beeches).

Inference of male and female relative fecundities: MEMM analyses

Male and female fecundities were jointly estimated with the pollen and seed dispersal kernels in a Bayesian framework implemented in the MEMM program (Oddou-Muratorio et al., 2018). MEMM is one of the recently developed spatially explicit mating models based on naturally established seedlings (see also Burczyk, Adams, Birkes, & Chybicki, 2006; Goto, Shimatani, Yoshimaru, & Takahashi, 2006; Moran & Clark, 2011; Oddou-Muratorio & Klein, 2008). These models provide joint estimates of individual male and female fecundities together with the pollen and seed dispersal kernels and mating system parameters, so that estimates of fecundity are not biased by the confounding effects of spatial and sampling designs (the arrangement of male/female parents and sampled seedlings).

Briefly, the Mixed-Effect Mating Model (MEMM) considers that each sampled seedling originates either (i) from a mother tree located outside the study site (implying seed immigration) or (ii) from a mother tree located within the study site. The latter case includes three possible origins of the fertilizing pollen: (i) pollen immigration, (ii) selfing, or (iii) pollination by a male tree located within the study site. The approach bypasses parentage assignation and focuses instead on the fractional contribution of all adults, either as female or as male parent, to each seedling (see Appendix A1 for details). For instance, the probability π_{Sij} of each sampled female tree *j* to contribute to the seedling pool at the spatial location of seedling *i* is modeled as:

$$\pi_{S_{ij}} = \frac{F_{Fj}\theta_S(d_{ij})}{\sum_{l:\text{mother}} F_{Fl}\theta_S(d_{il})} \quad \text{(equation 2)}$$

where F_{Fj} and F_{Fl} are the female fecundities of mother *j* and *l*, respectively; d_{ij} and d_{il} are the distances between seedling *i* and mother *j* and *l*, respectively; and ϑ_s is the seed dispersal kernel. Both the seed and pollen dispersal kernels (ϑ_s and ϑ_p) are modelled using a power-exponential function. All the parameters of the model are estimated in a Bayesian framework (Appendix A1). Note that F_F (and F_M) estimates are relative, with the average F_F-value (and F_M-) over the entire parent population fixed to 1.

Note that the fecundity estimates provided by MEMMs are related but not equivalent to the traditional resource-based estimates of female (i.e. the biomass/number of ovules, seeds, ovuliferous flowers or fruits) and male fecundity (i.e. the biomass/number of pollen grains or staminate flowers). First the latter estimate the resources allocated by each plant to reproduction while the former can only estimate a relative amount of pollen or seeds produced by each plant as compared to other plants. Second, the resource-based estimate is a pre-dispersal evaluation of seed and pollen production while MEMM estimates an effective amount of pollen achieving successful fertilization, and of seeds achieving successful germination. In consequence, MEMM-based estimates of fecundities account for individual effects (either maternal or genetic) that act independently on location to modify the success of mating, seed maturation or germination, or early survival during the post-dispersal processes preceding the sampling stage (Oddou-Muratorio et al., 2018).

For the estimation, we accounted for typing errors at microsatellite loci, with two possible types of mistyping: in the first type, the allele read differs only by one motif repeat from the true allele with a probability P_{err1}, while in the second type, the allele read can be any allele observed at this locus with a probability P_{err2}. We considered a mixture of the two error types, with $P_{err1} = 0.01$ and $P_{err2} = 0.01$. We ran 10 Markov chain Monte Carlo (MCMC) of 10,000 steps, each with additional 500 first MCMC steps as burn-in, checked that the different chains converged to the same value visually, and then combined the 10 chains together. Individual female (F♀) and male (F♂) fecundities were summarized by their median value across the 100,000 iterations.

Adult subsampling for dendrochronological analyses

We selected 90 trees within the protected plot for which we sampled cores to measure ring-width. These 90 trees were chosen to represent contrast in terms of defoliation and female fecundity (Figure S3). Cores were extracted in February 2016 at 1.30 m above ground. After sanding, cores were scanned at high resolution (1200 dpi). Boundary rings were read using CooRecorder v 9.0. Ring width were transcribed, individual series were checked for missing rings and dating errors and mean chronologies were calculated using Cdendro 9.0 (CDendro 9.0 & CooRecorder 9.0; Cybis Elektronik & Data AB. Sweden). Using the sum of ring width increments between 2002 and 2012 (Σrw), the growth of the 90 individuals between 2002 and 2012 was estimated as: $BAI_{wood}=\pi((DBH_{2002}/2+\Sigma rw)^2-DBH^2_{2002}/4)$.

Statistical analyses of the ecological drivers of growth and fecundities

Our objective herein was to test whether defoliation significantly affected individual growth and female/male fecundity. For each response variable independently (i.e., growth as measured by BAI, and fecundities as estimated with MEMM), we considered the following initial linear model:

$$BAI \text{ or } F♀ \text{ or } F♂ = DEF + DBH_{2002} + DBH_{2002}^2 + Compet_{dmax} + Dens_{dmax}$$

$$+ DEF{:}DBH_{2002} + DEF{:}Compet_{dmax} + DEF{:}\,Dens_{dmax} \quad \text{(equation 3)}$$

where all the predictors are quantitative variables (Table S2). Besides the target defoliation factor (DEF), this model includes one size-related factor (DBH_{2002}), and two competition-related factors ($Compet_{dmax}$ and $Dens_{dmax}$). Size and competition are considered here as "nuisance" parameters, susceptible to blur the signal between defoliation, growth and reproduction. A quadratic effect of DBH_{2002} was also included, as growth and sometimes fecundity are known to be proportional to basal area. Density and competition index can both be relevant to capture competition effect on growth or fecundity, and moreover, their influence may vary with the distance up to which competitors are accounted for. Therefore, we first selected the best $Compet_{dmax}$ and the best $Dens_{dmax}$ terms for each response variable independently using the model described by equation 3 without interaction terms, and retaining the d_{max} values leading to the highest R^2. Then, we included interactions terms (the three last terms in equation 3) to investigate specific effects of defoliation depending on individual size or on the level of competition.

The model was fitted on 432 focal adult beech trees within the protected plot (Figure 2) for which BAI was estimated from inventory data. All response variables were log-transformed to approach Gaussian distribution and to account for the higher variance associated to higher fecundity or higher growth. We visually inspected the relationship between each predictor and each response variable (Figure S4). For each response variable, we selected the most parsimonious model based on the AIC using the functions 'lm' and 'step' in R 3.3 (R Core Team 2018). The residuals were visually inspected through a plot of residuals vs predicted. Interaction effects were visualized with the package 'jtools' (Long, 2018).

Collinearity resulting from correlations between predictor variables is expected to affect statistical significance of correlated variables by increasing type II errors (Schielzeth, 2010). To evaluate this risk, we computed variance inflation factors (VIF) associated to each term retained in the best model with R package 'car' (Fox & Weisberg 2011).

Statistical analyses of the joint defoliation effects on female fecundity and growth

Our objective herein was to focus on the two variables (growth and female fecundity) responding to defoliation (see results), and to investigate how the relationship between these two variables varied with defoliation. We first compared the effects of defoliation on female fecundity vs growth after centring and normalizing fecundity and growth, and by using the best models fitted with equation 3 to estimate the effect of defoliation on these transformed variables.

Then, we investigated the individual correlation between raw relative female fecundity and growth for non-defoliated trees (DEF=0) versus defoliated trees (DEF>0). Note that a part of these correlations may be due to variation in size and/or competition among individuals. Moreover, they do not account for the quantitative nature of DEF. To overcome these limitations, we further investigated the trade-off between growth and female fecundity using the following linear model:

$$F♀ = BAI + DEF + DBH_{2002} + DBH_{2002}^2 + Compet_{dmax} + Dens_{dmax}$$

$$+ DEF{:}BAI + DEF{:}DBH_{2002} + DEF{:}Compet_{dmax} + DEF{:}\,Dens_{dmax} \quad \text{(equation 4)}$$

where BAI and the interaction between BAI and DEF are added to the model described by equation (3) above. A quadratic effect of DBH_{2002} was also included.

Results

Patterns of covariation of defoliation, tree size and competition

Recurrent crown defoliation was overall limited in the 432 individuals, with 95 trees with a non-null DEF-value (mean=0.36, Table S2). Defoliation increased with tree size; the significant interaction between DBH_{2002} and competition (mediated by Comp19) or density (mediated by Dens20) reflected a stronger effect of size on defoliation as competition increased (Figure S5).

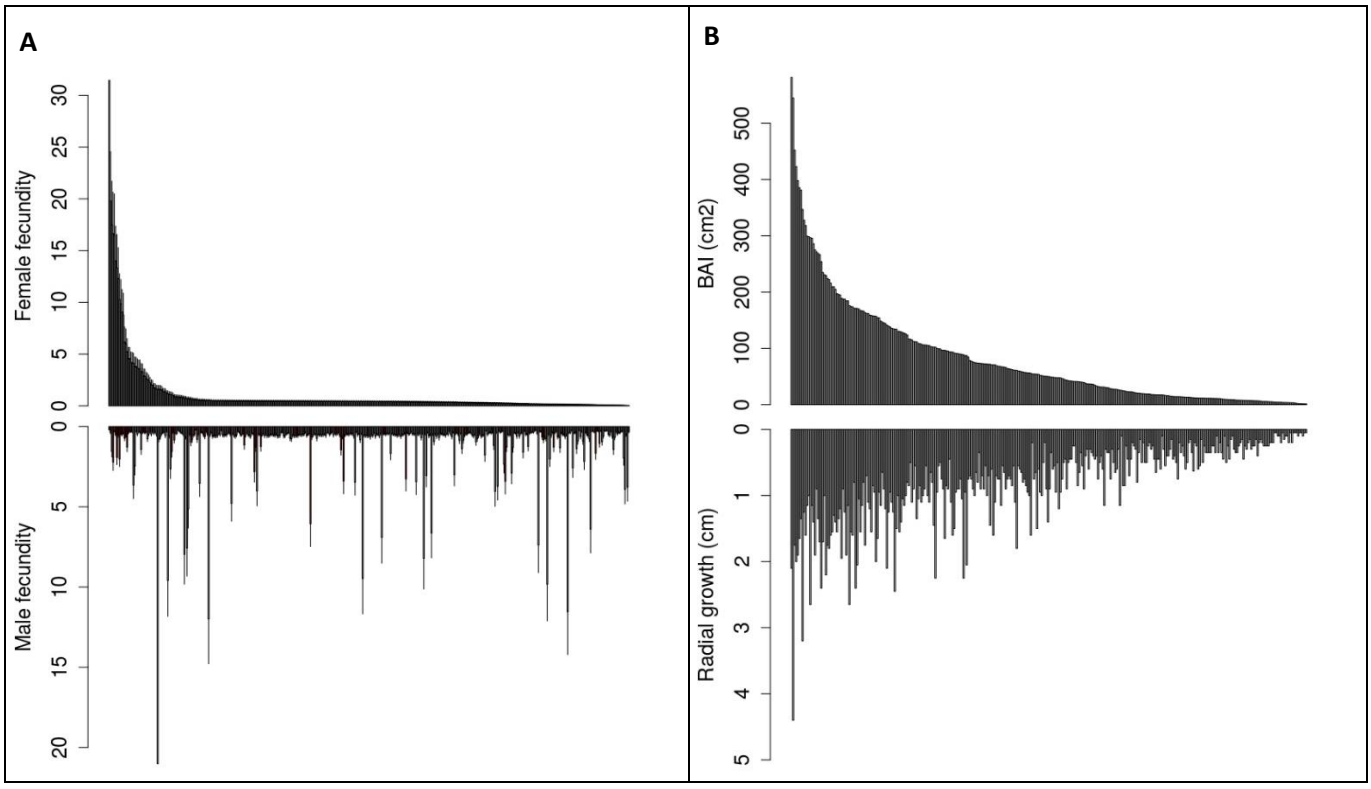

Figure 3: Distribution of individual (A) relative female (top) and male (bottom) fecundities estimated with MEMM, and (B) absolute growth estimated by BAI (top) or radial growth (bottom) for the 432 adult trees. Parents on the x-axis are ranked in decreasing order of female fecundity (A) or BAI (B).

Inter-individual variations in relative fecundities and growth

The distributions of relative female and male individual fecundities (F♀ and F♂) estimated by MEMM were strongly L-shaped (Figure 3A). Female fecundities varied from 0.03 to 32.44 (median=0.42, mean= 1, sd= 2.78), while male fecundities varied from 0.17 to 21.16 (median= 0.48, mean =1, sd= 1.86). By comparison, the distribution of growth values was less L-shaped than those of fecundity (Figure 3B). In the data set of 432 adult

trees, where cumulated growth from 2002 to 2012 was estimated through inventory data, radial growth varied from 0 to 4.4 cm (median=0.45, mean= 0.60, sd= 0.62), while BAI varied from 0 to 581.22 cm^2 (median=23.98, mean= 61.58, sd= 86.87).

In the subset of 90 cored trees, where cumulated growth from 2002 to 2012 was estimated through ring width data, radial growth varied from 0.17 to 2.70 cm (median=0.97, mean= 1.03, sd= 0.57), while BAI varied from 7.8 to 805.89 cm^2 (median=126.30, mean= 180.07, sd=172.7). Moreover, for these 90 cored trees, the correlation between inventory-based and ring-width-based radial growth was 0.84 (p-value<0.001), while the correlation between inventory-based and ring-width-based BAI was 0.68 (p-value<0.001). The lower correlation for BAI values was due to the largest trees, for which inventory data generally underestimated growth (Figure S6).

Ecological drivers of fecundities and growth

Defoliation, size and competition overall explained a significant part of the variation in growth (57%) and female fecundity (12%), while competition alone was found to marginally explain a small part of the variation in male fecundity (<1%). In the whole data set of 432 individuals, the most parsimonious model showed that female fecundity (F♀) significantly decreased with defoliation and competition (mediated by Compet10), while it increased with DBH_{2002} and density (mediated by Dens10; Table 1A). Moreover, the interaction between DEF and DBH_{2002} was significant, reflecting a weaker negative effect of defoliation on female fecundity as tree size increased (Figure 4A). By contrast, male fecundity (F♂) was only marginally (and negatively) affected by competition (mediated by Dens5, Table 1B). Finally, growth (as measured by BAI) significantly decreased with defoliation and competition (mediated by Compet7), and increased with DBH_{2002} and density (mediated by Dens10; Table 1C). By contrast with female fecundity, no interactions between defoliation and size were detected on growth. For all fitted models, variance inflation factors (VIF in Table 1) were all below 10, ruling out any serious multicollinearity issue. Diagnostic plots confirmed the quality of the fitted models (Figure S7).

To compare the effect of defoliation on fecundity and growth, we centred and normalized F♀ and BAI, and ran the best models for each response variable. The average decline in response to a one-unit increase in DEF was -0.06 for F♀ (S.E.= 0.10; measured in standard unit of trait) versus -0.10 for BAI (S.E.=0.04).

Table 1. Analysis of variance table for (A) *F♀*: female fecundity (B) *F♂*: male fecundity and (C) BAI: basal area increment, in response to ecological determinants included in equation (3). We show the results of the most parsimonious model: its adjusted R^2, the type III sum of squares (SSQ) and degree of freedom (df) associated to each term. For each predictor, we give the estimate of its effect, the standard error (S.E.) and associated t and p-value. Variance inflation factors (VIF) were computed with R package CAR. All the response variables were log-transformed. Results are based on the whole data set of 432 individuals for *F♀* and *F♂*, and on the 341 with non-null BAI for BAI.

Predictor	***R²***	**SSQ**	**df**	**Estimate**	**S.E.**	**t**	**p-value**	**VIF**
(A) log(F♀)	*0.12*						*<0.001*	
DEF		9.33	1	-0.349	0.111	-3.148	0.002	4.13
DBH_2002		11.97	1	0.013	0.004	3.564	<0.001	2.19
Compet10		7.9	1	-0.033	0.011	-2.896	0.004	1.43
Dens10		7.46	1	0.010	0.003	2.815	0.005	1.35
DEF:DBH_2002		7.28	1	0.006	0.002	2.780	0.006	4.61
residuals		401.29	426					
(B) log(F♂)	*0.004*						*0.097*	
Dens5		1.695	1	-0.01	0.01	-1.662	0.10	-
residuals		263.854	430					
(C) log(BAI)	*0.61*						*<0.001*	
DEF		4.89	1	-0.153	0.058	-2.646	0.00853	1.05
DBH_2002		139.39	2	15.494	1.167	13.275	<0.001	1.21
DBH_2002²				-5.539	0.886	-6.251	<0.001	
Compet7		20.92	1	-0.090	0.016	-5.473	<0.001	1.27
Dens14		4.78	1	0.005	0.002	2.617	0.00927	1.16
residuals		234.02	335					

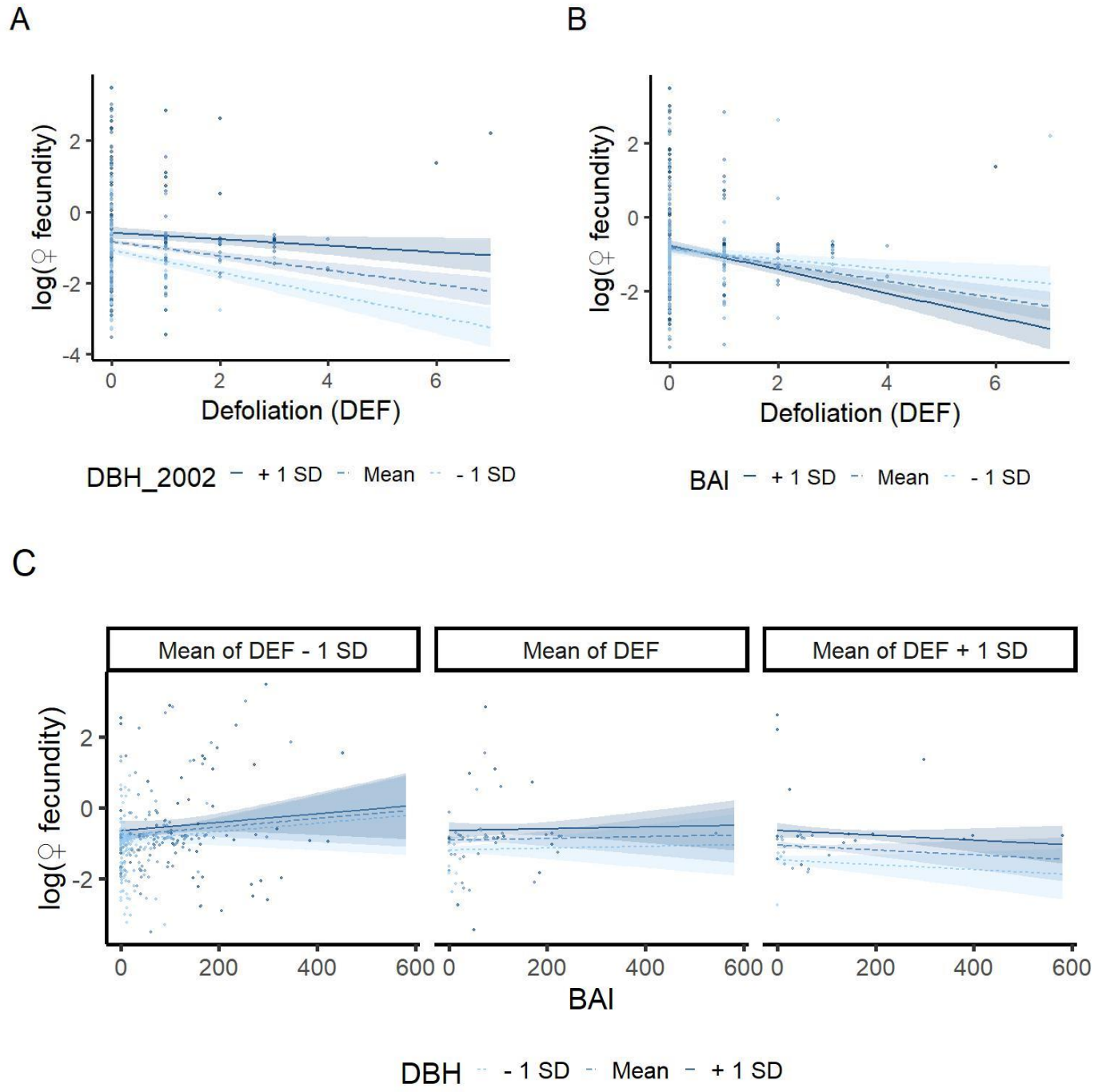

Figure 4: Interaction plots for (A) DEF and DBH_{2002} effects on female fecundity (B) DEF and BAI effects on female fecundity, (C) BAI, DBH_{2002} and DEF effects on female fecundity. Regression lines are plotted for three values of each moderator variable, corresponding to +/- 1 standard deviation from the mean. Confidence interval at 80% are shown around each regression line. Points are the observations.

Joint defoliation effects on female fecundity and growth

The raw F♀s and BAIs were significantly and positively correlated in the 337 non-defoliated trees ($cor_{F♀\text{-}BAI\text{-}nondef}$ = 0.31, p-value<0.001), but not in the 95 defoliated trees ($cor_{F♀\text{-}BAI\text{-}def}$=0.13, pval=0.2; Figure 5).

The linear model for F♀ including BAI as a predictor (equation 4) allowed us to disentangle the respective effects of defoliation, size and competition on the relationship between female fecundity and growth. In addition to the previous effects, a significant interaction between BAI and defoliation was detected (Table 2): F♀ overall decreased with increasing defoliation, but this decrease was faster and stronger for trees with a higher BAI (Figure 3B). The complex interaction between BAI, DEF and DBH_{2002} on F♀ resulted in a defoliation-dependent trade-off between growth and female fecundity: F♀ of the non-defoliated trees (Figure 3C, left panel) increased with BAI (no trade-off), whereas F♀ of the most defoliated trees (Figure 3C, right panel) decreased with increasing BAI (trade-off). Moreover, F♀ of small trees (Figure S8, left panel) always decreased in response to increasing defoliation, whatever their BAI, whereas the female F♀ of large trees (Figure S8, right panel) could increase in response to increasing DEF, at the expense of reduced BAI. Diagnostic plots confirmed the quality of the fitted models (Figure S9).

Table 2. Analysis of variance table for female fecundity, in response to ecological determinants included in equation (4). Results are based on the whole data set of 432 individuals. See Table 1 for legends.

Predictor	R^2	SSQ	df	Estimate	S.E.	t	P-value	VIF
	0.13						*<0.001*	
BAI		0.56	1	0.001	0.001	0.773	0.440	2.468
DEF		11.04	1	-0.384	0.112	-3.433	0.001	4.231
DBH		6.24	1	0.011	0.004	2.582	0.010	3.171
Compet10		7.49	1	-0.032	0.011	-2.828	0.005	1.444
Dens10		6.85	1	0.009	0.003	2.704	0.007	1.354
BAI:DEF		4.09	1	-0.001	0.001	-2.091	0.037	2.857
DEF:DBH		11.39	1	0.009	0.003	3.488	0.001	6.750
Residuals		397.03	424					

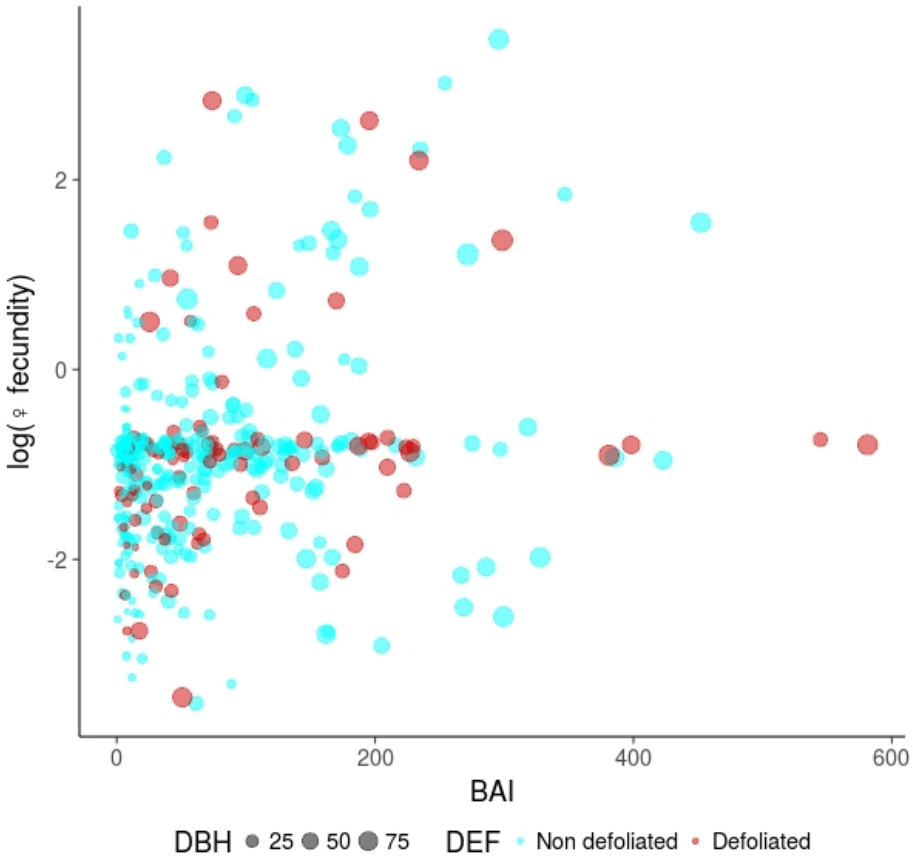

Figure 5: Correlation between growth, measured by the Basal Area Increment (BAI) and female fecundity (F♀), plotted on a log scale. The size of the dots is proportional to tree diameter (DBH_{2002}). This is a scatter plot of raw data, and not of model predictions.

Discussion

By investigating the among-individual variation in the impact of stress-induced defoliation on female/male fecundity and wood growth within a beech natural population at the warm, dry margin of the species distribution, this study brings new insights on the response to stress of a major European tree species. We show that crown defoliation was significantly associated to a decrease in wood growth and female fecundity, but not in male fecundity. A trade-off between growth and female fecundity was observed in response to defoliation, suggesting that some large defoliated individuals can maintain significant female fecundity at the expense of reduced growth. The consequences of these results on short-term evolutionary dynamics of the studied population are discussed.

The response of wood growth and reproduction to stress-induced crown defoliation.

The coordination between increasing crown defoliation and decreasing wood growth observed in this study is consistent with the temporal sequence of ecophysiological processes involved in tree

response to water stress and late frosts. During summer, low precipitation and high evaporative demand due to high temperatures and vapor-pressure increase water stress, which leads trees to close stomata, in order to reduce transpiration and protect the integrity of the hydraulic system by maintaining water potentials above irreversible embolism thresholds. Drought also directly impacts wood growth by limiting cell division and elongation of wood cells due to carbon limitation (Lempereur et al., 2015). Post-drought stomatal closure can prolong the decrease in photosynthesis and potentially affect carbon storage (Bréda et al., 2006), which may lead to a decrease in radial growth in subsequent years. Under severe drought, some branches can experience hydraulic failure or undergo carbon starvation, which leads to leaf fall. Leaf fall can then in turn have a negative effect on radial growth, first by decreasing photosynthesis and thus carbon availability in the years following defoliation. Secondly, leaf fall can induce allocation shifts that reduce the priority of growth relative to other sinks such as reserves storage, as observed in black oak (Wiley et al., 2017). On the other hand, when late frosts damage young leaves, beech trees can reflush, i.e. produce another cohort of leaves (Menzel, Helm, & Zang, 2015), at least for some parts of the crown. However, the time required to reflush leads to a shorter growing season, which directly reduces wood growth. For these non-mutually exclusive reasons, related to either carbon-, sink-, or temporal limitation of growth, a negative effect of crown defoliation on growth is often observed, especially on beech (Delaporte et al., 2016, this study).

Although seed production is recognized as being resource-limited in plants (Lloyd & Bawa, 1984), the ecophysiological processes involved in the response of tree sexual reproduction to physiological stresses are less well characterized than those involved in wood growth response. The negative effect of crown defoliation on female fecundity observed in this study is consistent with the expected decrease in photosynthesis and thus in carbon availability induced by leaf fall. Moreover, this result combined with the absence of crown defoliation effect on male fecundity is also consistent with the expected higher resource-limitation of female fecundity (costly nut-seeds) as compared to male fecundity in beech (Lloyd & Bawa, 1984; Obeso, 1988). This second expectation is also supported by the marked increase in female fecundity with increasing tree size and decreasing competition while male fecundity was only marginally (and negatively) affected by competition. Moreover, recent studies showed that many tree species use mainly current photosynthates to maturate their fruits, while flowers are produced from old carbon storage (Hoch, Siegwolf, Keel, Körner, & Han, 2013; Ichie et al., 2013). Altogether, our results suggest that beech reproduction is more limited by the carbon resources needed for maturating seeds than for those required for producing flowers. Although nitrogen storage and remobilization is usually a limiting resource for seed production, and particularly masting (Han & Kabeya, 2017), this may not be the case in our study site, where cow grazing could favour nitrogen enrichment.

Defoliation induced a trade-off between growth and reproduction

Several studies tested the existence of a negative correlation between growth and reproduction at the individual level, as a signature of the possible trade-off between these functions. The key assumption underlying this trade-off is that reproduction is costly and competes with growth for resources (Koenig & Knops, 1998; Obeso, 2002; Thomas, 2011). By contrast, the absence of correlation is usually interpreted as independence between these functions in terms of resource pool (Knops, Koenig, & Carmen, 2007; Obeso, 2002; Pulido et al., 2014). A trade-off between growth and

reproduction was already found for beech (Hacket-Pain, Friend, Lageard, & Thomas, 2015; Lebourgeois et al., 2018; Hacket-Pain et al., 2018). More precisely, Hacket-Pain et al. (2017) found for beech that masting years (i.e. high seed production) are negatively correlated with growth and this trade-off is more pronounced during drought years due to resource scarcity.

We found here a negative (respectively positive) correlation between growth and reproduction for defoliated (respectively non-defoliated) trees. Hence, among the defoliated trees, some individuals maintained significant female fecundity at the expense of reduced growth, and reciprocally. These results support the general idea that the correlation between reproduction and growth depends on the level of resource (Obeso, 2002; van Noordwijk & de Jong, 1986), a trade-off being present only under limiting resources, i.e. crown defoliation in our case. By contrast, the higher resource level of non-defoliated individuals could allow them to insure reproduction and growth with independent resource pool, as it was found also for *Fagus* genus (Yasumura, Hikosaka, & Hirose, 2006). Moreover, the detailed analysis of the interactions between defoliation, size and growth on female fecundity showed that those defoliated trees maintaining high female fecundity were the largest ones, suggesting that crown defoliation could shift the allocation of carbon to reproduction above a given tree size. Besides the literature on forest seed orchards and fruit trees orchards, one of the rare studies supporting such hypothesis is that of Wiley, Casper & Helliker (2017), who experimentally defoliated black oak, a tree species which maturates its acorns over two years. Recovery following defoliation was shown to involve substantial allocation shifts, with carbohydrate storage and already initiated reproduction cycles (i.e. maturation of 2-year acorn) being favored relative to growth and new reproductive cycles (i.e. flowering and production of new 1-year acorn).

The positive correlation between growth and reproduction for non-defoliated trees may also indicate an effect of the unobserved level of resource, which probably varies among individuals. More generally, elucidating the causal relationships between defoliation as an impact of stress, the (non-observed) level of resource, growth and reproduction would deserve further investigations, accounting for the complex multivariate relationships among the interrelated variables mapped on Figure 1. This could be achieved using for instance path analyses (Shipley, 2016) or other Bayesian tools introducing the level of resource as a latent variable (e.g., Journé et al., submitted). The use of such approaches in this study was however hampered by two main limitations. First, resource allocation between two compartments are difficult to handle in path analyses, and a reciprocal relationship between growth and reproduction such as depicted by the red double arrow on Figure 1 cannot be specified (Shipley, 2016). The solution to this problem usually consists in accounting for the time dimension, focusing on among-year lagged effects between annual variables (e.g. Hacket-Pain et al., 2018, Journé et al., submitted). However, this solution was intractable in this study, where growth and reproduction were measured as integrated values over the period 2002-2012. The second limitation stems from the weak ability of variance-covariance based methods such as path analyses to deal with non-normality. Whereas deviations from a Gaussian distribution are not necessarily crucial for predictor variables in a linear model, they cannot be handled in path analyses simultaneously with latent variable to our knowledge (Lefcheck, 2016).

Long-term consequences for population adaptive response to stress

In the studied population, some large, defoliated individuals maintained a high female fecundity under stressful conditions, at the expense of reduced growth. Moreover, as male fecundity was insensitive to crown defoliation, the less competed defoliated trees also contribute to reproduction through male function. Hence, we can reject the hypothesis H1 that the relationship between reproduction and growth does not change with increasing crown defoliation. Note however that the alternative hypothesis H2 (defoliation or stresses act like a cue stimulating reproductive performances at the expense of reduced growth) was only supported for some individuals. This response to stress could have major consequences for the short-term evolutionary dynamics of the population. Indeed, assuming that at least some of the traits underlying vulnerability to stresses are under genetic control, we showed here that the most vulnerable individuals (those that are the most impacted by stress) still contribute to regeneration, which could lead the population to evolve traits compromising its adaptation to stress. By contrast, if the defoliated individuals would decrease simultaneously their growth and reproduction (hypothesis H1), their potentially non-adapted genotypes could be purged more efficiently.

Deriving demo-genetic scenarios for the population adaptive response to stress and testing for a reproduction load would however require further investigations. First, the observed inter-individual variation in the level of defoliation is probably shaped in part by genetic variation but also by microenvironment variation and ontogeny, since the largest and most competed individuals were more susceptible to defoliation. Hence, the importance of genetic factors driving the level of defoliation remains to be characterised, in order to better decipher the intra-individual variation in the vulnerability to stress from that of the stress exposure, and to investigate possible evolutionary changes (Hamanishi & Campbell, 2011). Second, our MEMM-based estimates of fecundity have the advantage to integrate the whole regeneration processes and not just seed/pollen production. This is important as post-dispersal processes and recruitment patterns may compensate the decline in seed production in populations under stressful conditions, as suggested for drought by Barbeta et al. (2011). However, they also have the drawbacks to be relative, and to convey no information on the absolute contribution of defoliated or non-defoliated individuals to the regeneration, and thus on the demographic impact of defoliation.

Finally, investigating the population adaptive response to stress would ideally require accounting for the physiological mechanisms involved. For instance, when dealing with drought-induced defoliation, we would need to consider the two main ecological strategies widely acknowledged in plants for drought response: 1) the water economy strategy, where plants maintain low growth rates and low rates of gas exchange during droughts, and 2) the water uptake strategy, where plants have a more rapid instant growth through higher rates of gas exchange when water is available, typically spring in Mediterranean climate, allowing them to complete important biological functions before drought onset (Arntz & Delph, 2001). These two strategies rely on different combinations of physiological, morphological or phenological trait values (in particular those related to hydraulics and carbon-storage). Bontemps et al. (2017) demonstrated the co-existence of these two strategies in a drought-prone population of beech and showed a higher reproductive output of the water uptake strategy. In this context, defoliation could be one of the traits involved in the water uptake strategy,

allowing the maintenance of the water balance after drought onset. Indeed, if defoliated trees are characterized by higher xylem vulnerability but also higher hydraulic conductivity, the more a tree is efficient for transpiration and photosynthesis, the more it is vulnerable to drought (Cochard, Lemoine, & Dreyer, 1999).

Data accessibility

The data set analysed in this preprint is available online under the zenodo platform (DOI: 10.5281/zenodo.3516305). More detailed data (genotypes) and R scripts for statistical analyses are available from the corresponding author.

Supplementary material

The MEMM software for estimating female and male fecundities is available at: https://informatique-mia.inra.fr/biosp/memm.
Supplementary materials (Figures and Tables) for this preprint are available on bioRxiv (doi: https://doi.org/10.1101/474874).

Acknowledgements

We are grateful to our colleagues Francois Lefèvre and Etienne K. Klein, as well as to our PCIEcology editor Georges Kunstler and three anonymous reviewers for discussions and comments on previous version of this manuscript. We thank Nicolas Mariotte INRA URFM Avignon for wood core sampling and Jean Thevenet, INRA UEFM, Avignon for sample management. The study was partly funded by the EU ERA-NET BiodivERsA projects TIPTREE (BiodivERsA2-2012-15), and the ANR project MeCC (ANR-13-ADAP-0006). Version 4 of this preprint has been peer-reviewed and recommended by Peer Community In Ecology (https://doi.org/10.24072/pci.ecology.100033).

Conflict of interest disclosure

The authors of this preprint declare that they have no financial conflict of interest with the content of this article. SOM is a recommender for PCIEcology.

References

Adams, H. D., Zeppel, M. J. B., Anderegg, W. R. L., Hartmann, H., Landhäusser, S. M., Tissue, D. T., … McDowell, N. G. (2017). A multi-species synthesis of physiological mechanisms in drought-induced tree mortality. *Nature Ecology and Evolution*, *1*(9), 1285–1291. doi:10.1038/s41559-017-0248-x

Allen, C. D., Macalady, A. K., Chenchouni, H., Bachelet, D., McDowell, N., Vennetier, M., … Cobb, N. (2010). A global overview of drought and heat-induced tree mortality reveals emerging climate change risks for forests. *Forest Ecology and Management*, *259*(4), 660–684. doi:10.1016/j.foreco.2009.09.001

Anderegg, W. R. L., Kane, J. M., & Anderegg, L. D. L. (2013). Consequences of widespread tree mortality triggered by drought and temperature stress. *Nature Climate Change*, *3*(1), 30–36. doi:10.1038/nclimate1635

Barbeta, A., Peñuelas, J., Ogaya, R., & Jump, A. S. (2011). Reduced tree health and seedling production in fragmented Fagus sylvatica forest patches in the Montseny Mountains (NE Spain). *Forest Ecology and Management*, *261*(11), 2029–2037. doi:10.1016/j.foreco.2011.02.029

Bigler, C., & Bugmann, H. (2018). Climate-induced shifts in leaf unfolding and frost risk of European trees and shrubs. *Scientific Reports*, *8*(1), 1–10. doi:10.1038/s41598-018-27893-1

Bonnet-Masimbert, M., & Webber, J. E. (2012). From flower induction to seed production in forest tree orchards. *Tree Physiology*, *15*(7–8), 419–426. doi:10.1093/treephys/15.7-8.419

Bontemps, A., Davi, H., Lefèvre, F., Rozenberg, P., & Oddou-Muratorio, S. (2017). How do functional traits syndromes covary with growth and reproductive performance in a water-stressed population of Fagus sylvatica? *Oikos*, *126*(10), 1472–1483. doi:10.1111/oik.04156

Bréda, N., Huc, R., Granier, A., & Dreyer, E. (2006). Temperate forest trees and stands under severe drought: a review of ecophysiological responses, adaptation processes and long-term consequences. *Annals of Forest Science*, *63*(6), 625–644. doi:10.1051/forest:2006042

Burczyk, J., Adams, W. T., Birkes, D. S., & Chybicki, I. J. (2006). Using genetic markers to directly estimate gene flow and reproductive success parameters in plants on the basis of naturally regenerated seedlings. *Genetics*, *173*(1), 363–372. doi:10.1534/genetics.105.046805

Bykova, O., Limousin, J.-M., Ourcival, J.-M., & Chuine, I. (2018). Water deficit disrupts male gametophyte development in Quercus ilex. *Plant Biology*, *20*(3), 450–455. doi:10.1111/plb.12692

Bykova, O, Chuine, I., Morin, X., & Higgins, S. I. (2012). Temperature dependence of the reproduction niche and its relevance for plant species distributions. *Journal of Biogeography*, *39*(12), 2191–2200. doi:10.1111/j.1365-2699.2012.02764.x

Camarero, J. J., Gazol, A., Sangüesa-Barreda, G., Oliva, J., & Vicente-Serrano, S. M. (2015). To die or not to die: Early warnings of tree dieback in response to a severe drought. *Journal of Ecology*, *103*(1), 44–57. doi:10.1111/1365-2745.12295

Charrier, G., Ngao, J., Saudreau, M., & Améglio, T. (2015). Effects of environmental factors and management practices on microclimate, winter physiology, and frost resistance in trees. *Frontiers in Plant Science*, *6*(April), 1–18. doi:10.3389/fpls.2015.00259

Delaporte, A., Bazot, S., & Damesin, C. (2016). Reduced stem growth, but no reserve depletion or hydraulic impairment in beech suffering from long-term decline. *Trees - Structure and Function*, *30*(1), 265–279. doi:10.1007/s00468-015-1299-8

Dobbertin, M. (2005). Tree growth as indicator of tree vitality and of tree reaction to environmental stress: a review. *European Journal of Forest Research*, *124*(4), 319–333. doi:10.1007/s10342-005-0085-3

Flores-Rentería, L., Whipple, A. V., Benally, G. J., Patterson, A., Canyon, B., & Gehring, C. A. (2018). Higher

Temperature at Lower Elevation Sites Fails to Promote Acclimation or Adaptation to Heat Stress During Pollen Germination. *Frontiers in Plant Science*, *9*, 1–14. doi:10.3389/fpls.2018.00536

Galiano, L., Martínez-Vilalta, J., & Lloret, F. (2011). Carbon reserves and canopy defoliation determine the recovery of Scots pine 4 yr after a drought episode. *New Phytologist*, *190*(3), 750–759. doi:10.1111/j.1469-8137.2010.03628.x

Goto, S., Shimatani, K., Yoshimaru, H., & Takahashi, Y. (2006). Fat-tailed gene flow in the dioecious canopy tree species Fraxinus mandshurica var. japonica revealed by microsatellites. *Molecular Ecology*, *15*(10), 2985–2996. doi:10.1111/j.1365-294X.2006.02976.x

Hacket-Pain, A. J., Ascoli, D., Vacchiano, G., Biondi, F., Cavin, L., Conedera, M., … Zang, C. S. (2018). Climatically controlled reproduction drives interannual growth variability in a temperate tree species. *Ecology Letters*, *21*(12), 1833–1844. doi:10.1111/ele.13158

Hacket-Pain, A. J., Lageard, J. G. A., & Thomas, P. A. (2017). Drought and reproductive effort interact to control growth of a temperate broadleaved tree species (Fagus sylvatica). *Tree Physiology*, *37*(6), 744–754. doi:10.1093/treephys/tpx025

Hamanishi, E. T., & Campbell, M. M. (2011). Genome-wide responses to drought in forest trees. *Forestry*, *84*(3), 273–283. doi:10.1093/forestry/cpr012

Hampe, A., & Petit, R. J. (2005). Conserving biodiversity under climate change: The rear edge matters. *Ecology Letters*, *8*(5), 461–467. doi:10.1111/j.1461-0248.2005.00739.x

Han, Q., & Kabeya, D. (2017). Recent developments in understanding mast seeding in relation to dynamics of carbon and nitrogen resources in temperate trees. *Ecological Research*, *32*(6), 771–778. doi:10.1007/s11284-017-1494-8

Hedhly, A., Hormaza, J. I., & Herrero, M. (2009). Global warming and sexual plant reproduction. *Trends in Plant Science*, *14*(1), 30–36. doi:10.1016/j.tplants.2008.11.001

Hoch, G., Siegwolf, R. T. W., Keel, S. G., Körner, C., & Han, Q. (2013). Fruit production in three masting tree species does not rely on stored carbon reserves. *Oecologia*, *171*(3), 653–662. doi:10.1007/s00442-012-2579-2

Ichie, T., Igarashi, S., Yoshida, S., Kenzo, T., Masaki, T., & Tayasu, I. (2013). Are stored carbohydrates necessary for seed production in temperate deciduous trees? *Journal of Ecology*, *101*(2), 525–531. doi:10.1111/1365-2745.12038

Journé, V., Papaïx, J., Walker, E., Courbet, F., Lefevre, F., Oddou-Muratorio, S., & Davi, H. (submitted). A hierarchical Bayesian resource model to investigate trade-offs between growth and reproduction in a long-lived plant.

Karimi, F., Igata, M., Baba, T., Noma, S., Mizuta, D., Gook Kim, J., & Ban, T. (2017). Summer Pruning Differentiates Vegetative Buds to Flower Buds in the Rabbiteye Blueberry (*Vaccinium virgatum* Ait.). *The Horticulture Journal*, *86*(3), 300–304. doi:10.2503/hortj.MI-158

Lee, T. D. (1988). Patterns of fruit and seed production. In J. Lovett-Doust & L. Lovett-Doust (Eds.), *Plant reproductive ecology: patterns and strategies* (Oxford Uni). New York.

Lefcheck, J. S. (2016). piecewiseSEM: Piecewise structural equation modelling in r for ecology, evolution, and systematics. *Methods in Ecology and Evolution*, *7*(5), 573–579. doi:10.1111/2041-210X.12512

Lempereur, M., Martin-StPaul, N. K., Damesin, C., Joffre, R., Ourcival, J.-M., Rocheteau, A., & Rambal, S. (2015). Growth duration is a better predictor of stem increment than carbon supply in a Mediterranean oak forest: implications for assessing forest productivity under climate change. *New Phytologist*, *207*(3), 579–590. doi:10.1111/nph.13400

Lloyd, D. G., & Bawa, K. S. (1984). Modification of the Gender of Seed Plants in Varying Conditions. In M. K. Hecht & G. T. Prance (Eds.), *Evolutionary Biology* (pp. 255–338). Boston, MA: Routledge. doi:10.4324/9781315128634-1

McDowell, N. G., Beerling, D. J., Breshears, D. D., Fisher, R. A., Raffa, K. F., & Stitt, M. (2011). The interdependence of mechanisms underlying climate-driven vegetation mortality. *Trends in Ecology and Evolution*, *26*(10), 523–532. doi:10.1016/j.tree.2011.06.003

Meilan, R. (1997). Floral induction in woody angiosperms. *New Forests*, *14*, 179–202.

Menzel, A., Helm, R., & Zang, C. (2015). Patterns of late spring frost leaf damage and recovery in a European beech (Fagus sylvatica L.) stand in south-eastern Germany based on repeated digital photographs. *Frontiers in Plant Science*, *6*, 1–13. doi:10.3389/fpls.2015.00110

Moran, E. V., & Clark, J. S. (2011). Estimating seed and pollen movement in a monoecious plant: A hierarchical Bayesian approach integrating genetic and ecological data. *Molecular Ecology*, *20*(6), 1248–1262. doi:10.1111/j.1365-294X.2011.05019.x

Obeso, J. R. (1988). The costs of reproduction in plants. *New Phytologist*, *155:*, 321–348. doi:10.1046/j.1469-8137.2002.00477.x

Oddou-Muratorio, S., Gauzere, J., Bontemps, A., Rey, J. F., & Klein, E. K. (2018). Tree, sex and size: Ecological determinants of male vs. female fecundity in three Fagus sylvatica stands. *Molecular Ecology*, *27*(15), 3131–3145. doi:10.1111/mec.14770

Oddou-Muratorio, S., & Klein, E. K. (2008). Comparing direct vs. indirect estimates of gene flow within a population of a scattered tree species. *Molecular Ecology*, *17*(11), 2743–2754. doi:10.1111/j.1365-294X.2008.03783.x

Peñuelas, J., & Boada, M. (2003). A global change-induced biome shift in the Montseny mountains (NE Spain). *Global Change Biology*, *9*(2), 131–140. doi:10.1046/j.1365-2486.2003.00566.x

Pérez-Ramos, I. M., Ourcival, J. M., Limousin, J. M., & Rambal, S. (2010). Mast seeding under increasing drought: results from a long-term data set and from a rainfall exclusion experiment. *Ecology*, *91*(10), 3057–3068. doi:10.1890/09-2313.1

Petit-Cailleux, C., Davi, H., Lefevre, F., Garrigue, J., Magdalou, J.-A., Hurson, C., … Oddou-Muratorio, S. (under review). Combining statistical and mechanistic models to unravel the drivers of mortality within a rear-edge beech population. *PCIEcology*.

Pulido, F., Moreno, G., Garcia, E., Obrador, J. J., Bonal, R., & Diaz, M. (2014). Resource manipulation reveals flexible allocation rules to growth and reproduction in a Mediterranean evergreen oak. *Journal of Plant Ecology*, *7*(1), 77–85. doi:10.1093/jpe/rtt017

Quézel, P., & Médail, F. (2003). *Écologie et biogéographie des forêts du bassin méditerranéen*. Elsevier.

Sánchez-Humanes, B., & Espelta, J. M. (2011). Increased drought reduces acorn production in Quercus ilex coppices: Thinning mitigates this effect but only in the short term. *Forestry*, *84*(1), 73–82.

doi:10.1093/forestry/cpq045

Schielzeth, H. (2010). Simple means to improve the interpretability of regression coefficients. *Methods in Ecology and Evolution*, *1*(2), 103–113. doi:10.1111/j.2041-210X.2010.00012.x

Sherry, R. A., Zhou, X., Gu, S., Arnone, J. A., Schimel, D. S., Verburg, P. S., … Luo, Y. (2007). Divergence of reproductive phenology under climate warming. *Proceedings of the National Academy of Sciences*, *104*(1), 198–202. doi:10.1073/pnas.0605642104

Shipley, B. (2016). *Cause and Correlation in Biology*. *Cause and Correlation in Biology*. doi:10.1017/cbo9781139979573

Vacchiano, G., Hacket-Pain, A., Turco, M., Motta, R., Maringer, J., Conedera, M., … Ascoli, D. (2017). Spatial patterns and broad-scale weather cues of beech mast seeding in Europe. *New Phytologist*, *215*(2), 595–608. doi:10.1111/nph.14600

Wiley, E., Casper, B. B., & Helliker, B. R. (2017). Recovery following defoliation involves shifts in allocation that favour storage and reproduction over radial growth in black oak. *Journal of Ecology*, *105*(2), 412–424. doi:10.1111/1365-2745.12672

Yasumura, Y., Hikosaka, K., & Hirose, T. (2006). Resource allocation to vegetative and reproductive growth in relation to mast seeding in Fagus crenata. *Forest Ecology and Management*, *229*(1–3), 228–233. doi:10.1016/j.foreco.2006.04.003

Zhao, M., & Running, S. W. (2010). Drought-Induced Reduction in Global Terrestrial Net Primary Production from 2000 Through 2009. *Science*, *329*(5994), 940–943. doi:10.1126/science.1192666

Zimmermann, J., Hauck, M., Dulamsuren, C., & Leuschner, C. (2015). Climate Warming-Related Growth Decline Affects Fagus sylvatica, But Not Other Broad-Leaved Tree Species in Central European Mixed Forests. *Ecosystems*, *18*(4), 560–572. doi:10.1007/s10021-015-9849-x

Zinn, K. E., Tunc-Ozdemir, M., & Harper, J. F. (2010). Temperature stress and plant sexual reproduction: Uncovering the weakest links. *Journal of Experimental Botany*, *61*(7), 1959–1968. doi:10.1093/jxb/erq053

3 Contributions scientifiques de la thèse

Congrès nationaux et internationaux

— Mars 2017 Functional Ecology Conference La grande motte (FR). Présentation intitulé "Understand trees mortality causes by using a physiological process-based model". Dans la session Progress in vegetation modelling through better integration of experiments and modelling. 3

— Mars 2018, 5TH Young Natural History Scientits' Meeting, Paris (FR).Présentation orale intitulée "Combining statistical and mechanistic models to unravel the causes of mortality causes within rear-edge beech population." Dans la session Biodiversity Dynamics and Conservation. Résumé p.24 3

— April 2019,European Geosciences Union (EGU), Vienne (Au). Pré-sentation orale intitulée "Risk of fruit production failure caused by the inter-action of phenology changes and extremes events occurrence detected with aprocess-based model", dans la session Phenology and seasonality in climatechange. Résumé page 291 3

— Aout 2019,European Ecological Federation (EEF) , Lisbon (PT). Présentation orale intitulée "Combined effects of climate and management on beech tree vulnerability and net ecosystem exchange across Europe.", dans la session Forest response to climate change. Résumé page 297 3

Vulgarisation

— Fête de la science : Speed dating jeunes chercheurs, Rencontres avec des jeunes étudiants de l'Université d'Avignon, de l'Inra et du CEA (2018), animation de stand sur la phénologie et changement climatique (avec F. Jean en 2017, INRA URFM), sur le changement climatique et la reproduction (avec F. Jean en 2018, INRA URFM).

— Un chercheur à ma table, café des sciences spécial doctorant

— Intervention avec Hélène Fargeon sur la thématique du "Changement climatique et forêts" pour un cour en licence 1 de géographie sur les Grands défis climatiques, (2018).

Autres missions scientifiques

— Co-Auteure dans "Distribution of endemic bark beetle attacks and their physiological consequences on Aleppo pine", soumis dans Forest ecology and management.

— Participation à la rédaction d'un manuel d'utilisation de CASTANEA, avec Hendrik Davi et Journé Valentin.
`https://www.overleaf.com/read/nmyvszjkfxxh`

— Groupe de travail sur les cSDM à Sopron (Hongrie) organisé par NAIK ERTI (september - 2017)

— Présidente fondatrice de l'Association des jeunes Chercheurs d'Avignon pour la Communication et l'Intégration des Arrivants (2017/2018). Puis membre du conseil d'administration (2018/2019)

— Membre organisateur de la journée doctorale de l'ED 536 (sciences) (juin 2018)

— Participation à l'organisation du festival pint of science pour le compte d'ACACIA (mai 2019)

— Participation à l'organisation d'une soirée de vulgarisation scientifique " Les jeunes chercheurs discutent de front de science". (Avril 2019)

Understanding trees mortality causes by using a physiological process-based model

Cathleen Petit[1], Hendrick Davi, H.[1], S. Oddou-Muratorio[1]

[1]URFM, INRA, Avignon, France
cathleen.petit@inra.fr

Abstract

In this study we used a process-based model to describe mortality causes of forest trees under global change. We used CASTENEA to simulate over time the development of tree with different characteristics describing the tree life cycle (diameter, height, leaf traits) and growing rate in different environmental conditions (temperature, precipitation, soil water content). These simulations allow us to determine carbon and hydraulic physiological thresholds matching the best with tree mortality observed rate. This methodology was tested by varying each environmental parameter independently and by varying several environmental parameters at the same time on a mortality event of beech tree (*Fagus sylvatica*) in South-Eastern France. We observed several causes of tree mortality and observed different patterns responses to the drought.

Keywords: Process-based model, Climate change, mortality, Tree, Fagus sylvatica, beech tree

Combining statistical and mechanistic models to unravel the causes of mortality causes within rear-edge beech population

Cathleen Petit *† [1], Sylvie Muratorio , François Lefevre , Hendrik Davi

[1] Unité de Recherches Forestières Méditerranéennes (URFM) – Institut National de la Recherche Agronomique : UR0629 – Domaine saint Paul, 84000,Avignon, France

Several studies report increasing dieback of trees over temperate forests, a major issue in ecology is to understand the mortality physiological drivers. In this study we combine statistical and mechanistic models to investigate the causes of mortality in a major European tree species (*Fagus sylvatica*) at its south margin range, based on individual monitoring of 5600 trees since 2003. First we used logistic regression and survival analysis to characterise the respective effects on individual mortality by exogenous (competition) and endogenous (size, defoliation, fungi presence) biotic factors. Then the effect of annual climatic factors on mortality at population scale. Secondly, we used a process-based model CASTANEA to simulate over time the development of beech trees with different individual characteristics (height, diameter and leaf traits) in different environmental conditions to mimicking the surveyed population. The first analysis shows that a combination of exogenous (climatic and biotic) and endogenous factors caused tree mortality. Drought was associated to increased mortality at population level. At individual scale, crown defoliation and the *Oudemansiella mucida* (fungi) presence were both found to be early signs of mortality. We found that the competition increase the mortality at early life stage and suggest that mortality is driven by light competition. Secondly, we will compare the simulations of CASTANEA model with these statistical predictions, and investigate if extremely low hydric potential occur when mortality is caused by drought. With the combination of these two methods we hope to better understand the whole process driving tree to death.

Keywords: Mortality, Fagus sylvatica, Tree, Mechanistic model, Longitudinal analysis

*Speaker
†Corresponding author

24

Geophysical Research Abstracts
Vol. 21, EGU2019-14686-1, 2019
EGU General Assembly 2019

Risk of fruit production failure caused by the interaction of phenology changes and extremes events occurrence detected with a process-based model

Valentin Journé, Cathleen Petit, Sylvie Oddou-Muratorio, and Hendrik Davi
INRA, URFM, France (valentin.journe@inra.fr)

Many perennial species, such as trees, show large variations of fruit production between years (the so-called masting) which can have major consequences on forest dynamic and species interactions. Among other drivers of fruit production failure, years of reduced fruit production can be due to the increase of temperature and the resulting advance in vegetative and reproductive phenology and timing of extreme events, such as drought or late frost. Indeed, flowers may fail to complete their maturation due to a 'veto' effect, i.e. variation of climatic conditions, promoting pollen limitation, fruit abscission, or more generally inducing reproductive failure. This veto effect may alter reproductive cycle which in turn impacts forest ecosystem functioning. Our hypothesis is that interactions between shifts in phenology and "veto" effects have major consequences on reproductive tree cycle at species range scale, considering the increasing number of extreme climatic events associated to ongoing and predicted climate change. To investigate this hypothesis, we used a process-based model (CASTANEA) previously calibrated and validated on European beech, a major European temperate tree. The model simulates stocks and fluxes between forest and atmosphere, from physiological characteristics of tree species. We simulated fruit production across Europe with a scenario accounting for veto (frost or drought) and a scenario without veto in order to detect the species margins associated to reproduction failure for that species. The detailed comparison of the two scenarios allowed us to assess when and where the different "vetos" explain the reproductive failure and how they interact with phenology changes. This study highlight how extreme climatic events can disrupt phenology of reproduction and thus change species distribution.

30/07 | 11h00
PARALLEL SESSION I - T7.P1 - FORESTS RESPONSES TO CLIMATE CHANGE
Room 2.3.13 | Topic 7 - Climate and global changes (4); Topic 12 - Theoretical and evolutionary ecology (1)

OC-022 - (EEF2019-13972) - COMBINED EFFECTS OF CLIMATE AND MANAGEMENT ON BEECH TREE VULNERABILITY AND NET ECOSYSTEM EXCHANGE ACROSS EUROPE.

Cathleen Petit (France)[1]; Hendrik Davi (France)[1]; Sylvie Oddou Muratorio (France)[1]; François Lefèvre (France)[1]; Pieter Johannes Verkerk (France)[2]

1 - INRA, UR 629 Ecologie des Forêts Méditerranéennes, URFM;
2 - European Forest Institute

The impacts of climate and global change on forests are expected to be strong, with increasing tree mortality leading to changes in forest ecosystem services. Here, we investigate how management practices and climate jointly influence the ecophysiology of European beech across Europe. We used the process-based model CASTANEA to simulate the vulnerability and Net Ecosystem Exchange (NEE) of beech trees. The vulnerability integrates the risk of mortality related to hydraulic failure, carbon starvation and late frost. Simulations were run all over Europe, with a grid of 3174 cells, each measuring 45km by 45 km. Simulation were run from 1961 to 2005 under current climate, and from 2006 to 2100 using two contrasted climate change models (CM5 and HadGEM) with two scenarios of atmospheric carbon change (RCP 4.5 and RCP 8.5). Moreover, we considered different management patterns across Europe, (i) no management over Europe, (ii) unique managements over Europe, (iii) historical management adapted to the region. With CM5 without management, we find very little evolution of the vulnerability, independently of the increase in CO2 scenario. However, we found that beech vulnerability increases in the south of Europe due to extreme stresses (frost and drought). With CM5 and unique management scenarios, we find a slight increase in the NEE across Europe. This approach allows us to explore the NEE and vulnerability changes across Europe and if the management mitigate spatial differences under several climate change scenarios.

CASTANEA Manual

H. Davi, V. Journé, C. Petit-Cailleux

hendrik.davi@inra.fr

February 28, 2020

Contents

Chapter 1

CASTANEA model

CASTANEA is an ecophysiological process-based model, which simulate carbon, energy and water flux in monospecific forests. The model can be used for major European tree species : *Quercus ilex*, *Quercus pubescens*, *Quercus petraea*, *Fagus sylvatica*,*Pinus sylvestris*, *Pinus pinaster*, *Abies alba*, *Picea abies*, *Pinus halepensis*, *Pinus nigra*, *Pseudotsuga menziesii*, *Cedrus atlantica*, *Pinus uncinata*.

Tree structure is divided into five compartments, for aboveground and belowground biomass. These compartments include stem, branches, coarse and fine roots and reserves. Reserves are an unlocated compartments. Main processes are simulated at half-hourly scale (photosynthesis, maintenance and growth repsiration, soil heterotrophic respiration, transpiration and evapotranspiration) and at daily scale (carbon allocation, phenology of organs, leaf area index and water content).

The basic version of the model simulates an average tree at the stand scale, meaning that there are no variability between trees and no explicit competition between trees neither for light nor for water. The canopy is divided into different sublayer. The soil is divided into two layers: top soil (30 cm) and entire soil. A version under developement will take into account the subsoil in karstic soils.

Description can be found in several articles : Dufrêne et al. 2005; Le Maire et al. 2005; Loustau et al. 2005; Davi et al. 2006a; Davi et al. 2006b; Davi et al. 2008; Davi et al. 2009; Delpierre et al. 2009; Delpierre et al. 2012; Oddou-Muratorio and Davi 2014; Guillemot et al. 2014; Guillemot et al. 2015; Davi and Cailleret 2017; Guillemot et al. 2017.

Two versions of CASTANEA exist, one developed at the INRA Institute from Avignon (INRA-URFM), and another one at the CNRS Institute (ESE) from Paris (all previous studies did not combine the development of both two versions). The report present here the INRA version, developped by H. Davi, in `Java` language and implemented in Capsis (Computer-aided projection of strategies in silviculture, `http://capsis.cirad.fr/capsis/presentation`).

What do you need to know:

1. Have Capsis plateform on your computer to run CASTANEA model. The model can be updated and modified through Capsis server

2. Once you have the model, you need to have 1/ a climate file (e.g. with daily precipitation, temperature...), 2/ a species file (file with species characteristics, do not need to be modified) and 3/ an inventory file with site characteristics (e.g. soil structure, tree diameter,...)

3. Run simulation with capsis interface/terminal/R software

Adding note - February 28, 2020: The development of the model is still in progress for spatial simulation (PhD, C. Petit-Cailleux), resources allocation to reproduction compartment (PhD, V. Journé), water-stress and frost damage (H. Davi). The model will also run with the R software.

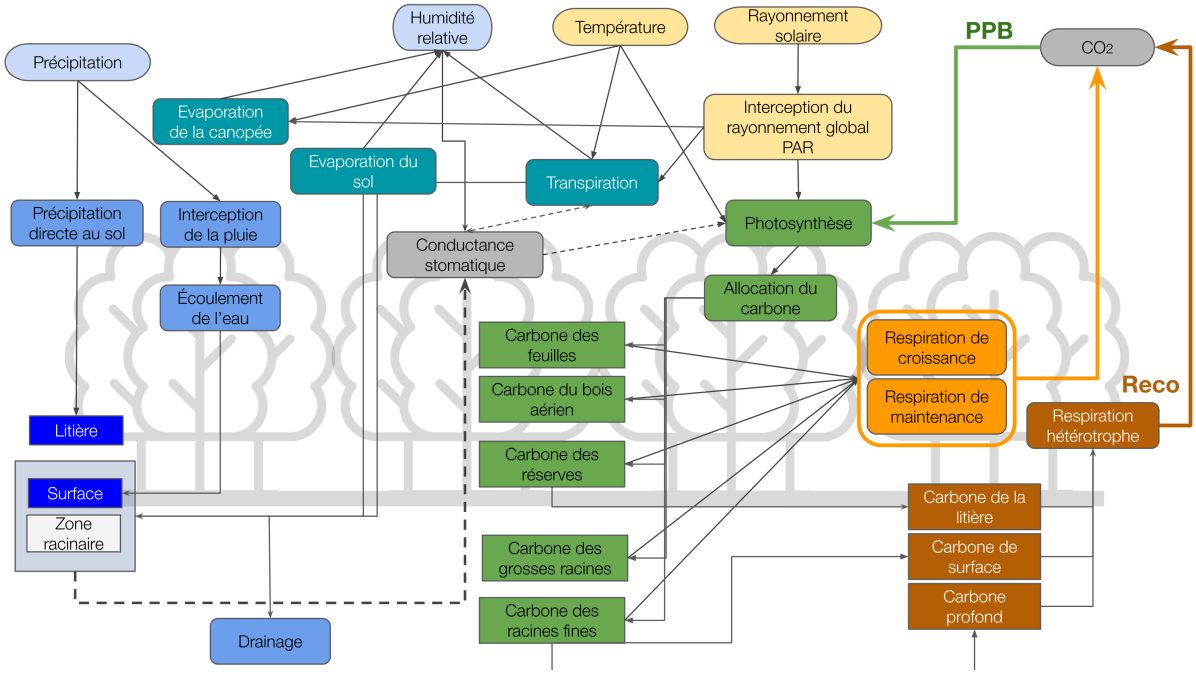

Figure 1.1: General overview of the CASTANEA process-based model.

Chapter 2

Capsis and CASTANEA guideline

Here, steps are described for Linux users.
All information provided in this document are coming from `http://capsis.cirad.fr` (it more than recommended to read directly the information on the website, which are updated, exist in French and English, for Linux, Mac and Windows). We also recommended to follow the courses in JAVA and/or Capsis functioning proposed by Capsis managers (Updating contact can be find thanks to the website).

2.1 Description of Capsis, SVN and CASTANEA

To use CASTANEA through the Capsis interface, that require to install SVN, Capsis and CASTANEA library in the user computer.

SmartSVN is a versioning system called (Subversion) on the `amap-dev.cirad.fr` server. The SmartSVN 'repository' contains all last versions of all the sources. It can rebuild all the older versions by applying the versioned differences from release to release if needed. SmartSVN software permit to share files between users by committing (share with the community information from your own local copy by implementing the shared-version with your local version) and updating (bring information from the shared-version in your local copy) local version. Hence you can find in your local version data files from other project in your different installed section of Capsis.

Capsis (Computer-Aided Projection of Strategies In Silviculture) is a software created to simulate the evolution of a forest stand under different scenarios and tools. It used, improved and implemented by several research team via the libraries which correspond to different model (physiology, phenology, light use, water drainage) all link to forest ecosystems. "Thanks to its flexible architecture, it is possible to integrate heterogeneous models (uneven-aged, several species) with various processes (growth, competition, mortality, regeneration, dispersion ...) and to run simulations in interactive or script modes. Some models can have very particular properties, *e.g.* radiative balance, genetics information at the individual level, internal biomechanics or wood quality."

More information about Capsis : http://www.inra.fr/en/Partners-and-Agribusiness/Results-Innovations-Transfer/All-the-news/Capsis

2.2 Installation for Linux user

All information and data available there: http://capsis.cirad.fr/capsis/download.

MORE COMMENTS

1. Ensure JAVA 1.8 is installed on your computer
2. Install SmartSVN : https://www.smartsvn.com/
3. Run it from the specific folder where it was installed from the terminal (open a terminal 

, and use cd to define software path):

   ```
   sh smartsvn.sh
   ```

When you have SmartSVN installed you can specify you working Capsis path.

You can run the installer:

```
java -jar capsis-setup-file-name.jar
```

or

Steps for the first installation of Capsis:

1. Open a new terminal and go in the folder where you want to install Capsis in local.

   ```
   cd /home/USER/PATH_OF_TARGET_FOLDER
   ```

2. Install capsis

   ```
   svn checkout --usernamecd https://amap-dev.cirad.fr/svn/capsis/trunk capsis4
   ```

We proposed here Linux commands to update and commit file to the server. However it is also possible to use directly the interface which is friendly use. Attention, when you modified a file, and after checked it (if the modified file is working), you must first 1/add the file (if it is a new file) ant then 2/commit the file to avoid conflicts in Capsis.

Some commands to modify file, and their path with the Linux terminal:

- To update:

```
svn up
```

- To commit:

```
svn ci
```

- To add script:

```
svn add bin/LIBRARY/model/MODELOutput.java
```

- To add data:

```
svn add data/LIBRARY/FILE.inv
```

- To remove files:

```
svn remove PATH/FILE
```

2.3 Run CASTANEA through the Linux console

Is useful to run CASTANEA with script when you reach to run lot of different scenarios.

Steps :

- In the capsis folder build a text file with command lines (here mycommand.txt)

  Example of content:

  ```
  sh capsis.sh -p script castaneaonly.myscripts.CastOnly4SA inventory.txt climate.txt
  ```

  (this command line say: run capsis with a the java scritp named CastOnlyS4SA (this scrip can be find in the folders : castaneaonly/myscripts) and with this inventaire and this climate)

- Transform `mycommand.txt` in executable file

  Console: `chmod + x mycommand.txt`

- Run it

  Console : `./mycommand.txt`

  (This mean execute mycommand.txt, "./" it can be find in this folder)

- Output

  Output files are storage in /var following this format :

`CastOnly4SA_inventory.txt_climate.txt_yearlyResults.log`

`CastOnly4SA_inventory.txt_climate.txt_init.log`

`CastOnly4SA_inventory.txt_climate.txt_ParamValue-.log`

This mean: I use CastOnly4SA script to run CASTANEA with this inventory file and this climate data as input and this is the yearlyResults ouput (or init, or ParamValue)

Chapter 3

Architecture CASTANEA Capsis

In this part, we describe 1/ data files used for simulations (we will explain later how to create and used this files for simulation) and 2/ the model, with small description for each **JAVA** scripts. Parameters (for species and stand characteristic) are present in data files, and are then read in scripts. A general overview of the CASTANEA model on the CAPSIS platform is presented in the following figure3.1

3.1 Data files

Data files are present in the folder capsis4 `:"/home/USER/.../capsis4/data/castaneaonly"`. In this folder you have two kind of files (inventories files + species files), one folder for phelib or fitlib files and another folder for climate files.

- climate : current climate data and future used for simulation. Other files are present for Ventoux site, O3HP, Fontblanche, Hesse...
  Example's working : `barbeau2006_2018.txt`

- species file : parameters values for different for all different species (12 in total). Parameters are based on literature and experimentations (for example value from linear regression between tree DBH and tree height, construction costs,median seed mass...).
  Example's working : `CastaneaSpecies3.txt`.

- inventory file : stand characteristics used for simulation. In this file you have all information for your site characteristic (soil) and tree population (age, size, DBH, LAI...).
  Example's working : `VentouxForPDGt.txt`.

- fit2018 file : This file will be used if you specify in your inventory file `phenoMode = PHENO_FIT2018`. You need to specify also in your inventory this option `fit2018FileName = fit2018/UniGauzere.fit2018`. This fit2018 file will run functions from another model present in Capsis plateform (PHENOFIT, developped

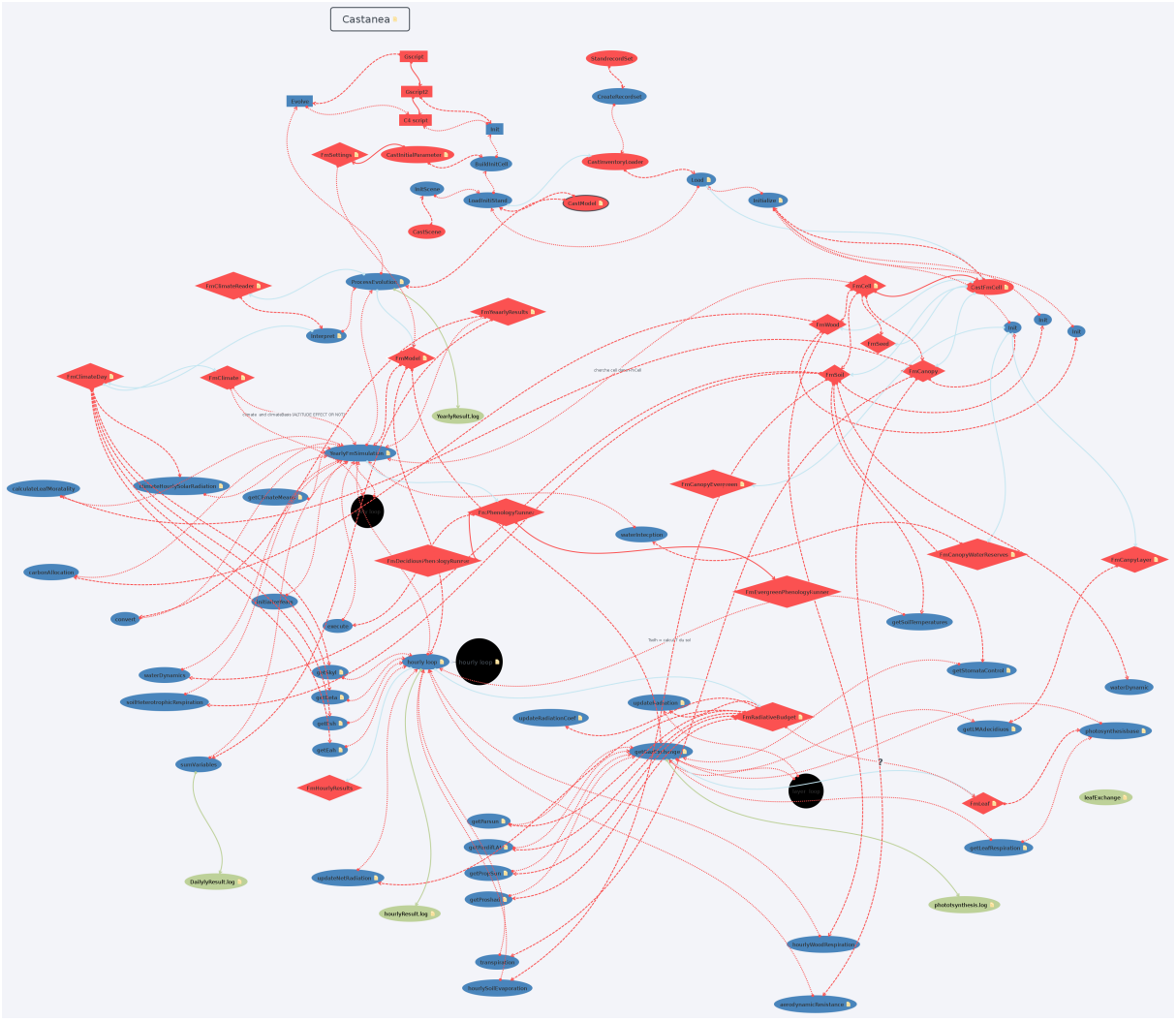

Figure 3.1: General overview of the CASTANEA process-based model on the CAPSIS version (updated in 2018, with all JAVA components.)

by I. Chuine). Contrary to initial version of CASTANEA model, we can now used many other phenology function (with higher accuracy). In this file we need to specify functions and values of parameters.
Example's working: `default.fit2018`

- phelib NOT USE NOW, IN PROGRESS : specific file for `FmPhenologyRunner` (description bellow), based on the Phelib model (present in the library `Phelib`; see Chuine et al, 1999 and Phenofit model from Chuine and Beaubien, 2001) which simulates leaf unfolding, flowering, fruit maturation and leaf senescence. Files are in the format XML.

3.2 Scripts CASTANEA model

Scripts are present in `:"/home/USER/.../capsis4/src/capsis/lib/castanea"` for the castanea library, and in `:"/home/USER/.../capsis4/src/castaneaonly/model"` for the model. All codes are in **JAVA** language. **JAVA** is an oriented object language, where to need to have class and objects. You can open scripts with an editor (e.g. Gedit, Notepad).
In these scripts you can find more details about the model (functions, sub-models...). In the following part, we present some useful information about these different scripts, mainly from the library, where you can find all process implemented in the model, and options that can be used (e.g. what process drive LAI, carbon allocation for wood). All class of castanea library are in `capsis/lib/castanea` defined as `Fm` at the head file name.

3.2.1 FmSpecies

Initial parameters, different parameters for species (call species file). They are parameters for respiration, biochemistry, allocation, allometry, reflectance, water, photosynthesis and phenology.

3.2.2 FmSettings

List of model settings, where you have initial parameters. Different kind of model are present, and can be modify or not by the user. It is possible to specify one of these models on the inventory file, in:

- `phenoMode =` : see section FmPhenologyRunner
- `LAImode =` : see section FmCanopy
- `stomataStress =` : see section FmSoil
- `temperatureEffectOnPhotosynthesis=` : see section FmLeaf
- `allocRemain =` : see section FmWood

- `allocSchema=` : to be improved
- `CO2mode =` : see section FmModel
- `ELEVATION_EFFECT =` : see section FmModel

3.2.3 FmCell

Define a square cell. Fluxes are at cell level and can be subdivided into other cell instances.

3.2.4 FmModel

for CO2 effect

- `CO2_FIXED` :
- `CO2_PAST_EVOLUTION` :
- `CO2_RCP2_6.6` :
- `CO2_RCP4_5` :
- `CO2_RCP6` :
- `CO2_RCP8_5` :

For elevation effect

- `ELEVATION_EFFECT_FIXED` :
- `ELEVATION_EFFECT_CONTINUOUS` :
- `ELEVATION_EFFECT_CONTINUOUS_NORTH` :
- `ELEVATION_EFFECT_CONTINUOUS_SOUTH` :

3.2.5 FmPhenology

Phenology object which establish a connection between CASTANEA and PHELIB. See **Fit5Phenology** and **FitlibPhenology.java** for more details.

3.2.6 FmPhenologyRunner

Simulate phenology of leaves and flowers. Different models of phenology are present. It is possible to specify one of these models on the inventory file, in the line `phenoMode =`

- PHENO_CASTANEA : initial module of phenology presented in Dufrene et al., 2005 (eq 9-11 for budburst and eq 16-19 for leaf fall). Budburst day after sum temperature exceed a threshold or after specific day. Same procedure for leaf fall. This module can also simulate a second flush after frost damage.
- PHENO_PHELIB : from Phelib library. Different sub-model which simulate leaf (from budburst to leaf senescence), flowers and fruits dynamics. Parameters initialized from the XML file input.
- |PHENO_FIT2018|: from phenofit function (I.Chuine library). Need to specify a phenology file in fit2018Filename option.

If using Phenofit phenology, the option is |fit2018Filename|= fit2018/FILENAME.fit2018

3.2.7 FmPhelibConnector

A CASTANEA connector to the PHELIB library (by Chuine). Read the phelib file (described above), to load 4 meta models, with the leaf model (2 phases, leaf dormancy break date and budburst date), flower model (2 phases, flower dormancy break date and flowering date) fruit maturation model (2 phases, fruit growth initiate date and fruit maturation date) and leaf senescence model (1 phase, leaf senescence date). Meta models are in the order : 1/leaf model 2/flower model 3/fruit maturation model 4/leaf senescence model. For 2 phases models, they may overlap; meaning that the second phase can start even if the first phase is not completed. See Chuine et Régnière, 2017 for details about philosophy and structure of phenology models.

3.2.8 FmWood

Carbon allocated to five compartments. Call parameters which define allocation coefficients to different structures. Description of calculation of respiratory coefficients for maintenance respiration.

- ALLOC_REMAIN_WOOD : surplus of resources allocated to wood
- ALLOC_REMAIN_RESERVES : surplus of resources allocated to reserves
- ALLOC_SCHEMA_DAVI2009 : allocation submodel from Davi et al 2009
- ALLOC_SCHEMA_REPRO : allocation submodel for reproduction. Application of cost of reproduction in resource allocation.

3.2.9 FmCanopy

Leaf functioning for deciduous and evergreen species.

- LAI_FIXED : LAI value is defined in the inventory file and stay the same during all the simulation; no LAI variation

- `LAI_NSC` :LAI value change with NSC (Non Structural Carbohydrates); LAI will depend of reserves (NSC)
- `LAI_DBSS_AND_DBH` : LAI will depend of DBSS (annual growth of reserve quantity) and DBH
- `LAI_NSC_AND_DBH` : LAI value change during simulation with NSC and DBH (diameter) of trees
- `LAI_NSC_DBH_AND_RDI` : LAI value change with NSC, DBH and relative density index.

3.2.10 FmCanopyEvergreen

Canopy functioning for evergreen species. Decrease photosynthetic capacity with leaf aging. Need to define specific parameters in species and inventory file, where you have details about number of cohorts.

3.2.11 FmCanopyLayer

A layer of leaves for the model. Calculate LMA and LAI of leaves and leaf surface. It is hypothesized that all leaf age are equally distributed in the canopy.

3.2.12 FmCanopyWaterReserves

Calculate daily water interception. In this part you have water interception (from stem, branch, depending of LAI...), which define water reaching the soil. Determine canopy water reserve.

3.2.13 FmLeaf

Leaf functioning

- `TEMPERATURE_EFFECT_BERNACCHI` :
- `TEMPERATURE_EFFECT_ARRHENIUS` :

3.2.14 FmSoil

Soil functioning.

- `STOMATA_STRESS_GRANIER` :
- `STOMATA_STRESS_RAMBAL` :

3.2.15 FmClimate

A set of days of climate, (called and loaded from climate files).

3.2.16 FmClimateDay

A day of climate, loaded from a climate file.

3.2.17 FmClimateReader

A format description to read a climate file at daily time step.

3.2.18 FmSeeds

Used to simulate buds and seeds number. Need to define two allocation, one to defined number of buds and one to defined final number of seeds mortality. It is also possible to active veto (such as drought and/or frost), which limit final number of seeds.

- `REPRO_INIT_STORAGE` : level of storage to determine a number of buds
- `REPRO_INIT_ALTERNATE` : similar to alternate bearing in fruit trees. Trade-off between current and future reproduction (i.e. null reproduction after a fruit crop).
- `REPRO_INIT_FIXED` : constant fraction of buds initiated
- `REPRO_INIT_CUE` : Difference during two summer temperature that defined number of buds.
- `REPRO_SURVI_SWITCHING` : if wood allocation is high, seed mortality is high (i.e. trade-off growth and reproduction)
- `REPRO_SURVI_MATCHING` : if wood allocation is high, seed mortality is low (i.e.positive correlation expected between growth and reproduction)
- `REPRO_SURVI_STORAGE` : if storage allocation is high, seed mortality is low (i.e.positive correlation expected between reserves and reproduction)
- `REPRO_SURVI_CST` : constant seed mortality

rateOfSeedProduction	rate of carbon allocated to seed production at the end of the year
Phelib file name	

Table 4.1: Species parameters. In this table we defined variable used. We defined also articles references and data used for all 12 species

Parameters	Species Parameters								
	Abies alba	**Cedrus atlantica**	**Fagus sylvatica**	**Pinus halepensis**	**Pinus nigra**	**Pinus sylvestris**	**Pinus uncinata**	**Quercus ilex**	**Quercus pubescens**
Leaf construction cost	1.21	1.21	1.2	1.32[A]	1.32	1.32[A]	1.32	1.294	1.2
Coarse roots construction cost	1.2	1.2	1.38	1.206	1.206	1.206	1.206	1.194	1.2
Fine roots construction cost	1.28	1.28	1.28	1.28	1.28	1.28	1.28	1.27	1.28
Wood construction cost	1.18	1.18	1.38	1.206[B]	1.206	1.206[B]	1.206	1.194	1.38
Rate of alive cells in stem	0.46	0.2[C]	0.245	0.2[C]	0.24[D]	0.24[D]	0.24[D]	0.15	0.21
Rate of alive cells in branches	0.46	0.34	0.42	0.2[C]	0.408	0.408	0.408	0.15	0.37
Rate of alive cells in coarse roots	0.46	0.2	0.26	0.2[C]	0.24	0.24	0.24	0.1	0.21
Initial [NSC]	0.15	0.15	0.15	0.15	0.15	0.15	0.15	0.15	0.2
Percentage of nitrogen in leaves	1.04	1.52	2.2	1.181	1.019[E]	1.33[F]	1.22[G]	1	1.85
[Nitrogen] in coarse roots	9,40E-04	9,40E-04	1,60E-03	1,18E-03[H]	8,50E-04[G]	0.001	8,50E-04[G]	4,00E-03	1,20E-03
[Nitrogen] in fine roots	8,20E-03	8,20E-03	0.007	8,27E-03[H]	8,10E-03	8,50E-03	8,10E-03	4,00E-03	9,90E-03
[Nitrogen] in branches	4,00E-03	4,00E-03	5,50E-03	1,18E-03[H]	4,90E-03[G]	1,80E-03	4,90E-03[G]	4,00E-03	5,50E-03
[Nitrogen] in stem	9,40E-04	9,40E-04	1,60E-03	5,91E-04[H]	1,42E-03[G]	1,60E-03	1,42E-03[G]	4,00E-03	1,20E-03
Predawn potential for growth cessation	-1.6	-2	-2.6[I]	-2.2	-2.28[I]	-2.1	-2.28[I]	-3.15[I]	-2.8
Initial carbon allocation coefficient to wood	0.42	0.42	0.1	0.42	0.42	0.3	0.42	0.1	0.2
Fine roots turnover	1	1	1[J]	1.5[J]	1.5	1.5[J]	1.5	1	1
Ratio between branches and total aboveground biomass	0.15	0.15	0.2	2,86E-01[K]	2,86E-01[K]	2,86E-01[K]	2,68E-01[L]	0.164	0.2
Parameters	**Abies alba**	**Cedrus**	**Fagus**	**Pinus**	**Pinus nigra**	**Pinus**	**Pinus**	**Quercus ilex**	**Quercus**

Parameters	Species Parameters								
	Abies alba	**Cedrus atlantica**	**Fagus sylvatica**	**Pinus halepensis**	**Pinus nigra**	**Pinus sylvestris**	**Pinus uncinata**	**Quercus ilex**	**Quercus pubescens**
		atlantica	**sylvatica**	**halepensis**		**sylvestris**	**uncinata**		**pubescens**
Ratio between coarse roots and total wood biomass	0.22	0.22	0.2	1,67E-01[O]	1,83E-01[M]	2,31E-01[M]	2,97E-01[N]	1[C]	0.2
Ratio between fine roots and leaves biomass	0.3	0.3	1	1.25[J, P]	1.25[J, P]	1.25[J, P]	6,54E-01[Q]	0.33[R]	1
Branches mortality	7,00E-05	7,00E-05	7,00E-05	2,19E-04[S]	1,37E-04[K]	7,00E-05[K]	1,37E-04	7,00E-05	7,00E-05
Leaf area	5,00E-04	1,04E-05[T]	1,80E-03	1,50E-03[H]	1,11E-04[E]	7,05E-03	1,06E-04[U]	3,70E-03	3,70E-03
Leaf Mass per Area of sun leaves	292	245[T]	100	392[V]	227[E]	246.7[C]	256.1[E]	224	93
Extinction coefficient of Leaf Mass per Area within the canopy	7,29E-02	7,29E-02	0.187	0.076[C]	0.076[C]	5,79E-02[C]	0.076[C]	0.14	0.187
Leaf angle	40	40[W]	24	48[H]	48[H]	51	48[H]	30	33.15
Branches angle	8.7	8.7	45	10	68.23[X]	10	68.23	40	45
Slope of the crown area to dbh relation	8,15E-02[C]	8,04E-02[Y]	1,08E-01[C]	8,52E-02[C]	8,31E-02[Z]	7,43E-02[Z]	4,35E-02[AA]	1,19E-01[C]	1,87E-01[AB]
Intercept of the crown area to dbh relation	6,95E-01[C]	6,28E-01[Y]	1.04[C]	2,31E-01[C]	9,19E-01[Z]	1,35E+00[Z]	7,31E-01[AA]	7,81E-01[C]	-1,61E+00[AB]
Slope of the height-dbh relationship	1.4	4,36E+00[AC]	1.75	2.554[AD]	2,49E+00[C]	2,17E+00[C]	1,23E+00[C]	1,79E+00	7,11E-01
Power coefficient of the height-dbh relationship	0.751	3,65E-01[AC]	0.665	0.45[AD]	3,85E-01	5,15E-01[C]	7,26E-01[C]	5,05E-01	0.867
Form coefficient of stem	0.52[AE]	0.41[AF]	0.515[AE]	0.522[AE]	0.498[AE]	0.473[AE]	0.541[AE]	0.62	0.5
Wood density	414	545.2[AG]	764	545[C]	481[AH]	493	502[AI]	613	550
Canopy clumping coefficient	0.46	0.46	0.79	0.58	0.58	0.47[C]	0.43[C]	0.4	0.6
Wood reflectance in PIR domain	0.3	0.5[AJ]	0.39	0.3[AJ]	0.3[AJ]	0.3	0.3	0.39	0.39

Parameters	Species Parameters								
	Abies alba	**Cedrus atlantica**	**Fagus sylvatica**	**Pinus halepensis**	**Pinus nigra**	**Pinus sylvestris**	**Pinus uncinata**	**Quercus ilex**	**Quercus pubescens**
Wood reflectance in PAIR domain	0.15	0.1[AJ]	0.16	0.1[AJ]	0.1[AJ]	0.15	0.15	0.15	0.16
Leaf reflectance in PIR domain	0.33	4,27E-01[AJ]	0.34	0.36[AJ]	0.36[AJ]	0.259	0.259	0.3	0.32
Leaf transmittance in PIR domain	0.225	0.4[AJ]	0.388	0.375[AJ]	0.375[AJ]	0.188	0.188	0.388	0.26
Parameters	**Abies alba**	**Cedrus atlantica**	**Fagus sylvatica**	**Pinus halepensis**	**Pinus nigra**	**Pinus sylvestris**	**Pinus uncinata**	**Quercus ilex**	**Quercus pubescens**
Leaf reflectance in PAR domain	0.09	0.05[AJ]	0.057	5,86E-02[AJ]	5,86E-02[AJ]	0.055	0.055	0.085	0.05
Leaf transmittance in PAR domain	0.045	0.04[AJ]	0.048	0.04[AJ]	0.04[AJ]	0.005	0.005	0.1	0.11
Water storage capacity per unit of leaf area	0.4	0.4	0.3[AK]	0.208[AL]	1,19E-01[AL]	0.208[AL]	0.208[AL]	0.2	0.2
Water storage capacity per unit of bark area	0.32	0.32	0.3	1,95E+00[AL]	1,83E-01[AL]	1,95E+00[AL]	1,95E+00[AL]	0.2	0.3
Slope of the water interception coefficient	0.85	0.85	0.85	2.7	2.7	2.7[AM]	2.7	2.3	0.85
Intercept of the water interception coefficient	1.5	1.5	1.9	1.5	1.5	1.9	1.9	1.9	1.9
Ratio between stem flow and through fall	0.35	0.35	0.35	0.09[AM]	0.09	0.09[AM]	0.09[AM]	0.35	0.35
Intercept of ball and berry relation	0.001	0.001	0.001	0.001[AN]	0.001[AN]	0.001[AN]	0.001[AN]	0.005	0.001
Slope of ball and berry relation	6.7	1,05E+01[AO]	11.8	12.5[C]	10	5.7[AN]	5.4[AP]	10.07	9.27
Roots to leaves resistance to flow transport per Area Sapwood basis	2,87E+04	2,87E+04	1,15E+04	4,50E+04[C]	4,50E+04	1,79E+04[AQ]	1,79E+04	3,18E+04	1,15E+04
Capacitance of trunk	0.04	0.04	0.04	0.04	0.04	0.04	0.04	0.04	0.04
Water potential inducing 50% loss of conductivity	-4.67	-5.482[AG]	-3.175	51[AG]	-2.92[AG]	-3.2[AG]	-4.18[AG]	-3.261	-2.475
Dependency between vcmax and leaf nitrogen	18	10.47[AO]	26	2,08E+01[AR]	1,34E+01	1,65E+01[AG]	2,56E+01[AP]	22	27

Parameters	Species Parameters								
	Abies alba	**Cedrus atlantica**	**Fagus sylvatica**	**Pinus halepensis**	**Pinus nigra**	**Pinus sylvestris**	**Pinus uncinata**	**Quercus ilex**	**Quercus pubescens**
density									
Curvature of the quantum response of the electron transport rate	0.7	0.7	0.7	0.7	0.7	0.57	0.9[AP]	0.7	0.7
Base temperature for forcing budburst	1	1	0	3.5	0	0	0	0[C]	3.5
Base temperature for leaf growth	0	0	0	0	0	0	0	11[C]	11[C]
Base temperature for forcing leaf fall	20	20	20	20	0	0	0	20	20
Date of onset of rest	70	70	78	1	1	1	1	48	48
Parameters	**Abies alba**	**Cedrus atlantica**	**Fagus sylvatica**	**Pinus halepensis**	**Pinus nigra**	**Pinus sylvestris**	**Pinus uncinata**	**Quercus ilex**	**Quercus pubescens**
Date of onset of ageing	213	213	213	213	213	213	213	213	213
Critical value of state of forcing (from quiescence to active period)	400	400	190	1500	1160	1000[C]	1000	600	600
Critical value of state of forcing (from leaf development to maximum LAI)	350	350	200	200	200	200	200	280	200
Critical value of state of forcing (from leaf development to leaf maturity)	424	424	424	1700[AS]	424	424	424	900	424
Critical value of state of forcing (from nstart2 to leaf fall period)	100	100	100	100	100	100	100	230	100
Critical value of state of forcing from nstart2 to end of wood growth	300	300	60	-	150	150	150	300	100
Maximum needle or leaves lifespan	11	3	1	3	3	3	3	3	1

Parameters	Species Parameters								
	Abies alba	**Cedrus atlantica**	**Fagus sylvatica**	**Pinus halepensis**	**Pinus nigra**	**Pinus sylvestris**	**Pinus uncinata**	**Quercus ilex**	**Quercus pubescens**
NSC biomass above which seeds are produced	200	200	100	200	200	200	200	250	250
[NSC] under which tree die	0.22	0.3	0.48	1.34	0.74	0.72	0.38	1.7	0.28
Carbon cost to produce one seed	0.08	5,63E-02	0.45	1,28E-01[AT]	2,76E-02[E]	4,88E-03[E]	6,75E-03[AI]	1,92E+09[E]	2.115[AU]
Rate of carbon allocated to seed production at the end of the year	1	0.08	0.03	0.15	0.15	0.15	0.15	0.5	0.005

A. Villar & Merino

B. J. Rodríguez-Calcerrada

C. Personal data

D. Glavan et al., 2012

E. TRY

F. Renecofor stands PS04 PS15 PS63

G. Dawes et al., 2016

H. Simioni et al., 2016

I. Martin et al., 2017

J. Santantonio and Grace (1987)

K. Snowdon and Benson (1992)

L. Lin et yang 2003

M. Halle & Nicole

N. R. Ruiz-Peinado et al., 2011

O. Jackson and Chittendon (1981)

P. Ryan et al., (1996a)

Q. Hagdorn et al., 2013

R. Lopez 2001 & Rambal 2004

S. Vennetier. Personal data (80 % in 10 years)

T. Matteo et al., 2012

U. Boratyńska et al., 2000

V. BDD Hendrik Davi

W. Falge epicea

X. Cetin 2016

Y. Fitted Alice Bertrand

Z. Condes et Sterba 2005

AA. Ameztegui et al., 2012

AB. Cermak et al. 2008

AC. Sault 2002-2005

AD. Serrano et al. 2005

AE. Deleuze 2015

AF. Courbet 1991

AG. URFM Database

AH. Oliva et al., 2006

AI. Tapias et al., 2004

AJ. Williams et al., 1991

AK. Aussenac 1968 (Assuming a LAI of 6 for beech)

AL. Llorens & Gallart 2000

AM. Calibrated using Aussenac 1969

AN. Medlyn database

AO. Calibrated using Ladjal et al.,

AP. Fernadez et Fleck 2015

AQ. Irvin et al., 1998

AR. Calibrated from H. Davi and G. Simioni database

AS. Calibrated on IRSTEA data on Font-Blanche site

AT. Moya et al. 2017

AU. Landergotta et al., 2012

4.1.2 Climate

To run simulation, it is necessary to have climate matching beginning of year simulation needed and period covering simulation. If climate data start in 1970, and you want simulation before 1970, CASTANEA did not extrapolate climate.

Climate input data is presented here with a minimum of 10 columns :

Abbreviation	Variable	Unit
y	year	
m	month	
d	day of year	
gr	global radiation	MegaJ/d
rh	relative humidity	%
ws	wind speed	m/s
p	precipitation	mm
tmax	max temperature	C°
tmin	min temperature	C°
tj	average temperature	C°

Columns have to be ordered as below, separated with  :

```
y m   d   gr  rh  ws  p   tmax    tmin    tj
```

4.1.3 Inventory file

In the species characteristic table one line correspond to one simulation. As exposed previously CASTANEA simulate "one average tree" (the model is not individual based). We present here an example of inventory file. We present also some options available.

```
## CastaneaOnly model
## Inventory file


# General Sites
fmCellWidth = 20
#Size of cells (in m)
year = 1991
#Simulation start year
latitude = 44.18
#North in WGS84 decimal
longitude = 5.28
```

```
#East in WGS84 decimal

#CASTANEA parameters
CO2mode = CO2_FIXED or CO2_PAST_EVOLUTION or CO2_RCP2_6.6 or CO2_RCP4_5 or
    CO2_RCP6 or CO2_RCP8_5
#Submodel to determine the CO2 evolution across years

ELEVATION_EFFECT = ELEVATION_EFFECT_CONTINUOUS or
    ELEVATION_EFFECT_CONTINUOUS_NORTH or ELEVATION_EFFECT_CONTINUOUS_SOUTH
#Submodel to determine the effect of elevation on environmental parameters
    (Climatic only)

predawnModel= PREDAWN_CAMP or PREDAWN_CASTANEA or PREDAWN_VG
# soil potential at the sunrise

frostEffectCoef = 0
#Frost Impact ratio on the tree (BUDBURST? LEAVES or more compartment) //
    to be improved

iFROST= 0  or 1 or 2 or 3
#0 No frost
#1 frost kill a % of leaves and no leave repulse
#2 frost fill a % leaves and they are no second flush
#3 frost fill a % of leaves and they are a second flush

simulationReproduction= TRUE
#If true simulation of reproduction
simulationDefoliation= FALSE
#If true simulation of defoliation
sureau= FALSE
#Sureau use ton compute hydraulic conductance and hydraulic failure.
    Another process model.

LAImode = LAI_FIXED or LAI_NSC or LAI_NSC_AND_DBH or LAI_NSC_DBH_AND_RDI or
     LAI_DBSS_AND_DBH or LAI_FROMBUDS or LAI_STAND or LAI_NSC_AND_STAND
```

```
#Submodel to determine the LAI variation through year (or not).

fixedTronviv = FALSE
#If true, ratio of living tree can variate through the time.

fixedAgeOftrees = FALSE
#If true, all trees keep the age given in the inventory file and all
    biomass are keep to their initialize value every year

initWoodByVolume = FALSE
#If chosen "true", that initiate the biomass of wood with a volume-biomass
    relationship instead of DBH-biomass relationship. (If it's true you have
     to specify in the table volume in (treevolume))

fixedRDI= FALSE
# If true, RDI varied in fonction of LAI?

phenoMode = PHENO_CASTANEA or PHENO_PHELIB or PHENO_FIT2018 or PHENO_FORCED
#Submodel used to determine tree phenology. Can be linked to PHENOFIT model
    .

fit2018FileName = file.fit2018
# In complement of phenomode, and if phenoMode = PHENO_FIT2018
# Specify the file where all phenology parameter are in (repro and
    vegetative). File with extension .fit2018

stomataStress = STOMATA_STRESS_GRANIER or STOMATA_STRESS_RAMBAL
#Submodel used to determine stomatal stress responses SOIL

vcmaxStress = FALSE
#If true a relationship between Vcmax and Psoil is use to compute Vcmax
    through the year

doughtOnRespiration = FALSE
# Do varied respiration proportion in summer
```

```
QDIXvar= FALSE
# ?

iKarst= 0 or 1
# no water in deep soil if 0
#if iKarst =1 a sub-model a soil water budget is activated

rootsCavitation = TRUE
#To allow or not cavitation in root systems

temperatureEffectOnPhotosynthesis= TEMPERATURE_EFFECT_BERNACCHI or
    TEMPERATURE_EFFECT_ARRHENIUS
#Submodel used to determine the temperature effect on photosynthesis in
    simulation

allocSchema= ALLOC_SCHEMA_DAVI2019 or ALLOC_SCHEMA_REPRO
#Submodel used to determine the different compartment allocation ratio.

allocRemain = ALLOC_REMAIN_RESERVES or ALLOC_REMAIN_WOOD
#Submodel used to determine the reserve allocation ratio

allocRepro = REPRO_OLD or REPRO_JOURNE
#submodel allocation to reproduction. If REPRO_JOURNE selected, need to
    specify to other argument below

initRepro= REPRO_INIT_STORAGE or REPRO_INIT_ALTERNATE or REPRO_INIT_FIXED
    or REPRO_INIT_CUE
#defined a number of buds

surviRepro= REPRO_SURVI_CST or REPRO_SURVI_SWITCHING or
    REPRO_SURVI_MATCHING or REPRO_SURVI_STORAGE
#defined seed survival

vetoFrost= TRUE
```

```
# impact seed numer, based on frost dammage (leinonen, 1996)

vetoDrought= TRUE
# impact seed numer, based on PLC (eq: Martin ecolet)

basicMeteoFile = Character
#is the name of the meteofile used to compute the effect of elevation

parameterPot = -2
#the parameter of the exponential relationship between soil water content
    and soil water potential

#option for simulations
output = 0 or 1 or 2 or 3
#0 write only yearly data
#1 write only yearly and daily data
#2 write yearly, daily and hourly data
#3 write yearly, daily and hourly data canopy layer by canopy layer

logPrefix = Character
#This allow to put the same prefix for all output from the same simulation

NB_CANOPY_LAYERS= Integer
#is the number of layer simulated to splitting up the canopy.

optional variables = -
#if "-", no optional variables.
#optinal variable available
## nitrogen LMA nc coefBeta MRN gfac slopePotGs Nstress Tsum woodStop GBV
    CRBV tronviv PotWood coefrac rootshoot aGF dateDeb rateOfSeed costSeed
    reservesToReproduce
```

Linked to this inventory file, we also need to add row with specific values, linked to different sites characteristics. Several row can be added in one inventory file, and with many different species. Columns must be separated with  . The last column correspond to the optional variable. If no optional variables are included in the inventory file, this column must have a space or a "-" (both in the argument `optional variables = -` and the last column). We present here one table we must provided site values and one table with optional variables currently in the model.

Abbreviation	**Variable**	**Unit**	**Notes**
Name	Name of Castanea Cell		
Species	Species code		1 = Holm oak, 2 = White oak, 3 = Oak, 4 = Beech, 5 = Scots pine, 6 = Maritime pine, 7 = Silver fir, 8 = Spruce, 9 = Aleppo pine, 10 = Pinus nigra, 11 = Douglas, 12 = Cedrus, 13 = Pinus uncinata
xc	X localisation	°	in wgs84
yc	Y localisation	°	in wgs84
zc	elevation	m	WARNING put to zero if climate is already corrected for elevation
soilHeight	soil depth	cm	
stone	stone content	%	
wfc	humidity at field capacity		
wilt	humidity at wiling point		
propMacro	proportion of macroporosity		
bulk	soil bulk		
SOLCLAYtop	clay proportion in topsoil (30 cm)		
SOLCLAYsol	clay proportion in all soil		
SOLFINtop	proportion of fine particles (clay + silt) in top soil		
SOLFINsol	proportion of fine particles (clay + silt) in soil		
SOLSANDtop	sand proportion in topsoil (30 cm)		
SOLSANDsol	sand proportion in all soil		
prac	fine roots proportion in top soil		

pracDeep	fine roots proportion in deep soil		only for karstic soils
deepSoilDep	deep soil depth		only for karstic soils
stoneDeep	stone content in deep soil		only for karstic soils
MacroDeep	proportion of macroporosity in deep soil		only for karstic soils
dbh	diameter at breast height	cm	
Nha	hectare density		
Vha	hectare volume	m^3/ha	
age	age of trees		Do not work well for old trees
clumping	canopy clumping		
LAI	Leaf Area Index		

Table 4.2: CASTANEA inventory file

Optional variable abbreviation	**Description**
nitrogen	nitrogen content in leaves
LMA	Leaf Mass per Area
nc	Dependency between VC_{max} and leaf nitrogen density
coefBeta	ratio VC_{max}/VJ_{max}
MRN	Respiration dependency of nitrogen of all organs
gfac	slope of the ball and berry relationship
slopePotGs	drought effect on Gs Rambal
Nstress	drought effect on Gs Granier
Tsum	Critical value of state of forcing (from quiescence to active period)
woodStop	Critical value of state of forcing from NStart2 to end of wood growth
GBV	allocation coefficient to wood
CRBV	construction cost of wood
PotWood	drought effect on growth
coefrax	ratio between fine roots and leaves biomass
rotshoot	ratio betwwen coarse roots and total wood biomass
aGF	slope of the height-dbh relationship
dateDeb	date of budburst, only for forcing budburst date, set to zero
rateOfSeedJourne	coefficient to defined number of reproductive buds from undifferentiated buds

costSeed	cost of seeds. How many grams of carbon needed to produce seeds
reservesToReproduce	levels of reserves needed for reproduction

Table 4.3: Optional variables. Values can be added at the end of the row, and must match ordering defined in the argument `optionalVariables =`

4.1.4 Phelib file

This part is not developed here. Currently in progress for the phenology part.

4.1.5 Fit2018 file

It is a one line argument separate by tab, with 8 expected arguments. CASTANEA species code, then five functions from phenofit and two parameters depending of the functions. Several functions can be used, to simulate leaf and reproductive phenology, and are present in : `capsis4/src/capsis/lib/phenofit/function`.
More details about functions can be found online with the PMP guide (`https://www.cefe.cnrs.fr/fr/recherche/ef/forecast/index.php?option=com_content&view=article&id=921&Itemid=154`). We present here the general structure and an example.

- CASTANEA species number
- `leafDevelopmentPhaseFunction`, simulate budburst date. Currently you can find three main different functions available to simulate budburst date e.g. UniChillThreshold; UniForc; Gauzere.
- `flowerDevelopmentPhaseFunction`, simulate flowering date. The same three function as previously. (Same underlying mechanisms).
- `leafSenescencePhaseFunction`, simulate the senescence date. Function available e.g. SenDelpierre.
- `fructificationPhaseFunction`, simulate the fruit growth and their maturation. Function available e.g. Fructification2Phases.
- `frostFunction`, simulate frost damages. Function available: Frost
- `senescenceSigma`, parameter link to phenology function. (SenDelpierre function, in Phenofit)
- `maturationSigma`, parameter link to phenology function. (Maturation of fruit in Fructification2Phases function, in Phenofit)

An example with Unichill: arguments must be separated with a ⇆ (Tabulation and not Enter as in our example)

7

UniChillThreshold(−61.1;12.977;−0.08;13;73.72483;32)

UniChillThreshold(−61.1;12.977;−0.08;13;73.72483;32)

SenDelpierre(13.38;29.95;1.0;2.0;570.6;0.1)

Fructification2Phases(−0.2;14.7297;9.0;5.002;100.0;3.7;0.6;2.0)

Frost(−6;−20;−5;−5;10;−16;−8;−8;−12;−12;10;16)

0.1

0.037

4.2 Output files

We present here must important files that it is possible to obtain from CASTANEA. As mentioned previously, several output can be used, such as hourly, daily and yearly files. We will present here these main three outputs, corresponding to results simulations.

Abbreviation	Variable	Unit	Notes
FmCellId			
X			
Y			
altitude			
species			
LAI	Leaf Area Index	unitless	
GPP	Gross Primary Production	gC/M2/year	
NPP	Net Primary Growth, difference between gross primary production and ecosystem respiration (plant + soil)	gC/M2/year	
ETRveg	Evapotranspiration of canopy	mm	
ETRsol	Evapotranspiration of soil	mm	
TR	tree transpiration	mm	
ETP	potential evapotransipration	mm	
StressLevel	Soil water stress index	Mpa/year	
gel	number of frost day inducing damages	days	
DBBV	wood growth	gC/m2/year	
DBF	leaf growth	gC/m2/year	
DBRF	fine roots growth	gC/m2/year	
Rauto	autotrophic respiration	gC/m2/year	
Rgrowth	growth respiration	gC/m2/year	
Rcanopy	canopy respiration	gC/m2/year	
Rhetero	heterotrophic respiration	gC/m2/year	
BSSmin	minimal NSC (Non Structural Carbohydrates) reached during the year	gC/m2/year	
endWood	date at which growth stops	DOY	
Delta13C	leaf 13C	‰	
year	simulation year		
BF	Leaves biomass	gC/m2	
BiomassOfReserves	Biomass of NSC	gC/m2	
Ctop	top soil carbon content	gC/m2	

Csol	all soil carbon content	gC/m2	
ratioReserves	ratio between [NSC] and [NSC] species value		
BiomassOfFineRoots	biomass of fine roots	gC/m2	
BiomassOfTrunk	biomass of trunk	gC/m2	
AliveWoodBiomass	alive biomass of wood	gC/m2	
LeafDormancyBreakDate	date of leaf dormancy break	DOY	
BBday	date of budburst	DOY	
FlowerDormancyBreakDate	date of flower dormancy break	DOY	Need fit2018 mode
FloweringDate	Day of year for flowering	DOY	Need fit2018 mode
FruitGrowthInitDate	Day of beginning fruit growth	DOY	Need fit2018 mode
FruitMaturationDate	Day of year for fruit maturation	DOY	Need fit2018 mode
LeafSenescenceDate	date of leaf fall simulated using phenofit	DOY	Need fit2018 mode
endLeaf	date of end of leaf fall	DOY	
Tmoy	annual mean temperature	°C	
Tmax	annual max temperature	°C	
Tmin	annual min temperature	°C	
Rg	annual mean global radiation	MJ/year	
PRI	annual sum of precipitation	mm/year	
RH	annuel mean relative humidity	%	
age	tree age		
rw	ring width increment	mm/year	
dbh	diameter at breast height	cm	
height	tree height	m	
seed	seed production	seed/tree	
RU	soil water content	mm	
drainage	soil water drainage	mm/year	
ca	CO2 atospheric concentration	ppm	
CrownProjection	crown projection	m2	
PLeafmin	yearly minimal of midday leaf water potential	Mpa	
DBHinit	initial diameter at breast height	cm	

TSUMBB	sum of temperature requirement	°C
g1	slope of ball and berry	
nc	ratio between Vcmax and leaf nitrogen density	
nf	leaf nitrogen content	%
LMA	leaf mass per Area	g dry matter/m2
coefrac	ratio between fine roots biomaass and leaf biomass	
GBVmin	minimal allocation coefficient to wood	
woodStop	date at whiche wood growth srops	DOY
CRBV	construction cost of wood	gC/gC
potsoiltowood	soil water potentail below which wood growth stops	Mpa
RDI	relative stand density index	stem/ha
treevolume	stem volume	m3
StandVolume	stand volume	m3/ha
climateFileName		
outputFile	Name defined in the argument logPrefix	
reservetoBud	reserve allocated to bud (reproduction)	
numberOfSeeds	number of seeds produced with the model reproduction allocation	seeds/m2
numberOfFruits	number of fruits produced, for coniferous (1 cone structure = 1 fruits with many seeds)	fruits/m2
rateOfEmptySeeds	rate of empty produced	

Table 4.4: CASTANEA output yearly file

References

Davi, H., Barbaroux, C., Dufrêne, E., François, C., Montpied, P., Bréda, N., and Badeck, F. (2008). "Modelling Leaf Mass per Area in Forest Canopy as Affected by Prevailing Radiation Conditions". *Ecological Modelling* 211.3-4, pp. 339–349.

Davi, H, Barbaroux, C, Francois, C, and Dufrene, E (2009). "The Fundamental Role of Reserves and Hydraulic Constraints in Predicting LAI and Carbon Allocation in Forests". *Agricultural and Forest Meteorology* 149.2, pp. 349–361.

Davi, H. and Cailleret, M. (2017). "Assessing Drought-Driven Mortality Trees with Physiological Process-Based Models". *Agricultural and Forest Meteorology* 232, pp. 279–290.

Davi, H., Dufrêne, E., Francois, C., Le Maire, G., Loustau, D., Bosc, A., Rambal, S., Granier, A., and Moors, E. (2006a). "Sensitivity of Water and Carbon Fluxes to Climate Changes from 1960 to 2100 in European Forest Ecosystems". *Agricultural and Forest Meteorology* 141.1, pp. 35–56.

Davi, H. et al. (2006b). "Effect of Aggregating Spatial Parameters on Modelling Forest Carbon and Water Fluxes". *Agricultural and Forest Meteorology* 139.3-4, pp. 269–287.

Delpierre, N. et al. (2009). "Exceptional Carbon Uptake in European Forests during the Warm Spring of 2007: A Data-Model Analysis". *Global Change Biology* 15.6, pp. 1455–1474.

Delpierre, N. et al. (2012). "Quantifying the Influence of Climate and Biological Drivers on the Interannual Variability of Carbon Exchanges in European Forests through Process-Based Modelling". *Agricultural and Forest Meteorology* 154-155, pp. 99–112.

Dufrêne, E., Davi, H., François, C., Maire, G. le, Dantec, V. L., and Granier, A. (2005). "Modelling Carbon and Water Cycles in a Beech Forest". *Ecological Modelling* 185.2-4, pp. 407–436.

Guillemot, J., Martin-StPaul, N. K., Dufrêne, E., François, C., Soudani, K., Ourcival, J. M., and Delpierre, N. (2015). "The Dynamic of the Annual Carbon Allocation to Wood in European Tree Species Is Consistent with a Combined Source–Sink Limitation of Growth: Implications for Modelling". *Biogeosciences* 12.9, pp. 2773–2790.

Guillemot, J., Delpierre, N., Vallet, P., François, C., Martin-StPaul, N. K., Soudani, K., Nicolas, M., Badeau, V., and Dufrêne, E. (2014). "Assessing the Effects of Management on Forest Growth across France: Insights from a New Functional–Structural Model". *Annals of Botany* 114.4, pp. 779–793.

Guillemot, J., Francois, C., Hmimina, G., Dufrêne, E., Martin-StPaul, N. K., Soudani, K., Marie, G., Ourcival, J.-M., and Delpierre, N. (2017). "Environmental Control of Carbon Allocation Matters for Modelling Forest Growth". *New Phytologist* 214.1, pp. 180–193.

Le Maire, G., Davi, H., Soudani, K., François, C., Le Dantec, V., and Dufrêne, E. (2005). "Modeling Annual Production and Carbon Fluxes of a Large Managed Temperate Forest Using Forest Inventories, Satellite Data and Field Measurements". *Tree physiology* 25.7, pp. 859–872.

Résumé

Les modèles corrélatifs prédisent un déplacement important de la niche bioclimatique des espèces sous changement climatique (CC), sans toutefois tenir compte de la variabilité des mécanismes physiologiques de réponse entre individus et populations aux sein d'une espèce. Les objectifs principaux de ma thèse sont d'étudier le risque de mortalité d'arbres forestiers européens majeurs, notamment le hêtre, face au CC, d'en comprendre les processus physiologiques sous-jacents, et d'évaluer comment la sylviculture et la variabilité plastique/génétique affectent la vulnérabilité des individus et des peuplements. Ce projet s'appuie sur la modélisation statistique et mécaniste, avec un modèle basé sur les processus (CASTANEA), et à différentes échelles spatiales. La première partie a permis de caractériser trois composantes du risque de mortalité (associée aux gelées tardives, à la cavitation hydraulique et à l'épuisement des réserves carbonées) dans une population de hêtre en marge sèche. La seconde partie a permis de localiser et d'évaluer les risques de mortalité chez cinq espèces d'arbres (conifère et feuillus) avec CASTANEA à l'échelle européenne. Les risques de mortalité augmentent avec le CC pour les conifères mais stagnent pour les feuillus, et sont atténués par la sylviculture chez toutes les espèces. Dans la troisième partie, j'ai utilisé CASTANEA pour simuler l'effet de la variabilité génétique intra- et inter-populations sur le risque de mortalité du hêtre face au CC à l'échelle européenne. La variabilité génétique augmentait l'aire de viabilité de l'espèce et diminue la vulnérabilité des peuplements. Mes résultats ouvrent de nouvelles perspectives pour proposer de nouvelles stratégies de gestion innovante des arbres, tenant compte de leurs ressource génétiques.

Mots-clés : modélisation basé sur les processus, mortalité, changement climatique, forêts

Abstract

Correlative models predict major shifts in the bioclimatic niches of species under climate change (CC), without however taking into account the variability of the physiological mechanisms between individuals and populations within a species. The main objectives of my PhD thesis are to study the risk of mortality of major European forest trees, in particular beech, under CC, to understand the underlying physiological processes, and to assess how forestry and plastic/genetic variability may affect the vulnerability of individuals and stands. This project is based on statistical and mechanistic modeling, with a process-based model (CASTANEA), and at different spatial scales. The first part allowed three components of the risk of mortality (associated with late frosts, hydraulic cavitation and the depletion of carbon reserves) to be characterised in a Beech population on the dry margin. The second part allowed to locate and assess the risks of mortality in five tree species (coniferous and deciduous) with CASTANEA on a European scale. The risks of mortality increase with CC for conifers but stagnate for hardwoods, and are mitigated by silviculture in all species. In the third part, I used CASTANEA to simulate the effect of intra- and inter-population genetic variability on the risk of beech mortality under CC on a European scale. Genetic variability increased the species' viability area and reduced the vulnerability of stands. My results open up new perspectives for proposing new innovative management strategies for trees, taking into account their genetic resources.

Mots-clés : process-based model, mortality, climate change, forests